DNA cleavage photoinduced by benzophenone-based sunscreens

by

Avashnee Sewlall

Submitted in fulfilment of the academic requirements for the degree of Master of Science in the School of Pure and Applied Chemistry, University of Natal, Durban.

2003

ABSTRACT

The topical application of sunscreens is widely practised to protect healthy and photosensitive skins from the sun. The benzophenone-derived sunscreens, *e.g.* 2-hydroxy-4-methoxy benzophenone-5-sulphonic acid (or benzophenone-4) and 2-hydroxy-4-methoxy benzophenone (or benzophenone-3), were ranked as the second and third most frequently used sunscreens, respectively, by the United States Food and Drug Administration (FDA) in 1996. These sunscreens are categorised as being 'safe' and 'effective'. However, it is well known that the parent compound, benzophenone, undergoes rapid hydrogen abstraction reactions on irradiation and is an extremely powerful radical generator. In addition, benzophenone has been shown to be a potent photosensitizer of thymine dimers in deoxyribose nucleic acid (DNA). More astounding to the sunscreen industry is the recent discovery that a group of non-steroidal anti-inflammatory drugs (NSAIDs) having the benzophenone backbone, *e.g.* ketoprofen, not only form thymine dimers when irradiated with DNA *in vitro*, but also photosensitize double stranded supercoiled DNA making it prone to single-strand break formation. Both these lesions, if unrepaired, may contribute to mutagenesis, carcinogenesis, inherited disease and eventually cell death.

The purpose of this investigation was to determine if a group of benzophenone-derived sunscreen agents has the ability to photosensitize the cleavage of DNA, whereby supercoiled DNA is converted to the relaxed circular and linear forms. The group of UV absorbers investigated in this study included benzophenone-4, benzophenone-3, 2,4-dihydroxybenzophenone (or benzophenone-1), 2,2'-dihydroxy-4,4'-dimethoxy benzophenone sulphonic acid (or trade name Uvinul DS49) and 2-phenylbenzimidazole-5-sulphonic acid (or trade name Eusolex 232). For comparison the parent compound benzophenone and the NSAID ketoprofen, a well-known photocleaver, were also studied.

Buffered aqueous solutions of the benzophenones were irradiated in the presence of DNA at wavelengths greater than 300 nm with an Osram 500 W/2 high-pressure mercury lamp in conjunction with a 10 mm thick Pyrex filter. The irradiated samples were analysed for DNA cleavage by agarose gel electrophoresis and for DNA binding by fluorescence spectroscopy. The photostability of the UV absorbers was also investigated. In addition, computational studies were conducted to obtain the lowest energy geometrical structures of these UV absorbers and hence determine if intercalation of these UV absorbers with DNA was possible.

From the photostability experiments conducted, it is apparent that the benzophenone-based UV absorbers were stable to photodecomposition when irradiated with UV light. They behaved in a manner different from their parent compound benzophenone, and from ketoprofen, where substantial photodegradation occurred upon UV irradiation. This is indicative of the rapid photoreactivity of the benzophenone backbone. The relative photostability of the UV absorbers was not anticipated and was attributed to the substituents present on the benzophenone backbone.

The agarose gel electrophoresis experiments however clearly showed that benzophenone, ketoprofen, benzophenone-1, Uvinul DS49 and Eusolex 232 cleave ϕX174 DNA when irradiated with UV light at wavelengths greater than 300 nm, while benzophenone-3 and benzophenone-4 did not. For these UV absorbers with the exception of benzophenone-3 and benzophenone-4, the number of single strand breaks in the DNA increased compared to when it was irradiated in their absence. In addition, the supercoiled DNA was converted to the relaxed circular and linear forms, the latter of which was undetected in the absence of the UV absorbers. Binding of benzophenone, ketoprofen, benzophenone-1 and Uvinul DS49 to calf thymus DNA was also detected by the fluorescence spectroscopy technique. However, this was not observed for Eusolex 232, benzophenone-3 and benzophenone-4, since they did not compete with ethidium bromide for DNA binding sites.

Where DNA cleavage did occur, the mechanism of this interaction had to be determined hence the motivation for the computational studies. From computational studies using PM3 semi-empirical calculations, it was determined that the benzophenone-based UV absorbers investigated, apart from Eusolex 232, displayed non-planar geometrical structures. This indicated that DNA intercalation of these sunscreen agents with DNA would at best be very limited, since only one half of the molecule could possibly interact with the bases of DNA. For benzophenone, ketoprofen, benzophenone-1 and Uvinul DS49, photosensitised type I and type II processes involving triplet energy transfer reactions has been identified in literature as being responsible for DNA cleavage. It was determined by *ab initio* calculations that Eusolex 232 exists in a planar structure unlike the other UV absorbers mentioned above that were non-planar. It was concluded that although Eusolex 232 has the ability to intercalate with the base pairs of DNA, it does not do so, as shown by its lack of binding to calf thymus DNA by the fluorescence spectroscopy study. Literature alludes to photooxidation by singlet oxygen in single stranded DNA via the type II reaction and type I electron transfer reactions in double stranded DNA as the mechanism responsible for DNA cleavage induced by Eusolex 232.

Benzophenone-3 and benzophenone-4 did not cleave DNA as was expected. This was attributed to the electron-donating groups –OH and $–OCH_3$ present on the benzophenone backbone, which are known to reduce the reactivity of the lowest triplet from n,π to π,π^*.

Preface

The experimental work presented in this dissertation was performed in the Schools of Pure and Applied Chemistry and Life and Environmental Sciences at the University of Natal, Durban from March 2000 to May 2002. The work was supervised by Professor Bice S. Martincigh and Dr Jenny Lamb.

These studies represent original work by the author and have not otherwise been submitted in any form for any degree or diploma to any tertiary institution. Where use has been made of the work of others it is duly acknowledged in the text.

Acknowledgements

I would like to extend my gratitude to the following people for their contribution to this research:

- Firstly my academic supervisor, Professor Bice. S. Martincigh from the School of Pure and Applied Chemistry for her interest in this subject.
- My co-supervisor, Dr Jenny Lamb from the School of Life and Environmental Sciences who assisted in the gel electrophoresis experiments.
- Dr Gert Kruger, for his assistance with the computational modelling and with the interpretation of the results.
- Dr Glenn Maguire, for this enthusiasm and ideas on fluorescence spectroscopy.
- University of Natal Medical School for use of their microscope and quartz cuvette.
- Technical Staff: Mr Logan Murugas, Mr Enoch Mkhize, Mrs Zarina Sayed-Ally, Mrs Saroj Naidoo, Mr Kishore Singh and Mr Bret Parel for their assistance.
- Mr Greg Moodley for his assistance with the ordering of chemicals.
- Ezekiel Chetty for his love, support, and help during my study.
- My family for their support and encouragement.
- My colleagues Rivash Panday, Ali M. Salim, Wally Waudo and Manomayi Venayagamoorthy for their support and friendship.
- Finally the National Research Foundation, for financing this project and awarding me a bursary and the University of Natal for a graduate assistantship.

Table of Contents

Chapter 3

Results and discussion

List of Figures

Chapter 1

Chapter 2

Chapter 3

List of Tables

Abbreviations

Avobenzone	Butyl methoxy dibenzoylmethane
Benzophenone-1	2,4-dihydroxybenzophenone
Benzophenone-3	2-hydroxy-4-methoxy benzophenone
Benzophenone-4	2-hydroxy-4-methoxy benzophenone-5-sulphonic acid
Bp	Base pairs
CPD	Cyclobutane pyrimidine dimer
DNA	Deoxyribonucleic acid or deoxyribose nucleic acid
EDTA	Ethylene diaminetetraacetic acid
EHMC	2-ethylhexyl-*para*-methoxycinnamate
Eusolex 232	2-phenylbenzimidazole-5-sulphonic acid
FDA	Food and Drug Administration
FID	Fluorescent intercalator displacement
HPLC	High performance liquid chromatography
IR	Infrared
NMR	Nuclear magnetic resonance
NSAIDs	Non-steroidal anti-inflammatory drugs
PABA	Para-aminobenzoic acid
Padimate-A	Amyl dimethyl PABA
Padimate-O	Octyl dimethyl PABA
PBS	Phosphate buffered saline
PM3	Parametric method number 3
Pst I	*Providencia Stuartii* restriction endonuclease
RNA	Ribonucleic acid
SSB	Single strand breaks
SPF	Sun protection factor
TBE	Tris-borate EDTA electrophoresis running buffer
Tris	*Tris*-(hydroxymethyl)-aminomethane buffer
Tris-HCl	*Tris*-(hydroxymethyl)-methylammonium chloride buffer
UV	Ultraviolet
Uvinul DS49	2,2'-dihydroxy-4,4'-dimethoxy benzophenone sulphonic acid
XP	*Xeroderma Pigmentosum*

Chapter 1

INTRODUCTION

The dramatic increase in the incidence of skin cancer over the past few decades has become a major cause of concern for scientists throughout the world. Exposure to sunlight and, in particular, ultraviolet (UV) radiation has been implicated as the principal cause for this epidemic. Consequently, the use of sunscreens has been practised for over 80 years now, in an effort to protect the skin from the adverse effects of the sun. However, recent studies have shown that sunscreens may actually inflict more damage than they prevent (Wolf *et al.* [1994], Westerdahl *et al.* [1995], Autier *et al.* [1998] and Westerdahl *et al.* [2000]). The photochemistry of sunscreens is therefore very important and it has gained increasing interest from researchers throughout the world. In this study the photochemistry of a group of benzophenone-derived UV absorbers, namely, benzophenone-1 (or 2,4-dihydroxy benzophenone), benzophenone-3 (or 2-hydroxy-4-methoxy benzophenone), benzophenone-4 (or 2-hydroxy-4-methoxy benzophenone-5-sulphonic acid), 2, 2'-dihydroxy-4, 4'-dimethoxy benzophenone sulphonic acid (trade name Uvinul DS49) and 2-phenylbenzimidazole-5-sulphonic acid (trade name Eusolex 232), has been investigated. In particular, this work focuses on the ability of these sunscreen active agents to photoinduce DNA strand breaks and DNA damage *in vitro*.

1.1 Deleterious effects of sunlight

Life on earth would be impossible without sunlight. Sunlight is necessary for the production of vegetation, food and vitamin D in the body and it is essential for emotional and physical well being. However, in excessive doses it does have harmful effects.

Sunlight consists of radiation of differing wavelengths. These are UV-radiation (190 - 400 nm), visible radiation (400 - 800 nm) and infrared (IR) (0.78 - 300 μm) radiation (Skoog *et al.* [1996]). Due to the filtering effect of the ozone layer, not all of this solar energy reaches the earth's surface. Of the total energy reaching the earth's surface, 60% is in the visible range, 25% in the IR range and 15% in the UV region (Sayre [1992]).

UV radiation can be subdivided into three regions. These are the UVA (320 – 400 nm), UVB (280 - 320 nm) and UVC (100 – 280 nm) regions. All of the UVC radiation however is filtered out by the ozone layer and oxygen. Only UVA (95%) and a small portion of UVB radiation (5%) reach the earth's surface (Larsen [1994]) (Figure 1.1).

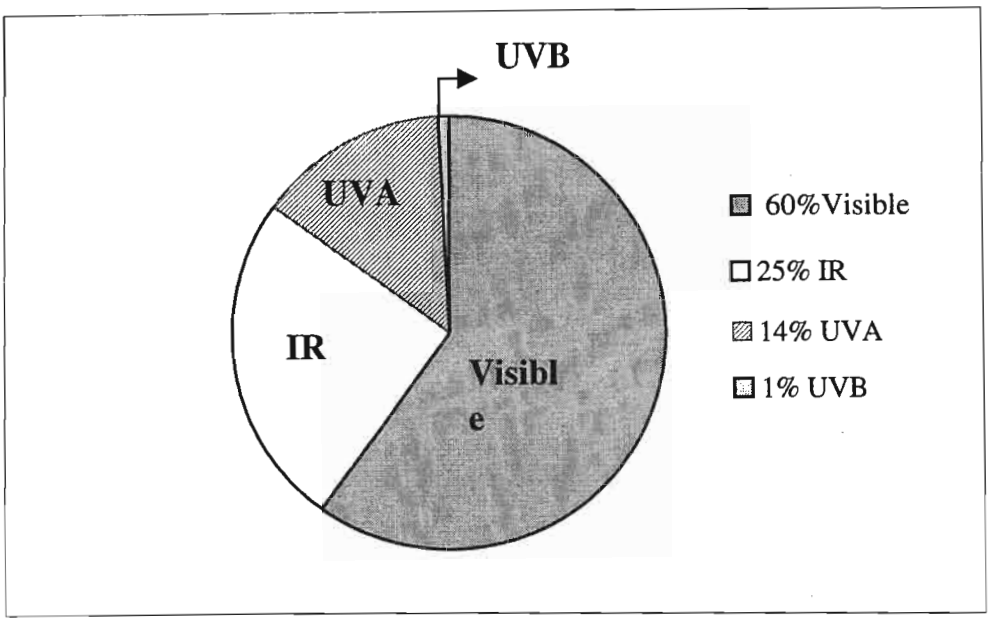

Figure 1.1: Solar radiation reaching the earth's surface.

Although UV radiation accounts for the smallest fraction of the solar energy reaching the earth's surface, it is of the highest energy since it has the shortest wavelength. Consequently, it has been implicated to be most harmful in inducing damage to living organisms. Efforts of dozens of researchers have revealed that overexposure to UV radiation induces a list of ailments including erythema (skin reddening), tanning, photoaging and skin cancer. The relationship between sunlight and skin cancer was recognized as early as 1894. It is now well established that UV radiation exposure is a significant factor contributing to skin malignancies in man (Glass & Hoover [1989], Lee [1989] and Higginson *et al.* [1992]).

Of the UV radiation reaching the terrestrial environment, UVB has been implicated to be the most destructive to living organisms although it is 100 times less abundant than UVA (Voss [2001]). UVB radiation has long been recognized as the principal cause of erythema, and is most significant in the induction of skin cancers (Green *et al.* [1997]). UVB radiation inhibits DNA, ribonucleic acid (RNA) and protein synthesis, and is responsible for most of the tissue damage that results in photoaging of the skin (Woodruff [2001]). UVA radiation, on the other hand, was once thought to be harmless due to its long wavelength region and low energy. It was only during the past decade that scientists have begun to understand fully the damaging effects of UVA radiation. UVA radiation has been shown to cause premature aging of the skin, with effects including roughening, blotchiness, sagging and wrinkles (Woodruff [2001]). UVA light penetrates deepest into the skin and has been implicated in the initial stages of suntanning. More importantly, it has been shown to suppress the immune function and contribute to the induction of skin cancers (Setlow *et al.* [1993]), which had previously not been thought to be the case.

UVC radiation, which is of the highest energy, would be the most potent if it were to reach the earth's surface, therefore depletion of the ozone layer is of great concern. The shortest measurable wavelength of solar radiation at sea level is 290 nm (Martincigh *et al.* [1997]). Continued deterioration of the ozone layer could mean that wavelengths shorter than 290 nm, *i.e.* the lower energy UVC wavelengths and the higher energy UVB, would be able to penetrate the stratospheric ozone layer and reach the terrestrial environment. This could have deleterious effects.

1.2 Skin cancer and UV radiation

The most common of all human cancers is that of the skin. There are three main types of skin cancer affecting man today. These are malignant melanoma, basal cell carcinoma and squamous cell carcinoma. The basal and squamous cell carcinomas are the most prevalent forms of skin cancer and are associated with long-term exposure to the sun (Voss [2001]), while malignant melanoma, which is linked to brief, intense periods of sun exposure is the rarest form of skin cancer, but the most deadly of the three (Larsen [1994]).

According to the National Cancer Registry of South Africa, there have been 149 815 histologically diagnosed cancer cases in South Africa over the period 1993-1995 (Sitas *et al.* [1998]). Of these, 41 713 cases were due to cancers of the skin, making skin cancer the most

commonly occurring form of cancer in South Africa during this period. In order to understand how these skin cancers occur, an understanding of the structure of human skin is required.

Human skin is composed of three main layers. These are the epidermis, dermis and the hypodermis. Only the epidermis and the dermis are affected by UV radiation. The epidermis, which is the top and the thinnest layer of the three (100 – 150 μm) consists of multiple layers of cells, while the dermis, a relatively thick layer, consists largely of collagen and elastic fiber (Young [1997]) (Figure 1.2). UVB rays penetrate the epidermis, while the longer wavelength UVA rays continue into the dermis. The cells found in the epidermis are the keratinocytes, the Langerhans cells and the melanocytes, with the keratinocytes being the main cell type. The keratinocytes in the basal layer undergo cell division and differentiate into several layers to eventually form the outermost layer of skin, the *stratum corneum* (Figure 1.2).

Basal cell carcinoma, which is the most common type of skin cancer, develops from the abnormal cell division of the keratinocyte cells of the basal layer of the epidermis, while squamous cell carcinoma develops from the spinous layer (Figure 1.2). Malignant melanoma arises from the abnormal cell division of the melanocyte cells. These cells, present in the innermost part of the epidermis, are the melanin pigment-producing cells, which not only give the skin colour, but also protect the body from UV radiation. However, in fair skin this protection develops only in part. Malignant melanoma accounts for more than 90% of all skin cancer deaths. Researchers have now estimated that for every 1% decline in the stratospheric ozone layer, a 3 - 5% increase in squamous cell carcinoma, 2 - 3% rise in basal cell carcinoma, and 1 - 2% increase in malignant melanoma is expected (Voss [2001]).

Studies conducted with polychromatic light sources in the hairless albino mouse show that UVB radiation is responsible for 70 - 80% of the cases of non-melanoma skin cancer (de Gruijl & van der Leun [1994]). In contrast, while studying a special hybrid fish (*Xiphophorus*) Setlow *et al.* [1993] have shown that 90% of melanoma cases are due to exposure to UVA radiation, which was once not thought to be the case. UVA light is a more likely cause of melanoma than UVB since it penetrates deeper into the skin and is therefore more likely to produce cancer in the deeper-lying melanocytes, while UVB expends its energy only in shallower tissues (Ainsleigh [1993]). However, researchers are now convinced that both UVB and UVA radiation can induce skin cancers.

After several decades of research, scientists now have a better understanding of how exposure to UV radiation leads to skin cancer. It is quite apparent that erythema is only a physical manifestation of the direct effects of UV radiation on the skin. What is unseen is the damage

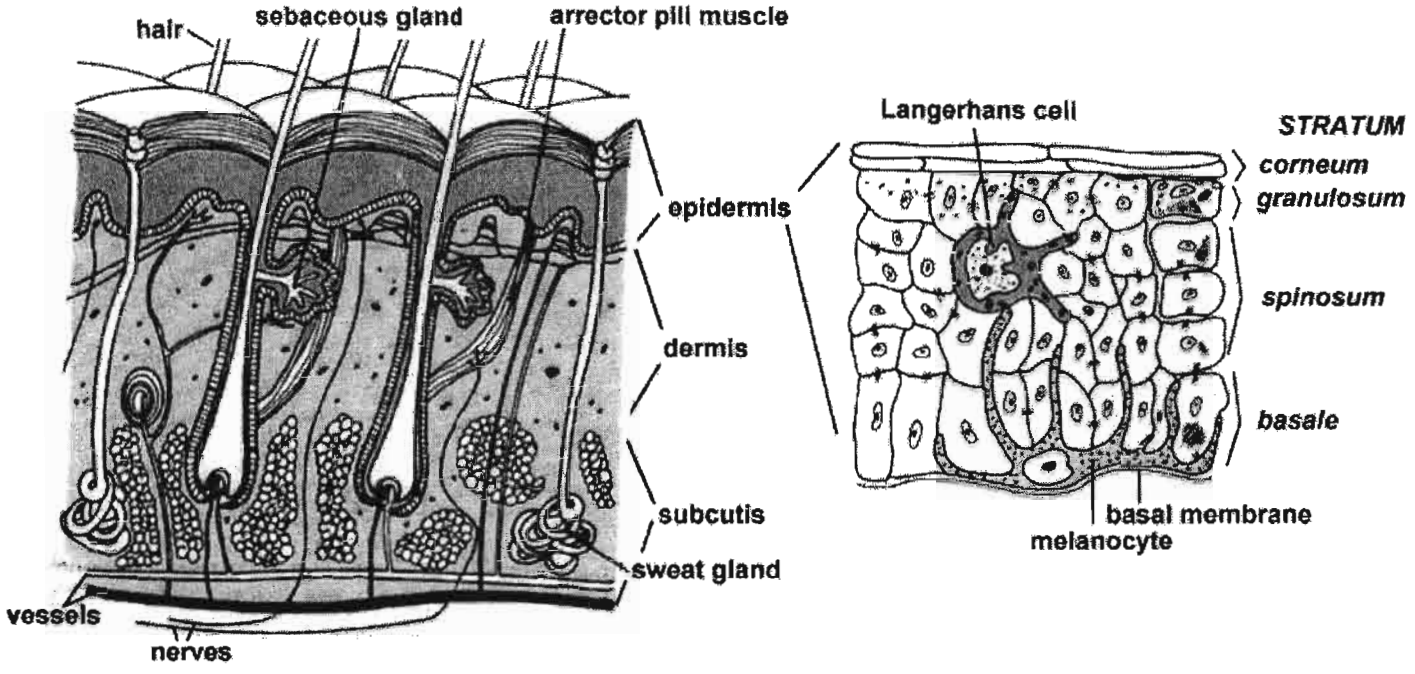

Figure 1.2: Structure of human skin showing the epidermis, dermis and hypodermis layers (http://herkules.oulu.fi/isbn9514266463/html/x563.html, Date accessed: 20 September 2002).

inflicted to cells within the epidermis. Each of these cells contains a nucleus in which lies the chromosome. Each chromosome is a strand of DNA coated with proteins. It has been well established that the DNA is susceptible to UV damage and it is this damage that is believed to induce malignancies in human skin.

1.3 DNA photochemistry

DNA is the macromolecule responsible for the storage and transmission of genetic information in living cells. The structure of the DNA molecule is dynamic and must be considered in order to understand its photochemistry.

The double helical DNA structure proposed by Watson and Crick (Alberts *et al.* [1989]) consists of two long anti-parallel polynucleotide chains that coil around a common axis (Figure 1.3). Each of the two strands is a polymer of nucleotides. A nucleotide comprises a nucleic acid base, which is joined to deoxyribose (a five-carbon sugar), which in turn is bonded to a phosphate group (Figure 1.4). On the inside of the helix are the bases, either pyrimidines (thymine and cytosine) or purines (adenine and guanine), linking the two anti-parallel DNA strands together with hydrogen bonds, while the sugar-phosphate backbone makes up the outside of the helix (Figure 1.3). The bases are specifically paired, that is, adenine (A) and thymine (T) pair, as do guanine (G) and cytosine (C). Two hydrogen bonds hold the AT base pair together, while three hydrogen bonds are formed between a GC base pair (Figure 1.5). During exposure of DNA to UV radiation, the bases are the principal targets of attack (Setlow & Ahmed [1980]). The bases have conjugated double bonds (Figure 1.5) with a bond energy suited to absorb UV radiation.

The sequence of nucleotides along the DNA backbone carries the genetic information, and serves as the template for synthesis of an exact copy of a complementary DNA strand upon replication (Figure 1.6). This governs the process of transcription of DNA into RNA, followed by translation into proteins. Preservation of the precise sequence of bases is essential, since any alterations would cause the transfer of incorrect genetic information, and if left unrepaired could cause gene mutations that could ultimately result in the formation of cancerous cells.

Numerous *in vitro* studies have shown that exposure of DNA to UV radiation results in the formation of specific photoproducts. These have been identified to be the cyclobutane pyrimidine dimer (CPD) and the (6-4) pyrimidine photoproduct, both formed between two

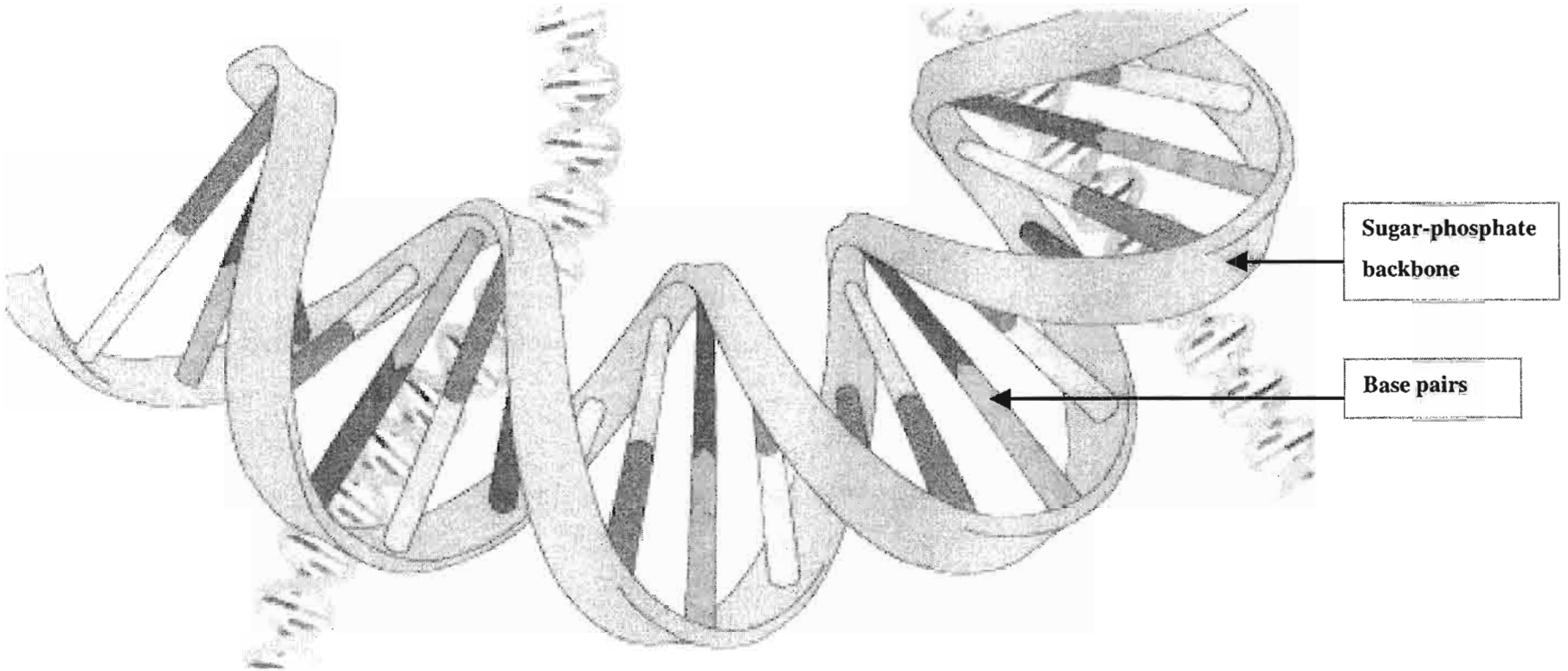

Figure 1.3: Model of the double helical Watson and Crick DNA structure (Brown [2003]).

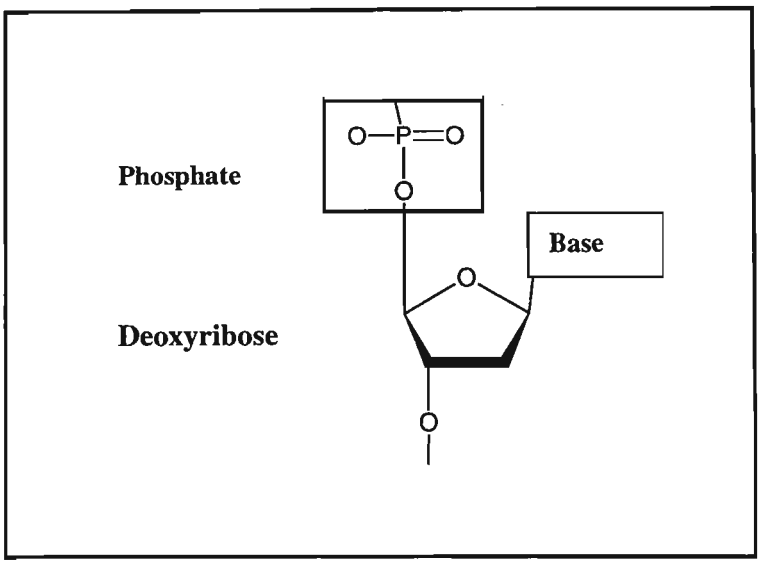

Figure 1.4: The repeating unit of DNA.

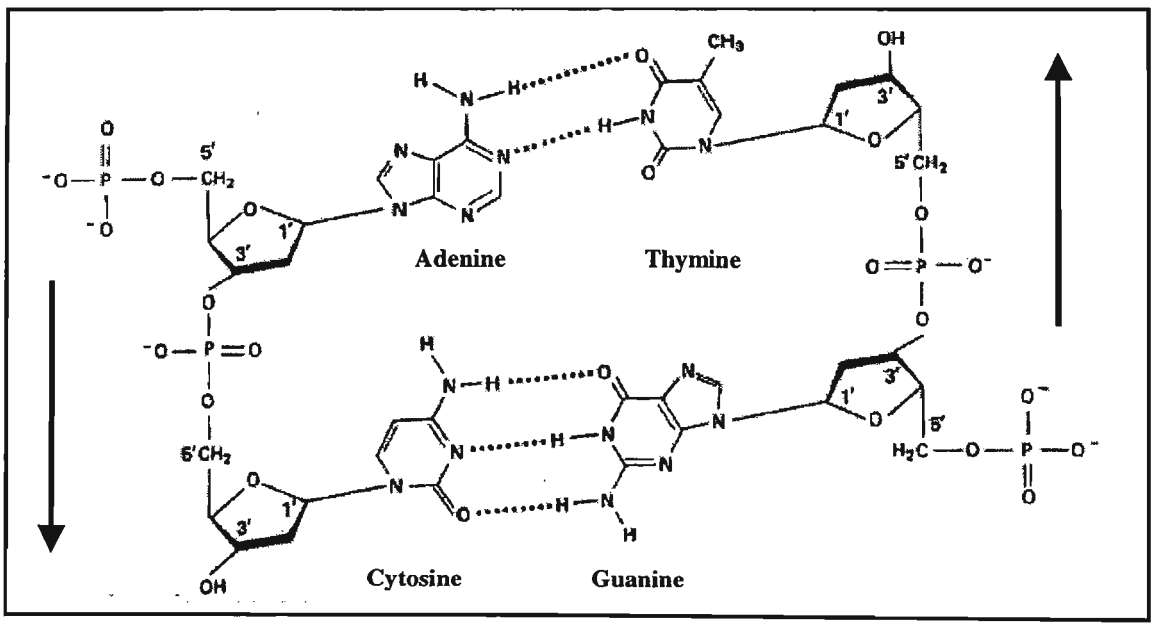

Figure 1.5: Interstrand hydrogen bonding between specific nucleic bases (Avers [1984]).

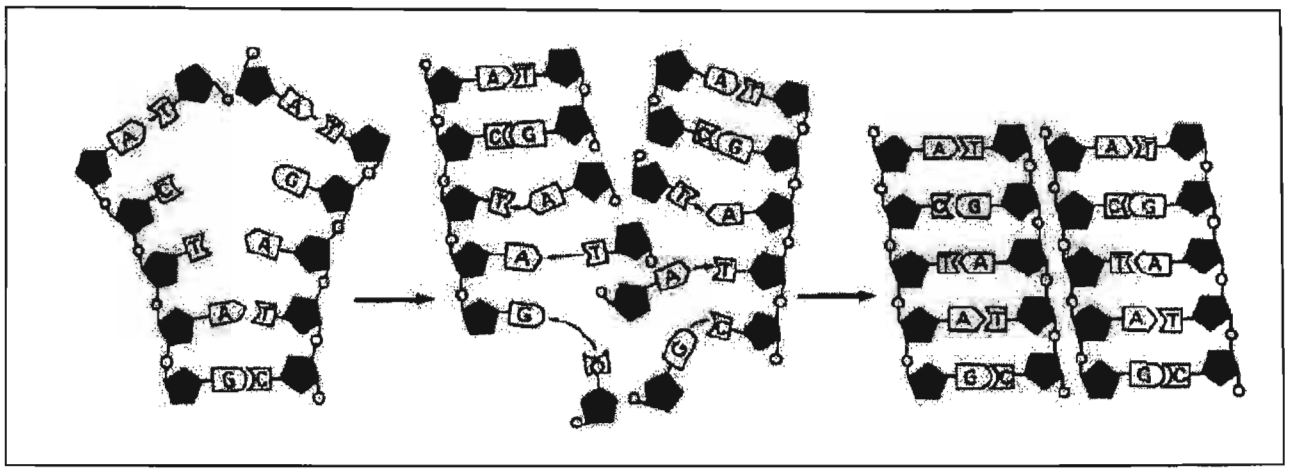

Figure 1.6: Synthesis of a new complementary DNA strand by replication, where the new DNA strand is an exact copy of the initial DNA sequence (Avers [1984]).

adjacent pyrimidine bases on the same DNA strand (Mathews & van Holde [1996] and Young [1997]) (Figure 1.7). The principal photoproduct in DNA is the CPD, which is formed when two adjacent pyrimidine bases in the same DNA strand become linked (Haseltine *et al.* [1980], Franklin *et al.* [1982] and Raghunathan *et al.* [1990]). The most prevalent of these dimers is that formed between two thymine bases, with thymine-cytosine occurring in smaller amounts. The (6-4) photoproduct, although more lethal, is, however, formed in smaller amounts and occurs when adjacent pyrimidines are linked across the 4-carbon of one to the 6-carbon of the other (Patrick [1977]).

The reaction mechanism for the formation of CPD agreed upon in literature is briefly outlined below (Sztumpf *et al.* [1967], Greenstock *et al.* [1967] and Brown & Johns [1968]). Initially absorption of a photon by the pyrimidine base promotes it from the ground state to its first excited singlet state. The singlet excited state is short-lived and rapidly undergoes intersystem crossing to the first excited triplet state. Population of the thymine triplet may also occur as a result of an energy transfer from a nearby excited molecule. This process is known as photosensitization and will be considered in Section 1.4.1. The excited pyrimidine then encounters an adjacent base in the ground state and reacts to form a dimer. Pyrimidine dimerization links the adjacent thymine residues, thereby causing uncoiling and bending in the DNA molecule. This distorts the helix in such a way that replication beyond this point is blocked (Mathews & van Holde [1996]).

Living cells are equipped with a number of repair mechanisms that are able to remove UV-induced lesions. One such repair system capable of removing thymine dimers in humans is known as excision repair. In this repair process the distortion in the DNA is recognized by a protein complex, which nicks the DNA on either side of the thymine dimer. This triggers the enzyme called DNA Polymerase I, which then inserts the missing bases (http://www.emunix.emich.edu/~rwinning/genetics/mutat4.html, Date accessed: 5 December 2002).

Cyclobutane pyrimidine dimers have been shown to be a major cause of mutagenic and carcinogenic events, especially in patients suffering with a condition known as *xeroderma pigmentosum* (XP). XP is a rare recessive hereditary disease in which repair to UV-induced damage is defective (Avers [1984]). Cleaver [1968] demonstrated that cells from individuals with XP, who were extremely prone to sunlight-induced skin cancer, were unable to excise pyrimidine dimers. More specifically, dimer formation is believed to induce mutations in the p53 tumor suppressor gene, a gene that plays an important role in cell division (Young [1997]).

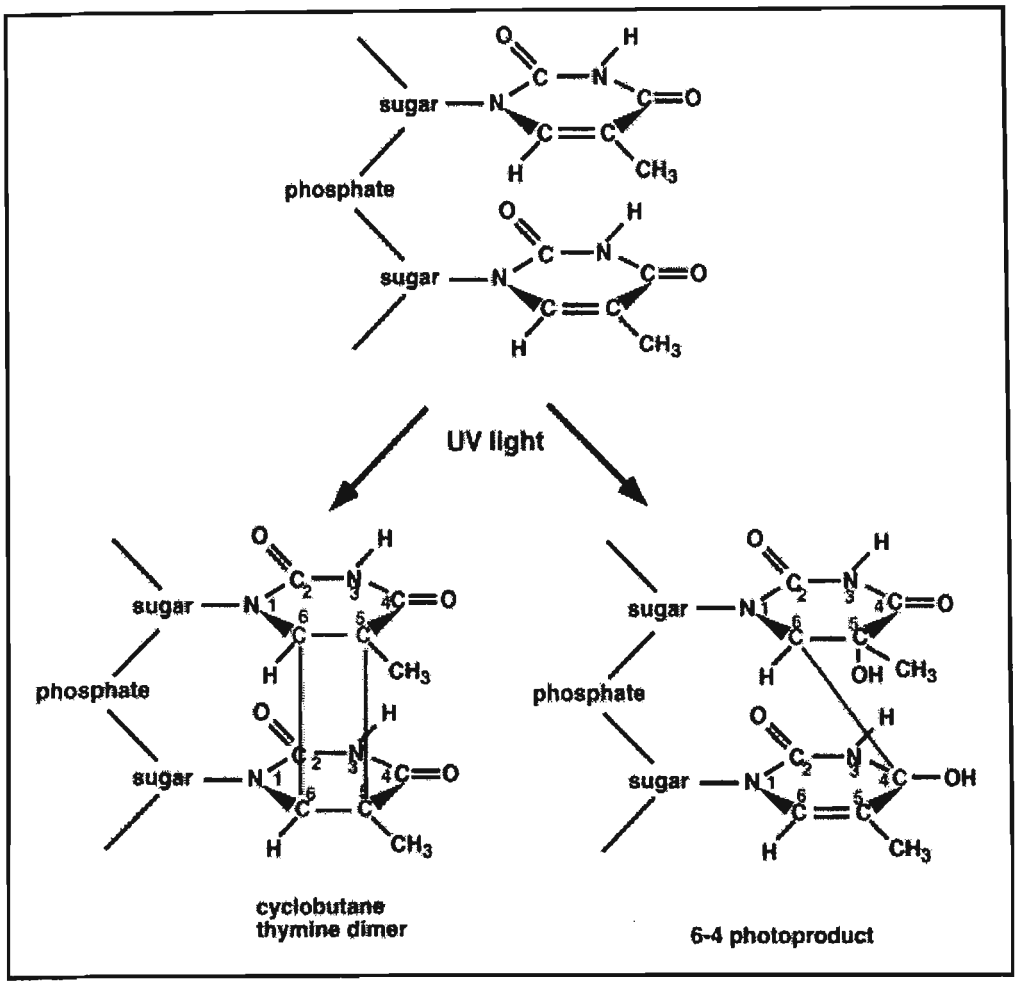

Figure 1.7 The two most common DNA photoproducts formed by UV irradiation of DNA (http://kukulkan.mcb.arizona.edu/~mhewlett/marty/alt411/modules/dimerrep.html, Date accessed: 25 September 2002).

This mutation is believed to be the initial process involved in the production of UV-induced skin cancers. A reduced capacity to excise pyrimidine dimmers in XP patients leaves them at a 2000-fold risk of developing malignant melanoma and a 4800-fold chance of forming squamous and basal cell carcinomas by the age of 20 (Voss [2001]).

In addition to tumor formation, pyrimidine dimers have also been shown to be involved in many pathways leading to tissue and cell damage including erythema, sunburn and suppressed immunity (Young [1997]). The effect of the (6-4) pyrimidine photoproduct is not yet fully

understood but studies have recently suggested that it too may be directly involved in mutagenesis (Mathews & van Holde [1996]).

1.4 The photochemistry of sunscreens

As a response to the high rates of skin cancer, sunscreens are now increasingly being used to protect the skin from the harmful effects of excessive exposure to UV radiation. The sunscreen industry is rapidly expanding and sunscreens are now incorporated into a wide range of products, from creams and moisturizers to cosmetics and shampoos. Sunscreen formulations are now made to be more effective, more cosmetically appealing and tolerable to the consumer.

The effectiveness of a sunscreen formulation is currently assessed in terms of its Sun Protection Factor (SPF). The SPF refers to the product's ability to screen or block out the sun's burning rays. It is interpreted as how much longer skin covered with sunscreen takes to burn compared to unprotected skin (Diffey [2001]). If unprotected skin takes 10 minutes before it starts to burn, then applying a sunscreen with a SPF factor of 15 will protect your skin from sunburn for 15 times longer (that is for 150 minutes). Today, a typical sun protection product consists of a UV absorber (sunscreen) in a base, which may be alcohol, oil, or more frequently an emulsion. The amount of UV absorber allowed in sunscreen formulations must be low to minimize side effects on users. The type and concentration of UV absorbers in sunscreens is strictly governed in most countries.

The UV absorbers can be broadly classified into two categories depending on their mode of action. These are either physical blockers or chemical absorbers. Physical blockers act as physical barriers that reflect and scatter UV radiation away from the skin. They include inorganic pigments such as titanium dioxide, iron oxides and zinc oxides, and generally offer broadband protection over both the UVA and UVB regions of the spectrum. Alternatively, chemical absorbers are organic molecules, which prevent sunburn by absorbing specific wavelengths of UV radiation. These absorbers are of paramount interest to this work and have been considered in detail in Section 1.4.1.

1.4.1 Chemical absorbers

Chemical absorbers can be classified as either UVA or UVB absorbers depending on their absorption spectrum. The UVA absorbers absorb the shorter wavelengths of UVA radiation (320 - 360 nm) and include compounds such as the benzophenones, anthranilates and dibenzoylmethanes. The UVB absorbers, on the other hand, are effective in absorbing the entire

UVB spectrum (290 - 320 nm) and include the para-aminobenzoate derivatives, cinnamates, and salicylates or their esters. The structures of the most commonly used chemical absorbers are shown in Figure 1.8.

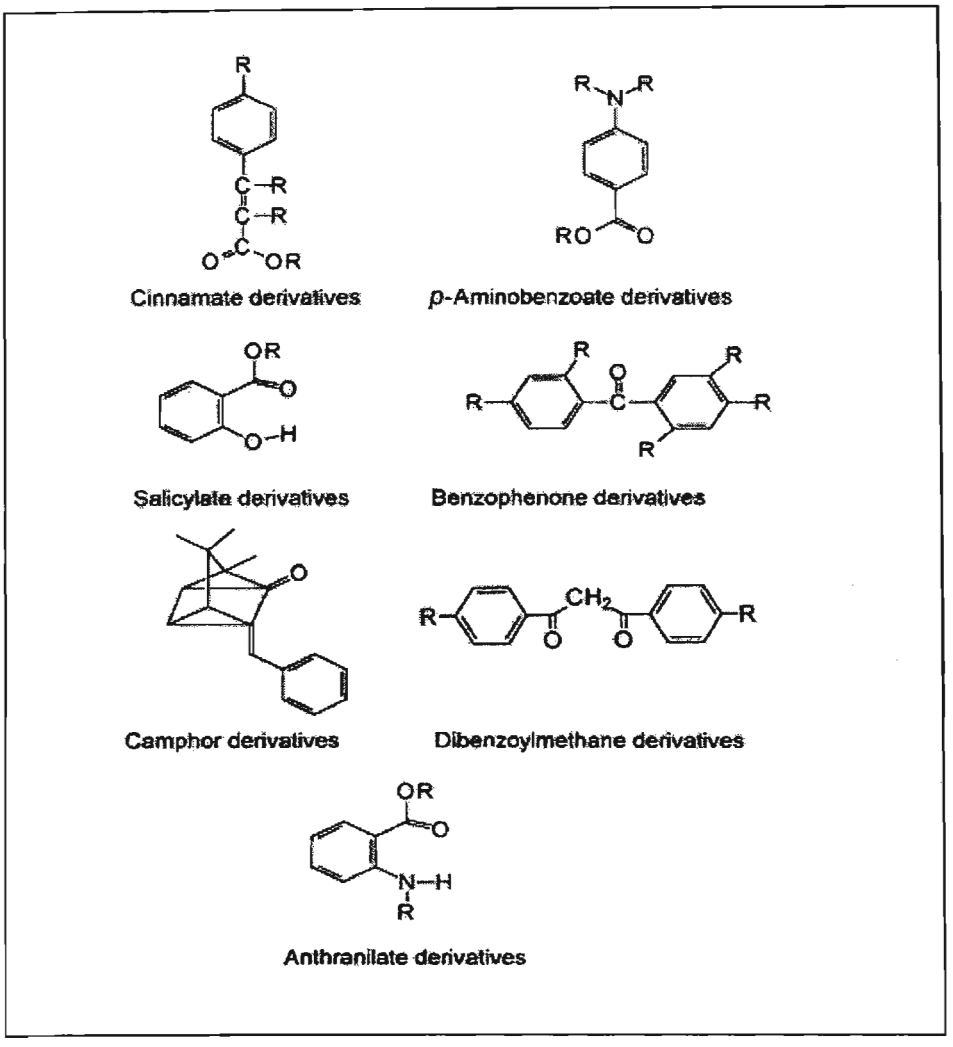

Figure 1.8: The most commonly used chemical absorbers in sunscreen formulations (Serpone *et al.* [2002]).

In general, most UVB absorbers are aromatic compounds conjugated with a carbonyl group and contain electron-releasing groups (such as amine, or methoxy) at the *ortho-* or *para-* positions of the aromatic ring. This allows for electron delocalisation, thereby allowing the compound to absorb radiation of the appropriate wavelength before it reaches the skin. The mechanism of absorption of light by chemical sunscreens and the possible pathways for the dissipation of the excess electronic energy have been illustrated in Figure 1.9 and will be briefly discussed below.

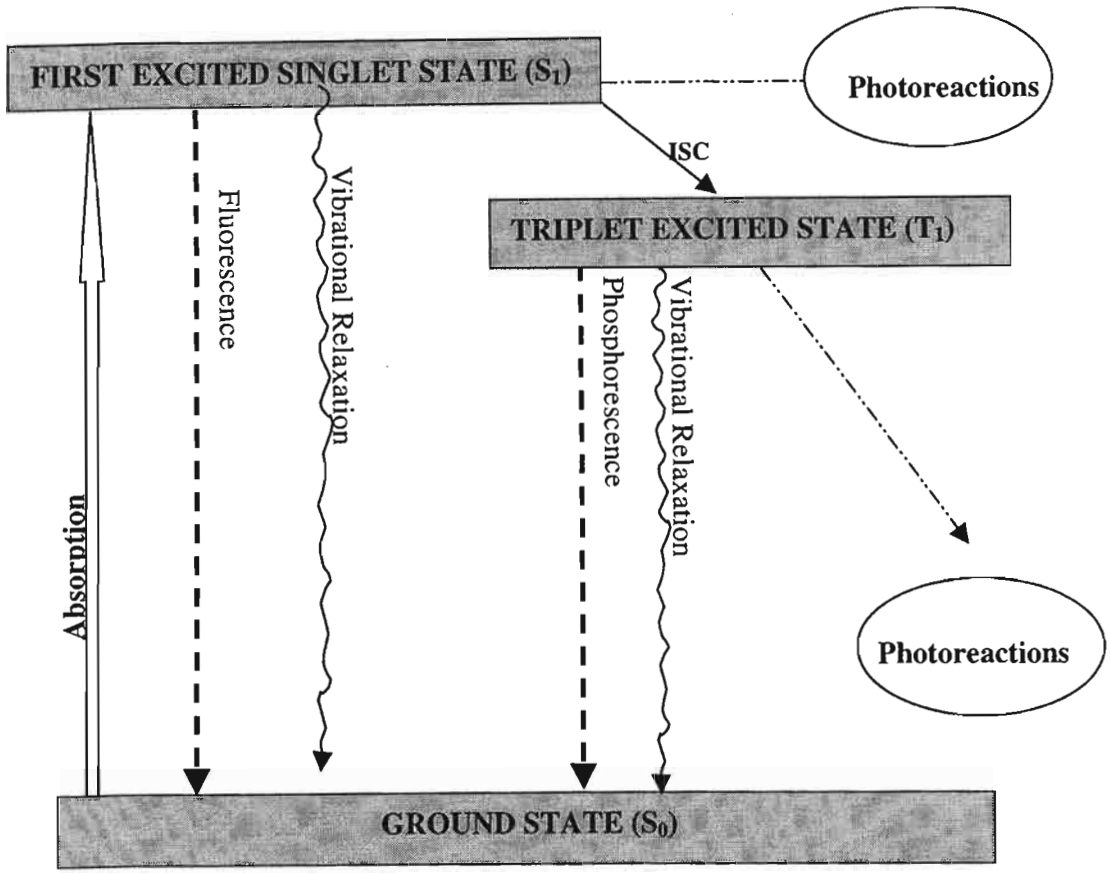

Figure 1.9: Mechanism of absorption of light and possible dissipation pathways for a chemical absorber.

Initially, the molecule absorbs a photon, which is a quantum of electromagnetic energy. This causes the energy of the molecule to increase and changes its electronic configuration. Before absorption, the orbital configuration of the electrons is the "ground" state, in which all the electrons are paired with opposite spin. On absorption of a photon, one of a pair of electrons is promoted to a higher energy level, but in doing so, it maintains its spin orientation. This is the first excited singlet state. The lifetime of the singlet excited state is short (10^{-9} - 10^{-8} seconds), and deactivation of the excited state occurs rapidly via one of the following pathways. Either the molecule in the singlet state can return to the ground state by emitting its energy thermally as heat through a series of vibrational relaxation transitions (nonradiative decay), or it could emit this energy as a photon of longer wavelength by a process known as fluorescence (radiative decay). These are the preferred routes for a sunscreen since the harmful radiation is dissipated in a harmless way, however this may not always be the case.

The excited molecule in the singlet state may react with another molecule to form photoproducts, or more commonly, it may transfer its energy by a radiationless process called

intersystem crossing (ISC) to populate the triplet excited state. In the triplet excited state the spin of one of the electrons of the pair is inverted. Again, it is least damaging for the triplet excited state to decay to the ground state via nonradiative (emission of heat) or radiative de-excitation (emission of a photon). The latter process is called phosphorescence since it occurs between two states of different spin. However, as the triplet excited state is long-lived, lasting 10^{-4} seconds (Turro [1978]) or longer, it is more likely to undergo a photochemical reaction or an energy transfer reaction.

The photochemical reactions include photoaddition/substitution, cycloaddition, photoisomerization and photofragmentation reactions. Any of these reactions may alter or destroy the UV absorption capacity of the sunscreen and are therefore undesirable. In addition, if the chemical absorber has the potential to penetrate the epidermis of the skin, the possibility exists for the occurrence of direct photochemical reactions between the sunscreen and biomolecules, such as DNA, in its vicinity or of indirect photochemical reactions via reactive intermediates, such as free radicals ($OH^{\bullet}$, $^1O_2$). These reaction products could be potentially carcinogenic.

Energy transfer reactions occur when the excited triplet returns to the ground state by transferring its energy to a nearby molecule. The excited triplet becomes the "donor" (D^*) and is known as the photosensitizer with the nearby molecule being the "acceptor" (A). This process is known as photosensitization. Upon the transfer of energy, D^* returns to the ground state in its original form while A is elevated to its excited state (A^*). The photosensitization process is illustrated in Reaction 1.1 below and will only occur if the energy of D^* is greater than that of A^*.

$$D^* + A \rightarrow D + A^* \qquad (1.1)$$

In some cases, this is the desired mechanism for energy dissipation, however, more commonly photosensitization leads to the formation of undesirable and often lethal products such as thymine dimers. Thymine, in the excited triplet state, can react with ground state thymine to yield thymine dimers which are potential precursors to skin cancer, as discussed in Section 1.3. The lowest triplet energy of a pyrimidine base is that of thymine which is estimated to be 314.8 kJ mol^{-1} (Lamola *et al.* [1967]). Any sunscreen having the lowest triplet energy higher than or similar to that of thymine could act as a photosensitiser and thereby increase the formation of thymine dimers.

The preferred energy dissipation pathway for an excited molecule will depend on a number of factors, which include the rates and activation energies of each competing reaction, the triplet energy and its lifetime, as well as the concentration and nature of the molecules. Ideally, a sunscreen should function by absorbing harmful UV radiation and then dissipating this energy either by nonradiative or radiative means. In this way the energy is given off in a harmless way and the sunscreen returns to the ground state such that it is able to absorb another photon of light, thereby repeating the process, which will protect the skin from UV damage. The skin penetration of the active ingredients should also be minimal thereby preventing any phototoxic reactions to the biological cells.

1.4.2 Controversy facing chemical sunscreens

The positive correlation between sunscreen use and the increased rates of skin cancer has now prompted scientists to re-evaluate the benefits of using sunscreens. Moan & Dahlback [1992] reported that in Norway during the period 1957 to 1984 the cases of melanoma increased by 440% for women and 350% for men, although there had been no change in the ozone layer over this period. In addition, studies conducted by Garland *et al.* [1992] suggest that the greatest increase in melanoma has been experienced in countries (such as Australia) where the use of sunscreens has been heavily promoted. The hypothesis that the use of sunscreens increases the risk of cancer, especially melanoma, has been further strengthened by a number of epidemiological case studies (Wolf *et al.* [1994], Westerdahl *et al.* [1995], Autier *et al.* [1998] and Westerdahl *et al.* [2000]). This now raises the possibility, though yet scientifically unproved, that sunscreens may play a very significant role in contributing to the skin cancer epidemic rather than preventing it.

Scientists do agree that most sunscreens protect the skin against sunburn and erythema, however, they are now re-examining their behaviour to determine if they protect the skin against non-erythema damages such as that to DNA and suppression of the immune system. Both of these are believed to be instrumental in the initiation of skin cancer. There is some evidence that regular use of sunscreens helps prevent the formation of actinic keratoses, that may be regarded as a precursor to squamous cell carcinomas (Dover *et al.* [1994]), however, the ability to protect against melanoma or basal cell carcinoma is not yet fully determined. Several *in vitro* studies on the photochemistry of sunscreens have been conducted, however, some of them are circumstantial since they may not reveal what sunscreens actually do when applied on the skin (Wu [1998]). Until the absorptivity of the active ingredients used in sunscreens is determined, these results should not be taken lightly since they indicate what sunscreens may be capable of

doing if they are absorbed through the skin and interact with the skins cells. Some of these studies are outlined below.

1. Para-aminobenzoic acid

Para-aminobenzoic acid (PABA) was the most common ingredient used in sunscreens in the 1980's. PABA was widely used as a chemical absorber to block UVB radiation, which at that time was thought to be the most lethal. However, PABA had some drawbacks such as stinging of the skin as well as photocontact allergic reactions, which have been well documented over the years. When the potential deleterious effects of PABA irradiation were recognized, its use as a sunscreen was discontinued. Firstly, it was found to photodegrade, when irradiated with Pyrex-filtered UV lamps, forming free radical intermediates (Chignell *et al.* [1980], Gasparro [1985] and Shaw *et al.* [1992]). In addition, Sutherland [1982] demonstrated that PABA has the potential to penetrate human cells, where it has the potential to increase the formation of thymine dimers in cellular DNA. The triplet state energy of PABA was calculated to be 311.2 kJ mol^{-1} (Osgood *et al.* [1982]), similar to that of the thymine base, thereby making energy transfer possible. This finding was supported by various researchers including Aliwell [1991] who showed the *in vitro* PABA-photosensitized formation of thymine dimers in pUC19 plasmid DNA. In addition, studies conducted by Gasparro & Battista [1987] and Shaw *et al.* [1992] suggested that PABA reacts directly with the DNA bases by forming photoadducts. Also, studies conducted by Allen *et al.* [1996] suggested that PABA is a good triplet sensitizer converting harmless triplet ground state oxygen (O_2) into singlet oxygen ($^1O_2$), which is known to be cytotoxic.

2. Esters of PABA

Due to the harmful effects of PABA, it has subsequently been replaced in sunscreens by its esters. These are Padimate-O (or octyl dimethyl PABA) and Padimate-A (or amyl dimethyl PABA). Although these esters are presently used in sunscreen formulations, some adverse effects have been reported. These include photofragmentation of Padimate-O (Roscher *et al.* [1994]), as well as the generation of reactive free radicals such as $^1O_2$ (Allen *et al.* [1995]) and $^{\bullet}OH$ (Knowland *et al.* [1993]), in illuminated solutions containing Padimate-O. Although padimate-O does not generate the thymine dimer, these free radicals have been shown to break DNA strands and inflict other damage to the base pairs (Knowland *et al.* [1993]). Padimate-O has also been shown by Kenny *et al.* [1995] to be absorbed through the skin where it is 32-36% metabolized. In addition, this sunscreen has also been negatively received by the sunscreen market since it has been shown to cause photoallergic and other skin related problems and was

therefore withdrawn in the late 1980's (Serpone *et al.* [2002]). In most countries, the sunscreen products available nowadays are PABA-free and have been replaced with cinnamates and salicylates as the UVB absorbers.

3. Cinnamates

Presently the most widely used UVB sunscreen in the world belongs to the cinnamate class of UV absorbers. This is 2-ethylhexyl-*para*-methoxycinnamate (EHMC). However, the cinnamate absorbers are subject to *trans-cis* photoisomerization across the ethylenic double bond (Morliere *et al.* [1982]). The *cis*-isomer is a less efficient UV absorber, therefore this type of isomerization results in a loss in the absorbing ability of these sunscreens. *Trans*-EHMC not only isomerizes to the *cis*-isomer but Broadbent *et al.* [1996] have demonstrated that it also dimerizes with itself by means of a (2+2) cycloaddition reaction across the ethylenic double bond, which also contributes to a loss in absorbing ability. In addition, although EHMC does not photosensitize the formation of thymine dimers since its triplet state energy is lower than that of thymine (Broadbent *et al.* [1996]), it has been shown to interact with DNA by photobinding to the bases (Kowlaser [1998]), which is potentially carcinogenic.

4. Butyl methoxy dibenzoylmethane

Butyl methoxy dibenzoylmethane, commonly known as avobenzone, is a frequently used UVA sunscreen. However, avobenzone not only photodegrades when illuminated in a non-polar solvent (Roscher *et al.* [1994]) but also produces carbon-centered free radicals that induce direct strand breaks on DNA on illumination *in vitro* (Damiani *et al.* [1999]). Photodecomposition of avobenzone into complex mixtures has also been demonstrated by Schwack & Rudolph [1995]. Today, avobenzone is often used in combination with EHMC to offer broad-spectrum protection, *i.e.* to cover both the UVA and UVB regions. However, it has been shown that using avobenzone in combination with EHMC in sunscreen formulations causes EHMC to photodegrade (Sayre & Dowdy [1999]). In addition, recent studies conducted by Panday [2002] have demonstrated that avobenzone photosensitises the photoisomerisation of EHMC in a non-polar medium.

5. Benzophenones

There is currently a wide range of benzophenone-based sunscreens on the market. Some of the benzophenone absorbers used are benzophenone-1, benzophenone-3, benzophenone-4 and 2,2'-dihydroxy-4-methoxybenzophenone (or benzophenone-8). However, benzophenone, the parent

compound to these UV absorbers, has been shown to be a potent photosensitizer of thymine dimers *in vitro* (Greenstock & Johns [1968] and Charlier & Hélène [1972]). In addition, the *in vitro* studies conducted by Bolton [1991] suggest that Uvinul DS49 and Eusolex 232, both UV absorbers having benzophenone-derived structures, also photosensitise thymine dimer formation. DNA damage by the latter sunscreen agent has also been confirmed by studies by Inbaraj *et al.* [2001]. This team demonstrated that free radical and oxygen species were involved in the photodamage of DNA by Eusolex 232. In addition, Eusolex 232, an approved FDA sunscreen agent has been shown to degrade by 90% in water, after only 10 minutes of irradiation at wavelengths greater than 290 nm and by 50% after 20 minutes of irradiation in acetonitrile (Serpone *et al.* [2002]).

Benzophenone-3, one of the more commonly used of the benzophenone class of sunscreens, has been shown to cause both contact and photocontact allergies (Bilsland & Ferguson [1993], Schmidt *et al.* [1998] and Berne & Ros [1998]). According to Darvay *et al.* [2001] and Trevisi *et al.* [1994], benzophenone-3 is the most common UV filter photoallergen. Studies conducted by Serpone *et al.* [2002] have shown benzophenone-3 to be photochemically unstable when irradiated in either a non-polar or a polar solvent at wavelengths greater than 290 nm. It degraded by 15% in acetonitrile, by 20% in water and by 90% in methanol. In addition, this team also demonstrated the significant photodegradation of benzophenone-3 in the presence of the physical absorber titanium dioxide. There is now evidence that benzophenone-3 is absorbed systemically following topical application to the skin. Studies conducted by Jiang *et al.* [1999] have shown that this UV absorber is absorbed by the skin in significant amounts (10% of applied dose) to warrant further investigation of its continued application in sunscreens. In addition, Schallreuter *et al.* [1996] reported that the oxidation of benzophenone-3 after topical skin application caused it to photofragment into benzophenone-3 semiquinone thus changing its properties. Benzophenone-3 has been shown to not only penetrate the skin but its metabolites have also been detected in urine after topical application (Felix *et al.* [1998] and Hayden *et al.* [1997]). However, Agin *et al.* [1998] reported that the amount of benzophenone-3 Hayden and his team detected was too small to be deemed harmful. Reports of the photochemistry of the other benzophenone sunscreens are less numerous and therefore this topic warrants investigation, and will be considered in this study.

1.5 Photosensitive benzophenone-derived drugs

Of concern to the sunscreen industry is the recent discovery that a group of 'non-steroidal anti-inflammatory drugs' (NSAIDs) having a benzophenone or a benzophenone-like chromophore

induce DNA photosensitization *in vitro*. NSAIDs are widely used in the treatment of rheumatic and arthritic diseases and include compounds such as ketoprofen, tiaprofenic acid and suprofen. The structures of these drugs appear in Figure 1.10. Included in this group of benzophenone-derived photosensitive drugs is fenofibrate, an anti-hyperlipoproteinemic drug, which at present is the most commonly used lipid-lowering agent in the world. A number of studies conducted by various researchers regarding phototoxicity and DNA photosensitization induced by these drugs appear in the literature.

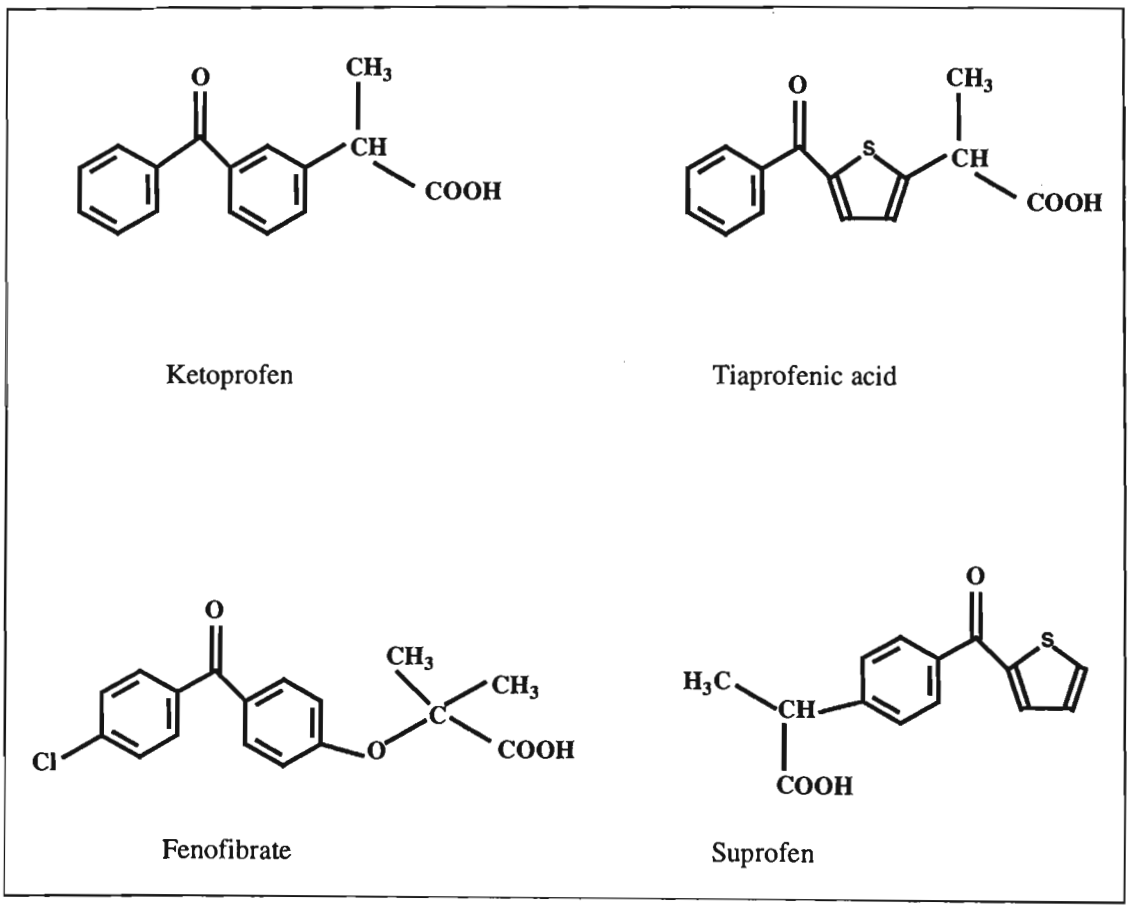

Figure 1.10: Chemical structures of the benzophenone-derived NSAIDs.

The NSAIDs have being shown to photosensitise chemical modifications to key biomolecules. These include lipid peroxidation, protein oxidation, protein cross-linking and DNA damage (Boscá & Miranda [2001], Lhiaubet *et al.* [2001], Marguery *et al.* [1998], Condorelli *et al.* [1995] and Boscá & Miranda [1998]). The DNA damage includes strand breaks, oxidation of bases as well as thymine dimerization (Artuso *et al.* [1991], Boscá & Miranda [2001] and Castrell *et al.* [1994]). Photoallergic, phototoxic and photosensitive reactions were also

reported with all the above benzophenone-derived drugs (Boscá & Miranda [1998]). Ketoprofen, the most widely used NSAID, has been shown to efficiently produce single strand breaks in supercoiled DNA as well as promote photodimerization of pyrimidine dimers (Boscà & Miranda [2001]). In addition, irradiation of ketoprofen in neutral aqueous media produced a number of benzophenone-containing photoproducts, which not only contributed to the photoallergic reactions and the phototoxicity of this drug, but also photosensitized linoleic acid peroxidation *in vitro* (Boscá *et al.* [1994]). Studies conducted by various researchers attribute the photosensitivity reactions of this group of drugs to the benzophenone chromophore.

Benzophenone is one of the most powerful and most potent radical generators known to man (Larsen [1994]). The powerful photoreactivity of the benzophenone chromophore is of concern to the sunscreen industry since benzophenone-derived absorbers are commonly incorporated in sunscreen formulations. Surprisingly few reports on the photochemistry of the benzophenone UV absorbers appear in the literature and therefore there is an urgent need to investigate the photoreactivities of these compounds.

1.6 Rationale and outline of this study

This work investigates the photochemistry of a group of benzophenone-derived sunscreens. These are benzophenone-1, benzophenone-3, benzophenone-4, Uvinul DS49 and Eusolex 232. The structures of these compounds appear in Figure 1.11.

Since these sunscreens all have the benzophenone chromophore with various substituents on the backbone, it is highly probable that they may behave in a similar manner to benzophenone. Therefore an investigation of their photochemistry is very important, in order to determine if their use in sunscreens can be considered "safe".

The benzophenone-based sunscreens have gained popularity in the sunscreen industry since they have the advantage of absorbing over a wider range of the UV spectrum than most other sunscreens. Therefore, they can be used alone or in combination with other sunscreens for maximum protection. According to the United States FDA's final monograph [2000] of approved sunscreen active ingredients, benzophenone-4, benzophenone-3 and Eusolex 232 make up three of the 14 chemical sunscreens substances permitted in the United States. In 1996, the former two were ranked as the second and third most frequently used UV absorbers in sunscreens, respectively, by the FDA (Steinberg [1996]). Eusolex 232 is widely used as a UVB filter in sunscreen formulations and cosmetic products such as moisturizers (Levy [2002],

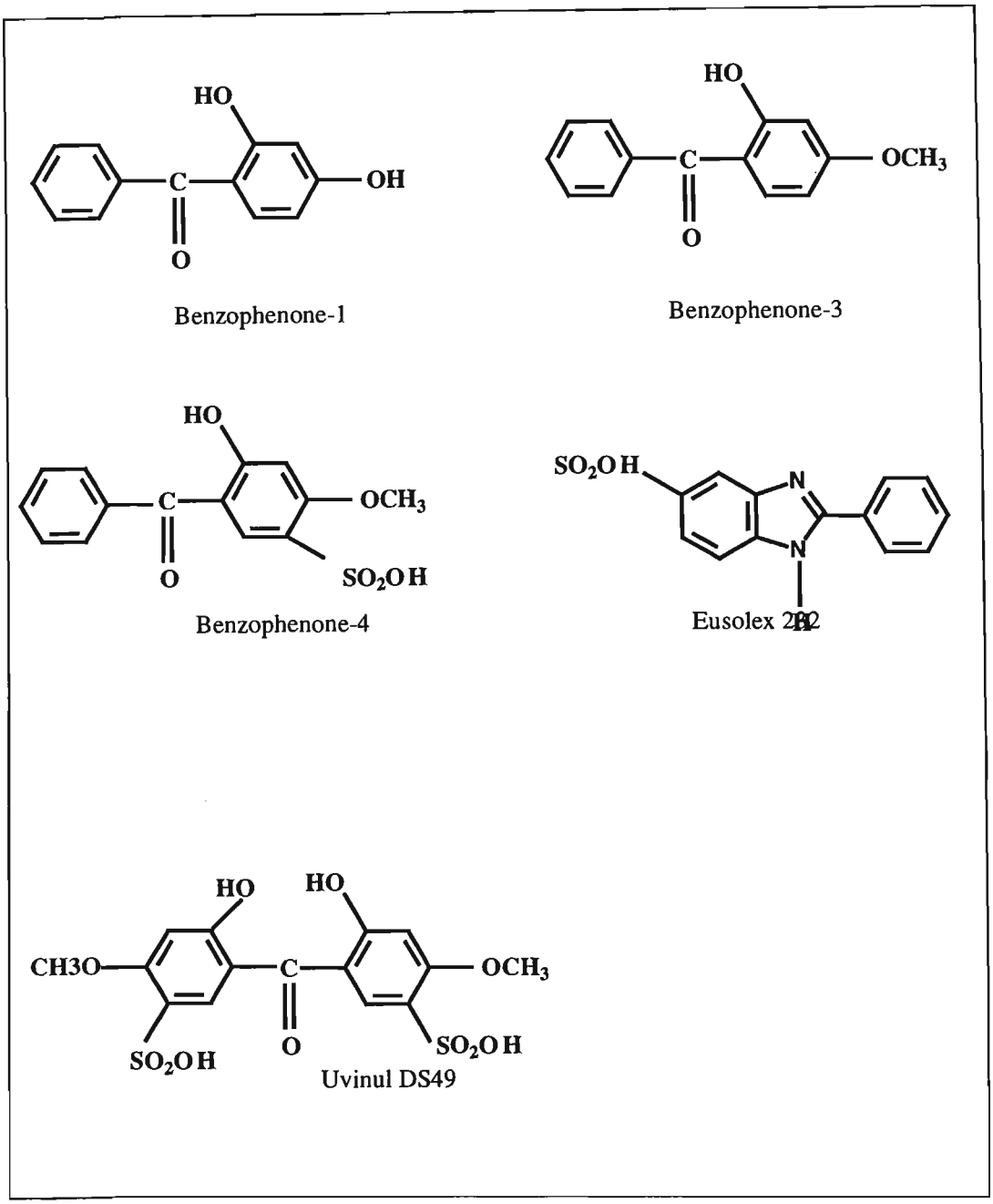

Figure 1.11: Chemical structures of the sunscreens under investigation in this study.

Stevenson & Davies [1999]). The other sunscreen absorbers being investigated have also found widespread use in sun protection. Benzophenone-1 is commonly used as a UV protector for nail lacquers and other cosmetics, in most countries. This sunscreen absorber, however, is only approved for use in protection of certain products from UV damage (http://216.239.39.120/translate_c?hl=en&ie=UTF-8&oe=UTF-8&u=http://www. abacovital.

com /fichastecnicas/filtros/benzofenone1.htm, Date accessed: 4 December 2002). Uvinul DS49, which often exists as the disodium salt in sunscreen agents, commonly referred to as benzophenone-9 or 2,2'-dihydroxy-4,4'-dimethoxy benzophenone-5,5-disodium sulfonate, is also only approved for product protection. (http://216.239.39.120/translate_c?hl=en&ie=UTF-8&oe=UTF-8&u=http ://www .abacovital .com/ fichastecnicas/filtros/benzofenone9.htm, Date accessed: 4 December 2002). The maximum allowed concentrations of these benzophenone-derived sunscreen agents in commercial products as drawn up by the various regulatory authorities is given in Table 1.1.

Of these UV absorbers, the photochemistry of benzophenone-3 has most often been considered in literature. Despite the controversy surrounding its use in sunscreen formulations, some of which has been discussed in Section 1.4.2, benzophenone-3 is still currently one of the most popular UV absorbers on the market. It is a cream coloured powder that has many of the favorable properties of a sunscreen, that is, it is insoluble in water, melts at a high temperature (66 °C) and has a low volatility. In addition, various studies have demonstrated the benefits of using it in a sunscreen. Some of these are outlined below.

The *in vivo* studies conducted by O' Kereke *et al.* [1995] and Robinson *et al.* [1994] suggest that benzophenone-3 does not induce genotoxic effects in Sprague-Dawley rats. The triplet state energy of benzophenone-3 as determined by Gozenbach *et al.* [1992] is 276.14 kJ mol^{-1}. This is much lower than the triplet state energy of thymine (314.8 kJ mol^{-1}) (Lamola *et al.* [1967]), thereby suggesting that thymine dimer photosensitization with this sunscreen is not possible. This was confirmed by studies conducted by Wolf *et al.* [1994], who demonstrated that skin treated with sunscreen formulations containing benzophenone-3 formed less thymine dimers compared to unprotected mouse skin. In addition, an *in vitro* study conducted by Sewlall [1999] suggests that irradiation of thymine in the presence of benzophenone-3 does not induce thymine dimerization. There is also evidence that irradiation of benzophenone-3 does not promote photosensitization of singlet oxygen, nor any other reactive oxidant species such as $OH^{\bullet}$ or the peroxy radicals (Allen *et al.* [1995]). However, although studies performed by Roscher *et al.* [1994] demonstrated that a solution of benzophenone-3 in a non-polar solvent irradiated for a period of 100 hours did not photodegrade, Serpone *et al.* [2002] appeared to prove otherwise (as mentioned previously). There is therefore a need to re-examine its photostability.

Table 1.1: Maximum allowed concentrations (%) of the benzophenone-based sunscreens in commercial sunscreens*.

Concentration allowed / %	USA	EUROPE	BRAZIL	JAPAN	AUSTRALIA	SOUTH AFRICA
Benzophenone					Approved	
Benzophenone-3	6	10	10	5	Approved	10
Benzophenone-4	10	5	10	Approved		
Benzophenone-1	Product protection	Product protection	3	Product protection		
Eusolex 232	4	8	8	Not approved	Approved	8
Uvinul DS49	Product protection	Product protection		Not approved		

*(Strange [1995], FDA final monograph [2000], & http://216.239.39.120/translate_c?hl=en&ie=UTF-8&oe=UTF-8&u=http ://www. abacovital .com/ fichastecnicas/filtros/filtros.htm&prev, Date accessed: 4 December 2002)

[The shading indicates that the sunscreen agent is currently under review (www.health.gov.au/tga/docs/pdf/sunscrai.pdf, Date accessed: 6 December 2002). A blank cell implies that the use of this sunscreen ingredient in a particular country has not been mentioned in literature.]

Due to the vast, often contradictory, literature available on the benzophenone sunscreens, in particular benzophenone-3, it is necessary to further investigate the photochemistry of this group of sunscreens. The aim of this study was to investigate the potential of the benzophenone-derived sunscreens, namely, benzophenone-1, benzophenone-3, benzophenone-4, Uvinul DS49 and Eusolex 232 to photosensitize the conversion of double stranded supercoiled DNA to the relaxed circular and linear forms. This investigation also included the parent compound, benzophenone, to provide a benchmark, since it has been examined

extensively in photochemical studies, as well as the UV-absorbing compound ketoprofen, since it is a well-known DNA photocleaver.

Briefly, buffered aqueous solutions of the sunscreens were irradiated in the presence of DNA at wavelengths greater than 300 nm. The DNA photocleavage potential of these UV absorbers was investigated by the technique of gel electrophoresis, while fluorescence spectroscopy enabled the DNA binding ability of these compounds to be determined. ϕX174 phage DNA and calf thymus DNA were used for the gel electrophoresis and the fluorescence spectroscopy experiments respectively. This study also included an investigation of the photostability of these UV absorbers. A pH of 7-8 was maintained throughout all the experiments conducted to replicate physiological conditions. Computational studies were also conducted to determine the lowest energy geometrical structures of the benzophenone-based sunscreen agents with the aim of determining if intercalation of these compounds with DNA was possible. Finally, the mechanisms of interaction of these sunscreens with DNA have been postulated.

Chapter 2 deals with the experimental techniques and procedures performed in this investigation, while Chapter 3 contains a discussion of the experimental results. This is followed by concluding remarks in Chapter 4.

Chapter 2

EXPERIMENTAL

The experimental techniques and procedures that will be discussed in this chapter are divided into four sections. These are:

- The irradiation techniques employed in this work in Section 2.1,
- UV absorption spectroscopy and the photostability investigation of the UV absorbers in Section 2.2,
- Agarose gel electrophoresis techniques and procedures to detect DNA cleavage in Section 2.3,
- Fluorescence spectroscopy to detect DNA damage induced by the UV absorbers in Section 2.4, and
- Computational studies using the semi-empirical and *ab initio* method to determine the geometrical structures of the UV absorbers in Section 2.5.

The materials and equipment used for the various experimental procedures are listed in Appendix A.

2.1 UV irradiation techniques and equipment

This investigation required the use of a light source of high intensity in both the UVB (280 - 320 nm) and the UVA (320 – 400 nm) wavelength ranges. This is the region in which the UV absorbers being investigated absorb UV radiation. For this investigation the source of UV light chosen was the Osram HBO 500W/2 high pressure mercury lamp. The lamp's suitability to this study will be discussed in Section 2.1.1. Section 2.1.2 describes the irradiation techniques used for this investigation while Section 2.1.3 discusses the irradiation cells used for the various experiments conducted.

2.1.1 Light source for the photosensitized irradiation of DNA

The Osram HBO 500 W/2 high pressure mercury lamp (shown in Figure 2.1) was the lamp of choice since it provided high luminance, strong ultraviolet radiation in the UVB and UVA regions, good light efficacy and high lamp stability. This lamp has also proven to be very successful for DNA photosensitization studies conducted by previous workers in this field (Thomas [1989], Bolton [1991] and Clemmett [1992]).

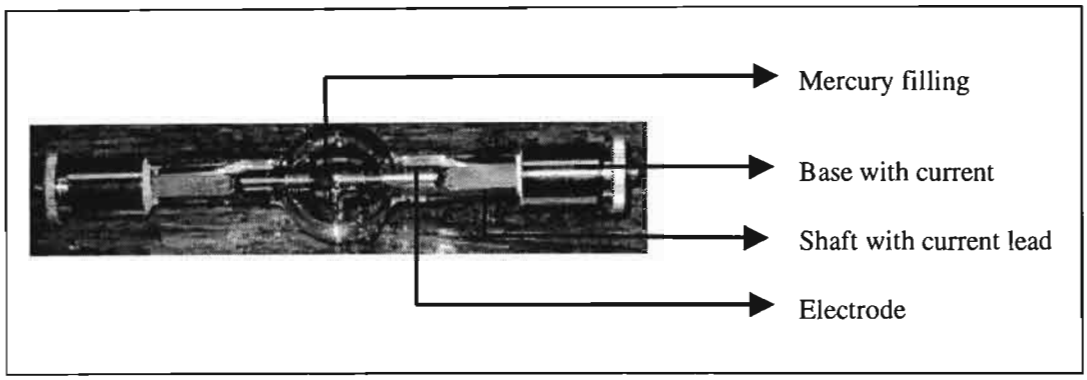

Figure 2.1: Top view of the Osram HBO 500 W/2 high pressure mercury lamp.

The radiation emitted from the HBO lamp consists of extensive pressure-broadened mercury spectral lines in the wide wavelength range of 260 nm to 700 nm (Figure 2.2). Therefore, isolation of the wavelengths of interest from this source would require the use of an appropriate filter. The filter used in this study was a 10 mm thick Pyrex filter. This filter has a short wavelength cutoff of about 300 nm and therefore only allows wavelengths greater then 300 nm to impinge on the irradiation cell (Figure 2.3). This enabled the wavelength of light emitted by the lamp when used in conjunction with the filter to be similar to that of sunlight incident on the earth's surface. The use of this filter minimized direct irradiation of DNA by UV light and allowed photosensitized DNA studies to be carried out.

2.1.2 Irradiation techniques

The Osram HBO 500W/2 high pressure mercury lamp used in this study is housed in an insulated steel box, which is connected to an external bracket, a Schreiber power pack, and an igniter (as shown in Figure 2.4 A).

The lamp housing is necessary due to the danger of UV radiation, glare and overpressure caused by the lamp during operation. The lamp is fixed vertically in front of a circular opening, which

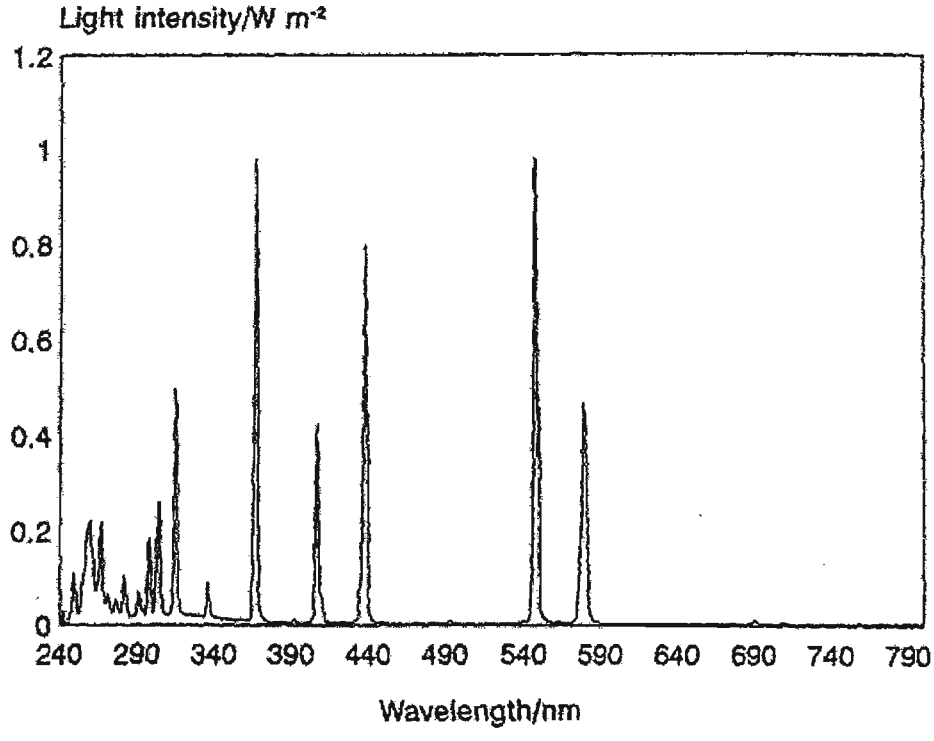

Figure 2.2: Output of the HBO 500W/2 high pressure mercury lamp (Broadbent [1994]).

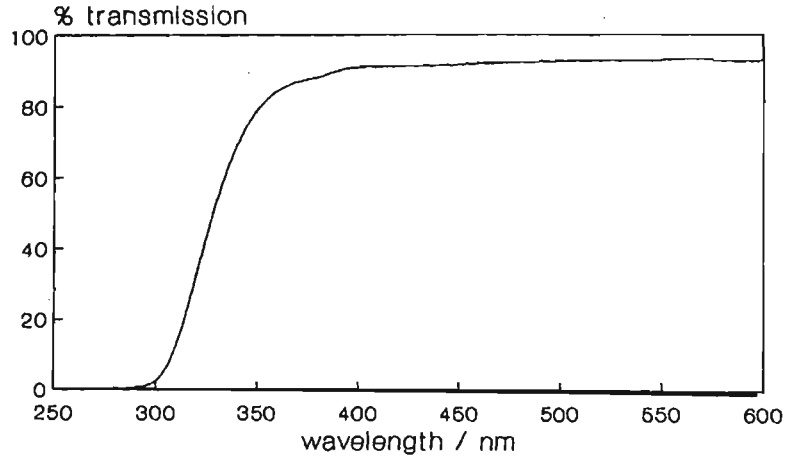

Figure 2.3 Transmission characteristics of the 10 mm thick Pyrex filter used for all irradiations carried out in this investigation (Broadbent [1994]).

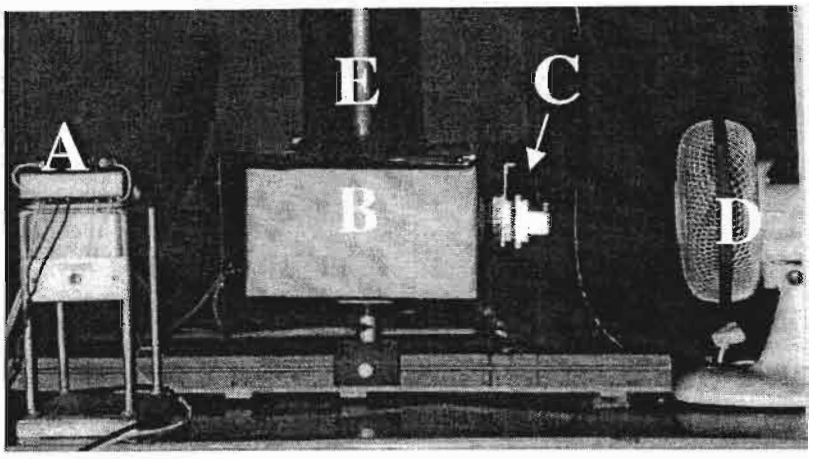

A: Front view of the ignitor (A) attached to lamp housing (B) and an external bracket (C). The cooling and extractor fans are represented by D and E respectively.

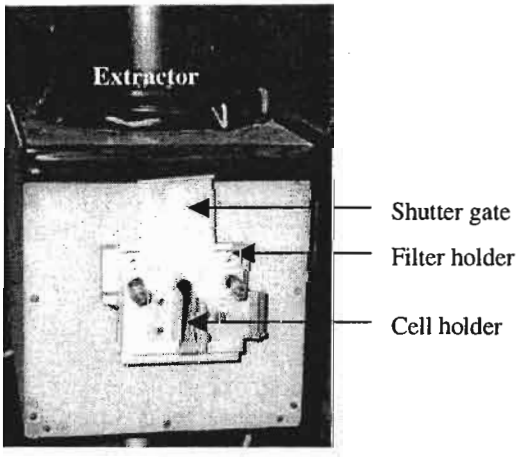

B: Side view of the external bracket attached to the lamp housing.

Figure 2.4: Lamp housing (A) and optical train (B) for the Osram HBO 500 W/2 high pressure mercury lamp.

enables the radiation to reach the irradiation cell. The irradiation cell is held in position by means of an external bracket, which is attached to the lamp housing (Figure 2.4B). The external bracket consists of a shutter gate, filter holder and cell holder. The shutter gate controls the light intensity impinging on the irradiation cell while the filter and cell holders hold the filter and the irradiation cell (or cuvette) respectively in place during irradiations. A cooling fan is also positioned directly behind the external bracket to cool the filter and the irradiated solution. The lamp housing is also fitted with an extractor fan, leading to the exterior of the building, to provide ventilation as well as to remove any ozone produced by the photolysis of oxygen.

The lifetime of the lamp is usually in the region of 400 hours (as recommended by the manufacturer). The lamp output does not vary significantly over the 400 hours. However, after this time, the intensity decreases dramatically and it is necessary to replace the lamp.

Before any irradiations were conducted, the lamp was allowed at least 15 minutes to warm up. This was necessary to reach thermal equilibrium. A Blak-Ray J-221 Longwave Photovoltaic UV intensity meter was used to measure the lamp output. Due to the low sensitivity of the meter, these measurements were only used to monitor the intensity of the lamp during the course of the experiments and to ensure that the intensity was stable.

2.1.3 Irradiation cells used for the various experiments

When choosing an irradiation cell (cuvette) to hold the sample for irradiation, it was important to ensure that the cell allowed radiation in the spectral region of interest to pass to the sample. Generally, for work in the UV region of the spectrum, quartz cuvettes are used (Skoog, West & Holler [1996]). For this investigation both 1 cm and 1 mm pathlength quartz cells were used. For the gel electrophoresis experiments, however, a different cell from the conventional type was needed. The experiments conducted required the use of a series of 5 mm internal diameter glass tubes due to the small sample volumes (5μl) to be irradiated. These tubes were preferred to the 1 mm pathlength cuvette since they enabled easy removal of the samples after irradiation. Each irradiation had to be performed separately in an individual tube. For this purpose Nuclear Magnetic Resonance (NMR) tubes were used since they were easily available, and did not absorb UV radiation in the region of interest.

The UV absorption spectrum for a typical NMR tube used as the irradiation cell for the electrophoresis experiments is shown in Figure 2.5. This spectrum was obtained by use of a Cary 1E UV-Visible spectrophotometer (details in Section 2.2.2). The tube had to be cut down

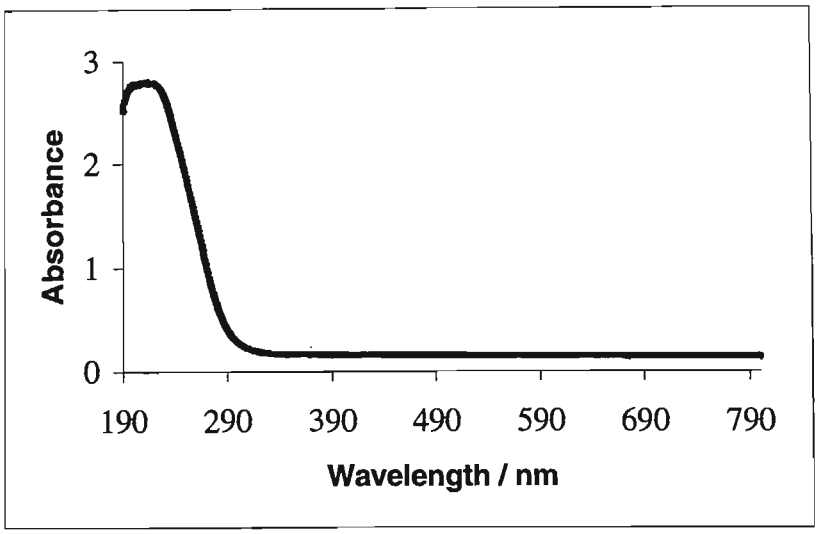

Figure 2.5: Absorption spectrum of the irradiation cell used for the electrophoresis experiments.

to size to fit into the sample holder. The instrument was zeroed against air, and when the measurement was taken the empty NMR tube was placed in the sample holder and was held in place with adhesive tape. From the spectrum it can be seen that the NMR tube absorbs short wavelength UV radiation up to about 300 nm and does not absorb in the longer UVB or UVA region, which is the region of interest for this study. Hence these tubes were suitable for use in this investigation. The tubes were cut down to about 4 cm in length so that they could fit in the cell holder and were fixed in place with adhesive tape during irradiation.

2.2 UV absorption spectroscopy

The benzophenone-derived compounds are widely used in sunscreen formulations because of their ability to absorb in the UV region of the terrestrial solar spectrum. Absorption spectroscopy was the analytical method employed to determine the nature of this absorption and, in particular, to investigate the photostability of the absorbers.

2.2.1 An introduction to absorption spectroscopy

Every molecule possesses a unique series of closely spaced energy levels, the lowest of which is known as the ground state. When a photon of radiation passes near a molecule with energy equal to the energy difference between the ground state and a higher electronic state, the energy

of the photon is transferred to the molecule. This results in an energy transfer from the ground state to the higher excited energy state (Skoog, West & Holler [1996]). This transition is known as absorption and can be depicted by Equation 2.1 as follows:

$$M + h\nu \longrightarrow M^{*} \qquad (2.1)$$

whereby a species M is converted to its excited state M^{*} by the absorption of a photon hν.

These transitions are responsible for the UV-visible absorption spectra observed for molecules. This process of absorption occurs in a brief period (10^{-6} – 10^{-9} seconds) and is specific to a characteristic structure (Skoog, West & Holler [1996]).

2.2.2 Instrumentation for absorption spectroscopy

The basic spectrophotometer consists of five main components. These are an energy source, a monochromator, a sample cell (and reference cell), a detector and a readout device (Figure 2.6).

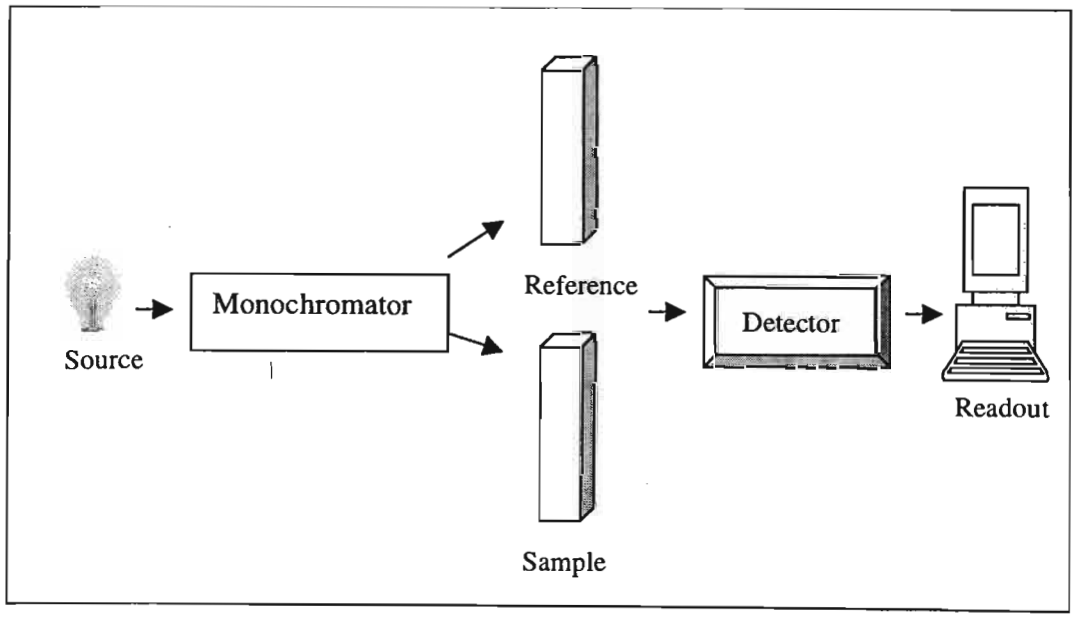

Figure 2.6: Schematic diagram of the optical components of a typical absorption spectrometer.

Radiation from the source first passes to the monochromator, which consists of gratings or prisms that permits isolation of a specific wavelength region. The monochromatic beam is then split into two, one passing through the absorbing sample, while the other passes through a reference cell. The reference cell contains the blank, which is essentially the solvent that has no analyte element. The detector alternatively samples the two beams and their ratio, as shown in Equation 2.2, which is determined electronically and displayed on a screen by the readout device.

$$A = \log \frac{P_{solvent}}{P_{solution}} = \log \frac{P_o}{P} \qquad (2.2)$$

where A is absorbance while p_o and p refer to the power of radiation after it has passed through cells containing the solvent (reference cell) and the analyte (sample cell) respectively. Essentially this is the difference between two signals.

Commercial spectrophotometers are available either as single-beam or double-beam instruments. A single-beam instrument normally allows monitoring of the sample at a single wavelength only, whereas with the latter, instrument absorbance is monitored as a function of wavelength (Skoog, West & Holler [1996]). However, with the single-beam spectrometer, measurements must be corrected for fluctuations in the light source, spectrometer efficiency, as well as variations in the sensitivity of the detector with wavelength (Lumb [1978]). Using a double or split-beam instrument eliminates the necessity of such corrections and therefore most commercial spectrometers used for analytical work today are dual beam. In this study the double-beam Cary 1E UV-Visible spectrophotometer was used.

2.2.3 Analysis of the photostability of the benzophenone-based sunscreens

Since UV absorbers are widely used in sunscreen formulations to protect the skin from the harmful rays of the sun, they are required to be stable towards photodecomposition in simulated sunlight in order to afford the desired protection to the consumer. The stability of the benzophenone-based sunscreens to UV radiation was assessed by UV spectroscopy. Samples of benzophenone, ketoprofen, benzophenone-1, benzophenone-3, benzophenone-4, Eusolex 232 and Uvinul DS49, as obtained from their suppliers, were analysed.

To dissolve the sunscreen absorbers, a solvent that reciprocated physiologically relevant conditions (pH 7 - 8) was desired. For this purpose a variety of buffers could have been used, with Tris-HCl buffer and phosphate buffered saline (PBS) being the most common. The Tris-HCl buffer, which is the acronym for *Tris*-(hydroxymethyl)-methylammonium chloride, was chosen due to its success as a physiological buffer. This buffer does not precipitate calcium salts as the phosphate buffer does, and is also stable in solution at room temperature for longer periods than the phosphate buffer.

Stock solutions of 1×10^{-3} M of all the UV absorbers were prepared in Tris-HCl buffer, except for benzophenone-3. Due to the very low solubility of benzophenone-3 in this buffer, a solution of 50% (v/v) ethanol / Tris-HCl buffer mixture was used as the solvent.

Tris-HCl was unavailable in the laboratory during the time of this investigation, therefore *Tris*-(hydroxymethyl)-aminomethane (or Tris) and hydrochloric acid (HCl) were used to obtain the desired pH. This buffer was comprised of 0.1 M Tris, 0.1 M NaCl and a volume of HCl to give a pH of 8. This involved dissolving 12.140 g of Tris and 5.844 g of NaCl in Millipore water , which was made up to one litre in a volumetric flask. When reference is made to Millipore water in this dissertation it refers to water that has been passed through a Millipore Milli-Q apparatus, which consists of ion exchange and organic removal resins. More details of the Tris-HCl buffer appear in Section 2.4.5. The pH of the buffer was measured with a Mettler 740 pH meter that had been calibrated with two buffers of pH 4.0 and 7.0. The pH of the Tris-HCl buffer was adjusted to 8 with 20 ml of 33% HCl. The buffer was filtered through a Millipore HV 0.45 µm filter, to remove particulates, after which it was autoclaved at 250 °F and 15 psi for 30 minutes.

Each sunscreen sample was irradiated at 5 minute intervals for a total irradiation period of 30 minutes with the Osram HBO 500W/2 high pressure mercury lamp coupled to the 10 mm thick Pyrex filter. A 1 mm pathlength quartz cuvette was used during the irradiations. After each irradiation an absorbance spectrum was recorded with the Cary 1E UV-Visible spectrophotometer using the same 1 mm pathlength cuvette. As a matched pair of cuvettes was not available, a baseline correction using a blank sample was performed before the UV measurements of the samples were taken. This was achieved by placing Tris-HCl buffer or the 50% (v/v) ethanol/ Tris-HCl buffer (in the case of benzophenone-3) in the sample cell and recording the spectrum over the wavelength region of interest. This blank spectrum was then electronically subtracted from that of the sample spectrum. The absorbance of the sample solution of interest was then measured from 190 nm to 400 nm at a scan rate of 600 nm min^{-1}.

The UV spectra obtained at this concentration did not conform to the Beer-Lambert law (shown by Equation 2.3 below), since for all the solutions the absorbance readings were greater than 1.5 absorbance units.

$$A = \varepsilon bc \tag{2.3}$$

where A is the absorbance of the analyte of interest, ε is the molar absorption coefficient of the analyte in $dm^3\ mol^{-1}\ cm^{-1}$, b is the pathlength of the cuvette in cm and c is the concentration of the analyte in mol dm^{-3}.

From Equation 2.3, it can be deduced that the absorbance of an analyte in solution is directly proportional to the concentration of that solution. However, deviations from Beer's law occur at high concentrations since the analyte molecules are packed so closely together that the charge distribution is distorted by neighboring molecules, resulting in changes in the absorption properties of the molecules (Atkins [1994]). All the samples were therefore serially diluted until absorbance readings below 1 (or just below 1.5) were obtained. This required concentrations of about 5.5 x 10^{-4} M. The resultant UV spectra of all the compounds under investigation are shown and discussed in Section 3.1.

2.3 Gel electrophoresis of DNA

The aim of this series of experiments was to investigate if the benzophenone-derived UV absorbers had the ability to cleave DNA *in vitro*. The DNA used in this series of experiments was supercoiled ϕX174 phage DNA obtained from Sigma. ϕX174 phage DNA was used for these experiments as opposed to calf thymus DNA (that was used for the fluorescence spectroscopy experiments) since it contains only a few genes and hence can be seen easily as a clear band on a gel.

In this section the technique of gel electrophoresis (Section 2.3.1), the gel electrophoresis apparatus used (Section 2.3.2) as well as the optimal electrophoresis conditions to ensure the efficiency of this procedure (Section 2.3.3) will be discussed. Solution preparations (Sections 2.3.4 – 2.3.5) as well as the gel electrophoresis nicking procedure to detect DNA cleavage (Sections 2.3.6 - 2.3.7) are also described. Finally Sections 2.3.8 - 2.3.10 describe the running, viewing and photography of the gels followed by quantification of the DNA bands.

2.3.1 The technique of gel electrophoresis

In gel electrophoresis the movement of small ions and charged macromolecules across a gel, under the influence of an electric field, is studied. Electrophoresis through agarose or polyacrylamide gels is the standard method used to separate and identify DNA fragments. This technique is simple, easy to perform and is capable of resolving mixtures of DNA fragments that cannot be separated adequately by other procedures. Agarose gels can be used to analyse double- and single-stranded DNA fragments from 70 base pairs (bp) to 800 000 bp, while polyacrylamide gels are used for smaller DNA fragments of between 6 bp and 1000 bp (Sedley P.G. & Southern E.M. [1982]). Since the ϕX174 phage DNA used in this study contained 5 386 bp as specified by the supplier (Sigma), agarose gel was used as the medium of separation for this investigation.

Agarose, which is extracted from seaweed, is a linear polymer. Agarose gels are cast by dissolving the required percentage of agarose in a heated solution of the desired buffer until a clear solution is achieved. The solution is then poured into a mold and allowed to harden, thus forming a matrix. The DNA to be separated is placed in sample wells made with a comb and a voltage is applied across the gel until separation is achieved. The DNA, which is negatively charged at neutral pH, migrates towards the anode. The rate of migration depends on a number of parameters such as the molecular size of the DNA, agarose concentration, conformation of the DNA, applied current and the composition of the electrophoresis buffer. Some of these factors will be discussed in more detail in Sections 2.3.3 and 2.3.4.

Agarose gel electrophoresis can be used as an efficient technique to detect DNA cleavage, since cleavage of supercoiled circular DNA produces different DNA forms which migrate through gels at different rates (Thorne [1996]). The ϕX174 phage DNA molecule is a single-stranded superhelix, which can exist in three distinct forms. These are the superhelical circular DNA (Form I), open circular DNA (Form II) and linear DNA (Form III) as illustrated in Figure 2.7.

Supercoiled (Form I) DNA has no breaks. Only one single strand break (SSB) per molecule is sufficient to convert DNA from Form I (supercoiled) to Form II (open circular) (Armitage [1998]). As Form II molecules sustain numerous SSB, it is increasingly likely that two SSB on opposite strands will be sufficiently close that intervening base pairs denature and hence produce Form III (linear) DNA. The bacteriophage ϕX174 DNA used in this series of experiments is a naturally occurring DNA molecule with a very small genome consisting of closed circular single stranded DNA.

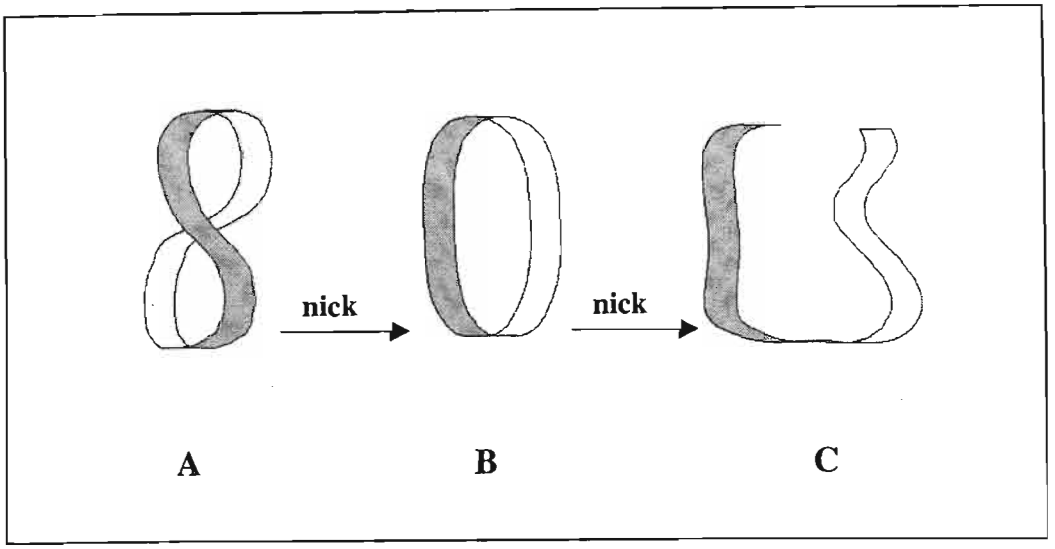

Figure 2.7: Schematic diagram showing the three DNA Forms, where A represents supercoiled Form I DNA, while B and C represent open circular Form II DNA and linear Form III DNA respectively.

The small compact Form I usually migrates the furthest, since it experiences the least resistance in an agarose gel. This is usually followed by the rodlike, linear Form III DNA molecules. The open circular Form II DNA molecules usually migrate the slowest (Boyer [1993]). Under some conditions, however, the migration rates may be different and Form II DNA may migrate faster than Form III DNA (Sambrook *et al.* [1989]).

The relative motilities of the three DNA forms depend primarily on the concentration of the agarose. They are also influenced by other factors such as the strength of the applied current, the ionic strength of the buffer and the density of the superhelical twists in Form I DNA. Since the three DNA forms migrate at different rates in different systems, it is important to run standards, which can be used to identify each of these forms.

2.3.2 The agarose gel electrophoresis apparatus

The apparatus used for agarose gel electrophoresis was a horizontal slab gel electrophoresis apparatus. The apparatus consisted of three main parts. These are: a casting tray, an electrophoresis tank and a power supply as shown in Figure 2.8.

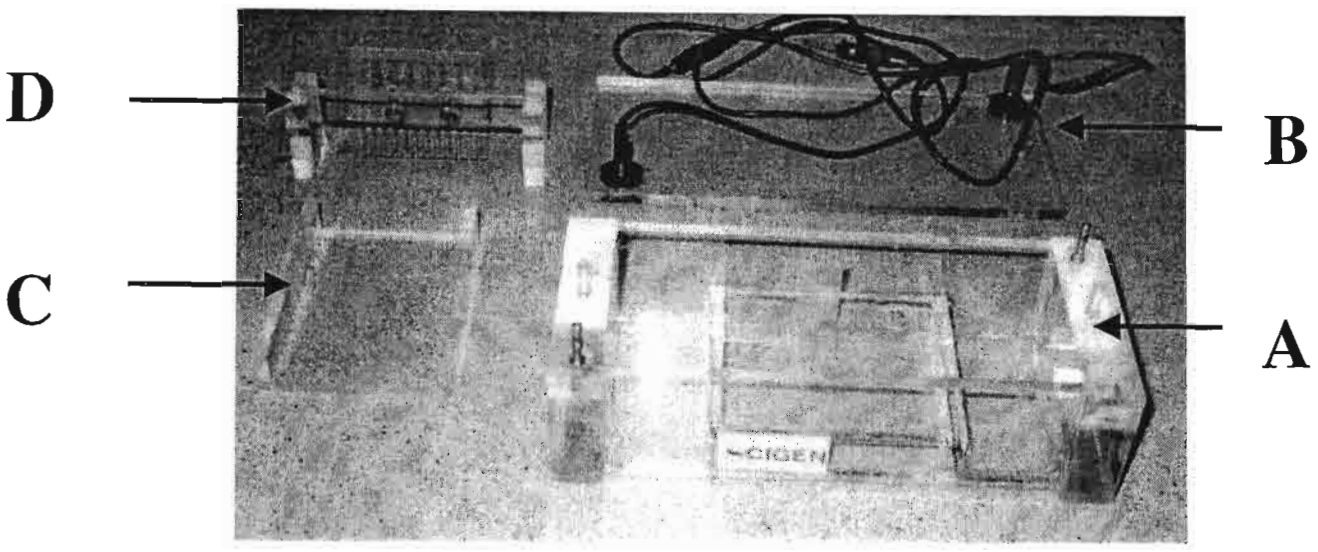

Figure 2.8: The horizontal slab agarose gel electrophoresis apparatus where A is the electrophoresis tank, B is the lid of the electrophoresis tank with leads to the power supply, C is the casting tray or gel mold and D is the comb used to form sample wells.

The casting tray or gel mold provides a shape for the gel as it polymerizes and is used to set the gel. The open ends of the casting tray are sealed with adhesive tape to provide a mold in which to set the gel. Plastic combs are used to form sample wells in the gels. The combs are placed at the cathodic end of the gel bed, to allow the negatively charged DNA molecules to migrate down the gel bed towards the anode. When forming sample wells, the comb is placed some 0.5-1 mm above the bottom of the gel bed. This prevents samples from leaking from one well to the other. Sample wells of about 1 cm in width and 1 cm in height were prepared such that a maximum volume of about 30 µl could be inserted into each well. The electrophoresis tank consists of two buffer reservoirs and a gel platform onto which the gel in the casting tray is placed when electrophoresis is performed. The lid of the tank contains two leads which when put into place are connected to the power supply. A power pack delivering up to 500 V at 400 mA was used.

2.3.3 Optimal electrophoretic conditions

There were many parameters that had to be considered to ensure optimal electrophoretic conditions. The most important of these are the agarose concentration and the applied current. When considering the optimal agarose concentration, it is important to produce a gel firm enough to be easily handled but yet not too concentrated, such that the matrix becomes too difficult for the DNA to move through, and hence separation would be more difficult to achieve. Using gels of different concentrations makes it possible to resolve specific size ranges of DNA molecules as shown in Table 2.1.

Table 2.1: Range of separation of DNA molecules in gels containing different amounts of agarose (Sambrook *et al.* [1989]).

Amount of agarose in gel (% w/v)	**Efficient range of separation of linear DNA molecules (size in kb)**
0.3	5 - 60
0.6	1 - 20
0.7	0.8 - 10
0.9	0.5 - 7
1.2	0.4 - 6
1.5	0.2 - 3
2.0	0.1 - 2

A very concentrated solution of agarose (e.g. 2% w/v) will offer good separation of the small DNA fragments (< 2 kilobases), however, the larger fragments will not separate due to their inability to move efficiently in the concentrated gel. Conversely, less agarose (e.g. 0.3% w/v) will offer better separation for the larger DNA fragments, while the smaller fragments will all migrate an equal distance thus providing no separation. It is important to achieve the best resolution of the DNA molecules at the chosen gel concentration. For conventional work, however, gels are often mixed at 0.8 - 1.0% (w/v) agarose. This normally separates DNA fragments larger than 500 bp but smaller than 70 000 bp. Since the DNA fragment size used for this investigation was 5 386 bp and hence fell within this range, both 0.8% (w/v) and1.0% (w/v) agarose gels were investigated to see which gave the best resolution. Although a 1.0% (w/v) agarose gel produced a firmer gel, the 0.8% (w/v) gel gave better separation of the DNA fragments and was chosen as the agarose concentration to be used for all further experiments.

The second factor of importance to be considered was the applied current. The optimum running current depends on the degree of resolution required, fragment size and the amount of time available. Electrophoresing smaller DNA fragments at high voltage gradients increases band sharpness as the smaller fragments diffuse faster. Conversely, large DNA fragments are best resolved by electrophoresing for longer times at low voltages, thus increasing separation but reducing the sharpness of the bands.

It is therefore important when choosing the optimum running current that a balance is struck between sharpness and separation. Another disadvantage of using too high voltages is the possibility that overheating of the electrophoresis buffer might occur during electrophoresis. Overheating distorts DNA bands and therefore must be avoided.

Agarose gels are typically run at 20 - 150 V, with the upper limit being heat dissipated. For this investigation 100 V was chosen as the optimum running voltage since it allowed good resolution of the DNA fragments under investigation.

2.3.4 Preparation of solutions for irradiation

Samples for irradiation consisted of solutions of ϕX174 DNA (Sigma) and solutions of the sunscreen UV absorbers of interest. The solutions that were prepared are briefly described below.

- **PBS buffer**

Biological cells maintain a constant pH by natural buffers, therefore it was necessary to use an artificial medium to mimic the natural environment of a cell. PBS was the buffer used to ensure that physiological pH (7.4) was maintained. The phosphate buffer was preferred to the Tris buffer used in Section 2.2.3 for the photostability experiments since it has been used with much success in gel electrophoresis of DNA.

A 5 mM phosphate buffer was prepared by dissolving 0.5884 g NaCl (10 mM), 0.7098 g Na_2HPO_4 (5 mM) and 0.6804 g KH_2PO_4 (5 mM) in approximately 200 ml of Millipore water, with sonication, and then making up the resulting solution to one litre in a volumetric flask. All reagents used were of analytical grade. The pH of the PBS buffer was measured with a Mettler 740 pH meter which had been calibrated with pH 4.0 and pH 7.0 buffer solutions. The pH was adjusted using 4 M NaOH. For all PBS solutions prepared the pH was maintained between 7.4 and 7.5. The buffer solution was filtered through a Millipore HV 0.45 μm filter to remove particulates. The solution was then autoclaved and refrigerated at about 7 °C.

- **ϕX174 DNA solution (75.4 μM DNA base pairs)**

Preparation of the ϕX174 DNA solutions for irradiation required appropriate dilution of the original DNA solution (as supplied by Sigma). The ϕX174 DNA was supplied with a total volume of 0.095 ml and a concentration of 10.5 A_{260} units/mL. A concentration of 14 nM in DNA molecule {or 75.4 μM DNA bp} was required for this series of experiments (Artuso *et al.* [1991]). Using the molecular mass of ϕX174 DNA to be 3.6 x 10^6 daltons (5386 bp per molecule) and the volume supplied, this corresponded to a 10-fold dilution of the original DNA. Special care had to be taken to ensure that no DNA was lost during handling of the sample since the volume purchased was very small. Before each irradiation, a 100 μl fresh working solution was prepared by very carefully transferring 10 μl of the original DNA solution to a sterilized plastic Eppendorf tube with a P 100 Gilson micropipette and making it up to 100 μl volume with 90 μl of the PBS solution.

- **Sunscreen solutions (45 μM or 0.2 nM)**

Stock solutions of the benzophenone-based sunscreens (45 μM or 0.2 nM) were prepared by dissolving the appropriate mass of reagent with PBS solution in sterile volumetric flasks. The

small masses required were weighed using the Mettler 6-digit mass balance. For benzophenone-3, PBS could not be used as the solvent since benzophenone-3 is completely insoluble in this buffer, therefore another solvent was sought. It was important to ensure that the DNA was stable in the chosen solvent and did not precipitate out or degrade. For this purpose high purity ethanol was used. However, DNA is known to precipitate in solutions with an ethanol content greater than 60% (v/v). Various mixtures of ethanol in PBS buffer were prepared and the dissolution of benzophenone-3 was tested. A 50% (v/v) ethanol / PBS solution proved successful and hence was used to dissolve the benzophenone-3.

- **Special precautions taken during preparation of solutions**

Considerable precautions were taken to ensure that all glassware used was properly cleaned and sterile. The presence of nucleases on glassware can result in the degradation of DNA in the samples upon storage. Furthermore, the PBS solution used for the preparation of samples for irradiation provides the ideal conditions for bacterial growth. The measures which were employed to minimize bacterial contaminants, and hence DNA degradation, are as follows:

- All glassware was firstly washed with chromic acid, followed by a 0.5% detergent wash.
- Sterilization of all equipment (glassware, Eppendorf tubes, pipette tips, etc.) and PBS solutions were carried out by autoclaving in the Wisconsin aluminium electric pressure steam sterilizer at 250 ^{0}F (121 °C) and 15 psi for 30 minutes.
- All solutions were wrapped in aluminum foil and stored in the cold at temperatures below 10°C. When required the solutions were allowed to attain room temperature before use, except for the DNA solution, which was used cold.
- Latex gloves were worn during the handling of the sterilized glassware and the solutions to minimize transfer of nucleases.

All these precautions were routinely performed with extreme care to ensure the validity and reproducibility of the results.

2.3.5 Preparation of solutions for electrophoresis

Solutions required for gel electrophoresis consisted of the electrophoresis buffer (tris-borate EDTA, where EDTA refers to ethylenediaminetetraacetic acid), the loading dye (bromophenol blue) and the staining dye (ethidium bromide).

- **Tris - borate EDTA electrophoresis running buffer**

The electrophoretic mobility of DNA is affected by the composition and ionic strength of the electrophoresis buffer. The buffer optimizes the pH and the ion concentration of the gel and its use is essential to ensure an efficient running gel. There are several different buffers available for electrophoresis of native DNA, but one of the most common buffers, which provides sufficient buffering power, is the tris-borate EDTA buffer (TBE).

A stock (10x) TBE solution was prepared by dissolving 108 g of T*ris*-(hydroxymethyl) aminomethane (or Tris), 55 g of boric acid and 40 mL of 0.5 mM EDTA (pH 8.0) in a one litre volumetric flask with Millipore water. The pH was measured with a Mettler 740 pH Meter and was adjusted with 33% HCl. The Tris present in the buffer helps maintain a constant pH in the solution while the boric acid provides the proper ion concentration. Furthermore, the TBE buffer contains EDTA, which serves to chelate divalent cations (*e.g.* magnesium) that are required for nuclease action. The electrophoresis buffer was transferred to storage bottles and autoclaved. When the buffer was required, a 10-fold dilution was made to give a working solution.

- **Bromophenol blue loading buffer**

A loading buffer is also required for gel electrophoresis. This buffer serves two purposes, *i.e.*, it increases the density of the sample, ensuring that the DNA sinks to the bottom of the well, and the buffer also contains a dye that enables the progress of an electrophoretic run to be visible and thus monitored. The loading buffer was prepared by adding 0.05 g of bromophenol blue to 75 ml of glycerol in a 100 ml volumetric flask. The mixture was brought to volume with a 250 mM Tris buffer (pH 7.2). This Tris buffer was prepared by dissolving 7.571 g of *Tris*-(hydroxymethyl)aminomethane with Millipore water in a 250 ml volumetric flask. The pH was adjusted with 2 M HCl. The loading buffer was stored in the refrigerator.

- **Ethidium bromide staining buffer**

The use of a staining dye in electrophoresis is essential. The staining dye serves as a convenient method to visualize DNA in agarose gels. For this purpose the fluorescent dye ethidium bromide was used (see Section 2.4.4 for the structure of the dye). Ethidium bromide contains a planar group, which enables it to intercalate between stacked bases of the DNA and this increases its fluorescence compared to the unbound dye on illumination. Hence, the DNA in an agarose gel can be detected by the fluorescence of the ethidium bromide bound to the DNA. The ethidium

bromide was prepared as a stock solution of 2 mg/ml in PBS, which was stored in the refrigerator and wrapped in aluminum foil to prevent dye degradation.

2.3.6 The DNA suitability assay

The purpose of this assay was to identify the three DNA forms. The ϕX174 DNA contained 85% supercoiled DNA (Form I), 15% open circular DNA (Form II) and no linear DNA (Form III) as specified by the supplier (Sigma). As the DNA may have degraded during transport and storage, it was necessary to perform the suitability assay.

A Form III DNA marker was required for this assay to identify the linear DNA band. For this purpose, the *Providencia Stuartii* (*Pst I*) restriction endonuclease was used. The *Pst I* enzyme has the following recognition sequence: 5'-CTGCA/G-3'. Once the enzyme recognises this specific sequence in the DNA, it will cleave DNA strands within this recognition site, thus converting the DNA to the linear form.

A mass of 1 μg of ϕX174 DNA was digested with 20 units of *Pst I* in the digestion buffer provided. The equivalent volume of DNA required for the suitability assay was calculated using the following relationships, that is, one unit of DNA is equivalent to 50 μg of DNA and a volume of 0.095 ml as specified by the supplier (Sigma). The enzyme was supplied as 15 units/μl, so the 20 units of *Pst I* required was equivalent to a volume of 1.33 μl. The assay used is shown in Table 2.2.

Table 2.2: Suitability assay used to identify the DNA Forms of the ϕX174 DNA

	EXPERIMENT	**CONTROL**
***Pst I* / μl**	1.3	0.0
ϕX174 DNA / μl	1.9	1.9
***Pst I* digestion buffer / μl**	3.0	3.0
Water / μl	23.8	25.1
Total / μl	30.0	30.0

The experimental and control samples were prepared as shown in Table 2.2 and transferred to two sterilized Eppendorf tubes using a Gilson P 100 micropipette. The tubes were then inserted in a polystyrene slab and floated on a water bath, which had been prepared to 37 °C. The DNA was

allowed to digest for 2 hours, after which 7 µl of loading dye was added to each tube. The agarose gel was prepared as discussed in Section 2.3.8. The experimental samples (*Pst I* digested ϕX174 DNA) were loaded into lanes 2, 4 and 6 while lanes 1, 3 and 5 were occupied by the control (no *Pst I* enzyme). Volumes of 5, 10 and 15 µl of each sample were loaded into lanes 1 and 2, 3 and 4, and 5 and 6 respectively. The gel was run and analysed as described in Sections 2.3.9 - 2.3.10. The results obtained are discussed in Section 3.2.1.

2.3.7 The DNA - agarose gel nicking assay to detect DNA cleavage

The DNA - agarose nicking assay that was performed in this investigation is an adaptation of that of Artuso *et al.* [1991]. Studies conducted by this research team demonstrated that a group of nonsteroidal anti-inflammatory drugs having benzophenone-derived structures photosensitize the formation of single strand breaks in double stranded ϕX174 DNA. From this group of benzophenone-derived drugs, ketoprofen was chosen as the standard photocleaver to verify the protocol implemented in this study. The preliminary experiment performed with ketoprofen and ϕX174 DNA appears in Table 2.3. Once the protocol proved to be successful, this technique was implemented to study the DNA photocleavage induced by the benzophenone-based UV absorbers. A mole ratio of DNA bp: UV absorber of approximately 1:3 was used (refer to Table 2.5) since, according to Marguery *et al.* [1998], this proved to be most successful in inducing SSB. A control experiment was set up in which ϕX174 DNA was irradiated alone for various time periods and gel electrophoresis was performed (refer to Table 2.4).

Listed below are tabulations of the assays used in this investigation, followed by a brief outline of the procedure.

Table 2.3: Experimental protocol for demonstration of ketoprofen photosensitization of DNA cleavage.

Sample	**1**	**2**	**3**	**4**
ϕX174 DNA (75.4 µM bp) /µl	5	5	5	5
Ketoprofen (45 µM) /µl	0	5	0	5
PBS (5 mM, pH 7.4) /µl	10	10	10	10
Irradiation period / min	0	0	30	30

Table 2.4: Experimental protocol to demonstrate DNA photocleavage induced by the irradiation of DNA alone (control).

Sample	1	2	3	4	5	6
ϕX174 DNA (75.4 μM bp) /μl	5	5	5	5	5	5
PBS (5 mM, pH 7.4) /μl	15	15	15	15	15	15
Irradiation period / min	0	5	10	20	30	45

Table 2.5: Experimental protocol to demonstrate DNA photocleavage induced by the irradiation of DNA in the presence of the benzophenone-derived UV absorbers using a UV absorber DNA bp ratio of 3.

Sample	1	2	3	4	5	6
ϕX174 DNA (75.4 μM bp)/μl	5	5	5	5	5	5
Sunscreen (0.2 nM)/μl	5	5	5	5	5	5
PBS * (5 mM, pH 7.4) /μl	10	10	10	10	10	10
Irradiation period / min	0	5	10	20	30	45

{*For benzophenone-3, the PBS was replaced by 50% (v/v) ethanol: 50% (v/v) PBS (refer to section 2.3.5).}

The samples for the individual nicking assays were prepared as stipulated in the tables above (refer to Section 2.3.4 for the preparations of the individual solutions). The mixtures were placed in sterilized NMR tubes, which served as the irradiation cells (see Section 2.1.3) and were capped. The tubes were wrapped in aluminum foil and placed on ice. The samples were irradiated with an Osram HBO 500W/2 high pressure mercury lamp in conjunction with a 10 mm thick Pyrex filter for the specific time periods indicated in the tables above. The use of the lamp is discussed in Section 2.1.1. Following irradiation, 5 μl of a loading dye comprising of a mixture of 250 mM Tris buffer (pH 7.2), 75% glycerol and 0.05% bromophenol blue was added to each sample (for the preparation of the loading dye, refer to Section 2.3.5). The samples were then loaded onto the gel as described in the following Section 2.3.8.

2.3.8 Running of the gel

A 0.8% agarose gel was prepared by adding 0.8 g of molecular grade agarose (Whitehead Scientific) to 100 ml of the TBE buffer (see Section 2.3.5 for preparation of the TBE buffer). The

agarose was dissolved by microwaving the mixture for a few minutes, until the contents just started to boil. The agarose solution was cooled to about 50°C and then poured into the casting tray, which had been sealed with adhesive tape. The comb was inserted into the mold to form the wells (refer to Section 2.3.2 for the electrophoresis apparatus used).

The gel was allowed 45 – 60 minutes to set at room temperature, after which the comb was carefully removed. The adhesive tape on the sides of the casting tray was removed before the casting tray was placed onto the gel platform in the electrophoresis tank. The gel apparatus was filled with TBE buffer solution such that the gel was covered to a depth of about 1 mm.

A volume of 25 µl of each sample was then loaded into the wells of the submerged gel using a P 100 Gilson micropipette. A fresh sterilized pipette tip was used for each sample transfer. After all the samples had been loaded the lid of the gel tank was closed and the electrical leads were attached. Electrophoresis was performed with a power supply set at 100 V and 100 mA.

When the bromophenol blue front reached the end of the gel, usually about 1.5 – 3 hours after the start of the run, electrophoresis was stopped. The gel was removed and placed in a staining bath where it was stained for 30 – 40 minutes in an aqueous solution of ethidium bromide (250 µl in 500 ml of water). This enabled the ethidium bromide to bind to the DNA such that it would fluoresce under UV light, thus allowing visualization of the DNA bands. During the staining process the staining bath was placed on a flask shaker (Scientific Engineering) to shake the gel. After the gel was stained, it was examined under UV light and photographed as described in Section 2.3.9. The bands were then quantified as described in Section 2.3.10.

2.3.9 Viewing and photography of the gels

To view and photograph the DNA bands in the agarose gel, a UV transilluminator connected to a camera apparatus was required, which in turn was connected to a computer installed with the imaging software.

The transilluminator provides the source of UV light which is required for the ethidium bromide stained DNA bands to be visualized. Ethidium bromide fluoresces when bound to DNA and illuminated with light of a wavelength of 302 nm, thus enabling DNA bands in an agarose gel to be detected. The transilluminator consists of a black box, with a Perspex sheet on the top and the UV source within. Two such gel photography systems were used, as they became available. These are the Syngene transilluminator connected to a Vacutec camera system (Figure 2.9) and

the Hoefer Scientific transilluminator connected to the CCTV camera (Matsushita Communications) (Figure 2.10).

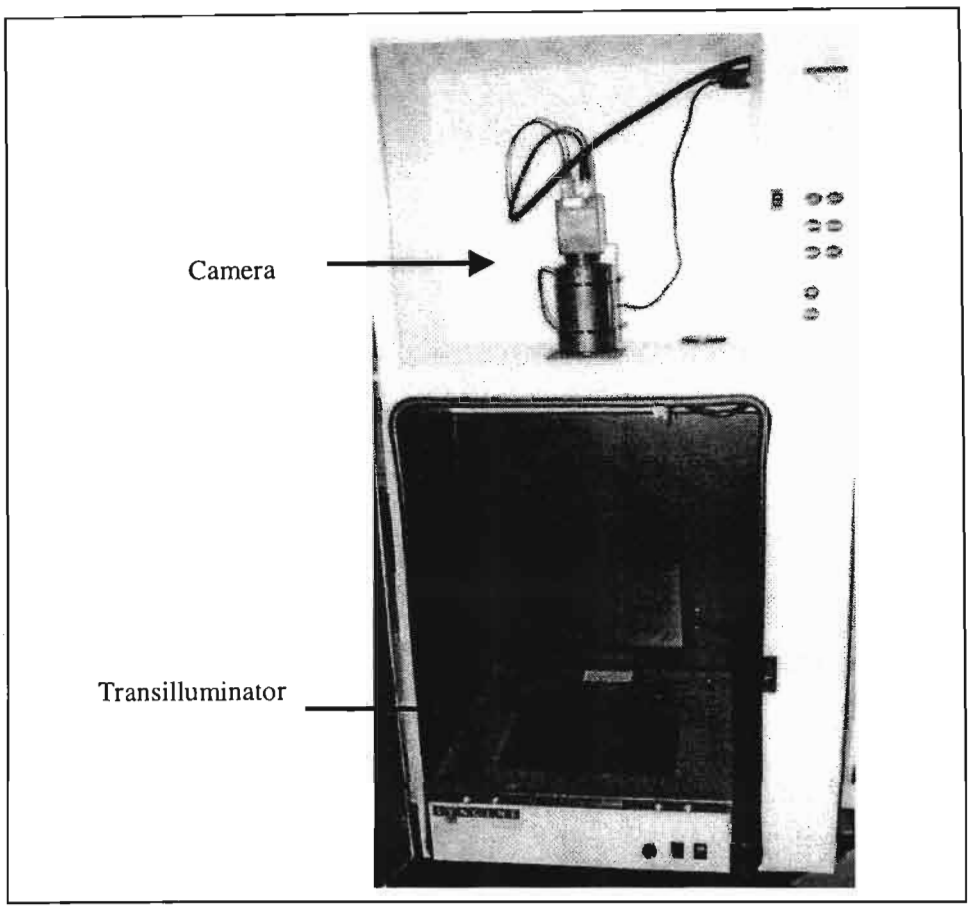

Figure 2.9: The Syngene transilluminator connected to a Vacutec camera system.

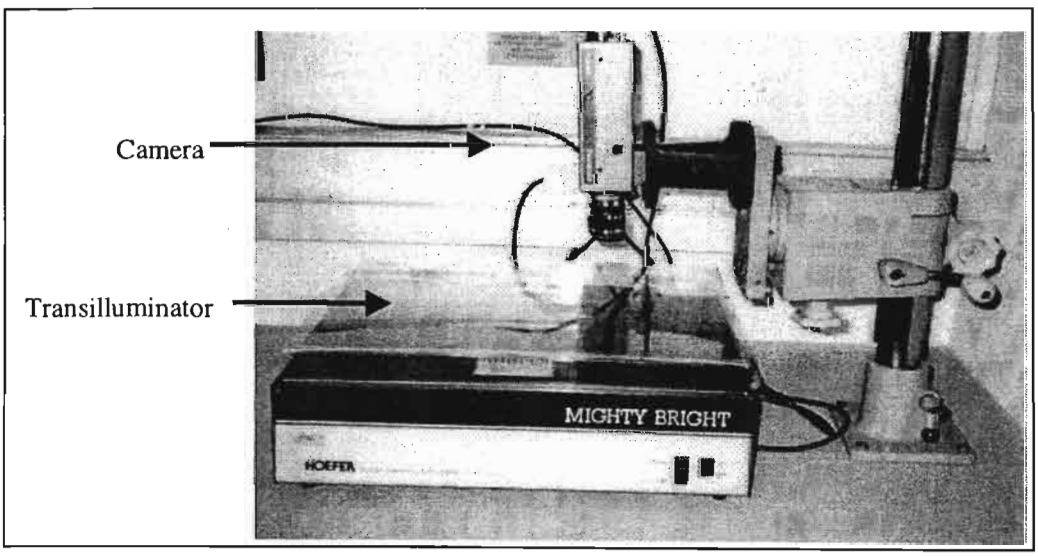

Figure 2.10: The Hoefer Scientific transilluminator connected to the CCTV camera (Matsushita Communications).

The viewing and photography of the gels was carried out in a dark room to limit the amount of light present. When viewing the gel, it was placed on the UV transparent perspex sheet, which serves as a UV-pass visible blocking filter allowing UV light to impinge on the gel. The attached camera was then set up and focused such that a picture with best resolution was obtained on the computer screen. After the best picture of the gel had been captured, the photograph could be further manipulated using the imaging software to emphasize certain aspects of the gel.

2.3.10 Quantification of the DNA bands

After the gels had been photographed, the bands were quantified to determine the relative composition of DNA in Form I (supercoiled), Form II (open circular) and Form III (linear). Initially this was carried out by means of the Hoefer Scientific densitometer GS 300 (Figure 2.11). When using this densitometer the negative films of the gel photographs had to be scanned in the transmittance mode. During the scan, the areas of the DNA bands in Forms I, II and III present in each lane were plotted on a graph plotter. The areas under the peaks were then cut out and weighed. This method was disadvantageous since it was time-consuming and allowed for human error and inaccuracies, therefore another method for DNA quantification was sought.

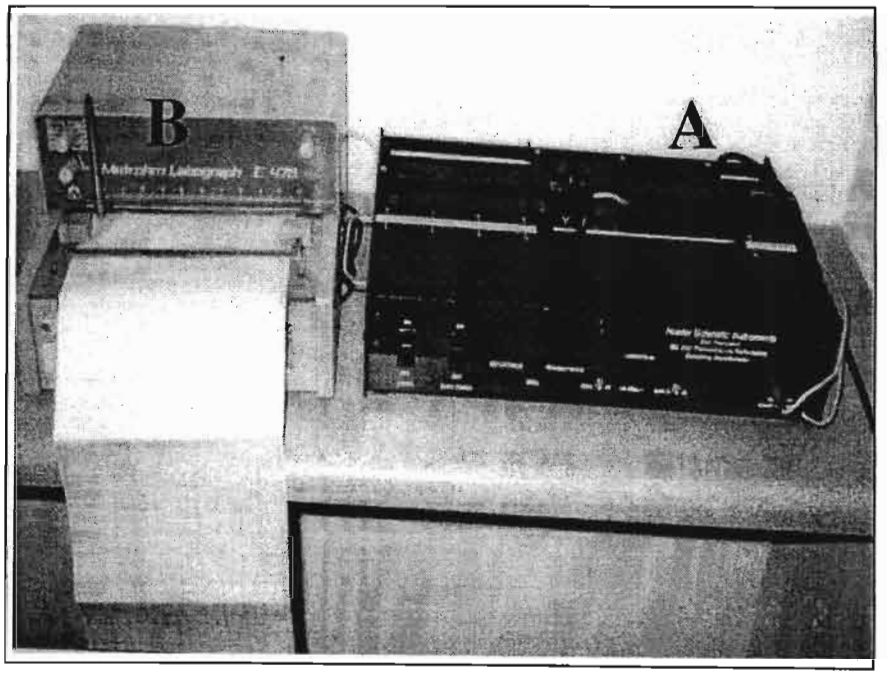

Figure 2.11: The Hoefer Scientific densitometer GS 300 (A) connected to a plotter (B).

The Scion Image software was purchased since it enabled direct quantification of the DNA bands to be carried out. This software was used in conjunction with the Hoefer Scientific transilluminator that had been connected to the CCTV camera (Figure 2.10). This system proved to be very efficient and accurate. It uses the logarithmic relationship between optical density and brightness to calculate the concentration of each band in an image. Each lane had to be marked using the appropriate software tools and the area under the peaks was then plotted.

The expressions for the percentage of DNA in Forms I, II and III following exposure to UV irradiation were adapted from Croke *et al.* [1988] and are shown below.

$$[I_F] = \frac{[I]}{[I] + [II] + [III]} \quad x \quad 100 \tag{2.5}$$

$$[II_F] = \frac{[II]}{[I] + [II] + [III]} x \quad 100 \tag{2.6}$$

$$[III_F] = \frac{[III]}{[I] + [II] + [III]} \quad x \quad 100 \tag{2.7}$$

where [I], [II] and [III] represent DNA Forms I, II and III respectively, while $[I_F]$, $[II_F]$ and $[III_F]$ are the fractional amounts of Form I DNA (supercoiled), Form II DNA (open circular) and Form III DNA (linear) respectively. This enabled normalization of the DNA Forms, which was necessary to compensate for variations in the volumes loaded in each lane.

When ethidium bromide intercalates with DNA, the dye causes an unwinding of the supercoiled DNA. This affects the centrifugal sedimentation rate and the electrophoretic mobility of DNA Form I (Boyer [1993]). Because ethidium bromide binds less efficiently to supercoiled DNA than to nicked and to linear DNA molecules, various correction factors have been used to estimate the relative proportions of Form I DNA. Roots *et al.* [1985] obtained a correction factor of 1.25, while Lloyd *et al.* [1978] and Ciulla *et al.* [1989] obtained values as high as 1.44 and 1.66 respectively. According to Croke *et al.* [1988] and Masnyk & Minton [1991], however, these corrections factors proved to be negligible. Since the variation in the published values for this correction factor is large, and the use of values determined by others under different gel, buffer or staining conditions may lead to significant errors in the quantitation of Form I, the use of the correction factor was omitted from all calculations in this work.

The number of SSB was calculated from the following expression (Hertzberg and Dervan [1984]):

$$SSB = \frac{I_0}{I} \tag{2.8}$$

where I_o is the initial concentration of Form I DNA and I is the concentration of Form I DNA after irradiation in the presence of the sunscreen absorbers.

The mean and standard deviations for the percentages of each DNA form as well as for the number of SSB were calculated and plotted against irradiation time. The effect of the sunscreen absorber was determined by comparing the DNA cleavage caused in its presence to that when it was absent (control). The gel scans and the resultant DNA cleavage induced by each of the benzophenone-derived compounds investigated in this study are discussed in Section 3.2.

2.4 Fluorescence Spectroscopy

Fluorescence spectroscopy was the second technique used to detect DNA damage photoinduced by the benzophenone-based sunscreen absorbers. This technique utilized displacement of ethidium bromide from the DNA base pairs as an indication of DNA damage. The DNA used for this series of experiments was calf thymus DNA. In this section, a brief introduction to fluorescence spectroscopy (Section 2.4.1), a description of the instrumentation that was used (Section 2.4.2) and the precautionary measures that were taken to ensure the success of this technique (Section 2.4.3) are discussed. The fluorescent intercalator displacement techniques and assay to detect DNA cleavage are outlined in Sections 2.4.4 - 2.4.6.

2.4.1 An introduction to fluorescence spectroscopy

Fluorescence spectroscopy is an important and powerful analytical technique for the investigation of biological material. Until the last decade radioactive labeling procedures and UV measurements were preferred whenever only the smallest amounts of a sample were available. However, recently, the development of sophisticated optical instruments, the supply of new fluorescent dyes, as well as the employment of lasers instead of lamps has turned fluorescence spectroscopy into a superior method. This technique owes its superiority to its sensitivity, which has reached an extremely high level. Fluorometric methods can detect concentrations of substance as low as one part in ten billion, with the sensitivity 1000 times greater than that of most other spectrophotometric methods (Guilbault [1973]). The process of fluorescence emission

occurs in a time scale between nanoseconds and milliseconds. Since in this time scale many important and dynamic events take place, this technique can provide information on a molecule that most other techniques cannot.

Upon absorption of a photon of light, a molecule goes from the ground state to the first excited singlet state as discussed in Sections 2.2.1. Now the excited state is short-lived and there are several ways an excited molecule can give up its excitation energy (refer to Section 1.4.1 for more details). One such de-excitation process is where the molecule rapidly loses its excess vibrational energy by collision with other excited molecules, and falls to the lowest vibrational level of the first excited state, in a process called collisional deactivation (depicted by short wavy arrows between vibrational energy levels in Figure 2.12). If all the excess energy is not further dissipated by collisions with other molecules, the electron returns to the ground electronic state, with the emission of a photon. This phenomenon is called fluorescence.

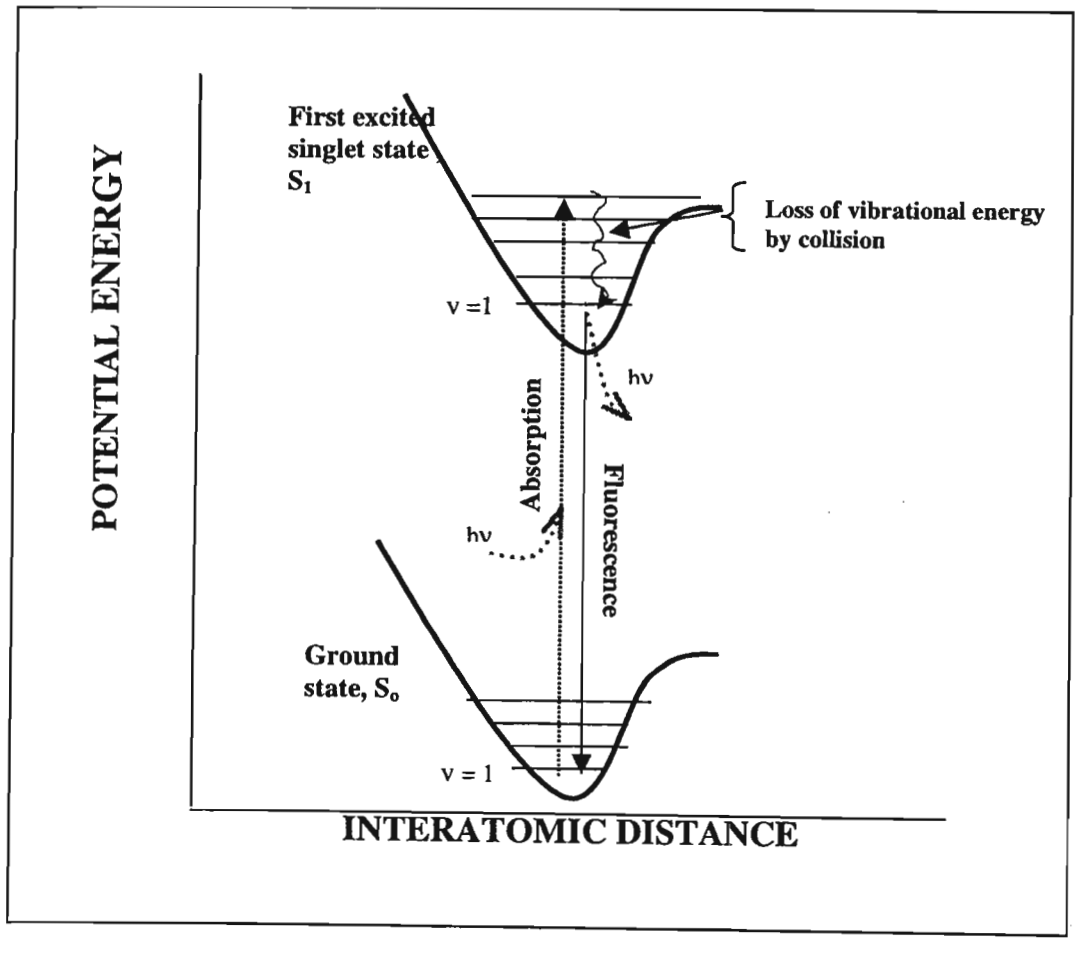

Figure 2.12: Schematic energy – level diagram showing fluorescence.

Fluorescence is generally complete after about 10^{-5} seconds (or less) from the time of excitation (Skoog *et al.* [1996]). Because some of the energy is lost in the brief period before emission can occur, the emitted energy (fluorescence) is lower and hence of a longer wavelength than that of the energy that was absorbed (absorption). Therefore fluorescence is always monitored at a longer wavelength than the excitation wavelength.

2.4.2 Instrumentation for fluorescence spectroscopy

A fluorescence spectrophotometer consists of the same basic components as found in an absorption spectrophotometer, *i.e.*, the light source, the wavelength selectors, a sample holder, a detector system and a readout. However, one major difference separates these two spectrophotometric techniques, *i.e.* for fluorescence the sample is measured at a 90° angle with respect to the source as apposed to 180 °C for absorption spectroscopy (Figure 2.13).

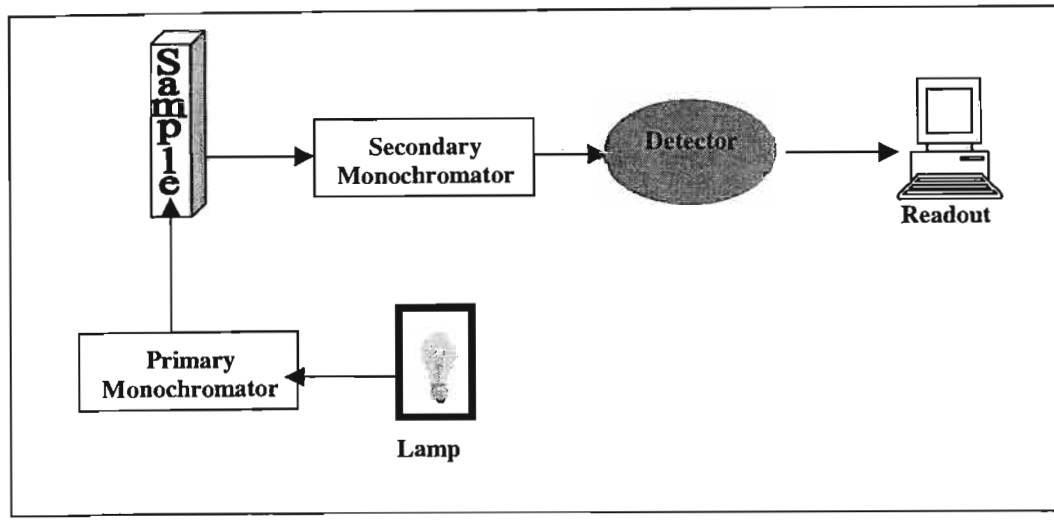

Figure 2.13: Schematic diagram of the optical components of a typical fluorescence spectrometer.

Energy from the light source first passes through the primary or excitation monochromator before it is transmitted to the sample in the sample holder. This serves to restrict the wavelength, which is important, since it greatly enhances both the selectivity and the sensitivity of the instrument. Fluorescence radiation emitted from the sample is propagated in all directions, but it is most conveniently observed at right angles to the excitation beam. At other angles increased scattering from the solution and the cell walls may cause large errors in the intensity measurement. This serves to limit the amount of incident light striking the detector and is characteristic of fluorescence spectroscopy. Only light emitted from the sample reaches the detector, so the

detector will register zero signal when no fluorescence occurs and an increase in signal indicates emission from the sample. This is the major reason for the sensitivity of this technique.

Energy emitted from the sample reaches the detector after passing through the secondary or emission monochromator. The monochromators consist of an entrance slit, a collimating mirror to produce a parallel beam of radiation, a grating to disperse the radiation into its component wavelengths and an exit slit (Skoog *et al.* [1996]). The slit widths are the most important parameter determining the resolution of the instrument. The signals from the detectors are then processed by the instrument electronics and are displayed on a computer screen.

For this study fluorescence was measured with a Perkin Elmer LS 50B luminescence spectrometer (Figure 2.14), using a quartz cell with a path length of 1 cm and a xenon discharge lamp as the light source.

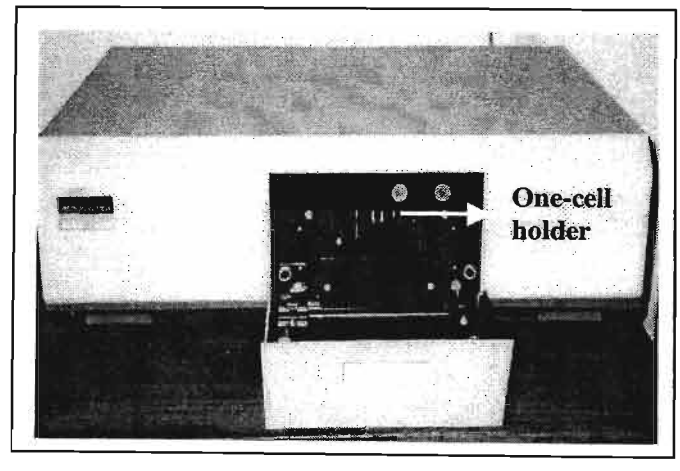

Figure 2.14: Perkin Elmer LS 50B luminescence spectrometer.

The excitation and emission slits were selected to be 10 nm and 5 nm respectively as these gave the best resolution. A high scan speed of 100 nm min^{-1} was used since the compounds under investigation reacted photochemically. The operation of the instrument was simple and required only a 50 second initializing period after which a measurement could be taken.

2.4.3 Precautionary measures

Fluorescence spectroscopy is an extremely sensitive technique, therefore considerable precautions had to be taken to ensure valid results.

Among the parameters examined, the first was the concentration effect. The concentration of the fluorescent species (C) and its fluorescence (F) is related by the following equation:

$$F = KC \tag{2.9}$$

When the fluorescence of a species is directly proportional to its concentration by the constant K, then Beer's law is obeyed. But when C becomes large enough that the absorbance is greater than 0.05, linearity is lost and this relation does not hold. This effect is called self-absorbance in which the analyte molecules absorb the fluorescence produced by other analyte molecules. At very high concentrations little of the radiation source actually penetrates the main bulk of the solution since most of it is absorbed by the solution confined to the front surface of the cuvette. The fluorescence emission becomes distorted and light scattering also becomes important. It was therefore important to measure the absorbance of the fluorescent species, before fluorescence was measured and to ensure that the absorbance was below 0.05 so as to prevent self-absorbance of the fluorescent species. If the absorbances of the solutions prepared were larger than 0.05 then the appropriate dilutions were made.

Another problem that is frequently encountered in fluorescence spectroscopy is quenching. Quenching is the reduction in the intensity of fluorescence due to a competing deactivating process, which results in a specific interaction between the exited species and another substance, as represented by Equation 2.10 below.

$$M^* + Q \longrightarrow M + Q^* \tag{2.10}$$

where M* represents fluorescent species M that is quenched by another species Q.

One of the most notorious quenchers is oxygen. Oxygen present in a solution at a concentration of 10^{-3} M can reduce fluorescence of a typical compound by 20% (Guilbault [1973]). It was therefore necessary to deaerate all solutions by bubbling nitrogen through the solutions for 10 – 15 minutes before irradiation. This was sufficient to remove the oxygen present in solution (Guilbault [1973]).

The UV radiation used for excitation may cause photochemical changes in the fluorescent compound, thus degrading its fluorescence emission. To overcome this problem, the longest wavelength radiation was always chosen for excitation since it had the lowest energy. Also the standard solutions of the fluorescent compounds were stored in opaque bottles, or if not, they were wrapped in aluminum foil to protect them from sunlight and fluorescent laboratory lights.

Temperature control of the fluorescent compounds also had to be exercised. This was important since in most molecules the quantum efficiency of fluorescence decreases with increasing temperature. This is due to the increased frequency of collision at elevated temperatures, which improves the probability of collisional relaxation. The change in fluorescence is normally 1% per 1^0C, however, in some compounds it can be as high as 5% (Guilbault [1973]). Therefore for maximum precision and accuracy it was important to take all measurements at the same temperature. In this study all samples were left to equilibrate to 25°C before fluorescence measurements were taken.

It was also necessary to ensure that all glassware and solutions were free of impurities since their presence can cause interferences. All the glassware, solvents and buffers were cleaned and treated in the same way as for agarose gel electrophoresis (Section 2.3.4). It was also very important that high quality solvents were used that were free of traces of contaminants which would interfere with fluorescence. Buffers were also not stored in plastic containers since leaching of organic additives could occur.

Finally, accurate pipetting and thorough mixing are critical for reproducible results. However, it was important to ensure that no air bubbles were present in the solution when fluorescence was measured. Air bubbles can cause scattering of light leading to inaccurate results.

2.4.4 The fluorescent intercalator displacement technique

Ethidium bromide (Figure 2.15) is a cationic dye that interacts with supercoiled DNA by intercalation. This fluorescent complex between ethidium bromide and DNA was first reported by Lepecq and Paoletti in 1967. When ethidium bromide is intercalatively bound to DNA a large increase in fluorescence is observed with intensity from 20 to 100 times that of the free dye (Strothkamp K. & Strothkamp R. [1994]). The intercalation model proposed by Lerman *et al.* [1961] suggests that the strong mode of binding of the ethidium bromide to DNA results in the intercalation of the phenanthiridium ring between adjacent base pairs on the double helix.

In the last decade a variety of drugs have been shown to interact with DNA in a similar manner (Rai *et al.* [1993] and Armitage *et al.* [1994]). One of the most successful techniques to detect drug-DNA binding has been the fluorescent intercalator displacement (FID) technique. The FID assay provides a rapid and readily reproducible measure of drug-DNA binding and interaction and requires only milligram quantities of drug and microgram quantities of DNA (Cain *et al.* [1978]).

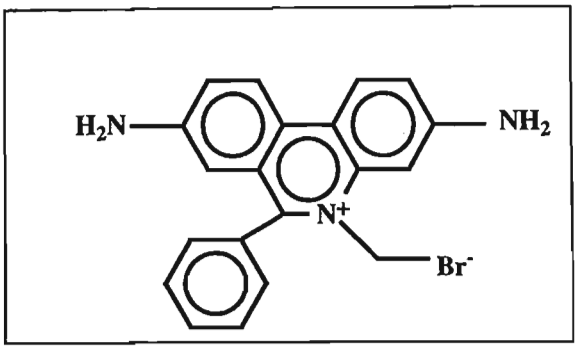

Figure 2.15: Chemical structure of ethidium bromide.

The FID technique utilizes competition of an added drug with ethidium bromide for DNA intercalation sites. Addition of a DNA binding compound would result in a decrease in fluorescence due to the displacement of the ethidium bromide bound intercalator. Several forms of DNA damage (including base intercalation, base oxidation, base liberation etc.) are believed to contribute to the loss of fluorescence. The fluorescent yield reduces to about 50% upon DNA denaturation in neutral solution and becomes very weak when intramolecular hydrogen bonds in single strands are further destabilized (Morgan & Pulleyblank [1974]). Thus the DNA-ethidium bromide fluorescence provides a convenient probe to detect DNA damage. The percentage fluorescence decrease is directly related to the extent of DNA binding.

For this assay calf thymus DNA was the DNA of choice as compared to the ϕX174 phage DNA that was used for the agarose gel electrophoresis experiments. This was due to the fact that calf thymus DNA is double stranded in contrast to the phage DNA that is single stranded. Due to the nature of the interaction between ethidium bromide and DNA, a double helix DNA was required to allow intercalation of the ethidium bromide, therefore calf thymus DNA was used.

The key to the assay is to employ an ethidium bromide concentration that saturates the DNA. This ensures that all the DNA intercalation sites are occupied by the intercalator (ethidium bromide) and therefore addition of a DNA binding compound results in the displacement of the intercalator from the DNA and not in binding at a vacant site. The molecular modelling studies of ethidium bromide intercalation with DNA have revealed that on binding, the base pairs in the immediate region are twisted by 10°, giving rise to an angular unwinding of -26°, while the intercalative base pairs are tilted 8° relative to one another (Sobell *et al.* [1977]). These changes in DNA conformation indicate that at maximal drug-DNA ratios, intercalation is limited to every other base pair, *i.e.* a neighbour exclusion model (Geall & Blagbrough [2000]). Also binding of the dye is saturated when one dye molecule is bound for every four or five base pairs (Nordmeier [1992]).

Studies performed on the FID assay have revealed that the assay is expected to perform best at a 1:2 ethidium bromide : DNA base pair ratio where all the intercalation sites are occupied (Boger *et al.* [2001]). The failure of this assay would be caused by using an inappropriate ethidium bromide : DNA ratio. Using a small ethidium bromide : DNA ratio (*e.g.* 1:4) would underestimate the binding of the compound since not all available intercalation sites would be occupied and hence compound binding could occur at sites where less or no intercalator would be displaced and would not significantly affect the fluorescence intensity. On the other hand, if the ethidium bromide concentration is raised above the optimal 1:2 ethidium bromide : DNA ratio (*e.g.* 2:1) then the fluorescence decrease would diminish due to an enhanced background fluorescence of the unbound ethidium bromide. Another important parameter for the assay is the compound concentration. The use of a near 6:1 ratio of DNA base pairs to compound, according to Boger *et al.* [2001], was necessary to provide the desired robust intensity of this assay.

For the success of the assay it was also important to ensure that binding took place exclusively at intercalation sites and not at the phosphate groups. At high salt concentration (> 0.5 M NaCl), ethidium bromide binds exclusively by intercalation with DNA with a resulting enhanced fluorescence (Geall & Blagbrough [2000]). However, at low salt concentration (≤ 10 mM), ethidium bromide can bind to the outside of the helix, where the fluorescence intensity is low. It was therefore necessary to ensure that the salt concentration was relatively high. This was provided by use of the Tris-HCl buffer, which ensured a relatively high salt concentration and minimized electrostatic binding of the benzophenone-based sunscreen absorbers to the phosphates.

The variable that is most crucial to the success of the assay, and most likely to be responsible for avoidable errors, is the quality of the DNA. In addition to the obvious concern of its constitution and purity, its concentration is critical. This was determined by absorption spectroscopy as will be discussed in Section 2.4.5.

Finally, the sensitivity of the assay is also dependent on the chosen excitation wavelength and the wavelength selected to monitor the fluorescence of ethidium bromide. Researchers in this field have used various excitation wavelengths. These include direct excitation of ethidium bromide at 540-546 nm (by Boger *et al.* [2001], Rai *et al.* [1993], Hansen *et al.* [1983], Cain *et al.* [1978] and Reinhardt & Krugh [1978]), 520-525 nm (by Birnboim & Jevcak [1981] and Strothkamp K. & Strothkamp R. [1994]), as well as 510 nm (by Armitage *et al.* [1994] and Mohtat *et al.* [1998]). In addition Geall & Blagbrough [2000] reported that indirect excitation of ethidium bromide at 260 nm by energy transfer from the DNA produces a more sensitive assay. When choosing the excitation wavelength it is important to ensure that the absorbance of the ethidium

bromide at this wavelength is below 0.05 units to prevent self-absorbance as discussed in Section 2.4.3, yet not too small such that fluorescence is not detected. When choosing the wavelength to monitor fluorescence, it is important to ensure that only the ethidium bromide absorbs or fluoresces at the chosen wavelength and that none of the other compounds used in the assay do (*i.e.* the benzophenone-based compounds, buffer and DNA).

2.4.5 Solutions required for the FID assay

A solution of 1 x 10^{-4} M DNA bp containing 1.67 x 10^{-5} M of the sunscreen compound, as well as a solution of 0.68 x 10^{-5} M of ethidium bromide was required for the assay. These concentrations ensured that a 1: 2 ethidium bromide: DNA bp ratio as well as a 6: 1 ratio of DNA bp to compound was maintained. The success of the assay was dependent on the concentrations used and therefore it was important to ensure that all solutions were accurately prepared. Preparation of all the solutions required for the assay will now be discussed.

1. Tris - HCl buffer

Firstly, the buffer used for this assay was the Tris-HCl buffer, as it is commonly known. The Tris-HCl buffer (or a buffer of similar composition) has been the buffer of choice of many researchers in this field (Strothkamp K. & Strothkamp R. [1994], Rai *et al.* [1993], Hansen *et al.* [1983], Birnboim & Jevcak [1981] and Reinhardt & Krugh [1978]). This buffer not only approximates physiologically relevant conditions (pH 7-8) but also represents a relatively high salt concentration, to minimize simple electrostatic binding to the phosphate backbone of the DNA. This buffer was comprised of 0.1 M Tris, 0.1 M NaCl and a volume of HCl to give a pH of 8. Preparation of the buffer has been described in much detail in Section 2.2.3. This buffer was used in the preparation of the other solutions required for the FID assay.

2. Solution containing calf thymus DNA (1 x 10^{-4} M DNA bp) and sunscreen (1.67 x 10^{-5} M)

A solution containing 1 x 10^{-4} M calf thymus DNA as well as 1.67 x 10^{-5} M sunscreen was prepared, with a total volume of 20 ml in a volumetric flask. Preparation of this solution required initially the preparation of individual stock solutions of each component, as discussed below and then mixing using the appropriate dilution factors as determined by absorption spectroscopy to give the final solution. Large volumes were not prepared since DNA is known to degrade when

stored for long periods. Preparation of the individual solutions as well as determination of the dilution factors is discussed below.

Preparation of the DNA stock solution:

A concentrated stock solution of calf thymus DNA was prepared by dissolving approximately 5 mg of calf thymus DNA in about 20 ml of Tris-HCl buffer in a sterilized stoppered 100 ml volumetric flask. Since the calf thymus DNA used was fibrous in nature, sterilized tweezers had to be used to handle the DNA when weighing. The handling period of the DNA was minimized to prevent contamination and degradation of the DNA by impurities. Dissolving the DNA required stirring the solution using a magnetic stirrer in the cold (2-9°C), until the solution appeared clear. This usually required 2-3 days of stirring in the cold.

Calf thymus DNA is known to contain many contaminants such as protein, water, sodium and others and therefore the concentration of the pure DNA in the stock solution had to be determined accurately. Although the percentages of sodium and water were specified by the supplier (Sigma), these could not be relied on since the water content may change on storage. Absorption spectroscopy was therefore used to determine the concentration of pure DNA in the stock solution. A Cary 1E UV-visible spectrophotometer and a matched pair of quartz cuvettes with a path length of 1 cm were used to measure the absorbance of the DNA in the stock solution. The instrument was zeroed with Tris-HCl buffer. The absorbance was measured at 260 nm, since pure DNA absorbs at this wavelength. A 10-fold dilution was made to the stock solution such that the absorbance at 260 nm was below one absorbance unit and hence obeyed the Beer Lambert law (Equation 2.3 in Section 2.2.3). The resultant absorption spectrum of the calf thymus DNA solution appears in Figure 2.16.

From this spectrum, the absorbance of the dilute DNA solution at 260 nm was determined to be 0.6239 units. It is generally accepted that calf thymus DNA with an absorbance of 1 unit at 260 nm, has an average concentration of 0.050 mg ml^{-1} (www.turnerdesigns .com/t2/doc/appnotes/s-0046.pdf, Date accessed: 2 December 2002). Using this conversion, this corresponded to 0.03120 mg ml^{-1} for the 10-fold diluted stock solution and therefore 0.3120 mg ml^{-1} for the stock DNA solution. A DNA concentration of 1 x 10^{-4} M in DNA bp was required for this assay. Using a molar mass of 660 g mol^{-1} for 1 bp of calf thymus DNA as supplied by the manufacturer, this corresponds to 0.066 mg ml^{-1} of DNA. Hence the dilution factor was determined to be 4.727.

DNA purity and quality were critical for the success of the FID assay. Protein is a common contaminant of DNA and it was necessary to establish whether the protein content was within the

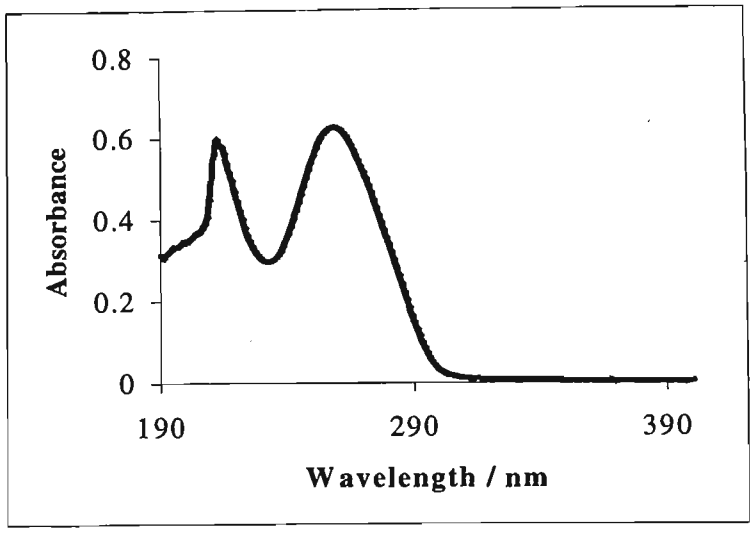

Figure 2.16: Absorption spectrum of a 10-fold diluted solution of calf thymus DNA with a concentration 0.03120 mg ml^{-1}.

acceptable limits to classify the DNA as pure. Proteins absorb UV light at 280 nm, therefore by comparing the ratio of the A_{260} reading (the wavelength at which pure DNA absorbs) to that at A_{280}, the presence of protein in the DNA solution can be evaluated. An A_{260}/A_{280} ratió of 1.8 orgreater indicates pure DNA. This analysis using the A_{260}/A_{280} ratio was first described by Warburg & Christian [1942] to assess protein purity in the presence of nucleic acid contaminants. Today, this method is commonly used to determine both nucleic acid purity and yield. The absorbance at 280 nm for the 10-fold diluted stock solution was 0.3379 units, therefore the A_{260}/A_{280} ratio was calculated to be 1.86. This indicated that the DNA solution was of high purity and therefore could be used for the FID assay.

Preparation of the sunscreen stock solution:

The mass required to prepare 1.67 x 10^{-5} M sunscreen was too small to be weighed. A 20 ml concentrated solution of 1 x 10^{-4} M sunscreen was prepared by dissolving the appropriate mass of sunscreen in Tris-HCl buffer. This corresponded to a dilution factor of 5.988.

Preparation of the final solution with 1 x 10^{-4} M DNA bp and 1.67 x 10^{-5} M sunscreen:

To prepare 20 ml of solution required 4.23 ml of DNA stock solution (dilution factor = 4.727 as discussed above), 3.34 ml of sunscreen stock solution (dilution factor = 5.988) and 12.43 ml of Tris-HCl buffer. For the control samples the 3.34 ml of sunscreen solution was replaced by Tris-HCl buffer, and in the case of benzophenone-3 50% (v/v) ethanol: Tris-HCl was used.

3. Ethidium bromide solution (0.68 x 10^{-5} M)

For the FID assay a 0.68 x 10^{-5} M solution of ethidium bromide was required. Since the mass required was too small to be weighed, a concentrated solution of 4 x 10^{-5} M was prepared and diluted to the required concentration. The solution of ethidium bromide was prepared by dissolving 0.000789 g of ethidium bromide in a 50 ml volumetric flask with Tris-HCl buffer. The concentration of this solution was determined accurately by measuring the absorbance at 480 nm and using a molar absorption coefficient of 5 600 M^{-1} cm^{-1} (Strothkamp K & Strothkamp R. [1994]). The Cary 1E UV-visible spectrophotometer and a matched pair of quartz cuvettes with a path length of 1 cm were used. The instrument was zeroed with Tris-HCl buffer. A 5-fold dilution of the ethidium bromide stock solution was made such that the absorbance at 480 nm was below one absorbance unit and hence obeyed the Beer Lambert law. The resultant absorption spectrum of the diluted ethidium bromide stock solution appears in Figure 2.17.

From the absorption spectrum of the 5-fold diluted ethidium bromide solution in Figure 2.17, the absorbance at 480 nm was determined to be 0.04898. Using the Beer Lambert law (Equation 2.3 in Section 2.2.3), where the molar absorption coefficient (ε) of ethidium bromide at 480 nm is 5 600 M^{-1} cm^{-1} (as supplied by the supplier) and the path length (b) was 1 cm, the concentration of the 5-fold diluted solution was calculated to be 8.65 x 10^{-6} M. Hence the concentration of the concentrated stock ethidium bromide solution was calculated to be 4.38 x 10^{-5} M. Since a 0.68 x 10^{-5} M solution of ethidium bromide was required, this corresponded to a dilution of 6.43 from the stock solution. A total volume of 100 ml of ethidium bromide was prepared by dissolving 15.56 ml of the stock ethidium bromide solution (4.38 x 10^{-5} M) with 84.45 ml of Tris-HCl buffer.

2.4.6 The FID assay for DNA cleavage

Binding of the benzophenone-based UV absorbers to the DNA bases would reduce the number of available binding sites for the intercalator ethidium bromide and would result in a decrease in the fluorescence intensity for an ethidium bromide-DNA solution, as discussed in Section 2.4.4.

The FID assay employed in this study is an adaptation of the work done by Boger *et al.* [2001] because this group of researchers utilized optimum conditions for the assay. However, they utilized a fluorescent plate reader that was able to analyse microvolumes (100 µl at a time) of solution. The Perkin Elmer LS 50B luminescence spectrometer that was available for this study was unable to analyse such small volumes. For the purpose of this study all the volumes utilized

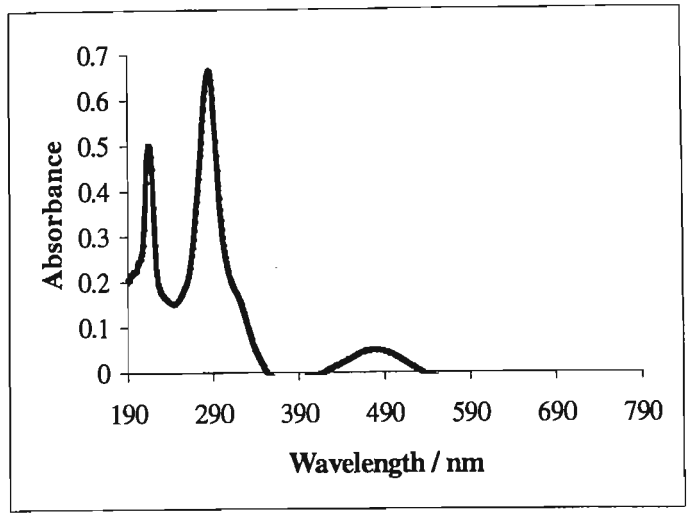

Figure 2.17: Absorption spectrum of a 5-fold diluted solution of ethidium bromide (8.65 x 10^{-6} M).

by Boger *et al.* [2001] were increased by 30-fold to accommodate the 3 ml quartz cuvette (1 cm path length) that was available.

For the FID assay, samples containing 0.36 ml of 1 x 10^{-4} M DNA bp and 1.67 x 10^{-5} M of the sunscreen compound of interest were irradiated at one minute intervals for a total irradiation period of 30 minutes (refer to Section 2.4.5 for preparation of the solutions). Irradiation was carried out with the Osram HBO 500W/2 high pressure mercury lamp in conjunction with a 10 mm thick Pyrex filter, using a 10 mm pathlength capped irradiation cell. Two control experiments were also conducted in the absence of any UV absorber. For the control samples, 0.36 ml of a solution only containing 1 x 10^{-4} M calf thymus DNA was used. The first of these controls was prepared in Tris-HCl buffer, and served as the control for all the UV absorbers except benzophenone-3. For benzophenone-3, the control required dissolving the calf thymus DNA in 50% (v/v) ethanol: Tris-HCl buffer. After each irradiation, the irradiated sample was removed from the irradiation cell and added to 2.64 ml of 0.68 x 10^{-5} M ethidium bromide in a fluorescence quartz cuvette. The sample was then incubated for 30 minutes by placing the cuvette in the sample holder of a DMS 300 UV-VIS spectrophotometer that was attached to a water-cooling system that had been equilibrated to 25°C. The fluorescence of the sample was then measured with the Perkin Elmer LS 50B luminescence spectrophotometer. The samples were scanned from 525 to 700 nm with excitation at 510 nm. The emitted fluorescence was monitored at 586 nm.

Due to the poor reproduciblity of this assay, for each of the UV absorbers under investigation the assay was performed at least in duplicate or triplicate. The percentage of binding sites remaining at a given time (t) was then calculated from the following equation (Armitage *et al.* [1994]):

$$\textbf{Percentage binding sites remaining} = 100\left(1-\frac{I_o - I_t}{I_o - I_{Buf}}\right) \tag{2.11}$$

where I_o, I_t, and I_{Buf} correspond to the fluorescence intensity of the solution at 586 nm before irradiation, after t minutes of irradiation, and of the buffer respectively. The average and the standard deviation for the percentage binding sites remaining after irradiation were then plotted. The results obtained are discussed in Section 3.3.

2.5 Computational Modelling

Computational modelling can be used to determine the energies and geometries of products, intermediates and transition states. In order to assess whether the benzophenone-based UV absorbers would be able to intercalate with DNA bases, the lowest energy geometries of these compounds were determined by means of computational modelling. By using an appropriate computational model, it can be ascertained whether these structures are planar (such as the common DNA intercalator, anthraquinone), in which case they would have a higher probability of intercalating with DNA, or non-planar, where intercalation would be limited or impossible.

There exist three different computational methods, namely *ab initio*, semi-empirical and molecular mechanics (Foresman & Frisch [1996], Hehre *et al.* [1998] and Leach [1996]). The first two methods are concerned with quantum mechanics and provide solutions to the Schrödinger wave equation, while the latter describes molecular properties in terms of energy potentials. The Schrödinger wave equation is represented by Equation 2.12 below:

$$H\psi = E\psi \tag{2.12}$$

where H is the Hamiltonian operator to the wavefunction, ψ is the wavefunction and E is the corresponding energy, which is known as the eigenvalue in quantum terms.

Ab initio, a Latin phrase, meaning from first principles, solves the wave function from basic principles. These calculations are theoretically pure and the most accurate that can be performed for computational modelling, however, they are most time-consuming and expensive, requiring large ultra-speed computers. In contrast, semi-empirical methods use approximations to simplify the solution to the Schrödinger equation so that it can be solved quickly. These approximations are obtained from experimental results and/or high level *ab initio* calculations. In addition, this method is relatively cheaper (several orders of magnitude) with regard to computer resources and time. Lastly, molecular mechanics uses force fields to determine energies and structures of normally much larger systems. Force fields include parameters such as bond lengths, angles, and charges, *etc.*, that are also obtained from experiment and/or *ab initio* calculations. Provided the force field has been verified as producing acceptable answers, one can normally get fairly accurate results with molecular mechanics within a very short time.

Semi-empirical calculations were chosen to find the lowest energy structures of the different molecules studied, with the exception of Eusolex 232, due to the ease of calculation. This method is extremely fast since it refrains from evaluating complex integrals and is able to generate results in minutes. The semi-empirical method has up to ten different approximations, from which the PM3 approximation (or the parametric method number 3) was chosen. The PM3 approximation is used primarily for organic molecules and has proved to be surprisingly accurate. For Eusolex 232, the semi-empirical calculation failed to give an accurate result so for this structure *ab initio* methodology was used.

2.5.1 Determination of the lowest energy, most stable structure for each UV absorber

The program used was Hyperchem and a conformational search was employed to find the low energy structures of each UV absorber. For each compound, energy scans were performed around a chosen dihedral angle(s) (refer to Section 3.4 for more details). The program has a conformational search algorithm, which varies the required dihedral angle(s) randomly to all possible values (+180° to -180°). An input structure is automatically created with random dihedral angles, and the structure is then optimized without any constraints. A new set of dihedral(s) is generated and the process is repeated. The program automatically overlays the products found and tests them for unique versus similar structures. In order to determine if the planar structure was stable, the required dihedral angles were then fixed (constrained) to force a flat structure and the energy obtained was compared to the lowest energy obtained from the optimization process.

To obtain the most stable structure for each of the UV absorbers under investigation, the energy profile for the different dihedral angles was of importance. The potential energy of a molecule is at a minimum for the most stable conformation and reaches a maximum when it is unstable (Morrison & Boyd [1992]). Depending on the value of the dihedral angle(s), the energy minimization algorithm might be trapped in a local minimum or the global minimum. This can be illustrated for butane as shown in Figure 2.18. A global minimum (the lowest point on the curve), corresponding to the anti-conformation (for the case of butane), as well as two local minima (at slightly higher energies), corresponding to the gauche conformations, can be seen. The gauche conformation has a slightly higher energy and is slightly less stable than the anti-conformation due to steric repulsion between the methyl groups. Also the maximum seen in this graph (4.4-6.1 kcal above the local minima) usually corresponds to an intermediate structure, *i.e.* a transition state, and it is representative of an unstable conformation.

A clear pattern was observed for each of the benzophenone-based structures studied after several starting structures were generated and optimized. The low energy structures were then optimized using PM3 for all the UV absorbers apart from Eusolex 232 and rank ordered by energy. For the latter, *ab initio* calculations were required, which took into account the electron delocalisation that contributed very strongly to the lowest energy structure for this UV absorber. The lowest energy structures corresponding to the most stable state for each UV absorber will be discussed in Section 3.4.

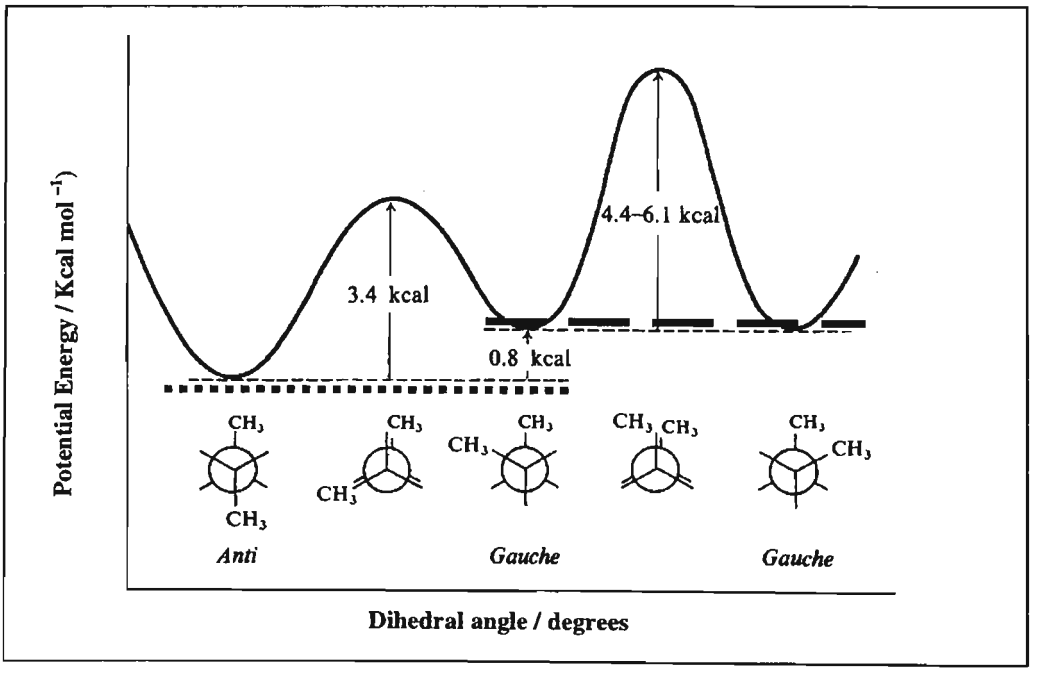

Figure 2.18: Potential energy changes during rotation about the C(2)-C(3) bond for n-butane showing a global (▪▪▪▪▪▪▪▪) and local (——— ———) minima (Morrison & Boyd [1992]).

Chapter 3

RESULTS AND DISCUSSION

The benzophenone-derived group of sunscreens is amongst the most commonly used sunscreen absorbing agents on the market today. However, the discovery that some UV absorbers containing the benzophenone backbone, for example, ketoprofen, amongst others not only form thymine dimers when irradiated with DNA, but also photosensitize DNA cleavage is of concern and has put the safety of the benzophenone sunscreens under the spotlight. In addition, it has been well established that the parent compound, benzophenone, is a potent free radical generator. It also induces thymine dimer formation when irradiated with DNA *in vitro*. The purpose of this investigation therefore was to determine if a group of benzophenone-derived sunscreens, that is, benzophenone-1, benzophenone-3, benzophenone-4, Uvinul DS49 and Eusolex 232 have the ability to photosensitize the cleavage of supercoiled DNA to the relaxed circular and linear forms. Binding of the UV absorbers to the DNA by intercalation has also being a focus of this investigation. Also included in this study were the parent compound, benzophenone, as well as the known DNA photocleaver, ketoprofen.

The experimental techniques employed to generate the necessary data have all been described in Chapter 2. Briefly, aqueous solutions of supercoiled DNA were irradiated in the presence of aqueous solutions of the benzophenones at wavelengths greater than 300 nm with an Osram 500 W/2 high pressure mercury lamp (Section 2.1). All solutions were buffered to pH 7-8 to maintain physiological conditions. The irradiated samples were analyzed by two separate techniques: these are gel electrophoresis (Section 2.3) and fluorescence spectroscopy (Section 2.4). The photostabilty of the UV absorbers have also been investigated (Section 2.2). Finally computational modelling was conducted to determine the lowest-energy geometrical structures of the benzophenone absorbers (Section 2.5).

This chapter deals with a discussion of results. Firstly, the photostablity of all the compounds analysed will be discussed (Section 3.1). This will be followed by a discussion of the results obtained for the photocleavage experiments of ϕX174 phage DNA as detected by agarose gel electrophoresis (Section 3.2), as well as DNA (calf thymus) binding as monitored by fluorescence spectroscopy (Section 3.3). In Section 3.4, the lowest-energy geometrical structures of the benzophenone absorbers, obtained from computational studies will be described and finally the mechanism for DNA photocleavage as induced by the various UV absorbers will be proposed in Section 3.5.

3.1 Photostability of the benzophenone-derived UV absorbers

The UV radiation reaching the earth's surface is comprised of no UVC, 5% UVB and 95% UVA radiation (Larsen [1994]). Previously it was thought that UVA radiation was harmless and that all skin ailments due to sun exposure, including skin cancer, were due to UVB radiation only. However, in the past decade it has been realized that UVA exposure is just as deadly as UVB. Nowadays sunscreen formulations offer protection against both these radiations by consisting of a mixture of UV absorbers that absorb UV radiation strongly in both regions. However for such a sunscreen to effectively protect skin from UV damage it should be stable to photodecomposition when subjected to sunlight. Hence the photostability of sunscreens is of importance.

In this series of experiments, the photostability of a group of benzophenone-derived UV absorbers was investigated with a Cary 1E UV-visible spectrophotometer. Absorption measurements were taken after specific irradiation periods at wavelengths greater than 300 nm as described in Section 2.2.3.

Dilute solutions of the UV absorbers (1×10^{-4} M - 6.5×10^{-4} M) were prepared in Tris-HCl buffer or 50% (v/v) ethanol/Tris-HCl buffer in the case of benzophenone-3. The concentrations of the UV absorbers used were such that the intensity of absorption at their absorption maxima was below 2 units to prevent deviations from the Beer Lambert law as discussed previously (Section 2.2.3). The absorption spectra of these compounds were recorded before exposure to UV radiation and after every 5 minutes of irradiation thereafter. The solutions were contained in a one mm pathlength quartz cell and were irradiated with an Osram HBO 500 W/2 high pressure mercury lamp whose output passed through a 10 mm thick Pyrex filter. The total irradiation period used to monitor the photostability of the UV absorbers was chosen to be 30

minutes since this irradiation period was similar to that used in the agarose gel electrophoresis experiments.

The UV absorbers studied in this investigation were classified as either narrow-spectrum or broad-spectrum absorbers. Their absorption spectra recorded prior to any UV radiation appear in Figure 3.1. Benzophenone, ketoprofen and Eusolex 232 were classified as the narrow spectrum absorbers since they absorb radiation only in the UVC and UVB regions of the spectrum (190 - 320 nm), with no absorption in the UVA region (Figure 3.1A). However, benzophenone-1, benzophenone-3, benzophenone-4 and Uvinul DS49 offer broad-spectrum protection (190 – 400 nm) and therefore were grouped together as broad-spectrum absorbers (Figure 3.1B). The results of the irradiation of the narrow- and broad-spectrum absorbers are presented below in Sections 3.1.1 and 3.1.2, respectively.

3.1.1 Photostability of benzophenone, ketoprofen and Eusolex 232

The UV absorbers, benzophenone and ketoprofen, have similar chemical structures and demonstrated similar photostability patterns towards UV radiation. It should however at the outset be mentioned that these UV absorbers are not used in sunscreen formulations and are included in this study simply as benchmarks for DNA photocleavage. However, the use of benzophenone is still under review in some countries like Australia (www.health.gov.au/tga/docs/pdf/sunscrai.pdf, Date accessed: 6 December 2002). It should further be noted that reference to these compounds as "UV absorbers" does not imply that they are used in sunscreens. Eusolex 232, the third of these UV absorbers, however, is approved for use in sunscreens in most countries. Eusolex 232 differs from the other two in that it does not possess the benzoyl chromophore, in addition it was found to have a very different photostability pattern.

Benzophenone

Benzophenone is the parent compound of the UV absorbers in this investigation (refer to its structure in Figure 3.2) and therefore knowledge of its photochemistry was important. The UV spectra that were recorded at the beginning of the experiment and after each 5-minute irradiation period have been superimposed and appear in Figure 3.2. The absorption spectrum of benzophenone without irradiation (see 1 in Figure 3.2) consisted of two peaks in the UV region, a strong band at 202 nm and a slightly weaker one at 258 nm. Upon irradiation, a rapid decline in height of both these peaks was observed. The results obtained here are in agreement with

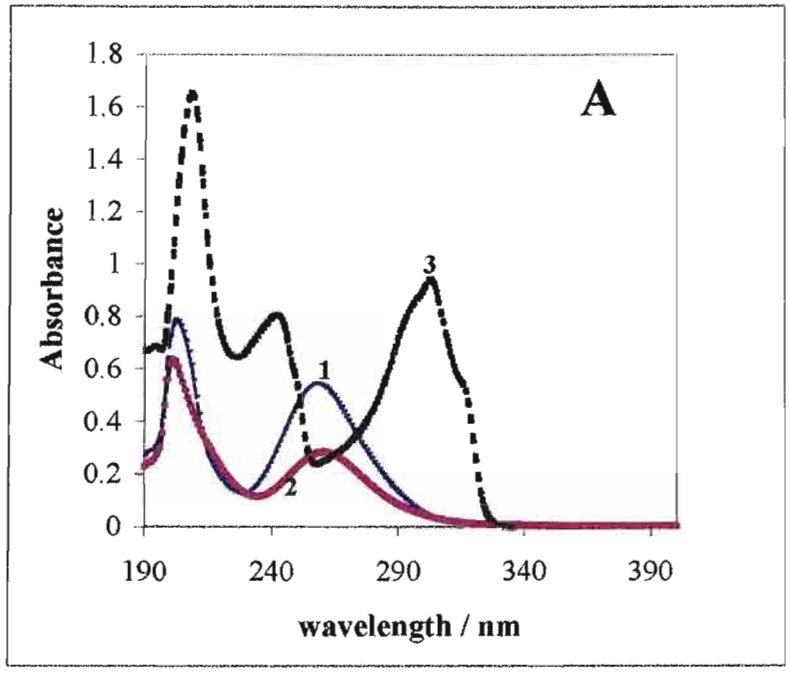

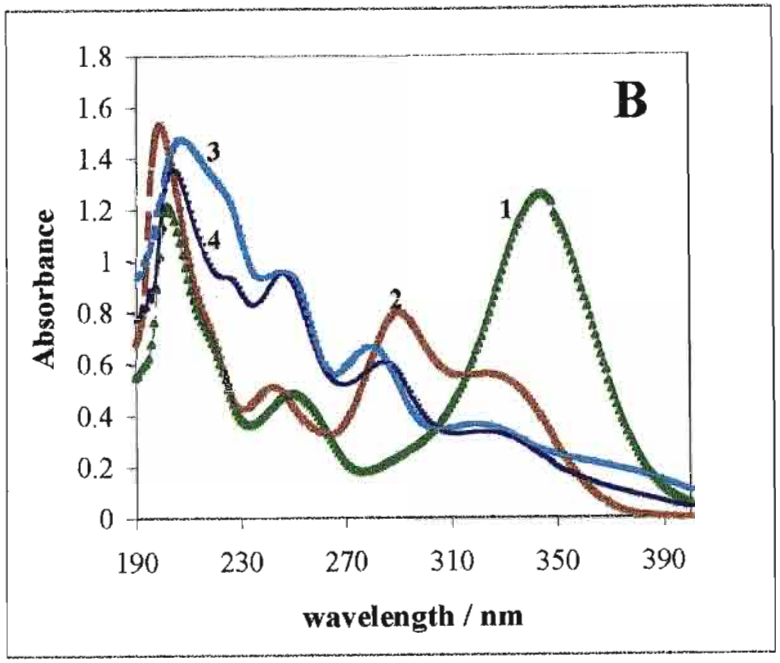

Figure 3.1 Absorption spectra of the narrow (A) and broad-spectrum UV absorbers (B).

In A: 1, 2 and 3 represent benzophenone (5.5×10^{-4} M), ketoprofen (1×10^{-4} M) and Eusolex 232 (5.5×10^{-4} M), respectively.

In B: 1, 2, 3 and 4 represent benzophenone-1 (5.5×10^{-4} M), benzophenone-3 (5.5×10^{-4} M), benzophenone-4 (5.5×10^{-4} M) and Uvinul DS49 (6.5×10^{-4} M), respectively.

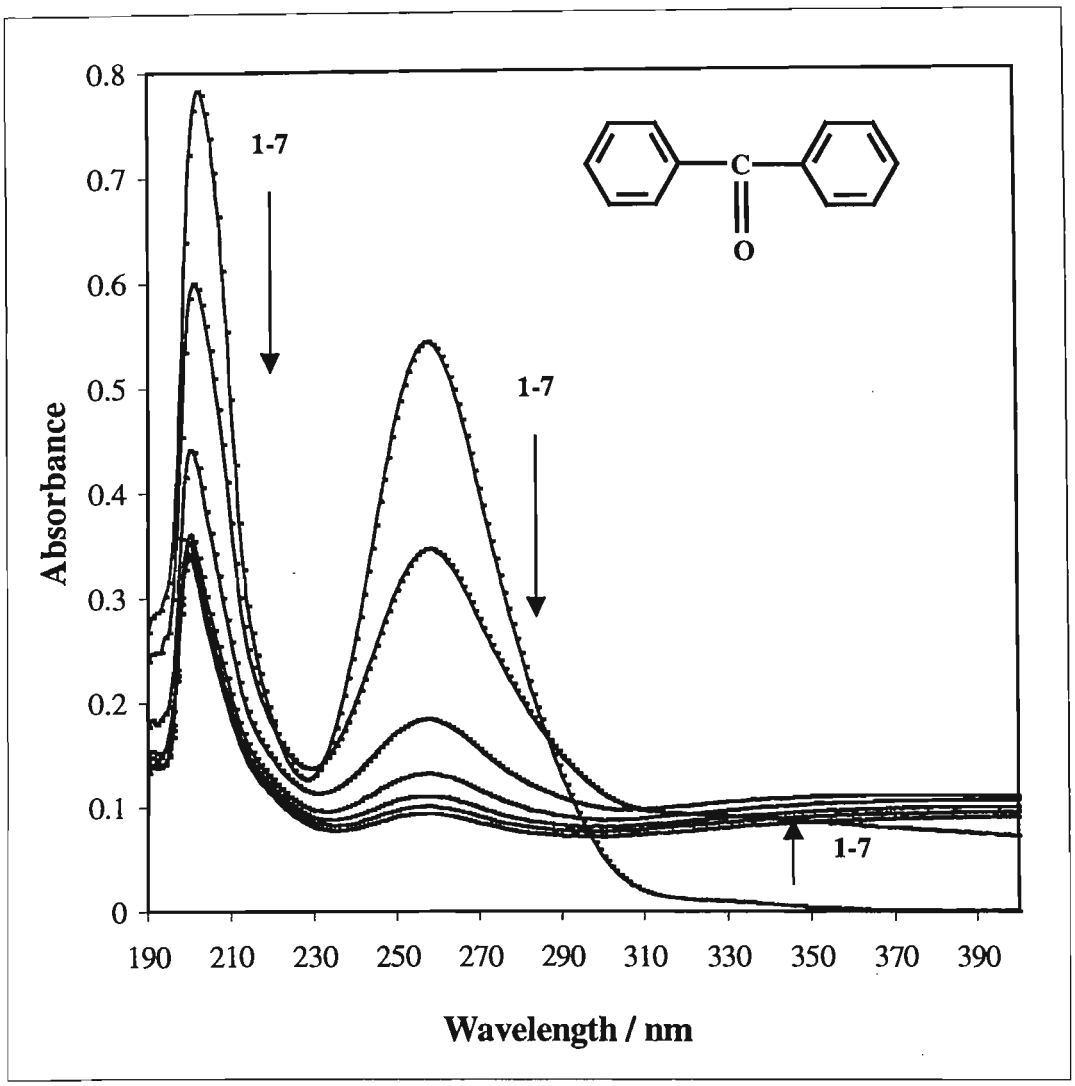

Figure 3.2: Changes in the absorption spectum of benzophenone (5.5×10^{-4} M) in Tris-HCl buffer with irradiation time where 1- 7 refer to 0, 5, 10, 15, 20, 25 and 30 minutes of irradiation, respectively.

with those obtained by Charlier & Hélène [1972], Ledger & Porter [1971] and Scaiano *et al.* [1982].

The absorbance at 258 nm was found to decrease dramatically from 0.5 units initially to 0.09 units after only 30 minutes of irradiation. The peak at 202 nm also decreased rapidly at first from 0.76 units without irradiation to 0.35 units after 15 minutes of irradiation and for the rest of the irradiation period this peak remained the same. Also for the first 5 minutes of irradiation, isosbestic points (points of intersection) occurred at about 220 nm, 230 nm and 287 nm, however, when the irradiation period was increased (5 - 30 minutes), deviations from these isosbestic points were observed. The absorbance decrease was also accompanied by an increase of absorbance on the red side of the band at 258 nm. This behaviour was indicative of a photochemical reaction and the possible formation of photoproducts absorbing in this wavelength region.

The percentage of photodegradation of benzophenone at its absorption maximum (258 nm) has been plotted against irradiation time and appears in Figure 3.3. From this Figure it can be seen that the percentage of photodegradation of benzophenone varied linearly with irradiation time for the first ten minutes of irradiation. Thereafter the curve levelled off suggesting a maximal formation of photoproducts. After only 20 minutes of irradiation about 80% of the benzophenone was degraded.

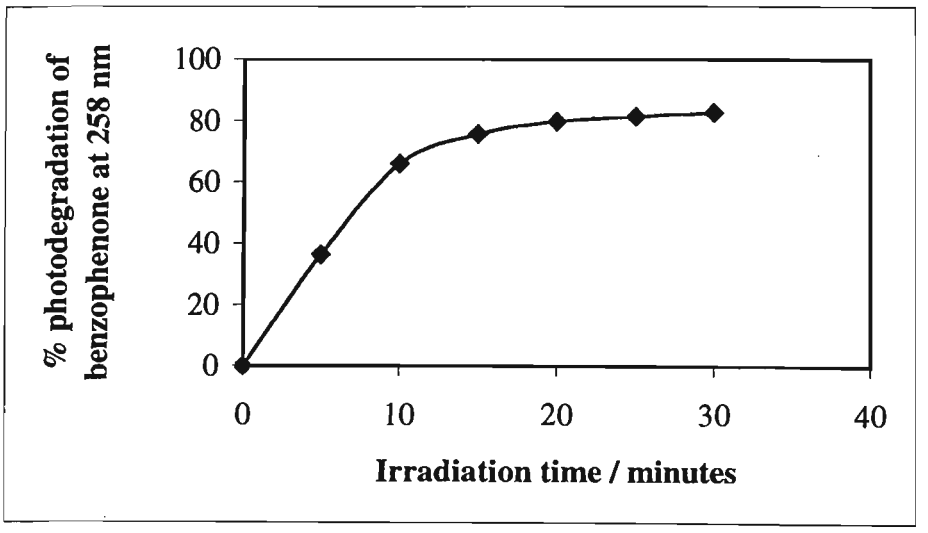

Figure 3.3: Percentage of photodegradation of benzophenone (5.5×10^{-4} M) in Tris-HCl buffer at 258 nm.

The photoreduction of benzophenone, and in particular the carbonyls, had been the subject of many photochemical studies in the 1900's and therefore the primary processes involved in its photochemistry are now largely understood. The mechanism involved in the photodegradation of benzophenone is shown in Figure 3.4 (Boscá & Miranda [1998]).

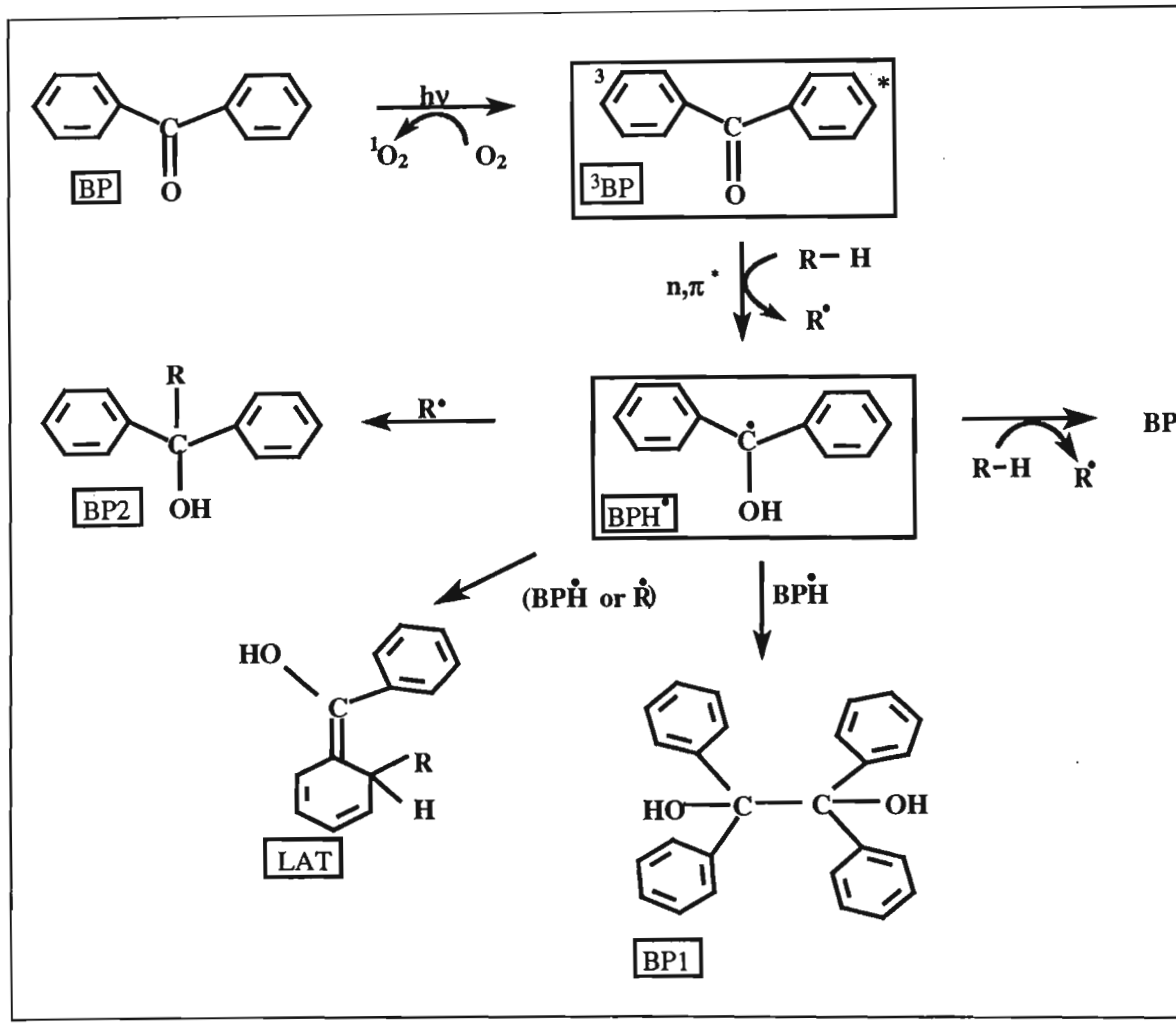

Figure 3.4: The mechanism of photodegradation of benzophenone (BP) (Boscá & Miranda [1998]).

Irradiation of benzophenone with UV light causes excitation of benzophenone from the ground state to its first excited singlet state (Figure 3.4). The efficiency of the intersystem crossing to the triplet state is determined by the quantum yield (ϕ_{ISC}), where a high value of ϕ_{ISC} indicates that intersystem crossing to a higher state occurs. Since ϕ_{ISC} for benzophenone is approximately one (Lamola & Hammond [1965]), the first excited state quickly intersystem crosses to the

triplet state (^{3}BP). In the excited triplet state, the electronic configuration of the molecule is n,π*, which implies that one of the lone pairs of electrons is promoted from a non-bonding orbital to the antibonding π orbital upon absorption of a photon. This leaves an unpaired electron in the non-bonding orbital located on the benzoyl carbonyl oxygen causing the excited oxygen to become electrophilic.

In the ^{3}n,π* state the characteristic primary reaction is hydrogen abstraction preferably from the surrounding solvent molecule resulting in the formation of a ketyl radical (BPH$^\bullet$). The resulting ketyl radical may either disproportionate to yield benzophenone (BP) again or it may dimerise to give benzopinacol (BP1) or even recombine with an alkyl radical to form a tertiary alcohol (BP2). Other usual products are the so-called light absorbing transients, which are formed by the recombination of BPH$^\bullet$ with itself or with other alkyl radicals. These species have been found to have an absorption at about 330 nm (Boscá ' & Miranda [1998] and Scaiano *et al.* [1982]). However, the major photoproducts are the hydroxybenzophenones and the benzopinacols. The hydroxyl radical adduct of benzophenone is known to occur at long UV wavelengths of approximately 390 nm (Ledger & Porter [1971]). These photoproducts formed at the longer UVA wavelengths accounts for the increase in absorbance observed in Figure 3.2, after about 290 nm.

The above results clearly support the lack of photostability of benzophenone towards sunlight-simulated light as it has been previously demonstrated (Charlier & Hélène [1972], Ledger & Porter [1971] and Scaiano *et al.* [1982]). Benzophenone decomposed almost completely in UV light, producing various photoproducts after only a short irradiation period thus demonstrating its inability to act appropriately as a sunscreen UV absorber. Luckily the use of benzophenone is not approved in sunscreen formulations in most countries. However in Australia its use is still under review (www.health.gov.au/tga/docs/pdf/sunscrai.pdf, date accessed: 6 December 2002). This is a definite cause for concern since it is quite clear from these results and results published elsewhere by other researchers that benzophenone's lack of photostability makes it an inefficient UV absorber, therefore its use in sunscreens should be strictly disapproved.

Ketoprofen

Ketoprofen, a non-steroidal anti-inflammatory drug, used in the treatment of arthritic diseases, is a UV absorber having the benzophenone chromophore (refer to its structure in Figure 3.5). Although this compound is not used in sunscreen formulations, its photostability was investigated so that a better understanding of its mechanism of DNA cleavage could be attained.

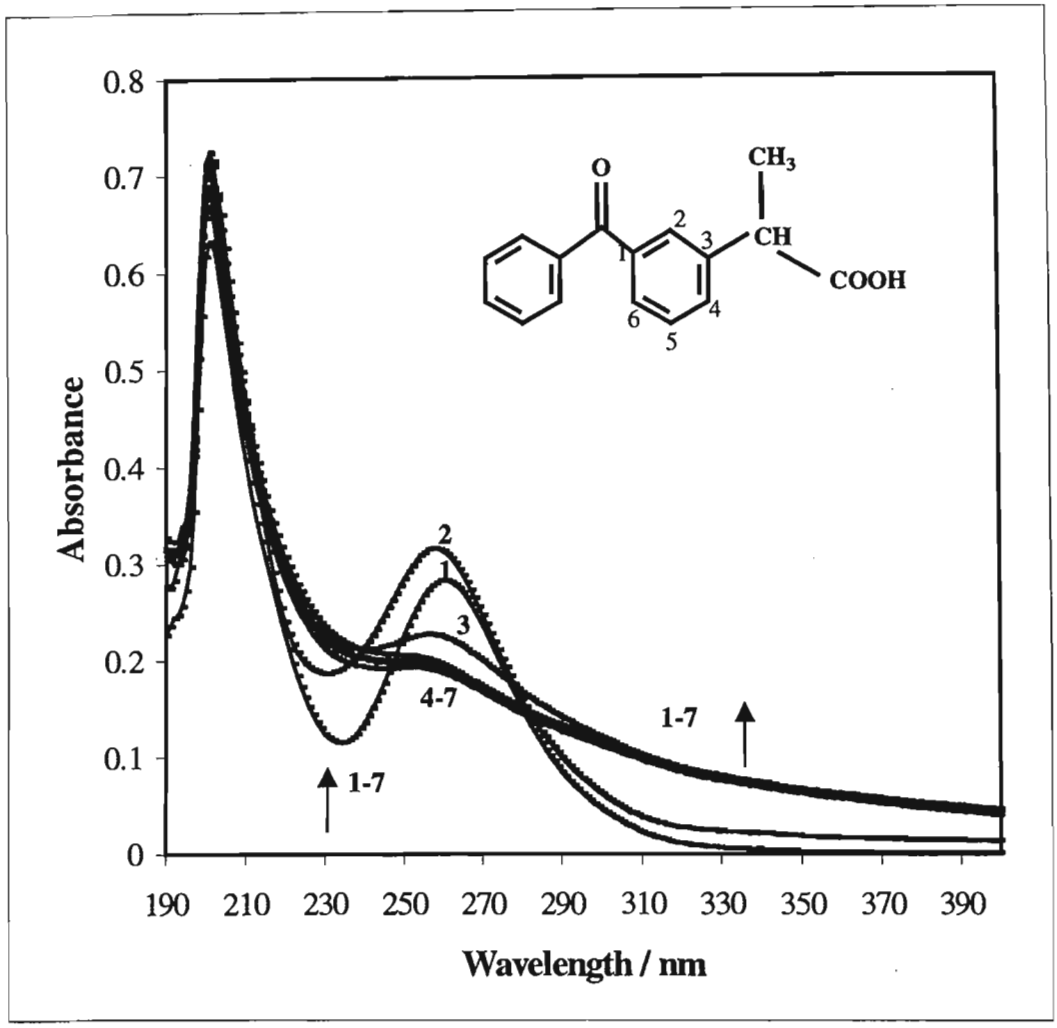

Figure 3.5: Changes in the absorption spectrum of ketoprofen (1 x 10^{-4} M) in Tris-HCl buffer with irradiation time where 1-7 in the Figure refer to 0, 5, 10 and 15 to 30 minutes of irradiation, respectively.

The absorption spectrum of ketoprofen without irradiation appeared very similar to that of benzophenone. It consisted of two peaks in the UVC region, that is, a major one at 201 nm and a weaker absorption band at 256 nm (Figure 3.5). This was attributed to the 3-benzoylpropanoic acid chromophore. When the 1 x 10^{-4} M solution of ketoprofen was irradiated, a rapid consumption of the compound at 256 nm was observed, but only after the first five minutes of irradiation. The absorbance band at 256 nm initially increased from 0.290 to 0.305 absorbance units (0-5 minutes) and thereafter for the rest of the irradiation period (5-30 minutes), a dramatic decrease in absorbance from 0.305 to 0.191 absorbance units was observed. The increase in absorbance for the first minutes of irradiation could have been due to the formation of a photoproduct, which on further irradiation degraded. Also it should be noted that increases in absorbance on both the red and blue sides of this band were observed. This behaviour was also observed during the irradiation of benzophenone, and again was indicative of a photochemical change.

The percentage of photodegradation of ketoprofen at 256 nm as a function of irradiation time appears in Figure 3.6. From this Figure it can been seen that only about 30% of ketoprofen was photodegraded after the entire irradiation period, compared to 80% photodegradation for benzophenone (Figure 3.3). The initial drop in photodegradation after the first five minutes could probably be attributed to the accumulative absorbance of another photoproduct that absorbed at 256 nm and thereafter degraded.

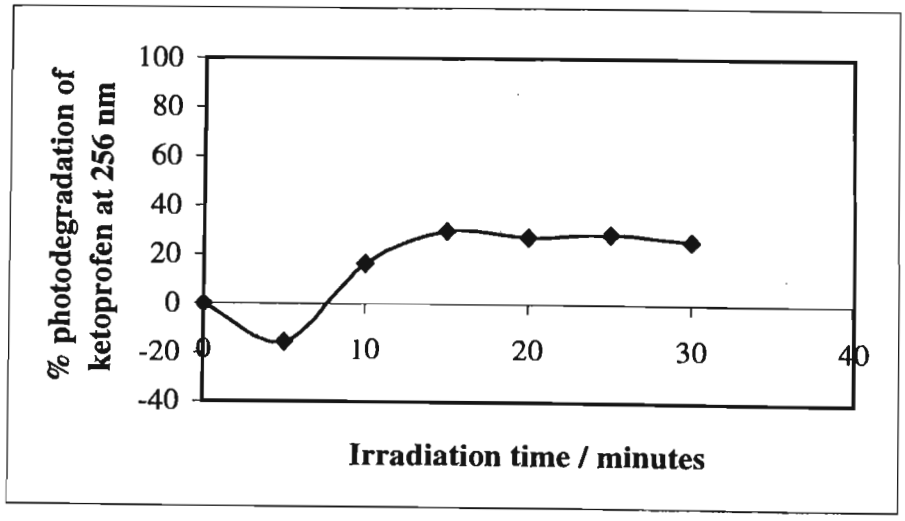

Figure 3.6: Percentage of photodegradation of ketoprofen (1 x 10^{-4} M) in Tris-HCl buffer at 256 nm.

Several studies have dealt with the photochemistry of ketoprofen (Boscá *et al.* [1994], Boscá & Miranda [1998] and Lhiaubet *et al.* [2001]). Nine different photoproducts have been identified in literature. The major photoproduct reported has always been 3-ethylbenzophenone whose yield according to Boscá *et al.* [1994] reaches a maximum, then progressively decreases on further irradiation. The photochemical reactivity of ketoprofen is dependent on the nature of its triplet-excited state. The lowest triplet state of ketoprofen is (n,π^*) with characteristics similar to its parent compound benzophenone (Lhiaubet *et al.* [2001]). The triplet state of ketoprofen leads to the formation of a ketyl radical by hydrogen abstraction from the solvent. This is characteristic of the (n,π^*) of benzophenone (Lhiaubet *et al.* [2001]).

A brief outline of the mechanism involved in the photodegradation of ketoprofen follows (Figure 3.7). Ketoprofen (1) exists at physiological pH (pH 7-8) as the dissociated acid (1^-) (Boscá *et al.* [1994]). On irradiation, the dissociated acid undergoes decarboxylation, which results in the formation of the benzylic radical ($2^\bullet$) and the evolution of carbon dioxide. This process is also associated with the ejection of an electron, which in the presence of oxygen would be scavenged to give the superoxide radical anion. Hydrogen abstraction by the benzylic radical results in the formation of 3-ethylbenzophenone (2). However, the benzylic radical may also in the presence of oxygen (or superoxide anion) produce a number of oxygenated products, one of which is shown as 3 in Figure 3.7. On further irradiation, the benzophenone chromophore of 2 becomes excited, and as for benzophenone (Figure 3.4) undergoes hydrogen abstraction. This explains the reduction in the yield of 3-ethylbenzophenone as observed by Boscá *et al.* [1994]. Hydrogen abstraction by the benzophenone chromophore produces the corresponding ketyl radical ($2H^\bullet$) from which various photoproducts similar to those formed with benzophenone are then possible.

These results clearly demonstrate lack of stability of ketoprofen towards UV radiation. These findings support those of Boscá *et al.* [1994], Boscá & Miranda [1998] and Lhiaubet *et al.* [2001]. Luckily, ketoprofen is not used in sunscreens as a UV absorber and its use therein should not be allowed.

Eusolex 232

The UV absorber 2-phenylbenzimidazole-5-sulphonic acid, commonly known by its trade name as Eusolex 232, is frequently used in sunscreen formulations. It has a benzophenone-derived

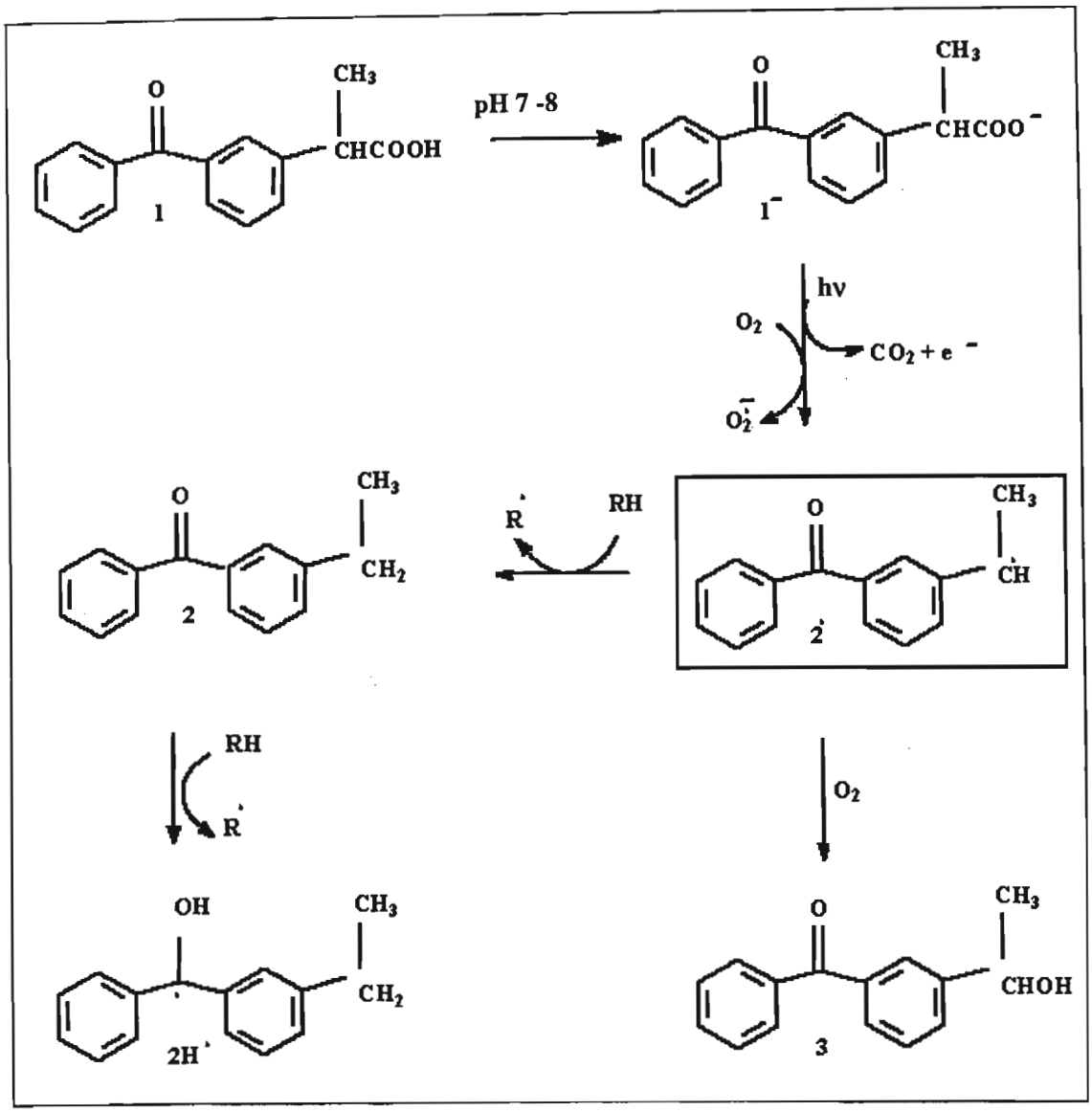

Figure 3.7: The mechanism of photodegradation of ketoprofen (Boscá *et al.* [1994]).

backbone, where the benzoyl chromophore has been substituted with an indole group, and a sulphonic acid group appears at the 5 position (structure in Figure 3.8).

The absorption spectrum of Eusolex 232 had 3 absorption peaks, one in the UVB region of the spectrum and two in the UVC region (Figure 3.8). When this spectrum was compared to that of benzophenone, the following observations were made. The absorption peak at 208 nm had been

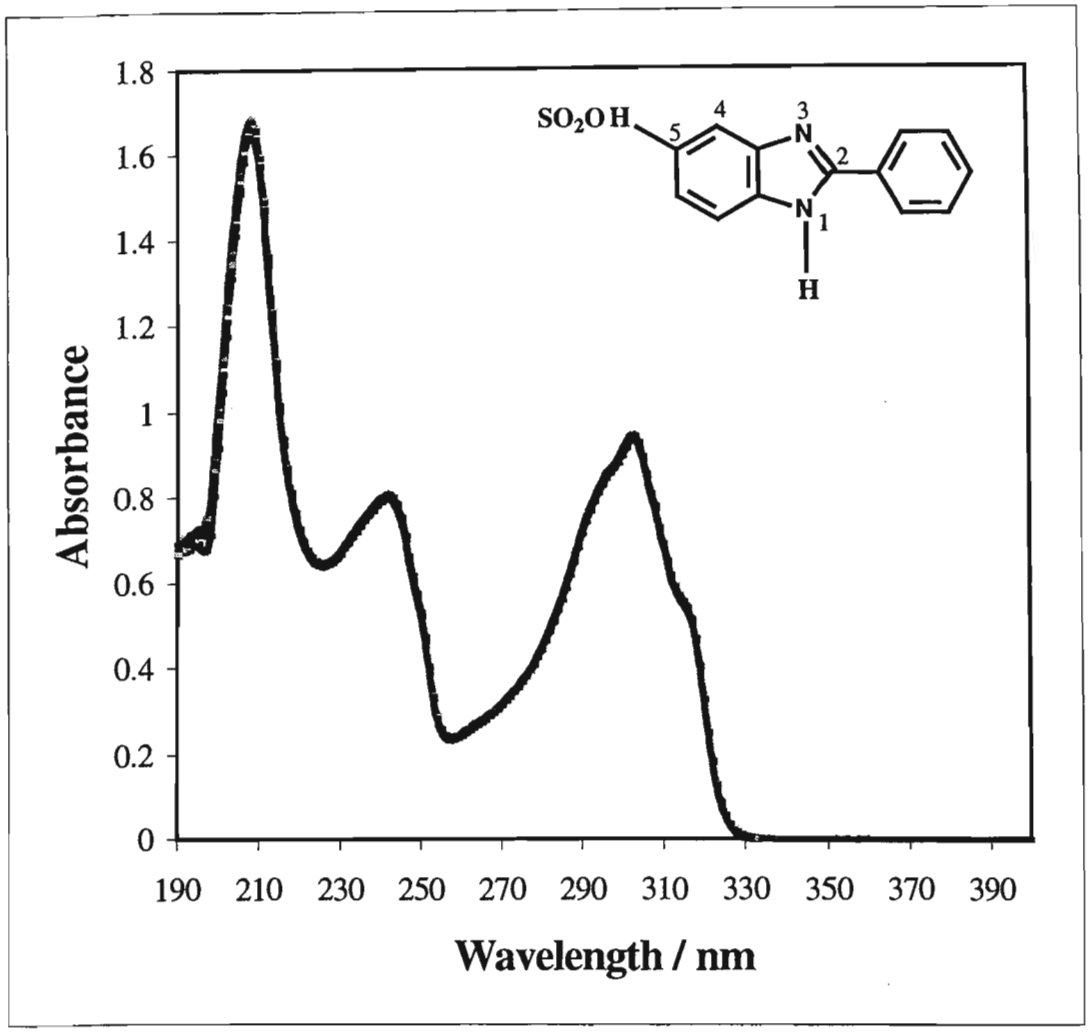

Figure 3.8 Changes in the absorption spectrum of Eusolex 232 (5.5×10^{-4} M) in Tris-HCl buffer after 0, 5, 10, 15, 20, 25 and 30 minutes of irradiation.

shifted to a slightly lower wavelength compared to benzophenone, while the transition maximum at 258 nm for benzophenone now appeared at 303 nm. This was be attributed to the 2-phenylimidazole chromophore. The appearance of another transition at 242 nm was assigned to the phenyl sulphonic acid chromophore.

Irradiation of a solution of Eusolex 232 (5.5 x 10^{-4} M) in Tris-HCl buffer with an Osram HBO 500W/2 high pressure mercury lamp at wavelengths greater than 300 nm induced no changes in the UV spectrum as can be seen from Figure 3.8. Even after 30 minutes of irradiation, it is quite clear that Eusolex 232 was very stable against UVB and UVA radiation and did not undergo any photodegradation at 303 nm (Figure 3.9). These findings support those obtained by Stevenson & Davies [1999] and Chignell *et al.* [2002] who also reported Eusolex 232 to be stable towards photodecomposition under UV irradiation.

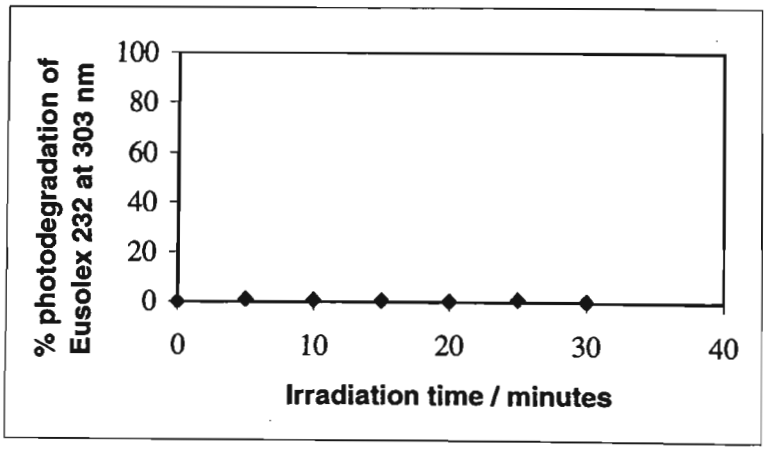

Figure 3.9: Percentage of photodegradation of Eusolex 232 (5.5 x 10^{-4} M) in Tris-HCl buffer at 303 nm.

Therefore, it can be concluded that in terms of photostability, Eusolex 232 behaved like an ideal UV absorber and when used in sunscreen formulations it would effectively protect human skin from UV radiation.

3.1.2 Photostability of benzophenone-1, benzophenone-3, benzophenone-4 and Uvinul DS49

The broad-spectrum absorbers studied in this investigation were benzophenone-1, benzophenone-3, benzophenone-4 and Uvinul DS49. In order for these compounds to act

effectively as UV absorbers in sunscreens or cosmetics they must display photostability towards UV radiation.

All of these UV absorbers have the benzophenone chromophore and demonstrated similar photostability patterns towards UVB and UVA radiation, however, their behaviour to UV radiation differed substantially from that of their parent compound benzophenone. These UV absorbers are grouped according to similar chemical structures and discussed below.

Benzophenone-1 and Benzophenone-3

Benzophenone-1 (or 2,4-dihydroxybenzophenone) and benzophenone-3 (or 2-hydroxy-4-methoxybenzophenone) absorb UV radiation in both the UVB and UVA regions of the spectrum (Figures 3.10 and 3.11 respectively). They are considered as broadband filters and are incorporated in cosmetics and sunscreen formulations to offer broad-spectrum protection.

The small difference in structure between benzophenone-3 and benzophenone-1 was reflected in their UV spectra, where benzophenone-1 offered a greater absorption in the UVA region of the spectrum than benzophenone-3. This was attributed to the replacement of the methoxy substituent in benzophenone-3 with the hydroxyl substituent in benzophenone-1.

When the absorption spectra of benzophenone-1 and benzophenone-3 were compared to that of benzophenone, the following observations were made. The absorption maximum at 201 nm present in benzophenone (Figure 3.2) appeared in both these UV absorbers (Figures 3.10 and 3.11). The absorbance maximum at 258 nm for benzophenone, however, was now shifted to 344 nm for benzophenone-1 and for benzophenone-3 it appeared at 290 nm with a shoulder in the band at about 330 nm. These shifts in absorbance in the spectra of benzophenone-1 and benzophenone-3 could be attributed to the para-hydroxybenzoyl and the para-methoxybenzoyl chromophores respectively. The appearance of another transition at 249 nm in benzophenone-1 and around 242 nm in benzophenone-3 could be due in both cases to the *ortho*-hydroxy substituent on the benzoyl chromophore.

Upon irradiation of 5.5 x 10^{-4} M solutions of benzophenone-1 and benzophenone-3 in Tris-HCl and 50% (v/v) ethanol: Tris-HCl buffers respectively, both these UV absorbers appeared fairly stable against UV radiation at wavelengths greater than 300 nm. Benzophenone-3, however, showed a greater stability towards UV radiation in the polar Tris buffer when compared to benzophenone-1 and underwent almost no photodegradation (Figure 3.12). These findings are

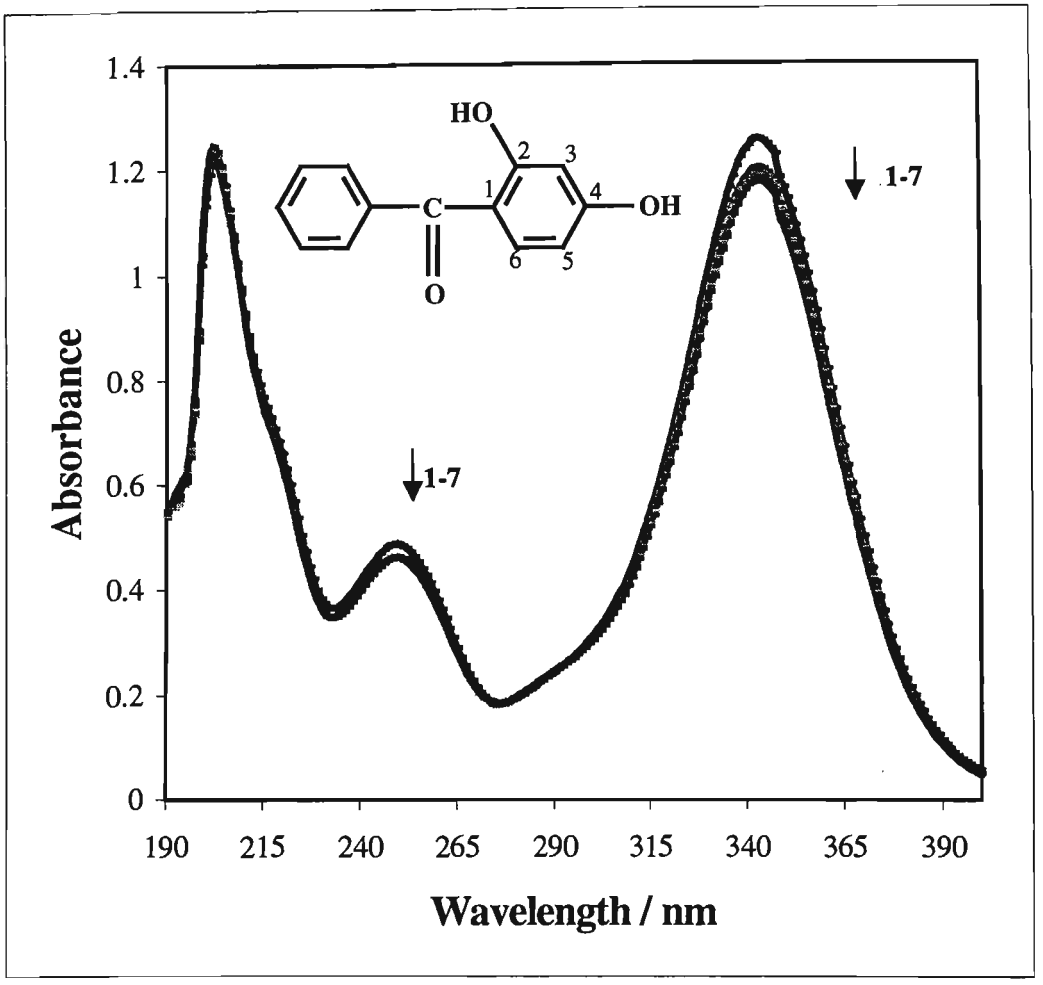

Figure 3.10: Changes in the absorption spectrum of benzophenone-1 (5.5×10^{-4} M) in Tris-HCl buffer with irradiation time where 1-7 refer to 0, 5, 10, 15, 20 , 25 and 30 minutes of irradiation, respectively.

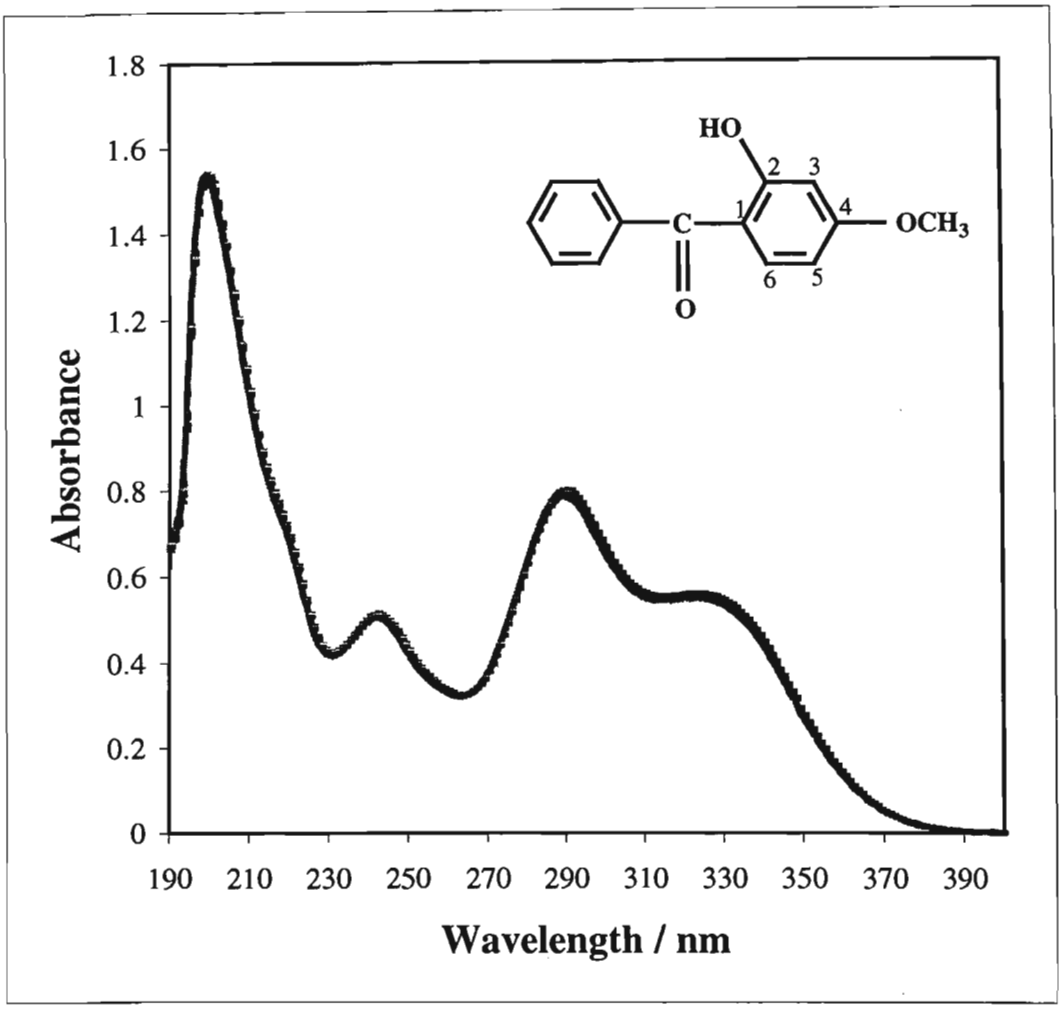

Figure 3.11: Changes in the absorption spectrum of benzophenone-3 (5.5×10^{-4} M) in 50% (v/v) ethanol:Tris-HCl buffer after 0, 5, 10, 15, 20, 25 and 30 minutes of irradiation.

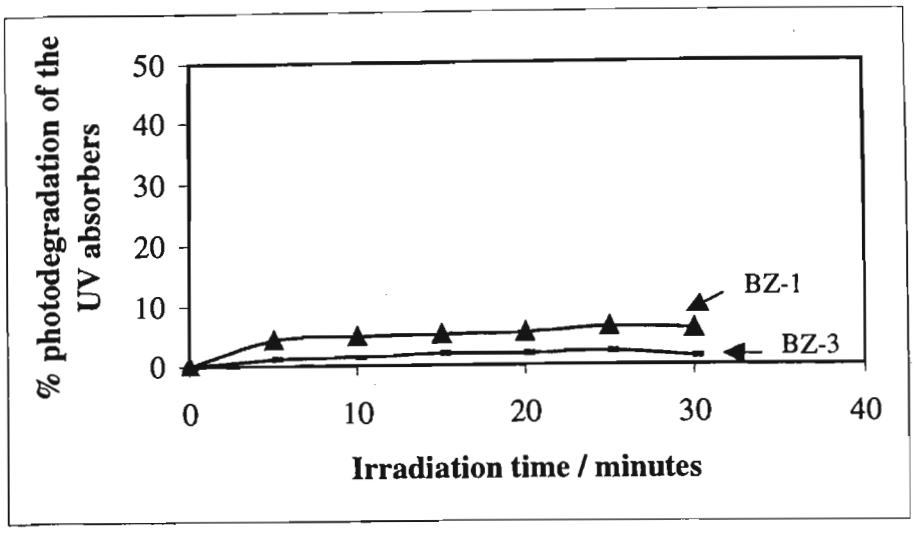

Figure 3.12: Comparison of the percentage of photodegradation of benzophenone-1 (BZ-1) (at 344 nm in Tris-HCl buffer) and benzophenone-3 (BZ-3) (at 322 nm in 50% (v/v) ethanol: Tris-HCl buffer) for solutions of same the concentration (5.5 x 10^{-4} M).

in agreement to those obtained by Roscher *et al* [1994] who demonstrated the photostability of benzophenone-3 even after 100 hours of irradiation with UV light. This team used a non-polar solvent compared to the polar Tris-HCl buffer, which was used in this study. However, these findings do contrast with the photochemical studies performed by Serpone *et al.* [2002] using an Oriel 1000 W Hg/Xe lamp. This team demonstrated that benzophenone-3 degrades by 20% in water and by 90% in the polar solvent methanol after two hours of irradiation.

In the case of benzophenone-1, the absorption spectra revealed that after 30 minutes of irradiation a small change in the absorption maximum at 344 nm had occurred. However, this change was negligible when compared to benzophenone since only about 5% of benzophenone-1 photodegraded (Figure 3.12).

The lack of photodegradation of both benzophenone-1 and benzophenone-3 could be attributed to the substituents present on the benzophenone chromophore. Literature reveals that intermolecular hydrogen abstraction by benzophenone is dependent on the polarity of the solvent and on the substituent present. Substituted benzophenones have been shown to display dramatic differences in their photoreactivity (Calvert & Pitts [1967], Boscá & Miranda [1998]).

It has been well established that the hydrogen-atom abstracting state of benzophenone is the lowest n,π* triplet (Calvert & Pitts [1966]). The presence of electron-donating substituents such as *para*-amino, *para*-hydroxy, *para*-phenyl or *para*-dimethylamino groups greatly reduces the tendency for intermolecular hydrogen-atom abstraction in polar solvents (Boscá & Miranda [1998]). In contrast, the reaction still proceeds in non-polar solvents. The quenching of photoreduction in polar solvents by electron-donating substituents on the benzophenone chromophore can be attributed to a change in the nature of the lowest triplet state from $^3(n,\pi^*)$ to $^3(\pi,\pi^*)$. This change brings about a decrease in the chemical reactivity of the lowest triplet state of the benzophenone chromophore. The attachment of electron-withdrawing groups, however, demonstrates high efficiency for hydrogen abstraction since these groups do not alter the typical n,π* character of the lowest triplet state (Boscá & Miranda [1998]). Therefore it can be deduced that the electron-donating substituents, that is, -OH in benzophenone-1 and -OH and $-OCH_3$ in benzophenone-3, are responsible for the lack of photodegradation in these two UV absorbers in the polar solvent water.

In addition, for some benzophenones intramolecular hydrogen abstraction reactions involving photoenolization have been proposed as being responsible for the quenching of the benzophenone photoreduction (Calvert & Pitts [1967]). According to Tarras-Wahlberg *et al.* [1999], certain substituted benzophenones can act as sensitizers and catalyze photodecomposition reactions. The mechanism of this photoreaction is illustrated for benzophenone-3 in Figure 3.13.

Since both benzophenone-1 and benzophenone-3 have demonstrated stability towards photodecomposition when exposed to UV light, they can be considered as efficient UV absorbers when used in sunscreen formulations.

Benzophenone-4 and Uvinul DS49

Benzophenone-4 (or 2-hydroxy-4-methoxy benzophenone-5-sulphonic acid) and Uvinul DS49 (or 2,2'-dihydroxy-4,4'-dimethoxy benzophenone sulphonic acid) are both wide range UV absorbers, absorbing in both the UVA and UVB regions (Figures 3.14 and 3.15 respectively). The absorption spectra of both these UV absorbers differed substantially from that of benzophenone. This is attributed to the substituents present on the benzophenone chromophore. In addition to the hydroxyl and methoxy groups, benzophenone-4 and Uvinul DS49 both contain the sulphonic acid substituent. The presence of the sulphonic acid group makes both these UV absorbers water-soluble.

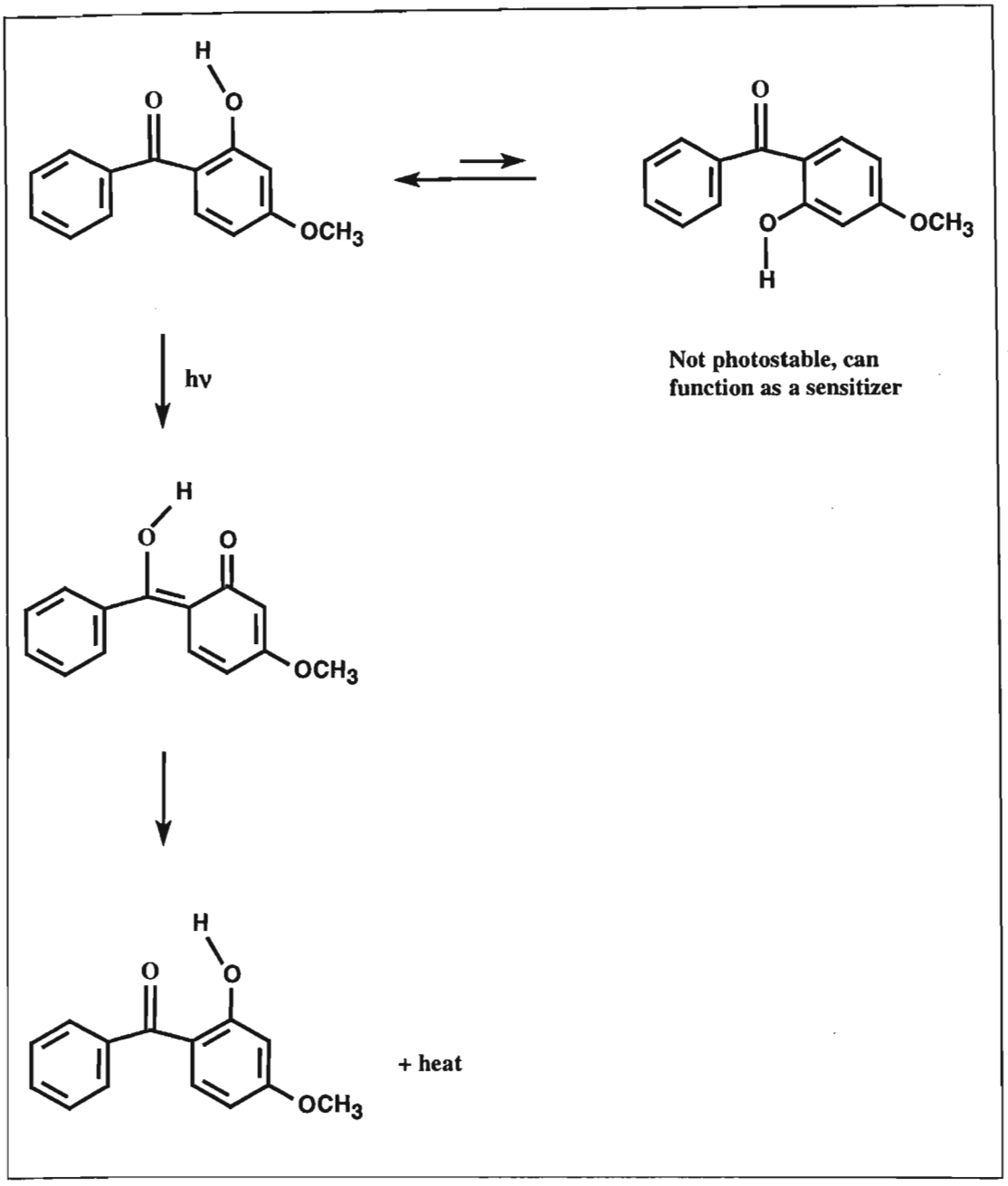

Figure 3.13: Photoreaction mechanism of benzophenone-3 (Tarras-Wahlberg *et al.* [1999]).

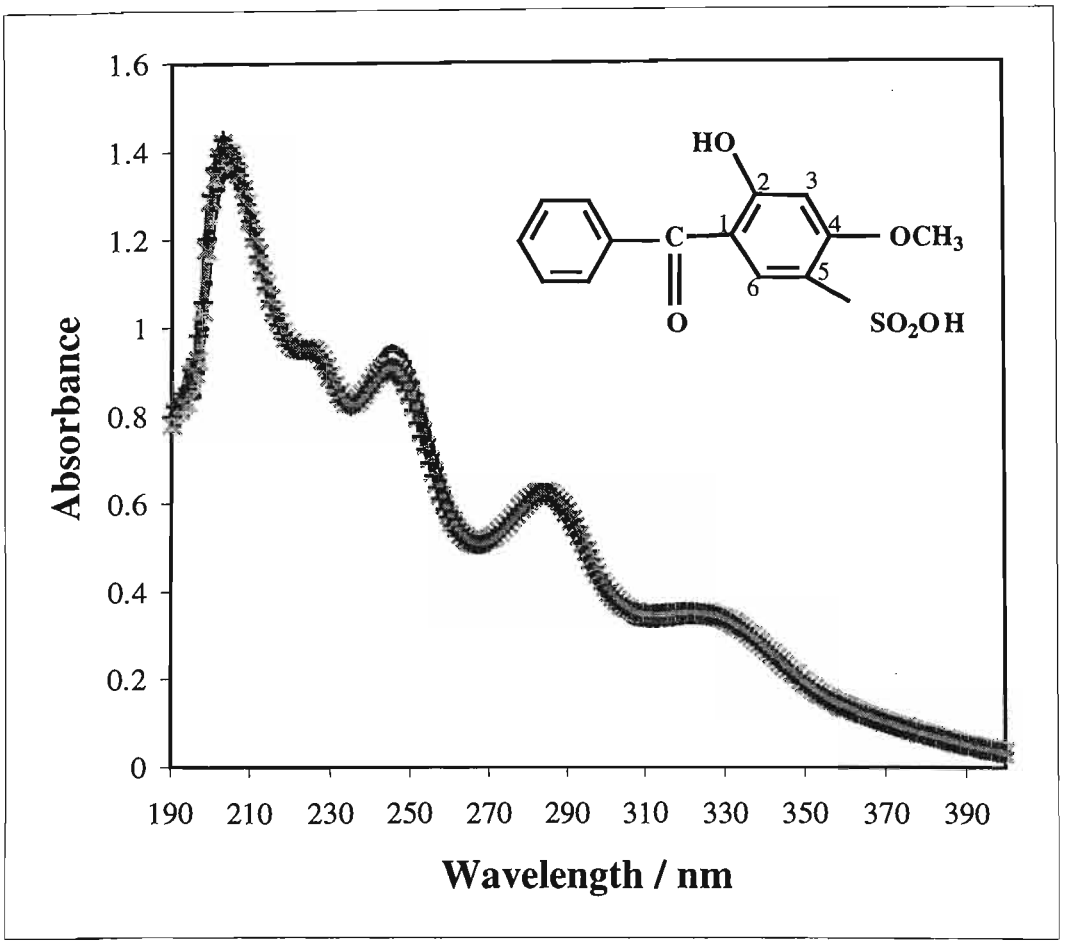

Figure 3.14: Changes in the absorption spectrum of benzophenone-4 (5. 5x 10^{-4} M) in Tris-HCl buffer after 0, 5, 10, 15, 20, 25 and 30 minutes of irradiation.

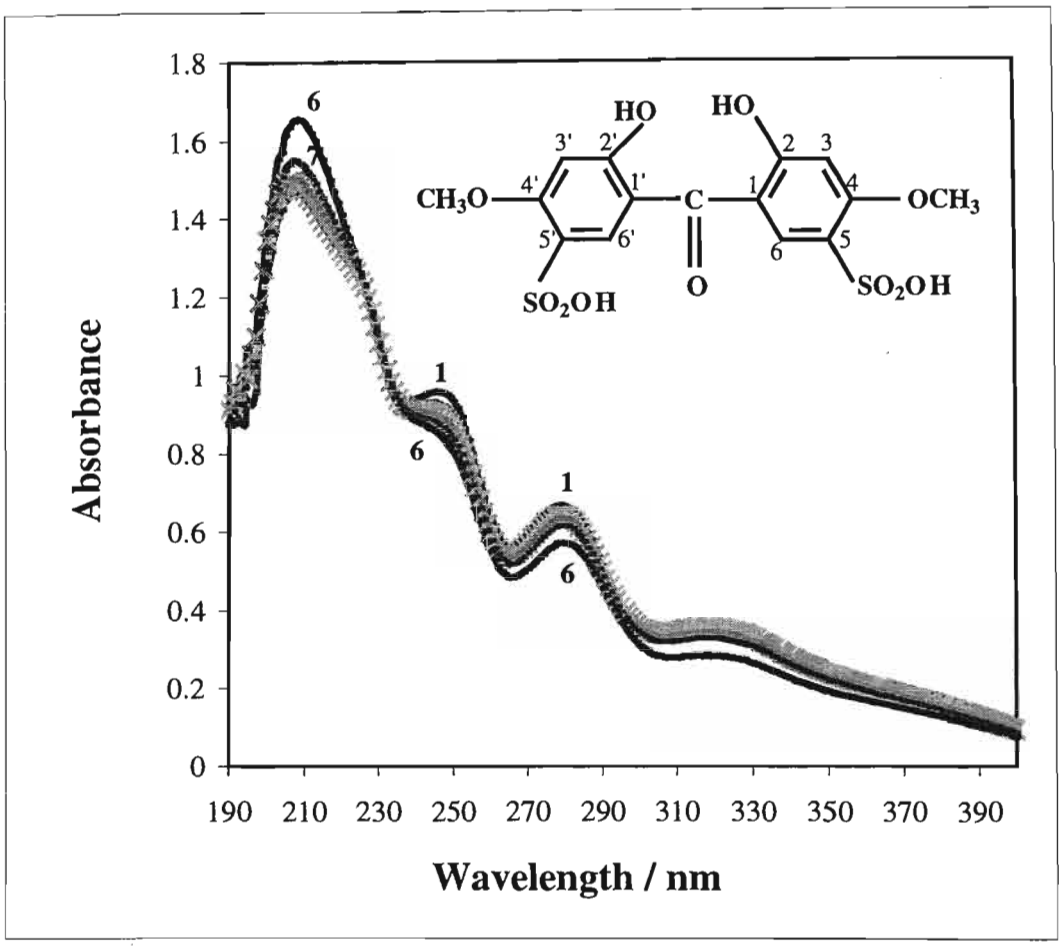

Figure 3.15: Changes in the absorption spectrum of Uvinul DS49 (6.5×10^{-4} M) in Tris-HCl buffer after 0, 5, 10, 15, 20, 25 and 30 minutes of irradiation.

When the spectrum of benzophenone-4 was compared to that of benzophenone-3 similar absorbance peaks were observed, except the presence of the sulphonic acid group in benzophenone-4 greatly increased the intensity of the absorbance at about 245 nm. The absorbance spectra of benzophenone-4 and Uvinul DS49 were very similar due to the presence of the same substituents on the benzophenone backbone. The addition of a 2-OH, 4-OCH_3 and 5-SO_2OH on both the phenyl groups in Uvinul DS49 did not cause any significant change in the absorption spectrum when compared to that of benzophenone-4.

Upon irradiation of benzophenone-4 (5.5×10^{-4} M) and Uvinul DS49 (6.5×10^{-4} M) in Tris-HCl buffer with an Osram HBO 500W/2 high pressure mercury lamp at wavelengths greater than 300 nm, both these UV absorbers appeared fairly stable against UV radiation. After 30 minutes of irradiation no changes in the absorption spectrum of benzophenone-4 were observed. For Uvinul DS49, however, the absorbance peaks at 245 nm, 279 nm and 318 nm decreased slightly for the first 25 minutes of irradiation, while an increase in absorbance at 208 nm was observed. Thereafter, for the last five minutes of irradiation the opposite effect was observed, that is, the absorbance peaks at 245 nm, 279 nm and 318 nm increased, while that at 208 nm decreased. The biggest change in absorbance was observed at 208 nm where the absorbance increased from 1.472 units to 1.655 units during the first 25 minute irradiation period, and thereafter dropped to 1.550 units.

Figure 3.16 compares the percentage of photodegradation of benzophenone-4 and Uvinul DS49 at 321 and 318 nm respectively. What is clear here is that Uvinul DS49 was not as photostable as benzophenone-4 when illuminated with UV light. The maximum amount of Uvinul DS49 that photodegraded is about 25%, which occurred after 25 minutes of irradiation at 318 nm and thereafter photodegradation decreased. This could possibly be due to the photodegradation of Uvinul DS49 during the first 25 minutes of irradiation, and on further irradiation a photoproduct possibly was formed which contributed to an accumulative absorbance at 318 nm after 30 minutes of irradiation. However, this level of photochemical change was relatively small if one compared it to that of benzophenone.

This relative lack of photodegradation can be attributed to the substituents present on the benzophenone chromophore. Benzophenone-4 and Uvinul DS49 both possess two electron-donating groups (-OH and -OCH_3) and one electron-withdrawing group (-SO_2OH). Ideally, the presence of the electron-withdrawing group should not alter the $^3(n,\pi^*)$ state and should promote hydrogen abstraction while the electron-donating groups should not, as discussed previously (Boscá & Miranda [1998]). Since photodegradation of benzophenone-4 did not occur and that of Uvinul DS49 was limited, it can therefore be assumed that the effect of the

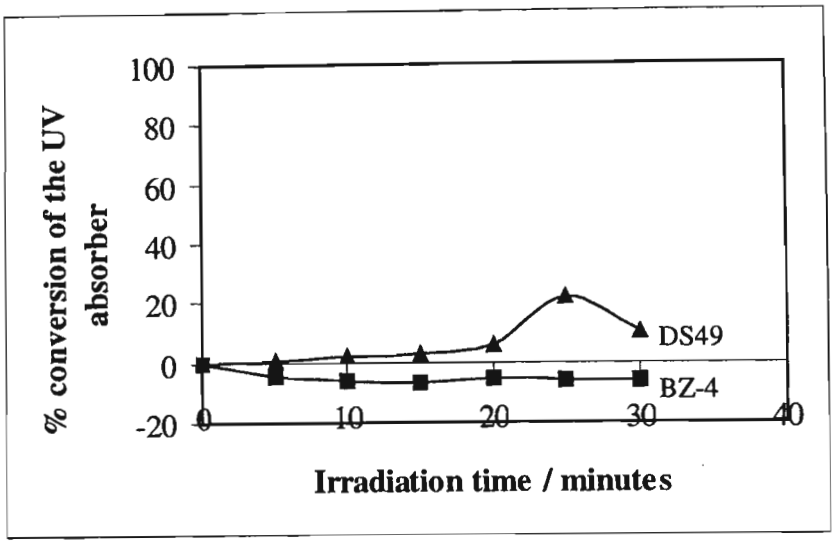

Figure 3.16: Comparison of the percentage of photodegradation of benzophenone-4 (BZ-4) (at 321 nm) and Uvinul DS49 (DS49) (at 318 nm) for solutions of similar concentration (5.5×10^{-4} M and 6.5×10^{-4} M respectively) in Tris-HCl buffer.

electron-donating groups was greater than that of the electron-withdrawing groups which resulted in the quenching of hydrogen abstraction by these UV absorbers.

The above results have demonstrated that the UV absorbing agent benzophenone-4 was photochemically stable and will act as an effective UV absorber when used in a sunscreen formulation, while Uvinul DS49 appeared relatively stable and the little photodegradation that was seen was not to the same extent as that for the parent compound benzophenone.

3.2 Gel electrophoresis to detect DNA cleavage

Agarose gel electrophoresis is the standard method used to separate and identify nucleic acids. The DNA-agarose nicking assay adapted from Artuso *et al.* [1991] was performed to identify DNA cleavage induced by the presence of a group of benzophenone-based UV absorbers. The experimental procedures conducted have been described in Section 2.3 and a discussion of these results will now follow.

Section 3.2.1 describes the identification of the three forms of ϕX174 DNA by the suitability assay. These forms demonstrate different migration rates in an electrophoresis system and can be identified by their migration rates. Preliminary experimental results obtained for the known photocleaver ketoprofen, appear in Section 3.2.2. The results for the photocleavage activity of

benzophenone, benzophenone-1, benzophenone-3, benzophenone-4, Uvinul DS49 and Eusolex 232, which were demonstrated by irradiating these UV absorbers (50 μM) for specific time periods (0 - 45 minutes) at wavelengths greater than 300 nm in the presence of buffered aqueous solutions of ϕX174 DNA (18.85 μM) appear in Sections 3.2.4 - 3.2.5. A mole ratio of DNA bp: UV absorber of 1: 2.7, i.e. approximately 1: 3, was used since studies conducted by Marguery *et al.* [1998] suggest that this mole ratio is required to obtain the maximum number of SSB. Due to the extreme sensitivity of this technique, small volume changes during DNA handling and irradiation of the samples, variations in lane-to-lane gel loading, as well as differences in pipetting became increasingly significant, and therefore it was necessary to perform the assay at least in duplicate. A control experiment, which was set up in the absence of the UV absorbers, was subjected to the identical conditions as the experiments and the results obtained for the control appear in Section 3.2.3.

3.2.1 Identification of the DNA Forms by the suitability assay

The suitability assay was necessary since it enabled the DNA Forms I, II and III to be identified. The assay involved digesting ϕX174 DNA with *Pst 1* enzyme (which cleaves the circular Form I DNA only once) and running this digest on a 1% agarose gel against a control of undigested DNA. The undigested ϕX174 DNA was found to contain 80% supercoiled and 20% nicked circular DNA, as stipulated by the supplier (Sigma). This enabled DNA Forms I and II to be identified in the undigested DNA control. *Pst 1* catalyses the formation of double strand breaks and converts supercoiled Form I DNA to the linear Form III (Smith *et al.* [1976]) thus enabling the linear DNA Form III to be identified in the digested sample. The samples were prepared and loaded as described in Section 2.3.6 after which electrophoresis was performed. The ethidium bromide-stained agarose gel was viewed with a Hoefer transilluminator and was photographed with a digital camera, since at this point the electrophoresis photography system was not set up.

The photograph of the ethidium bromide stained agarose gel showing the three DNA forms appears in Figure 3.17. From the control lanes 1, 3 and 5 (undigested ϕX174 DNA), the fastest migrating bands (lower band in lanes 1, 3 and 5) corresponded to approximately 80% of the DNA sample and represented the supercoiled Form I DNA. The band of slower electrophoretic mobility in the control lanes corresponded to approximately 20% DNA and was the nicked circular DNA Form II.

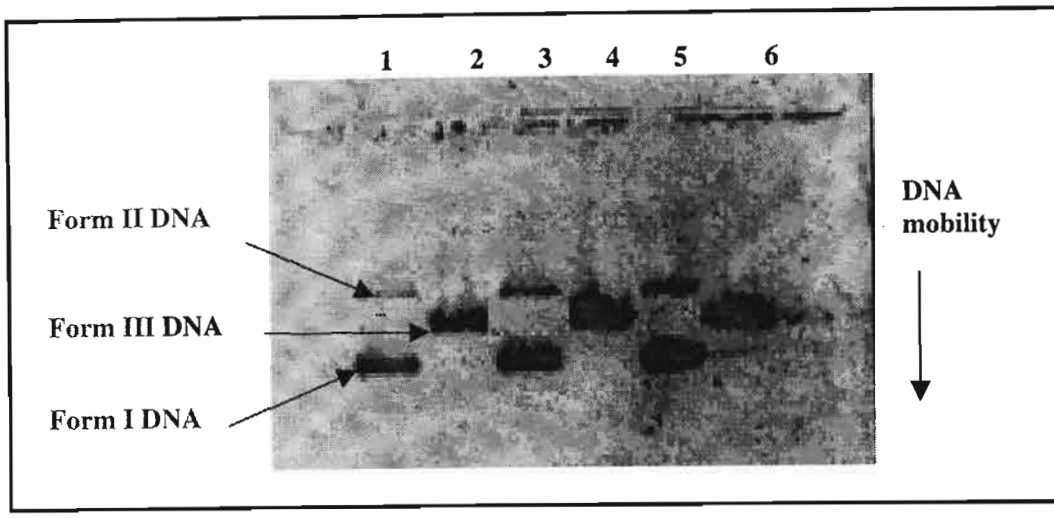

Figure 3.17: Ethidium bromide-stained agarose gel showing enzymatic cleavage of ϕX174 DNA with *Pst 1*. The DNA samples were treated with the enzyme for two hours at 37°C. Lanes 1, 3 and 5 contain 5, 10 and 15 µl, respectively, of undigested ϕX174 DNA (control) while lanes 2, 4 and 6 contain 5, 10 and 15 µl of *Pst 1* digested ϕX174 DNA.

Volumes of 5, 10 and 15 µl of the *Pst 1* digest, which were loaded into lanes 2, 4 and 6 respectively, showed the presence of only one band. This was attributed to the linear DNA (Form III), since digestion of ϕX174 DNA with the enzyme *Pst 1* catalysed double strand breaks in supercoiled DNA and converted it to the linear form. From this assay it was concluded that the compact Form I DNA migrated the fastest, followed by the rod-like linear Form III DNA, while the nicked circular Form II DNA had the slowest mobility. These rates of DNA migration were used to identify the DNA Forms in all the agarose gels analysed.

3.2.2 Ketoprofen photosensitization of DNA cleavage

To ensure that DNA photocleavage could be successfully detected by the DNA-agarose nicking assay, a preliminary electrophoresis experiment was performed using the known photocleaver ketoprofen. Artuso *et al.* [1991] have shown by *in vitro* studies that under UV irradiation, ketoprofen, a drug having the benzophenone chromophore and used for the treatment of arthritic diseases, photosensitizes DNA cleavage. Ketoprofen was therefore used as a standard to assess the sensitivity of the electrophoresis system.

The samples were prepared as described in Table 2.3 of Section 2.3.7. Samples 1 and 3 contained DNA alone in a buffered solution and served as the control, while samples 2 and 4 contained in addition to the buffered DNA, ketoprofen, and were the experiments. To demonstrate the photocleavage activity of the drug, ϕX174 DNA (18.85 μM) was irradiated for 30 minutes at wavelengths greater than 300 nm in the presence or in the absence of a buffered aqueous solution of ketoprofen (11.25 μM). The irradiations were carried out with an Osram HBO 500 W/2 high-pressure mercury lamp in combination with a 10 mm thick Pyrex filter. The photosensitized DNA cleavage was followed by agarose gel electrophoresis as described in Section 2.3.8. Samples 1-4 were loaded into lanes 1-4 respectively. A Hoefer Scientific transilluminator was used to view the gel and the gel was photographed with the aid of a digital camera. The reverse image of the ethidium bromide-stained agarose gel appears in Figure 3.18.

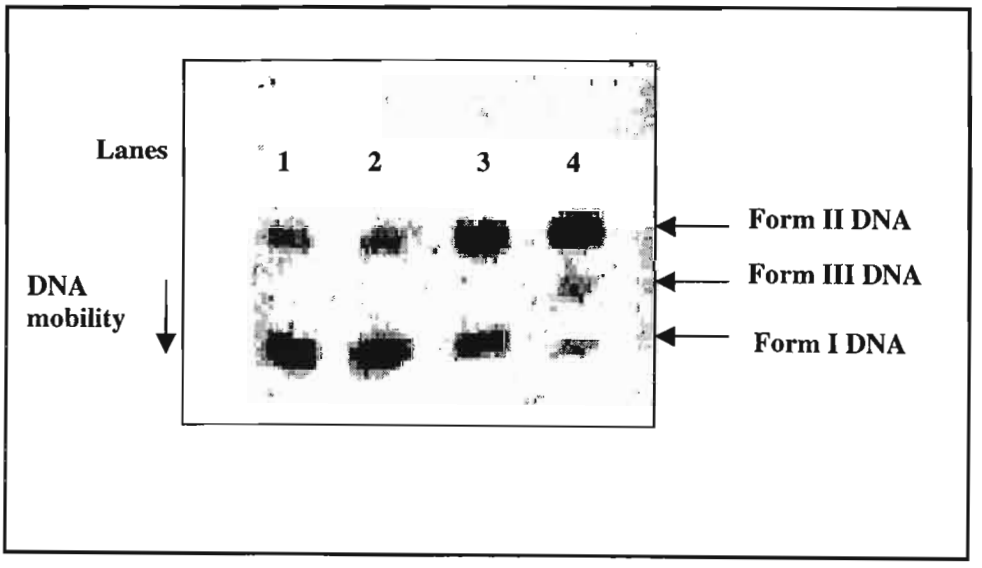

Figure 3.18: Agarose electrophoresis gel showing cleavage of ϕX174 DNA in the presence of ketoprofen (KP). Lane 1: no KP, no irradiation (dark control), Lane 2: KP present, no irradiation, Lane 3: no KP, with 30 minutes irradiation (light control) and Lane 4: KP present, with 30 minutes irradiation.

From Figure 3.18 it can be seen that the original DNA content in lane 1 (dark control) was approximately 80% in the supercoiled Form I DNA (lower band) and 20% nicked circular DNA Form II (top band). In the presence of ketoprofen, but in the absence of irradiation, no change in the DNA composition was observed (see lane 2). Upon irradiation of ϕX174 DNA for 30

observed as evidenced by the increase in the amount of Form II DNA and the decline in the amount of Form I DNA. Cleavage was even more significant in the presence of ketoprofen (compare lanes 3 and 4), as a distinct band of intermediate mobility between DNA Forms I and II, identical to that observed by the treatment of supercoiled DNA with *Pst I* (see Figure 3.17) was also present. This band was due to the linear DNA Form III.

When the ϕX174 DNA was irradiated alone at $\lambda > 300$ nm for 30 minutes, 40% of the DNA was in the supercoiled form, with the remaining 60% in the nicked circular. The proportions of DNA Forms produced on irradiation of the DNA in the presence of ketoprofen for 30 minutes was approximated to be 5% supercoiled (Form I DNA), 85% nicked circular (Form II DNA) and 10% linear DNA (Form III DNA). These results agree with those obtained by Artuso *et al.* [1991], and this technique was used to study the photocleavage efficiency of the benzophenone-derived UV absorbers under investigation.

3.2.3 Photocleavage of ϕX174 DNA at $\lambda > 300$ nm (control)

UV irradiation of DNA at wavelengths characteristically absorbed by the common nucleic acid bases (240 - 280 nm) is known to induce SSB with low yields (Rahn & Patrick [1976]). In order to determine the extent of cleavage induced by the irradiation of DNA alone at wavelengths greater than 300 nm, ϕX174 DNA (18.85 μM) was irradiated for a total irradiation period of 45 minutes with an Osram HBO 500W/2 high pressure mercury lamp, in conjunction with a 10 mm thick Pyrex filter. This assay served as the control and has been tabulated in Section 2.3.7 (Table 2.4). Due to the extreme sensitivity of this technique, the control was repeated several times. The ethidium bromide-stained agarose gel as well as the densitometric lane graphs for each gel (where available) appear in Figures 3.19 - 3.24.

The gels in Figures 3.19A and 3.20A were viewed and photographed with a Syngene transilluminator that had been connected to a Vacutec camera system (Figure 2.9 in Section 2.3.9). For this photography system the Hoefer Scientific densitometer was used to quantify the DNA bands (Figure 2.11 in Section 2.3.10) and the lane graphs obtained appear in Figures 3.19B and 3.20B respectively. This required cutting and weighing of the respective peaks as described in Section 2.3.10. The gels in Figures 3.21 - 3.24, however, were viewed and photographed with a Hoefer Scientific transilluminator that had been connected to a Panasonic CCTV camera (Figure 2.10 in Section 2.3.9). Quantitation of the DNA bands was by means of the Scion imaging software and the densitometric lane graphs appear with the respective gels.

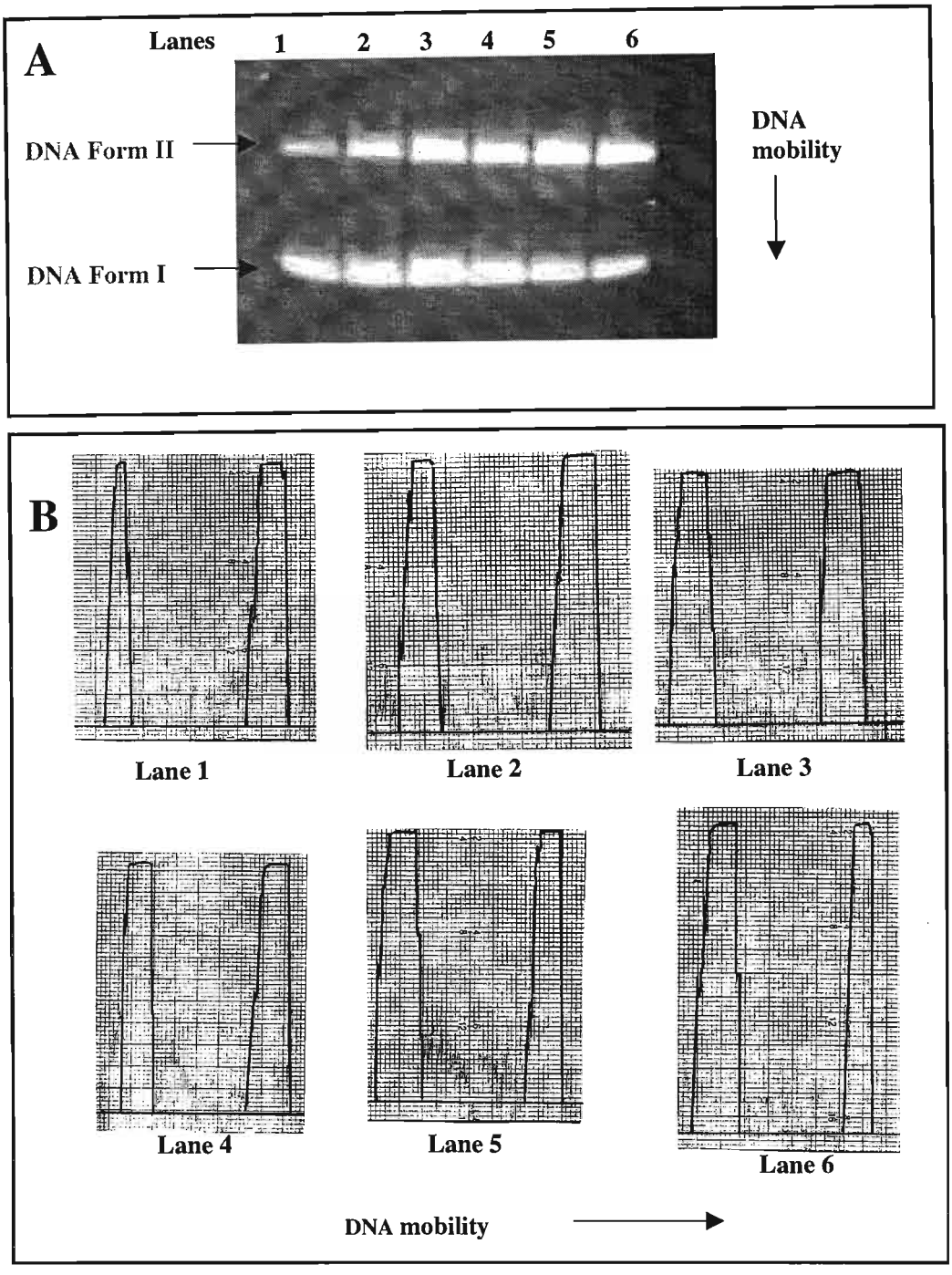

Figure 3.19: The ethidium bromide-stained agarose gel (A) and the densitometric lane graphs (B) showing ϕX174 DNA (18.85 μM) photocleavage induced by irradiation of DNA alone. DNA samples in lanes 1-6 were irradiated for 0, 5, 10, 20, 30 and 45 minutes, respectively (RUN 1).

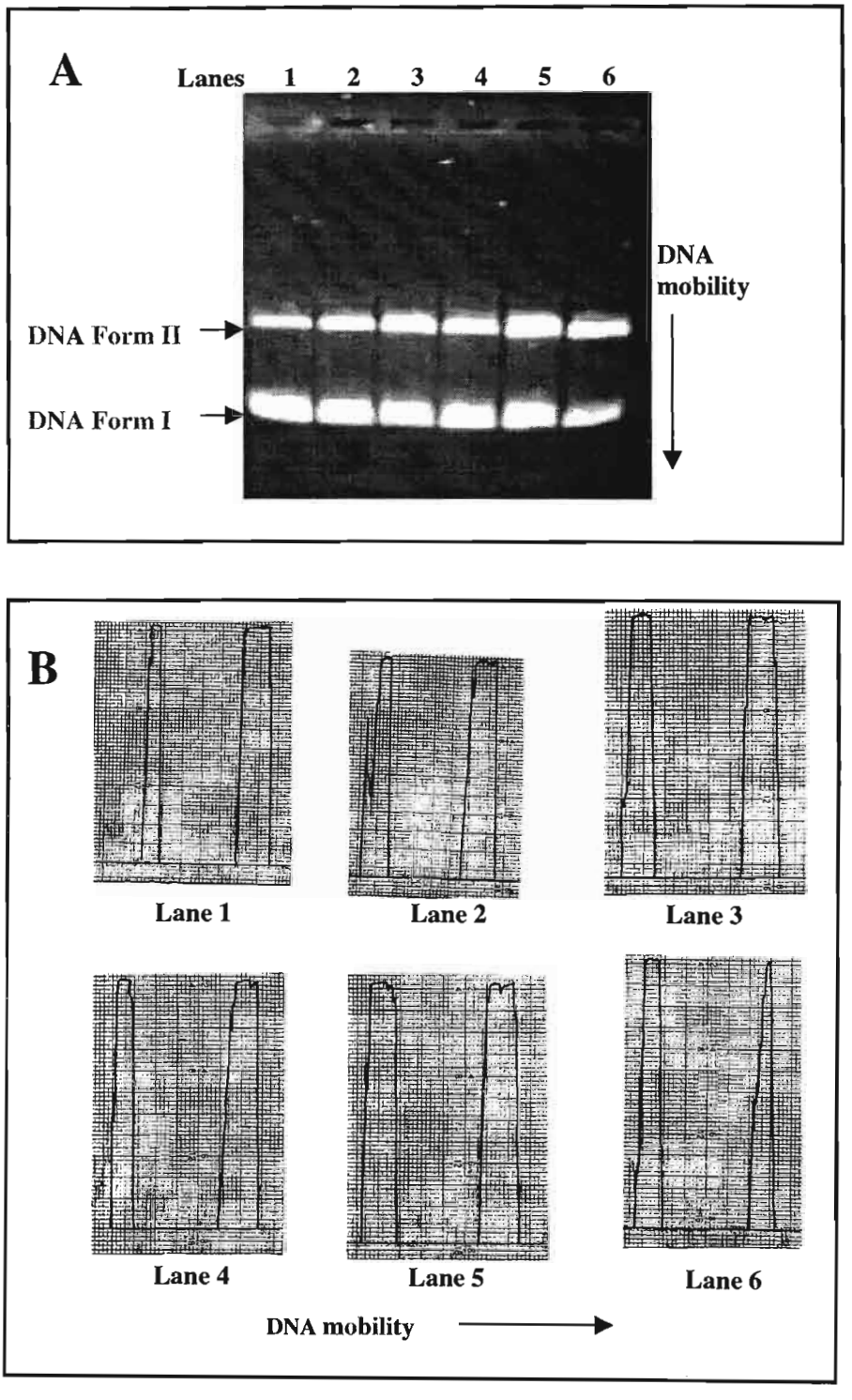

Figure 3.20: The ethidium bromide-stained agarose gel (A) and the densitometric lane graphs (B) showing ϕX174 DNA (18.85 μM) photocleavage induced by irradiation of DNA

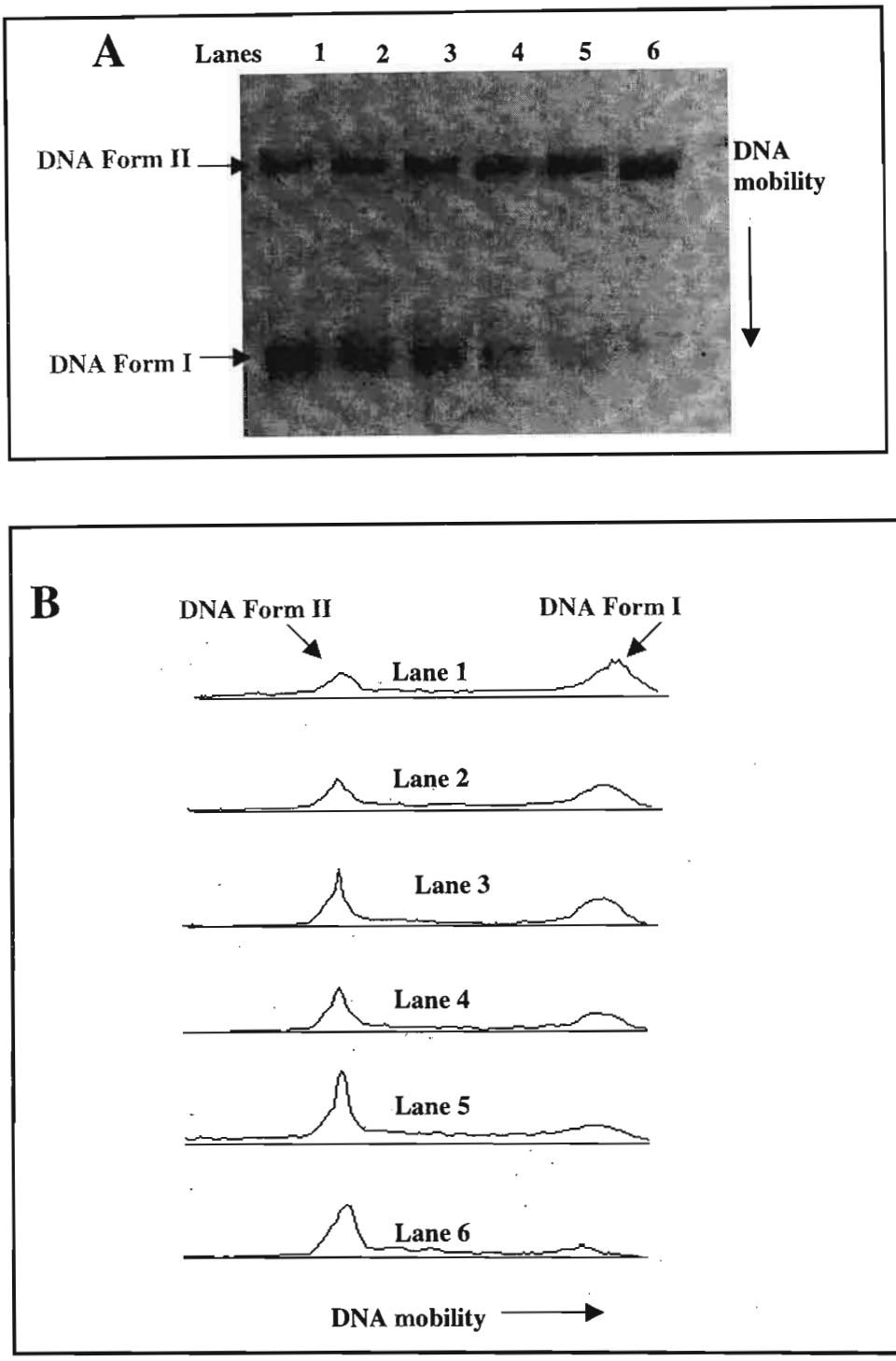

Figure 3.21: The ethidium bromide-stained agarose gel (A) and the densitometric lane graph (B) showing ϕX174 DNA (18.85 μM) photocleavge induced by irradiation of DNA alone. DNA samples in lanes 1-6 were irradiated for 0, 5, 10, 20, 30 and 45 minutes, respectively (RUN 3).

irradiation of DNA alone. DNA samples in lanes 1-6 were irradiated for 0, 5, 10, 20, 30 and 45 minutes, respectively (RUN 3).

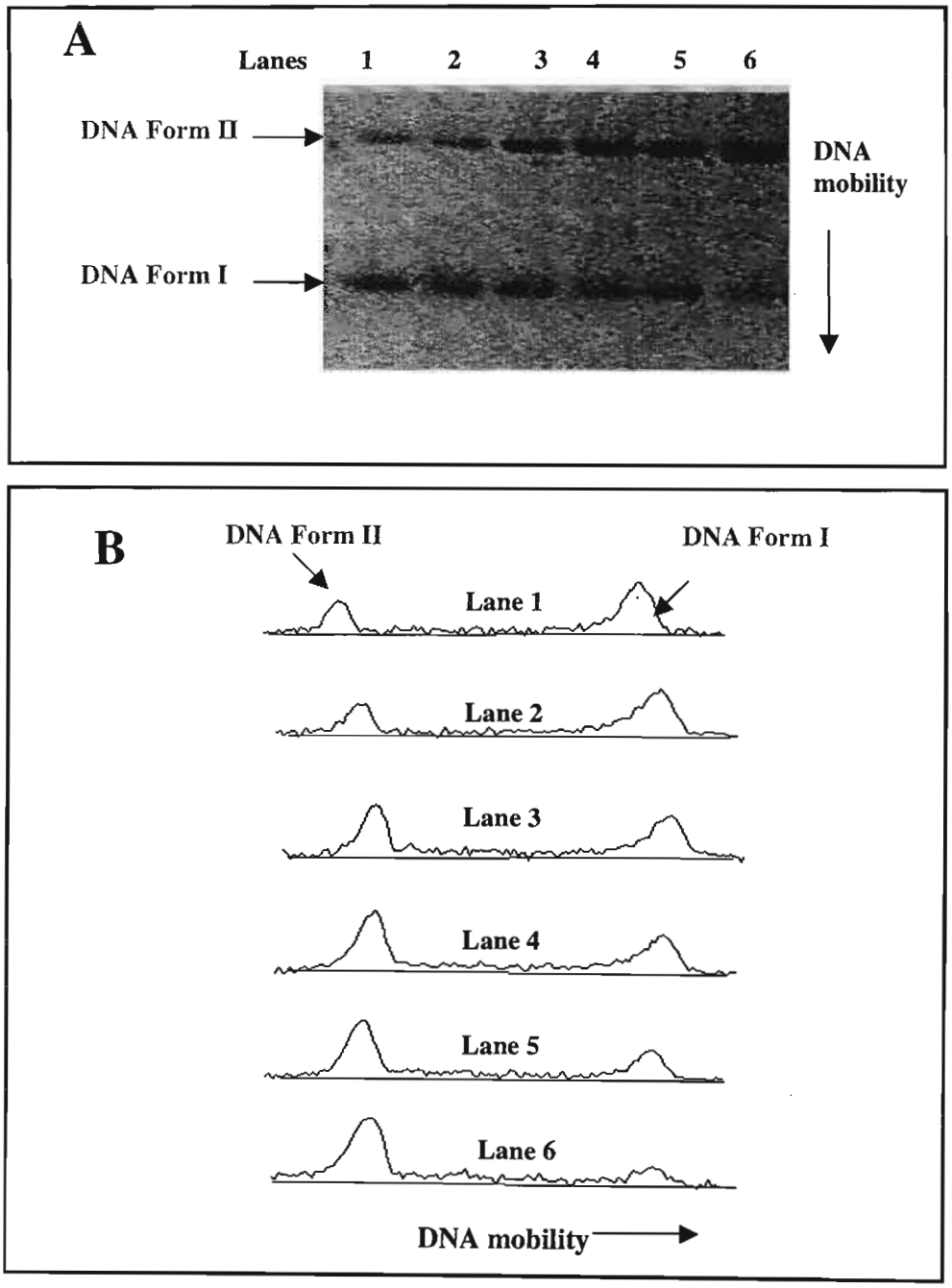

Figure 3.22: The ethidium bromide-stained agarose gel (A) and the densitometric lane graph (B) showing ϕX174 DNA (18.85 μM) photocleavge induced by irradiation of DNA alone. DNA samples in lanes 1-6 were irradiated for 0, 5, 10, 20, 30 and 45 minutes, respectively (RUN 4).

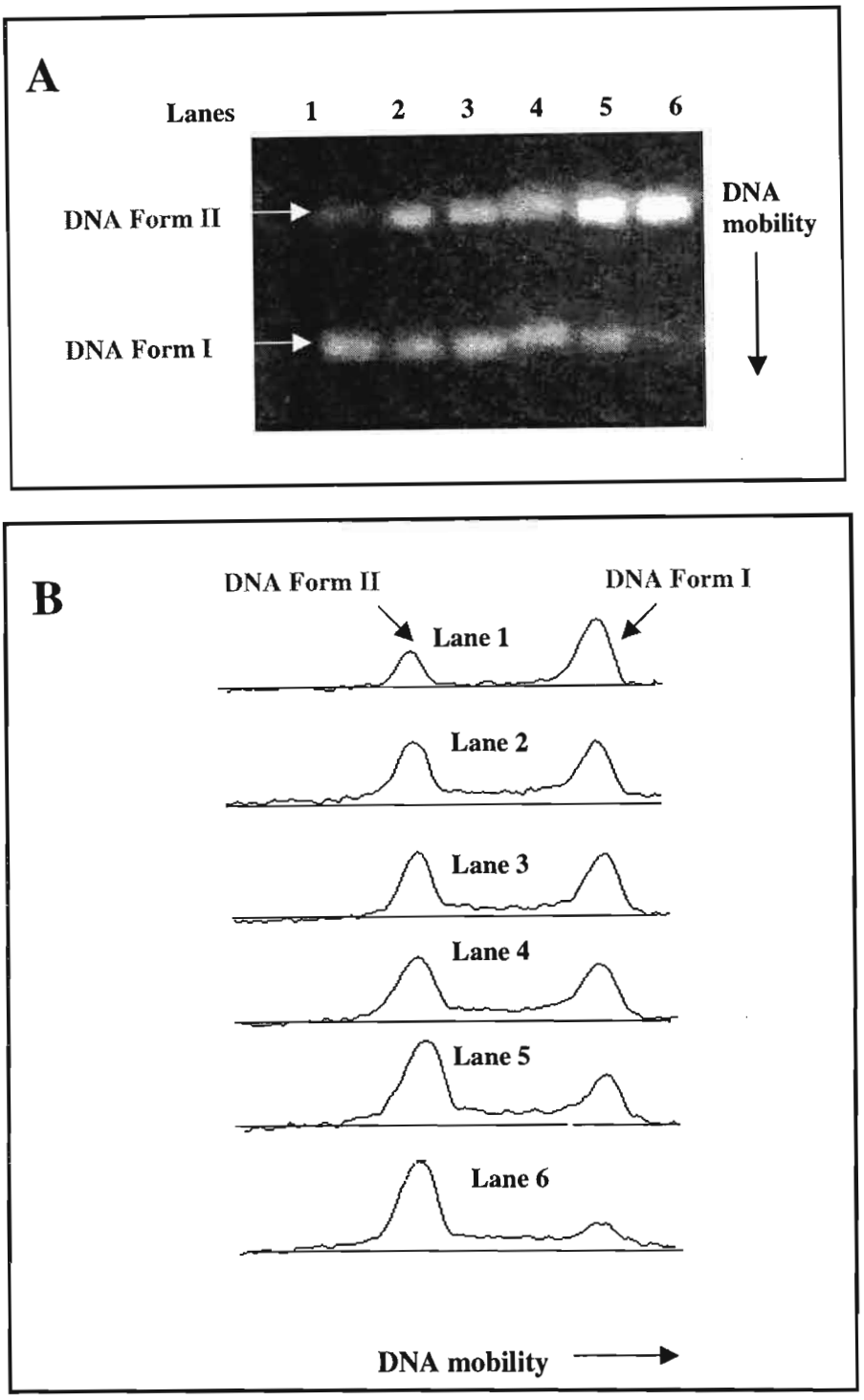

Figure 3.23: The ethidium bromide-stained agarose gel (A) and the densitometric lane graph (B) showing ϕX174 DNA (18.85 μM) photocleavage induced by irradiation of DNA alone. DNA samples in lanes 1-6 were irradiated for 0, 5, 10, 20, 30 and 45 minutes, respectively (RUN 5).

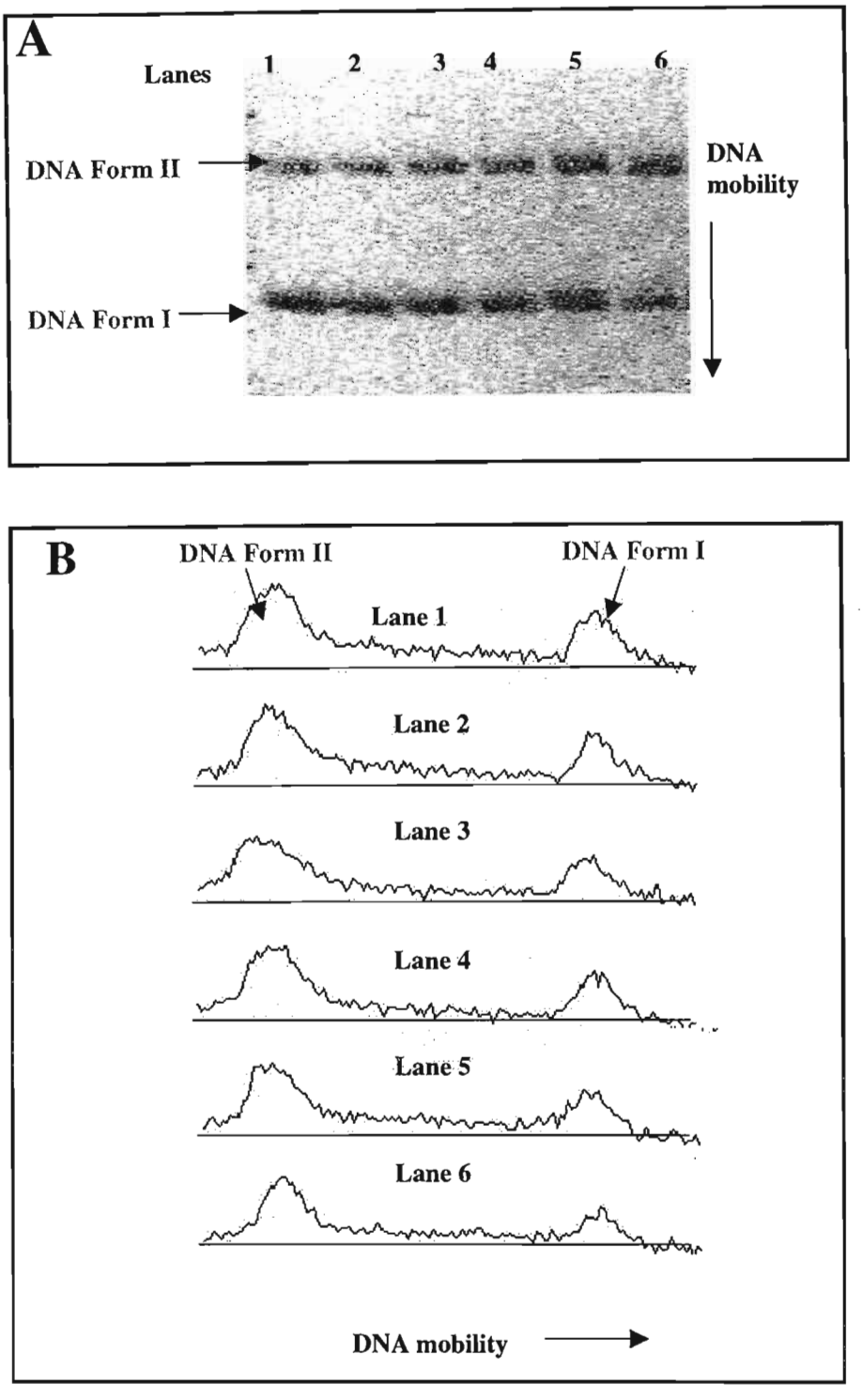

Figure 3.24: The ethidium bromide-stained agarose gel (A) and the densitometric lane graph (B) showing ϕX174 DNA (18.85 μM) photocleavage induced by irradiation of DNA alone. DNA samples in lanes 1-6 were irradiated for 0, 5, 10, 20, 30 and 45 minutes, respectively (RUN 6).

From Figures 3.19 - 3.24 it can be seen that when ϕX174 DNA was irradiated for a total irradiation period of 45 minutes at wavelengths greater than 300 nm, only two DNA forms were present. These corresponded to the supercoiled Form I DNA (lower band in each lane) and the nicked circular DNA Form II (upper band in each lane). No linear Form III DNA was detectable. The means and standard deviations for DNA Form I, II and III as well as for the SSB, were plotted against the irradiation time (0 - 45 minutes) and appear in Figures 3.25 - 3.28 respectively. The raw data used in the statistical analysis can be found in the Appendix B1.

Initially, without irradiation, the DNA composition was 68% DNA Form I, 32% DNA Form II and no DNA Form III (Appendix B1 and Figures 3.25-3.26). After 45 minutes of irradiation the supercoiled Form I DNA decreased from 68% to 35%, the nicked circular Form II DNA increased from 32% to 65% while there was still no DNA Form III present. This implies that after 45 minutes of irradiation of DNA at wavelengths greater than 300 nm, 49% of the original supercoiled DNA Form I was nicked to the circular Form II DNA. The number of SSB induced on the DNA reached a maximum of 0.79 after 45 minutes of irradiation (Figure 3.28). It can be concluded that when ϕX174 DNA was irradiated at wavelengths greater than 300 nm the extent of DNA cleavage and the number of SSB produced was not significant to form linear (Form III) DNA. Figures 3.25 - 3.28 will now serve as the control graphs against which the effects of the benzophenone-derived UV absorbers under investigation will be compared.

3.2.3 DNA photocleavage by benzophenone, benzophenone-1, Uvinul DS49 and Eusolex 232

Benzophenone-1, Uvinul DS49 and Eusolex 232 demonstrated a similar DNA photocleavage pattern to that of their parent compound, benzophenone, and therefore have been grouped together in this discussion.

Benzophenone, the parent compound of the UV absorbers under investigation, was included in this study to gain insight into the DNA photocleavage ability of this group of UV absorbers. Studies conducted by Kilfoil & Salter [1988] have shown benzophenone to be a potent photosensitizer of thymine dimerization *in vitro*. In addition, *Bolton* [1991] and Bolton *et al.* [1992] demonstrated that Uvinul DS49 and Eusolex 232 also promoted thymine dimer formation in DNA.

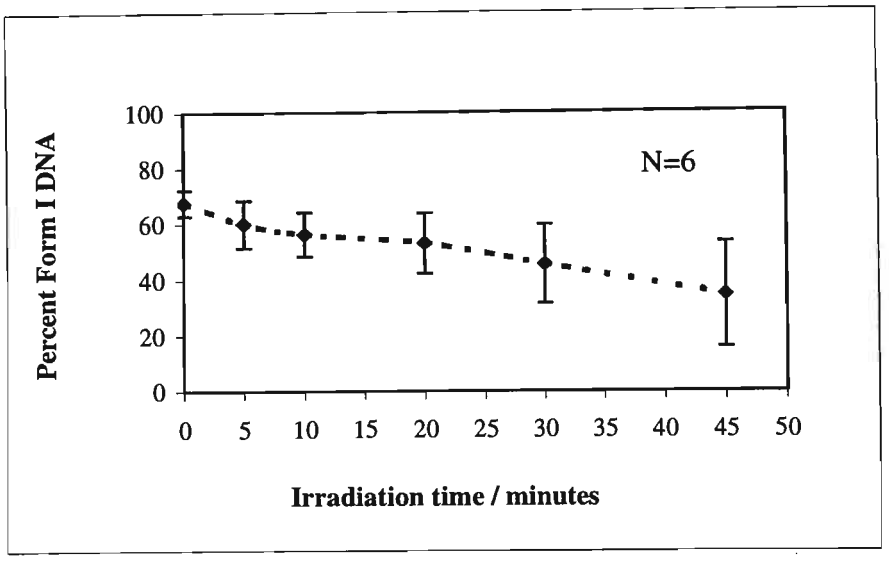

Figure 3.25 Change in the percentage of supercoiled DNA Form I induced by the irradiation of ϕX174 DNA (18.85 μM) DNA at $\lambda > 300$ nm. The error bars indicate the standard deviations and N refers to the number of replicates.

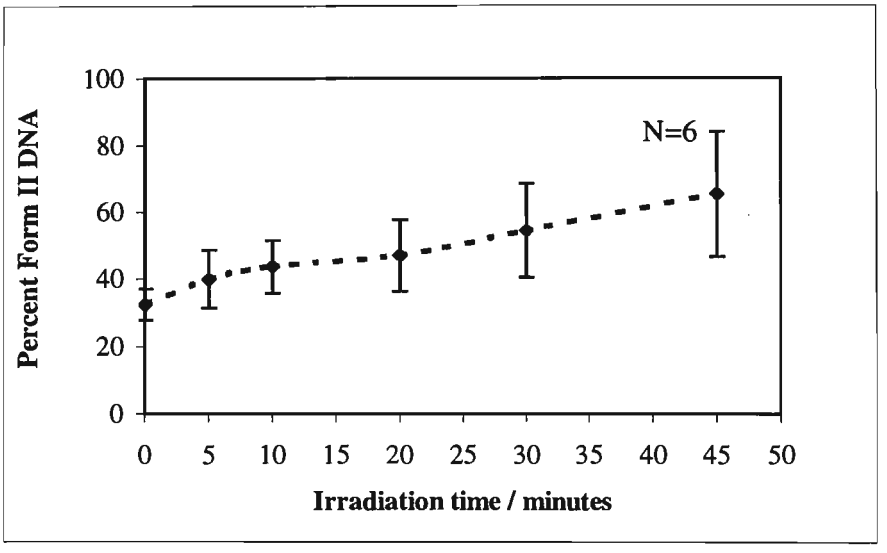

Figure 3.26: Change in the percentage of nicked circular DNA Form II induced by the irradiation of ϕX174 DNA (18.85 μM) at $\lambda > 300$ nm. The error bars indicate the standard deviations and N refers to the number of replicates.

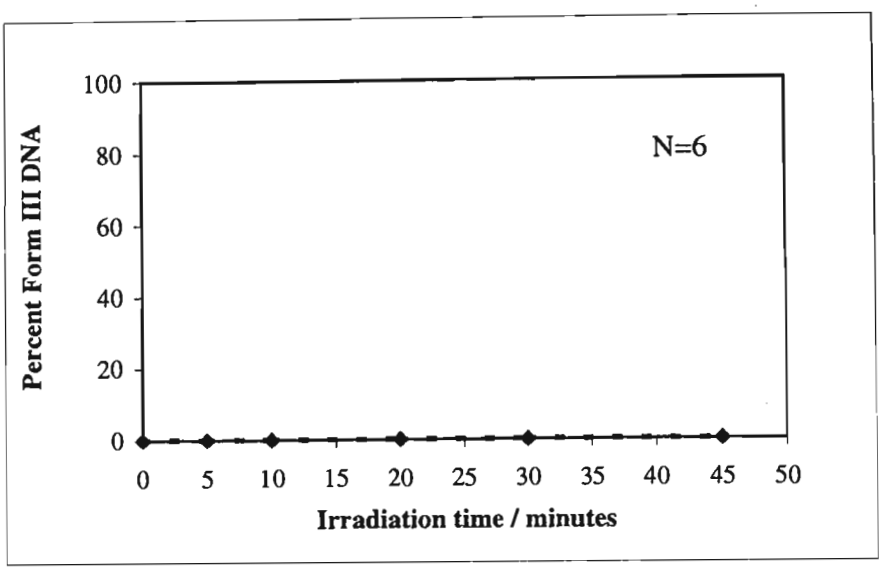

Figure 3.27: Change in the percentage of linear DNA Form III induced by the irradiation of ϕX174 DNA (18.85 μM) at λ > 300 nm, and N refers to the number of replicates.

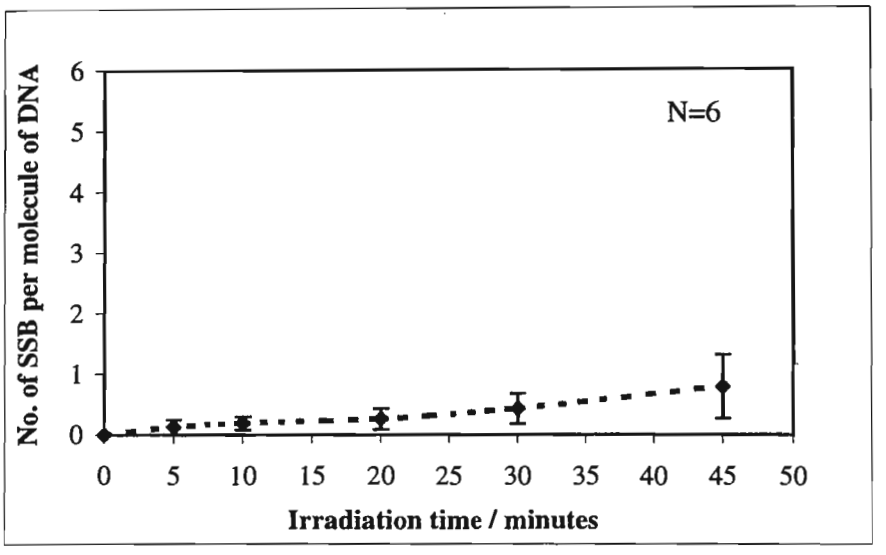

Figure 3.28: Change in the mean number of SSB per DNA molecule induced by the irradiation of DNA at λ > 300 nm. The error bars indicate the standard deviations and N refers to the number of replicates.

The ethidium bromide-stained agarose gels showing DNA cleavage induced by the presence of benzophenone, benzophenone-1, Uvinul DS49 and Eusolex 232 appear in Figures 3.29-3.30, 3.31-3.33, 3.34-3.36 and 3.37-3.39 respectively.

From Figures 3.29 - 3.39 it can be seen that three DNA Forms were present. These were the supercoiled DNA Form I (lowest band in each lane), the nicked circular Form II DNA bands (upper band in each lane), as well as a band of intermediate mobility, which occurred only in those lanes in which the samples were irradiated for longer periods. This band was attributed to the linear DNA Form III, which was due to an increase in the nicks on the DNA Form II molecule that are within 5-10 base pairs of the first (Kochevar & Dunn [1990]). Furthermore, as the irradiation time was increased from 0 - 45 minutes (except in Figure 3.29 where the maximum irradiation period is 30 minutes) the amount of supercoiled DNA Form I decreased, while the composition of the nicked circular DNA Form II and the linear DNA Form III appeared to increase. From Figures 3.29 and 3.30, it can be seen that irradiation of ϕX174 DNA in the presence of benzophenone required only about 15 minutes of irradiation, for the DNA to be converted to the linear Form. In contrast about 20-30 minutes of irradiation was required to produce the linear Form III DNA when benzophenone-1 (Figures 3.31-3.33), Uvinul DS49 (Figures 3.34-3.36) or Eusolex 232 (Figures 3.37-3.39) was present.

The linear DNA band appeared as a distinct, well-defined band, in all the agarose gels except for that in Figure 3.39, in which ϕX174 DNA was irradiated in the presence of Eusolex 232. Here a broad smear band between DNA Form I and II replaced the linear DNA band. At the higher irradiation doses, this smear DNA band acquired a sharp edge, the position of which coincided with Form III linear DNA.

The mean percentage of the DNA in Forms I, II and III as well as the number of SSB induced on the DNA after treatment with each UV absorber have been plotted against irradiation time (Figures 3.40-3.43 respectively). Included in these figures are the control graphs, which depict irradiation of the DNA in the absence of the UV absorbers (shown by the dotted lines). Error bars represent the standard deviation at each irradiation time for each UV absorber. The large error bars are representative of the large variations that are typical of this assay. However, it should be noted that the trends observed are always the same. The results of the DNA photocleavage experiments for benzophenone, benzophenone-1, Uvinul DS49 and Eusolex 232 can be found in Appendices B2 - B5 respectively.

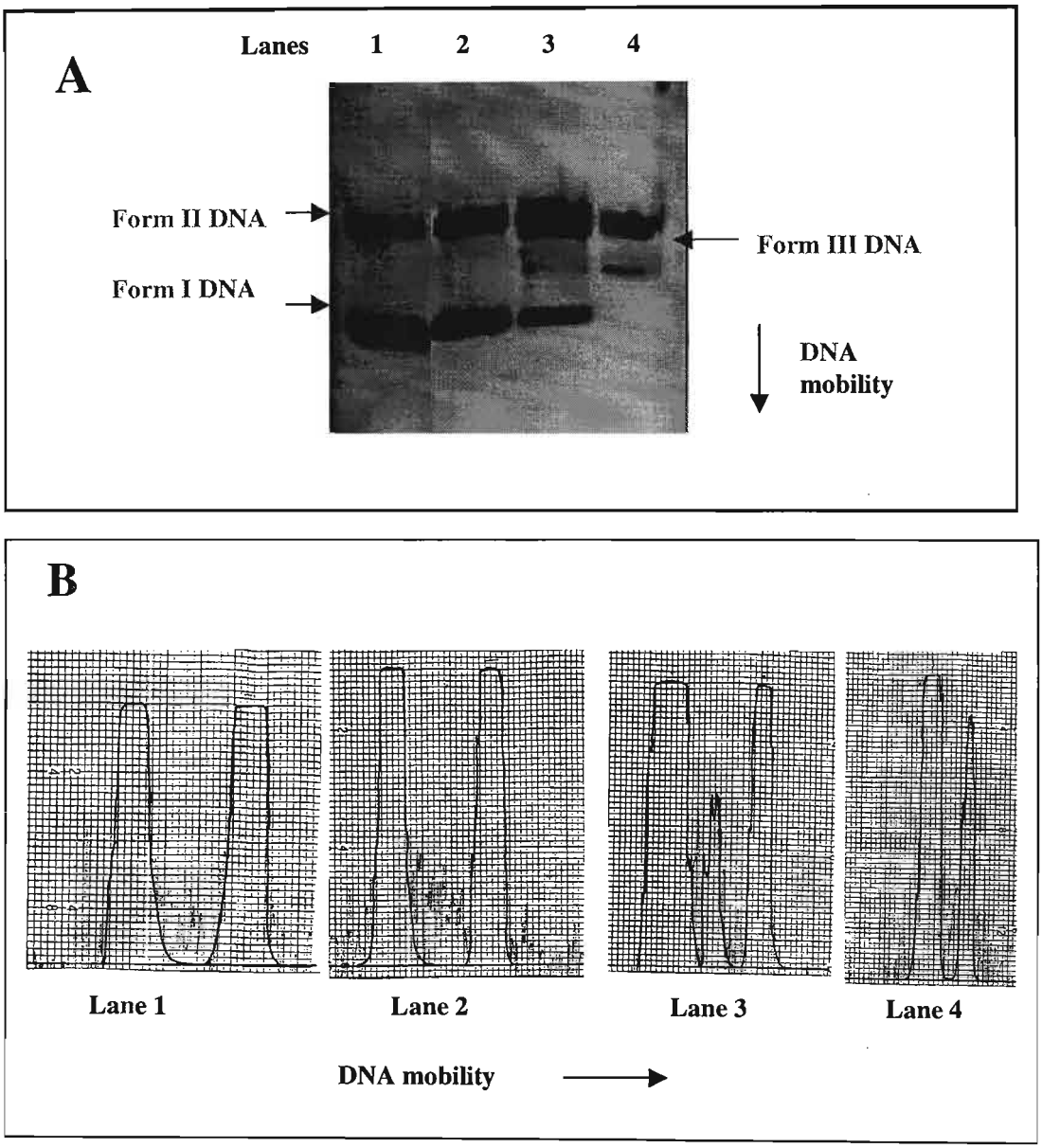

Figure 3.29: The ethidium bromide-stained agarose gel (A) and the densitometric lane graphs (B) showing cleavage of ϕX174 DNA (18.85 μM) photosensitised by benzophenone (50 μM). Lanes 1-4 contain DNA in the presence of benzophenone that had been irradiated for 0, 5, 15 and 30 minutes, respectively (RUN 1).

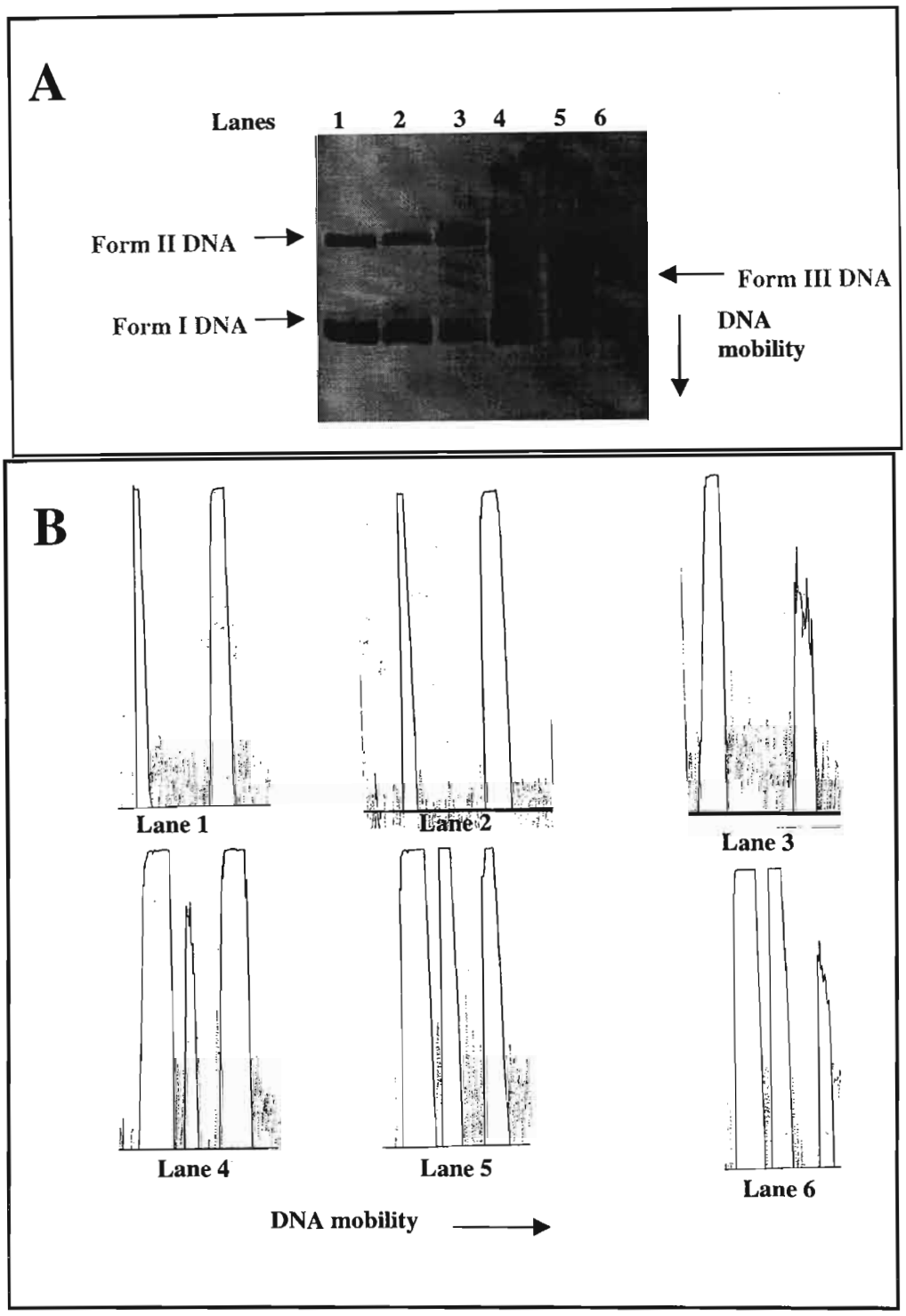

Figure 3.30: The ethidium bromide-stained agarose gel (A) and the densitometric lane graph (B) showing cleavage of ϕX174 DNA (18.85 μM) photosensitised by benzophenone (50 μM). Lane 1: DNA alone, no irradiation (dark control), Lanes 2-6 contain DNA irradiated in the presence of benzophenone for 0, 10, 15, 30 and 45 minutes, respectively (RUN 2).

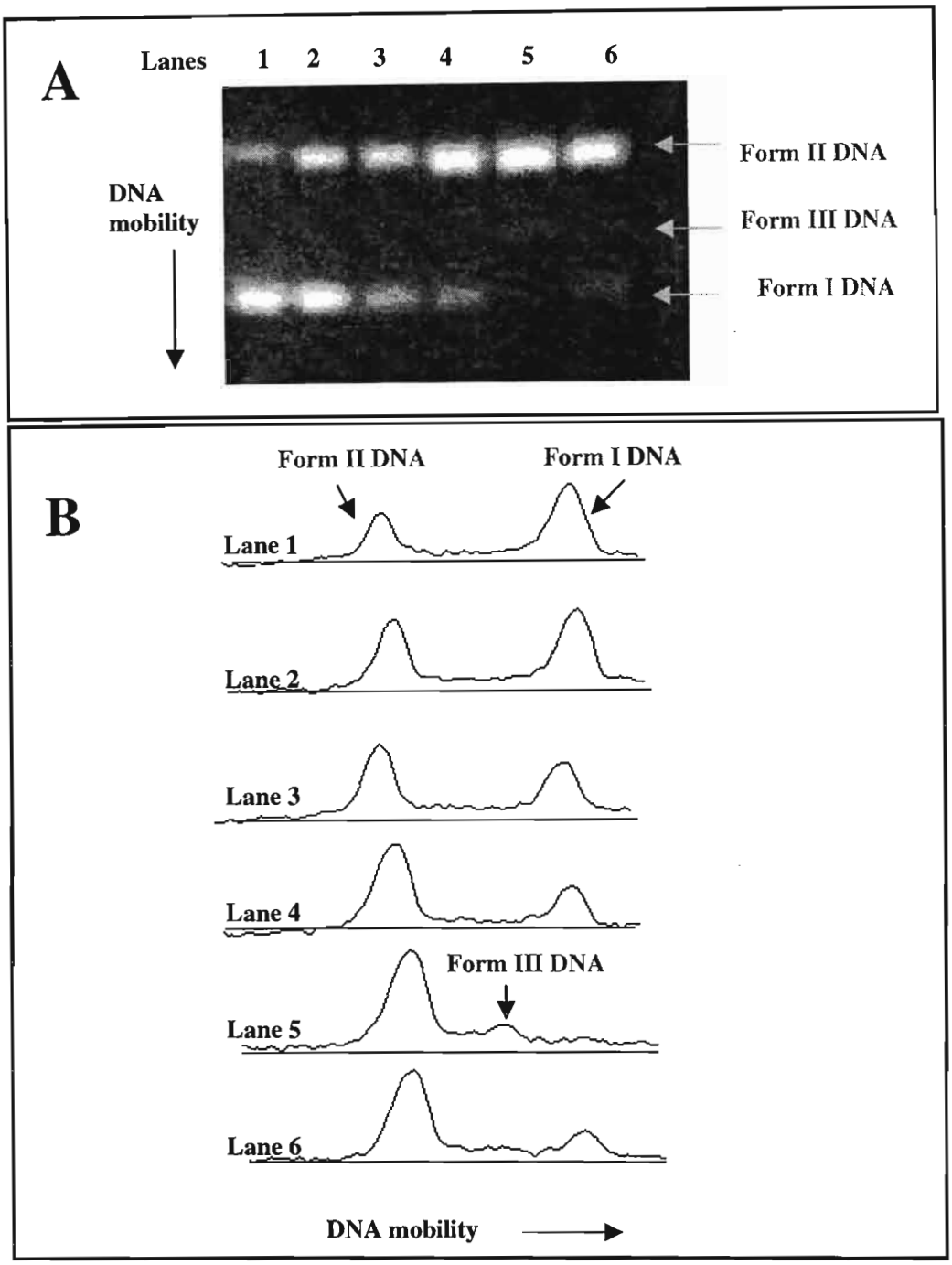

Figure 3.31: The ethidium bromide-stained agarose gel (A) and the densitometric lane graph (B) showing cleavage of ϕX174 DNA (18.85 μM) photosensitised by benzophenone-1 (50 μM). DNA samples in lanes 1-6 were irradiated for 0, 5, 10, 20, 30 and 45 minutes, respectively (RUN 1).

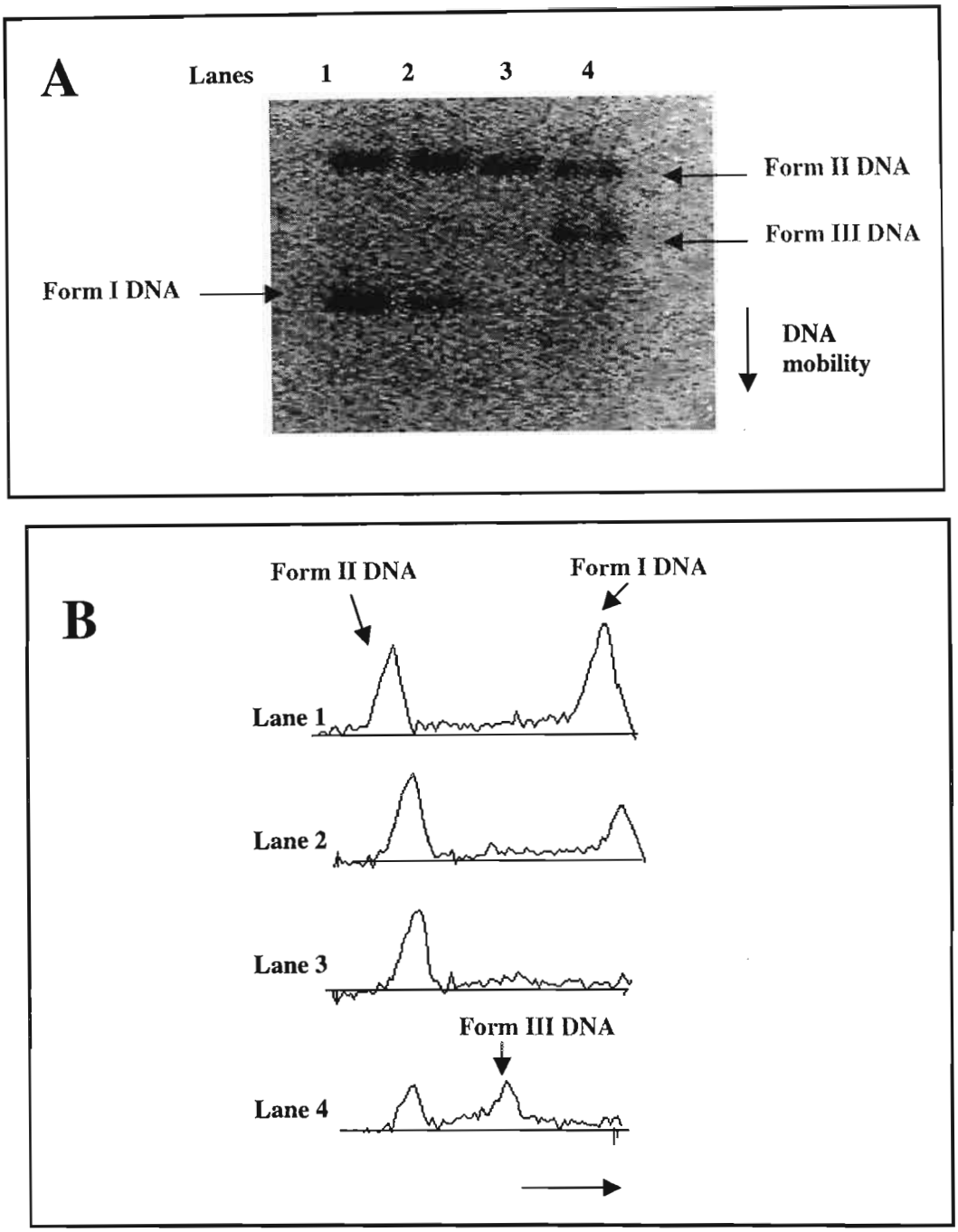

Figure 3.32: The ethidium bromide-stained agarose gel (A) and the densitometric lane graph (B) showing cleavage of ϕX174 DNA (18.85 μM) photosensitised by benzophenone-1 (50 μM). DNA samples in lanes 1-4 were irradiated for 5, 20, 30 and 45 minutes, respectively (RUN 2).

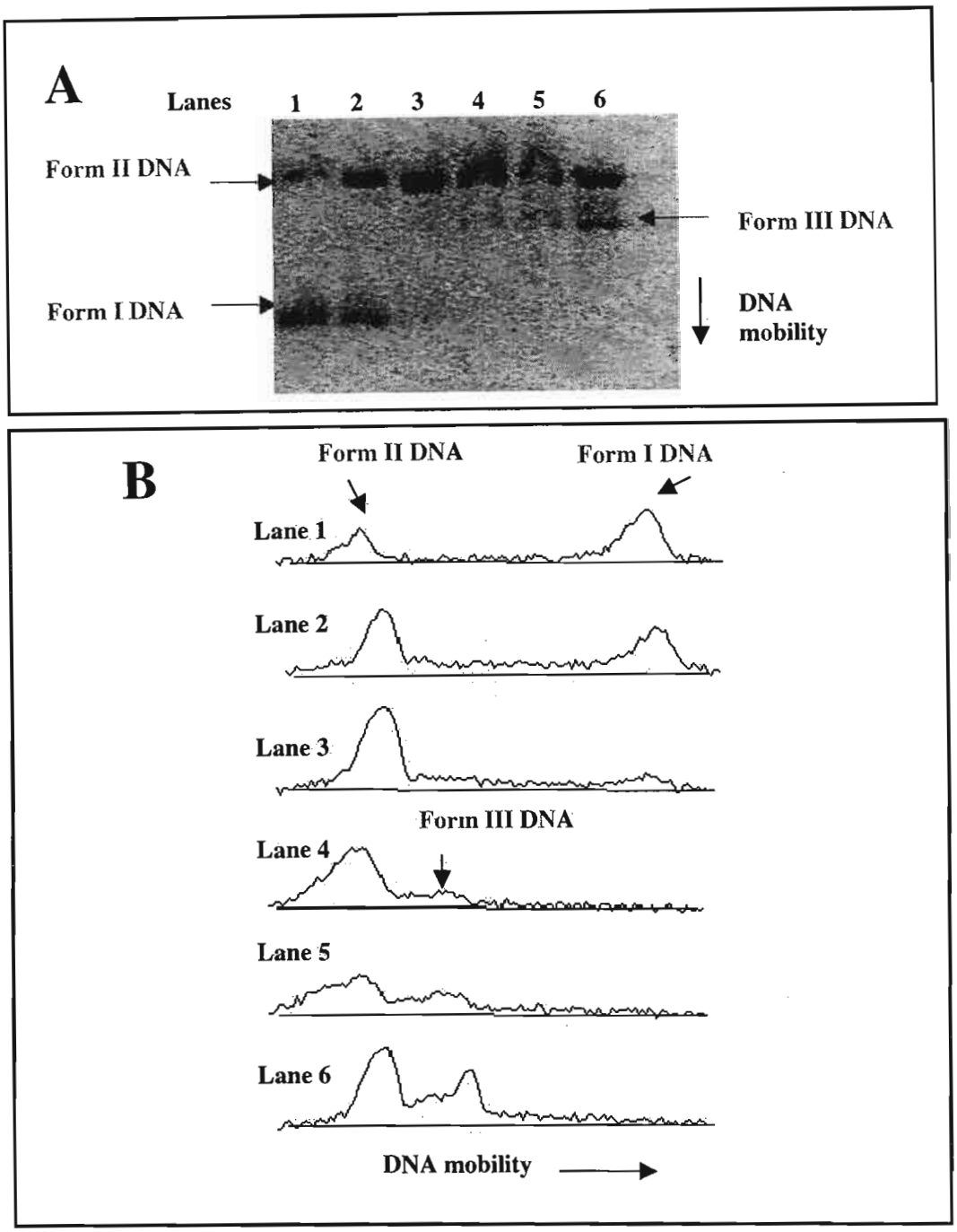

Figure 3.33: The ethidium bromide-stained agarose gel (A) and the densitometric lane graph (B) showing cleavage of ϕX174 DNA (18.85 μM) photosensitised by benzophenone-1 (50 μM). DNA samples in lanes 1-6 were irradiated for 0, 5, 10, 20, 30 and 45 minutes, respectively (RUN 3).

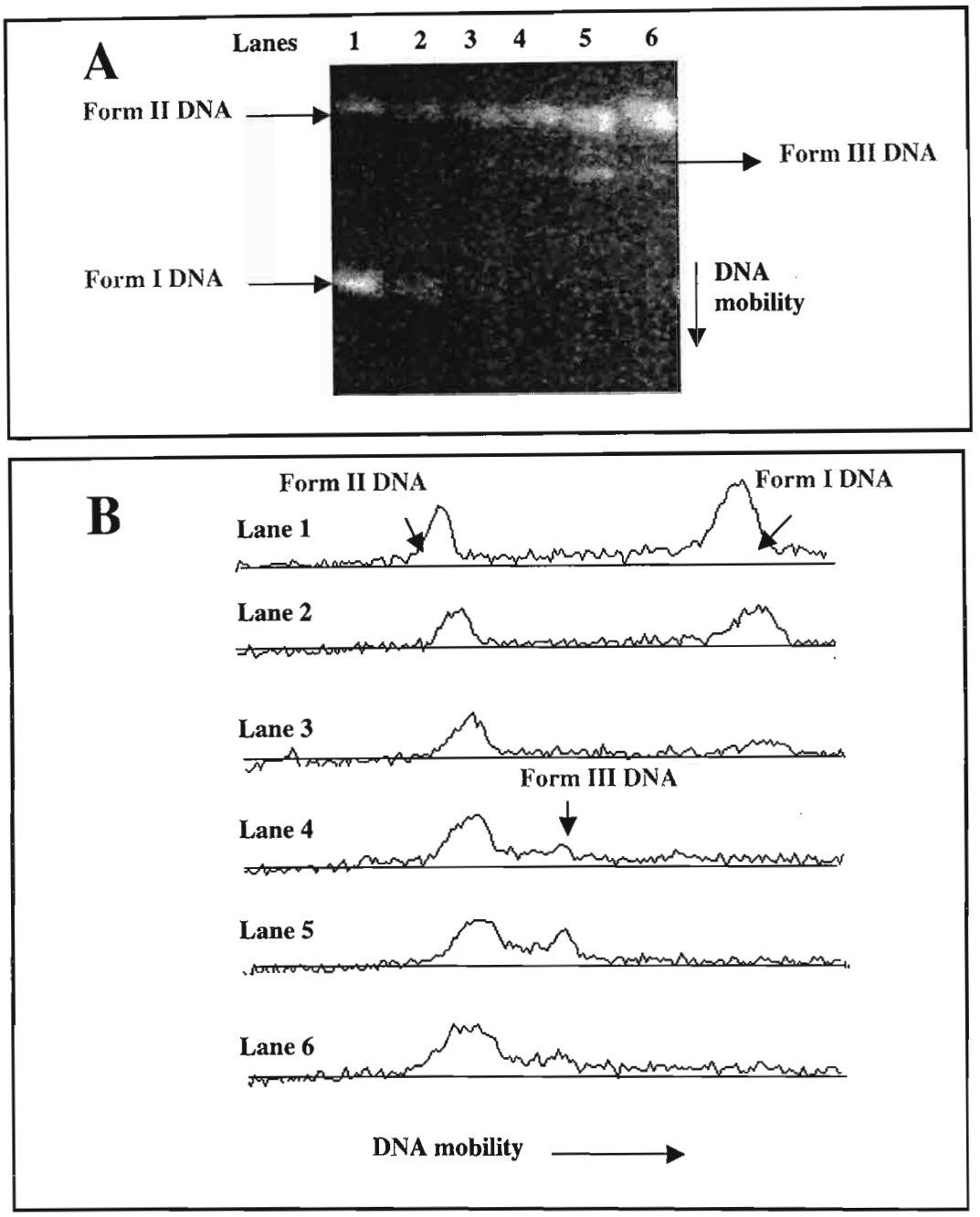

Figure 3.34: The ethidium bromide-stained agarose gel (A) and the densitometric lane graph (B) showing cleavage of ϕX174 DNA (18.85 μM) photosensitised by Uvinul DS49 (50 μM). DNA samples in lanes 1-6 were irradiated for 0, 5, 10, 20, 30 and 45 minute, respectively (RUN 1).

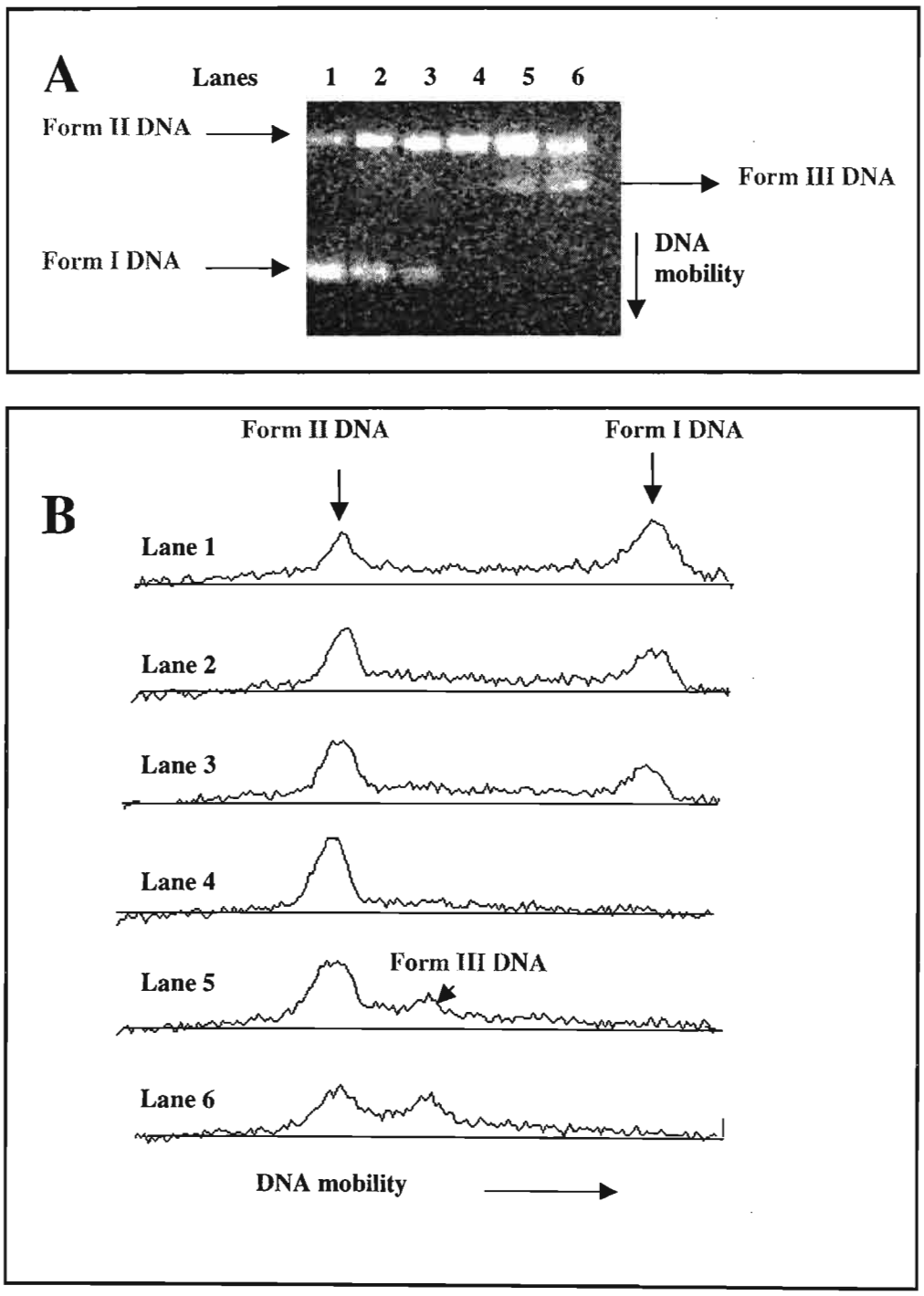

Figure 3.35: The ethidium bromide-stained agarose gel (A) and the densitometric lane graph (B) showing cleavage of ϕX174 DNA (18.85 μM) photosensitised by Uvinul DS49 (50 μM). DNA samples in lanes 1-6 were irradiated for 0, 5, 10, 20, 30 and 45 minutes, respectively (RUN 2).

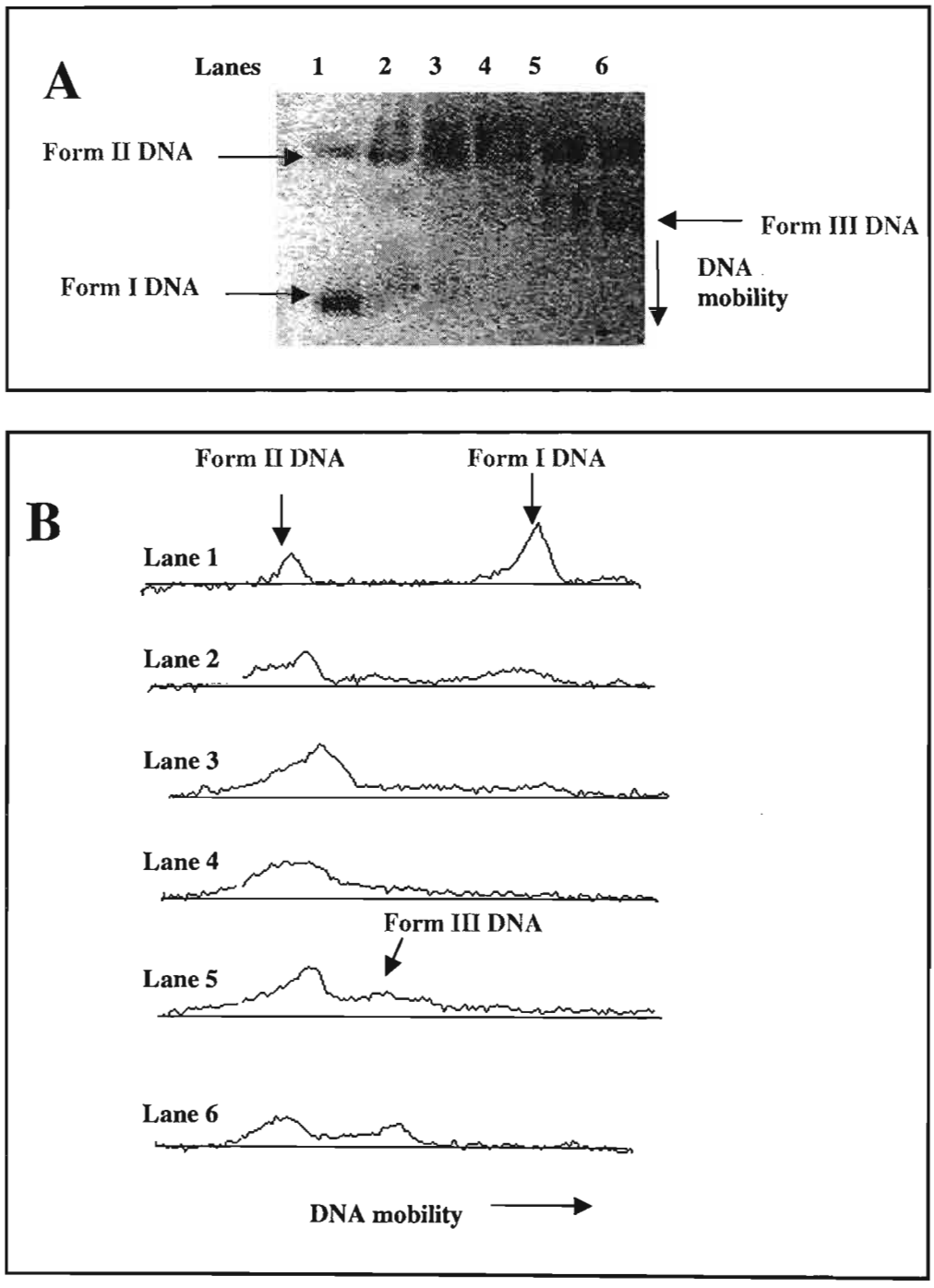

Figure 3.36: The ethidium bromide-stained agarose gel (A) and the densitometric lane graph (B) showing cleavage of ϕX174 DNA (18.85 μM) photosensitised by Uvinul DS49 (50 μM). DNA samples in lanes 1-6 were irradiated for 0, 5, 10, 20, 30 and 45 minutes, respectively (RUN 3).

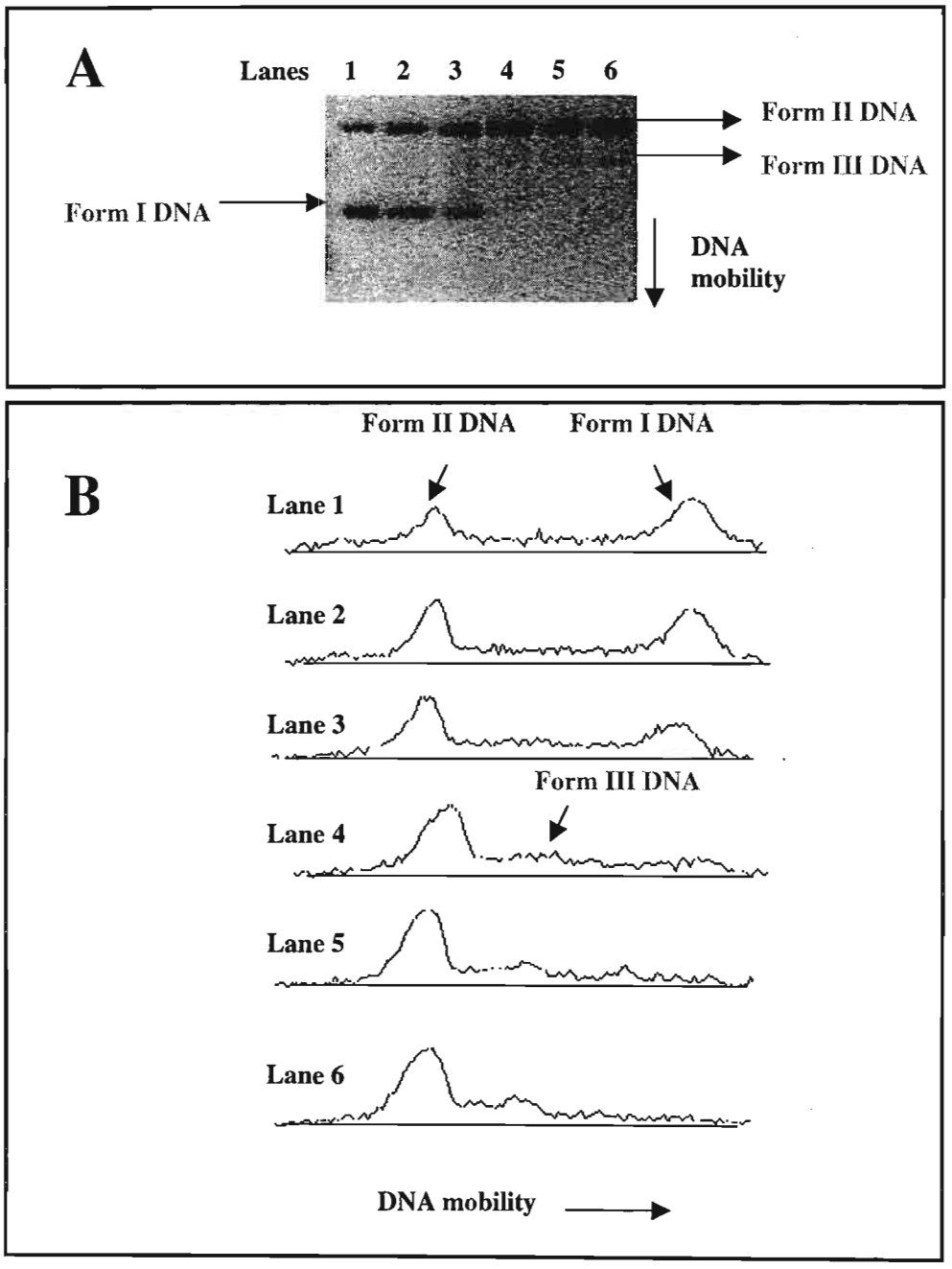

Figure 3.37: The ethidium bromide-stained agarose gel (A) and the densitometric lane graph (B) showing cleavage of ϕX174 DNA (18.85 μM) photosensitised by Eusolex 232 (50 μM). DNA samples in lanes 1-6 were irradiated for 0, 5, 10, 20, 30 and 45 minutes, respectively (RUN 1).

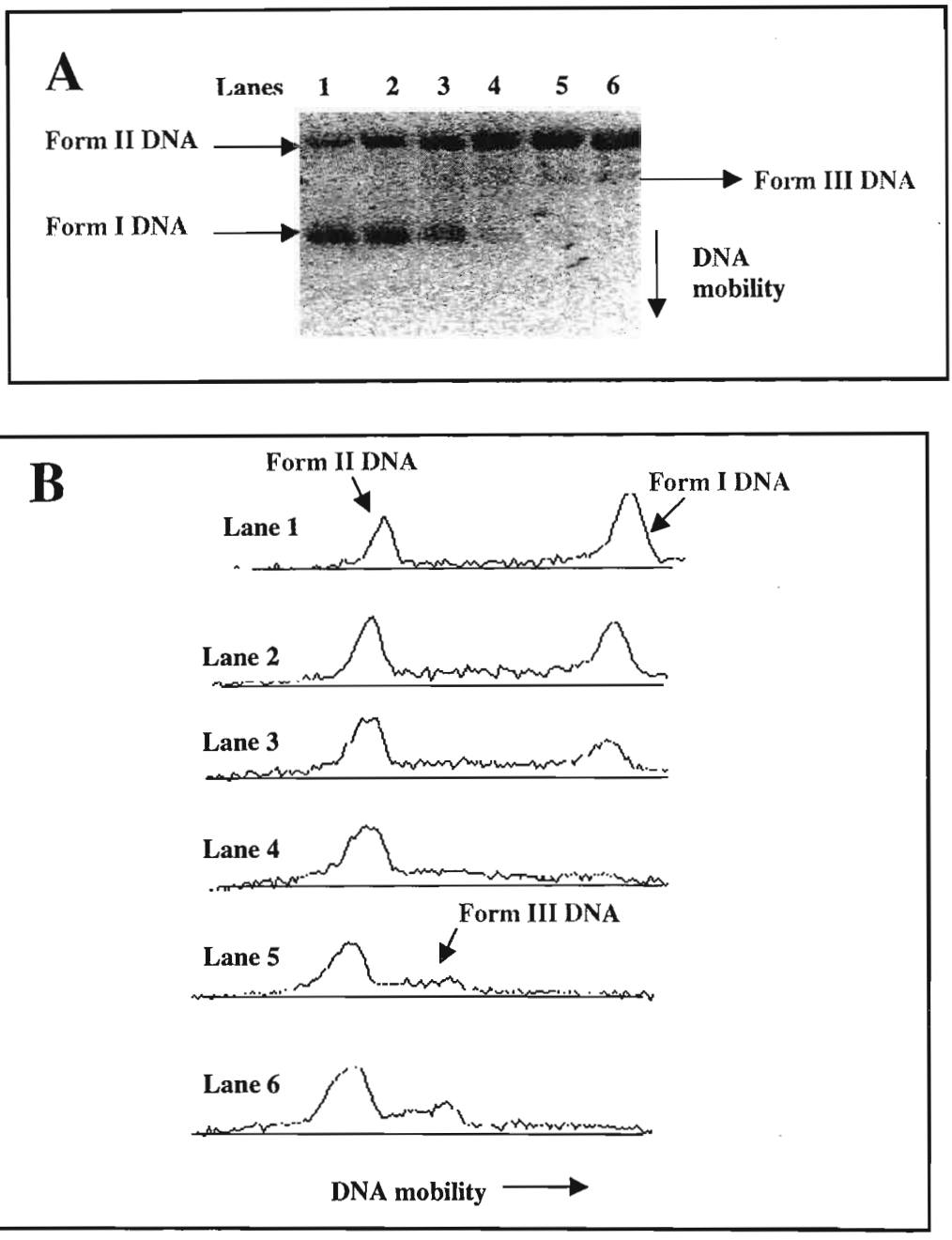

Figure 3.38: The ethidium bromide-stained agarose gel (A) and the densitometric lane graph (B) showing cleavage of ϕX174 DNA (18.85 μM) photosensitised by Eusolex 232 (50 μM). DNA samples in lanes 1-6 were irradiated for 0, 5, 10, 20, 30 and 45 minutes, respectively (RUN 2).

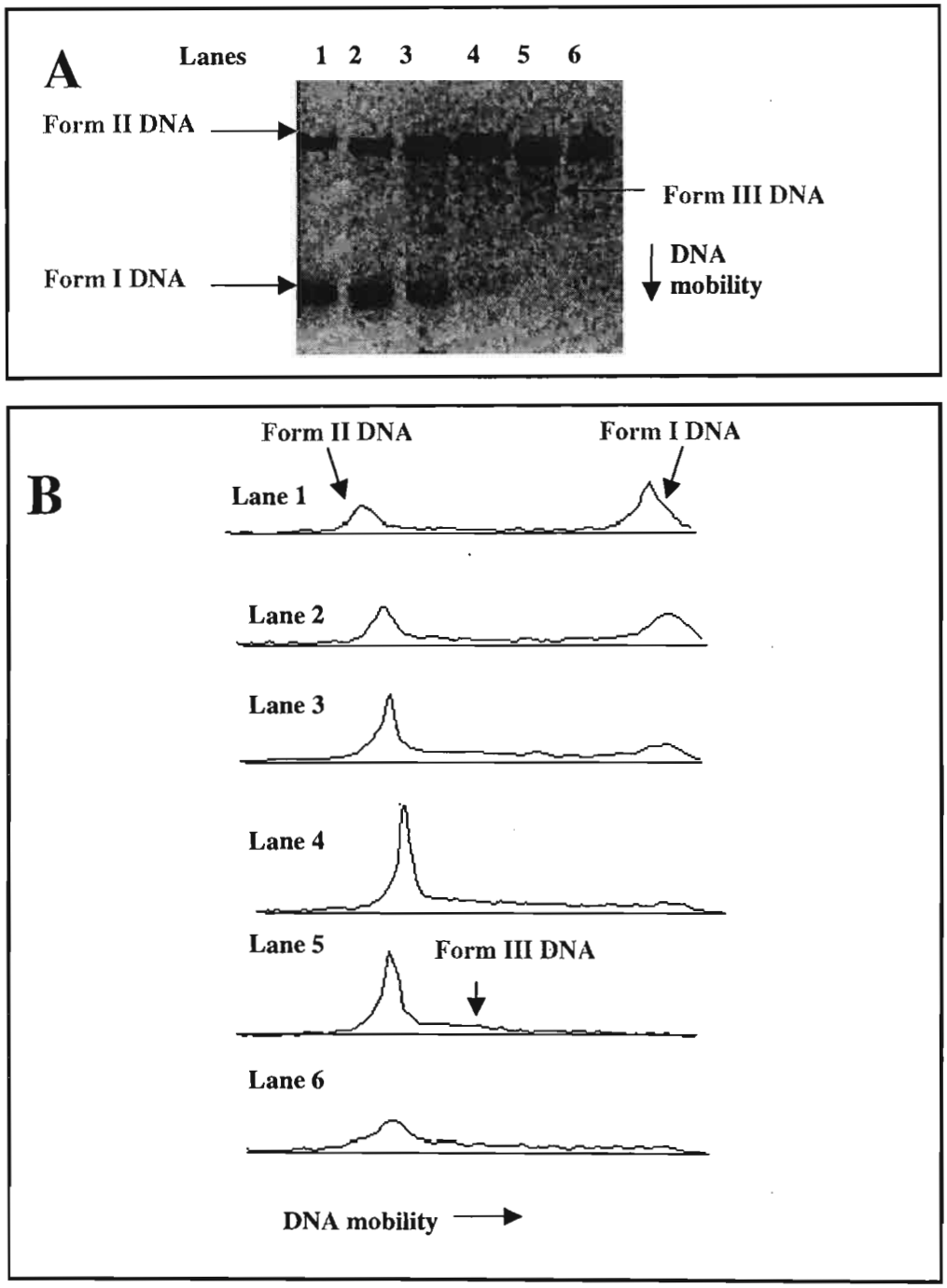

Figure 3.39 The ethidium bromide-stained agarose gel (A) and the densitometric lane graph (B) showing cleavage of ϕX174 DNA (18.85 μM) photosensitised by Eusolex 232 (50 μM). DNA samples in lanes 1-6 were irradiated for 0, 5, 10, 20, 30 and 45 minutes, respectively (RUN 3).

From Figure 3.40, it is apparent that irradiation of ϕX174 DNA in the presence of benzophenone, benzophenone-1, Uvinul DS49 or Eusolex 232 dramatically reduced the amount of DNA in the supercoiled form compared to when the DNA was irradiated alone. After 45 minutes of irradiation of the DNA in the presence of benzophenone, the supercoiled DNA Form I content was reduced from 59 % to 15% (Appendix B2). This indicates that 74% of the supercoiled DNA was nicked compared to only 49% when the irradiation was carried out in its absence (see control in Figure 3.40). Benzophenone-1, Uvinul DS49 and Eusolex 232 behaved similarly and induced decreases in the DNA Form I content from, 65% to 11%, 67% to 10 % and 64% to 8% respectively (Appendices B3-B5). This implies that 87% of the supercoiled DNA was nicked in the presence of Eusolex 232, followed by 86% in the presence of Uvinul DS49 and 83% when benzophenone-1 was present. When this is compared to the control, where only 49% of the supercoiled DNA was nicked to the circular form it can be seen that irradiation of the DNA in the presence of these UV absorbers increased the nicks in the supercoiled DNA by almost 2- fold.

The formation of the DNA Form II which arises from a SSB per DNA molecule, was increased in the presence of the UV absorbers, compared to when they were absent (control) (Figure 3.41). However, on closer examination, it can be seen that the DNA Form II content reached a maximum around 20-30 minutes of irradiation and thereafter declined. At this maximum point it is possible that the number of nicks on the DNA Form II had reached its optimum level such that many are within 5-10 bps of the first, and on further irradiation they are now converted to the linear DNA Form III. The DNA Form III content, which was undetectable when the DNA was irradiated alone, was increased significantly when the irradiations were performed in the presence of the UV absorbers, as can be seen in Figure 3.42. The percentage of linear DNA produced after 45 minutes of irradiation of ϕX174 DNA, was largest when benzophenone was present (35%), followed closely by benzophenone-1 (31%), then Uvinul DS49 (29%) and finally Eusolex 232 (17%).

The number of SSB was also much larger in the presence of these UV absorbers than in their absence. It can be seen that the number of SSB reached a maximum after about 20-30 minutes and thereafter declined. The maximum number of SSB from Figure 3.43 was formed when the DNA was irradiated in the presence of Eusolex 232, which induced 3.4 SSB per mole of DNA after 30 minutes of irradiation compared to 0.43 in its absence (see control). This was followed by Uvinul DS49, which induced 2.3 SSB per mole of DNA (after 20 minutes), and then benzophenone-1 with 2.3 SSB per DNA mole (after 30 minutes), and finally benzophenone with 2.1 SSB per DNA mole (after 30 minutes).

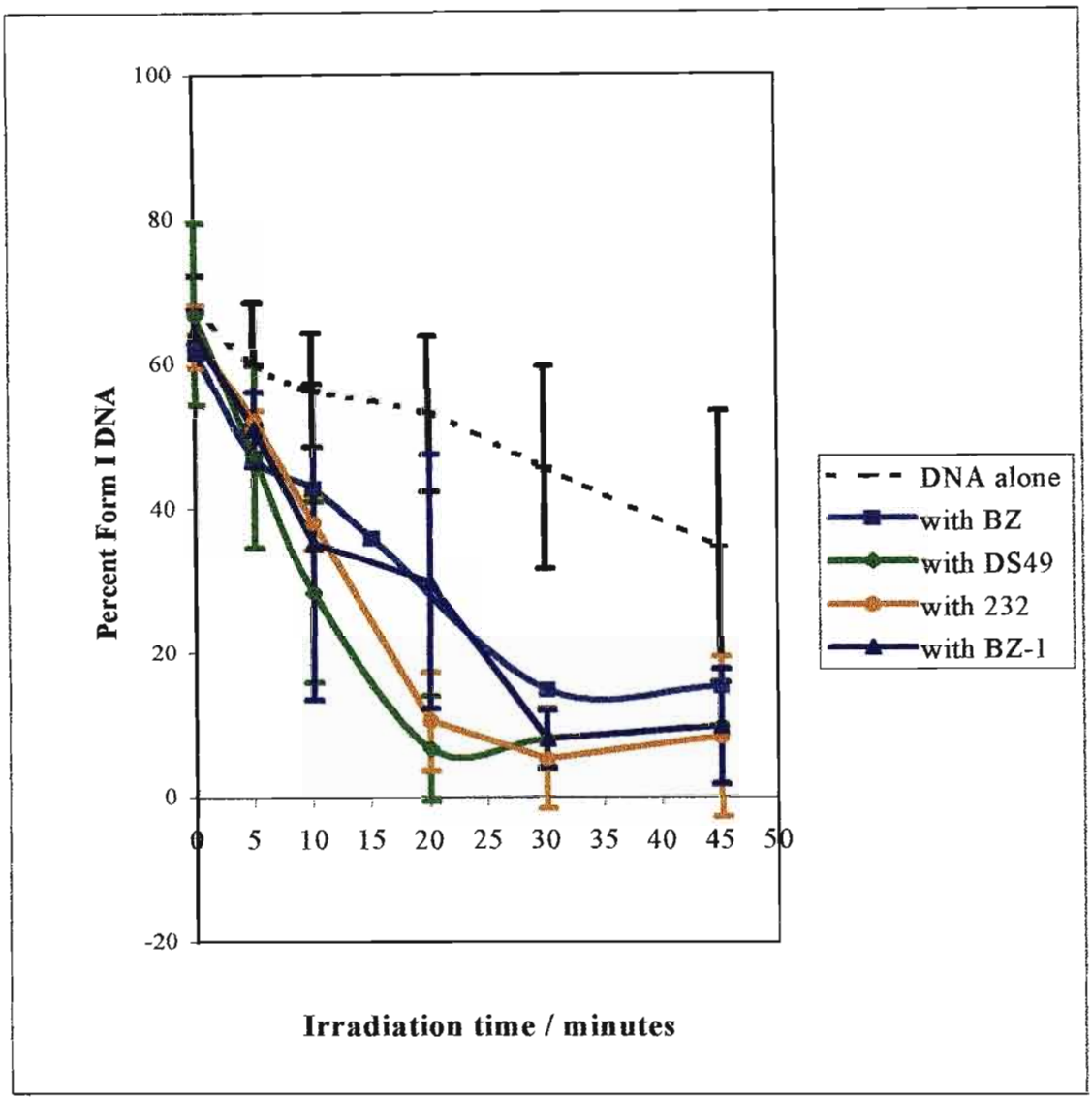

Figure 3.40: Change in the percentage of supercoiled DNA Form I induced by the irradiation of ϕX174 DNA in the presence of benzophenone (BZ) [N=2], benzophenone-1 (BZ-1) [N=3], Uvinul DS49 (DS49) [N=3] and Eusolex 232 (232) [N=3]. The dashed line shows the control, which represents DNA irradiated alone [N=6] and N refers to the number of replicates.

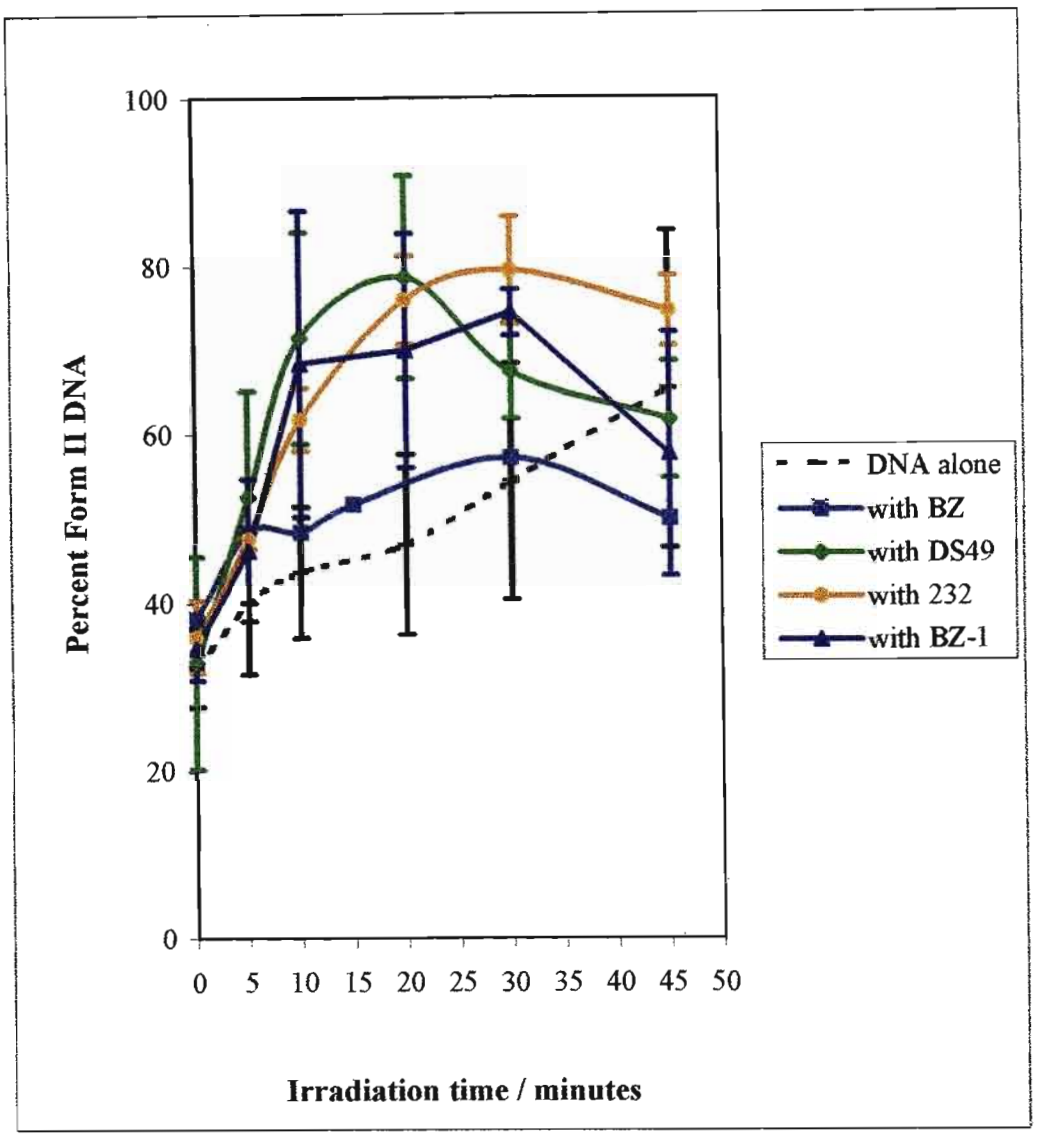

Figure 3.41: Change in the percentage of nicked circular DNA Form II induced by the irradiation of ϕX174 DNA in the presence of benzophenone (BZ) [N=2], benzophenone-1 (BZ-1) [N=3], Uvinul DS49 (DS49) [N=3] and Eusolex 232 (232) [N=3]. The dashed line shows the control, which represents DNA irradiated alone [N=6] and N refers to the number of replicates.

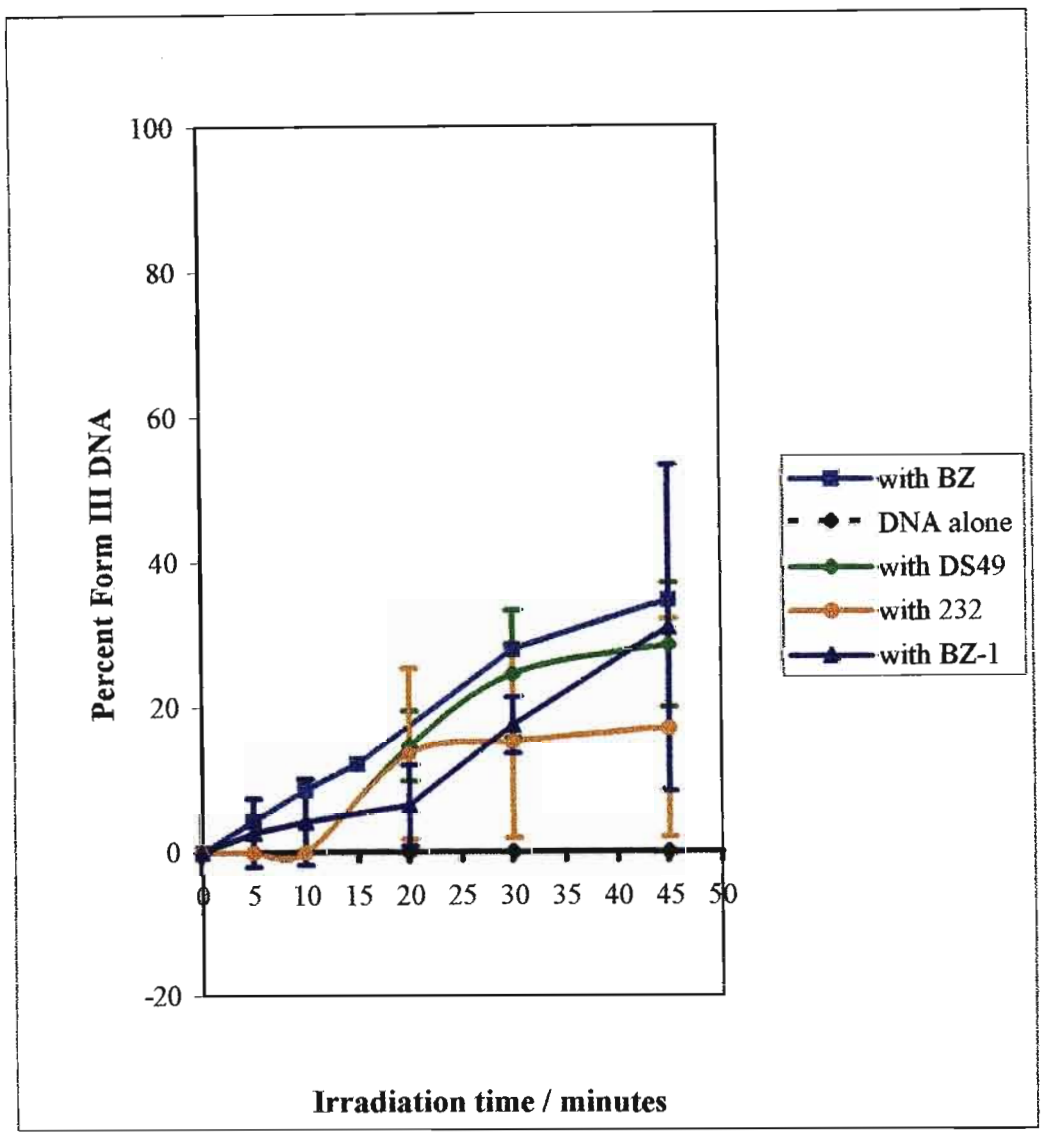

Figure 3.42: Change in the percentage of linear DNA Form III induced by the irradiation of ϕX174 DNA in the presence of benzophenone (BZ) [N=2], benzophenone-1 (BZ-1) [N=3], Uvinul DS49 (DS49) [N=3] and Eusolex 232 (232) [N=3]. The dashed line shows the control, which represents DNA irradiated alone [N=6] and N refers to the number of replicates. (The dashed line, which shows the control, coincides with the solid line and is zero along the x-axis.)

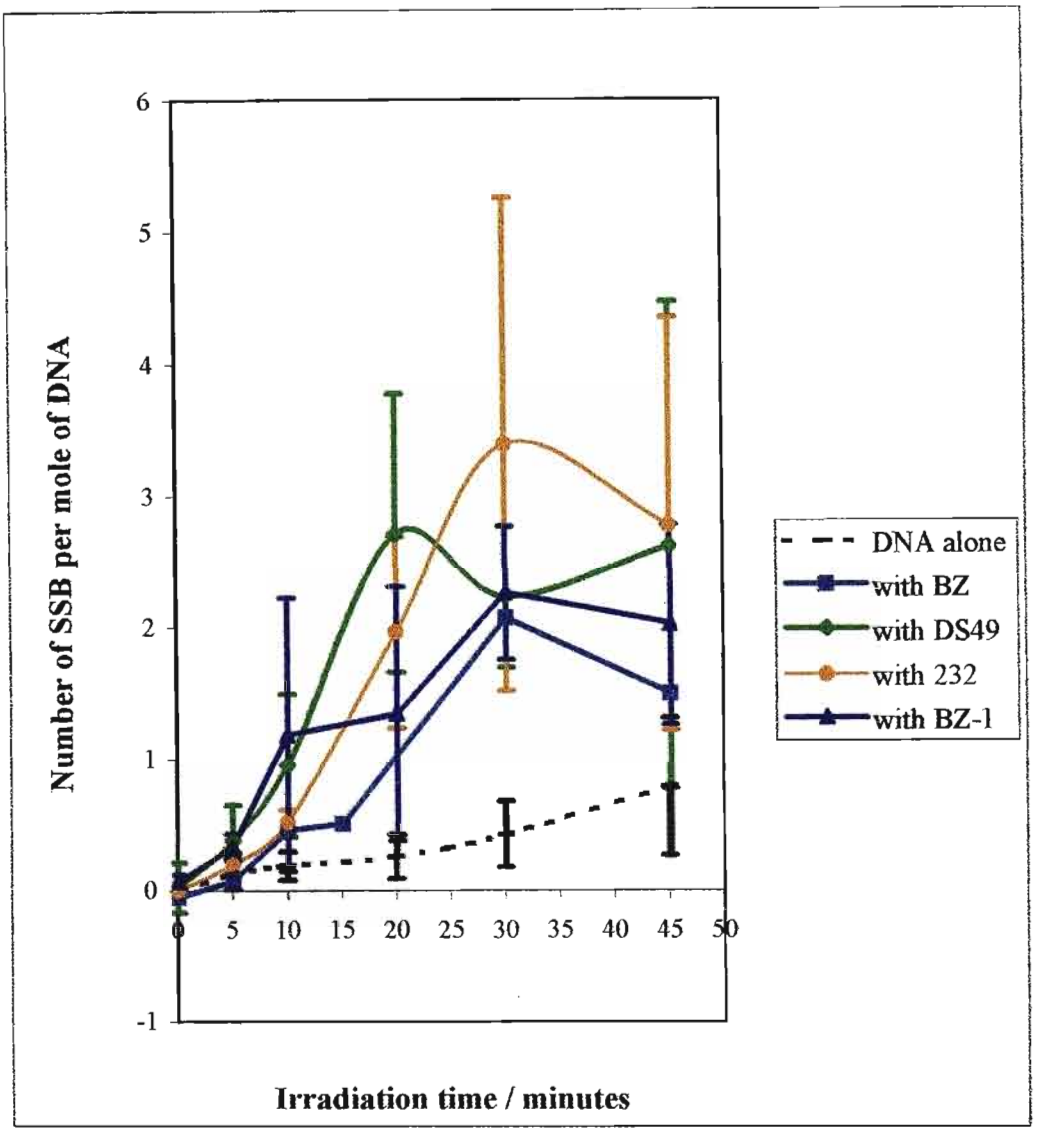

Figure 3.43: Change in the number of SSB per mole of DNA induced by the irradiation of ϕX174 DNA in the presence of benzophenone (BZ) [N=2], benzophenone-1 (BZ-1) [N=3], Uvinul DS49 (DS49) [N=3] and Eusolex 232 (232) [N=3]. The dashed line shows the control, which represents DNA irradiated alone [N=6] and N refers to the number of replicates.

The photocleavage trend observed here suggests that irradiation of DNA in the presence of benzophenone, benzophenone-1, Uvinul DS49 and Eusolex 232 greatly enhanced DNA photocleavage in that order. This is a definite cause for concern since these UV absorbers are approved for use in sunscreen and cosmetic formulations, apart from benzophenone, the use of which is currently being reviewed. If these UV absorbers were to be absorbed through the skin and enter human cells then DNA strand breaks would be able to occur in the body. If these are left unrepaired, they may contribute to mutagenesis, carcinogenesis, inherited disease and eventually cell death.

3.2.4 DNA photocleavage by benzophenone-3 and benzophenone-4

Benzophenone-3 and benzophenone-4 demonstrated similar DNA photocleavage patterns. However, their behaviour differed substantially from that of the parent compound benzophenone as well as from the other UV absorbers discussed above. The ethidium bromide-stained agarose gels showing DNA cleavage induced by the presence of benzophenone-3 and benzophenone-4, appear in Figures 3.44-3.46 and 3.47-3.48 respectively.

From Figures 3.44-3.48, it can be seen that only two DNA Forms were present. These were the supercoiled DNA Form I (lower band in each lane), and the nicked circular DNA Form II (upper band in each lane). What is also evident is that the relative amounts of DNA forms remained constant in the case of benzophenone-3 (see lane graphs in Figures 3.44-3.46) irrespective of the irradiation period.

However, for benzophenone-4 (Figures 3.47-3.48) as the irradiation time was increased, the composition of the supercoiled DNA Form I content decreased slightly while that of the nicked circular DNA Form II was slightly increased.

The mean percentage of the DNA in Forms I and II as well as the number of SSB induced on the DNA after treatment with benzophenone-3 and benzophenone-4 have been plotted against irradiation time in Figures 3.49-3.51 respectively. Included in these figures are the controls (represented by the dotted lines), which depict irradiation of the DNA in the absence of the UV absorbers. Error bars represent the standard deviation at each irradiation time for the UV absorbers. As mentioned before these error bars are large, which is typical of this assay. The results of the DNA photocleavage experiments for benzophenone-3 and benzophenone-4 can be found in Appendices B6 and B7 respectively.

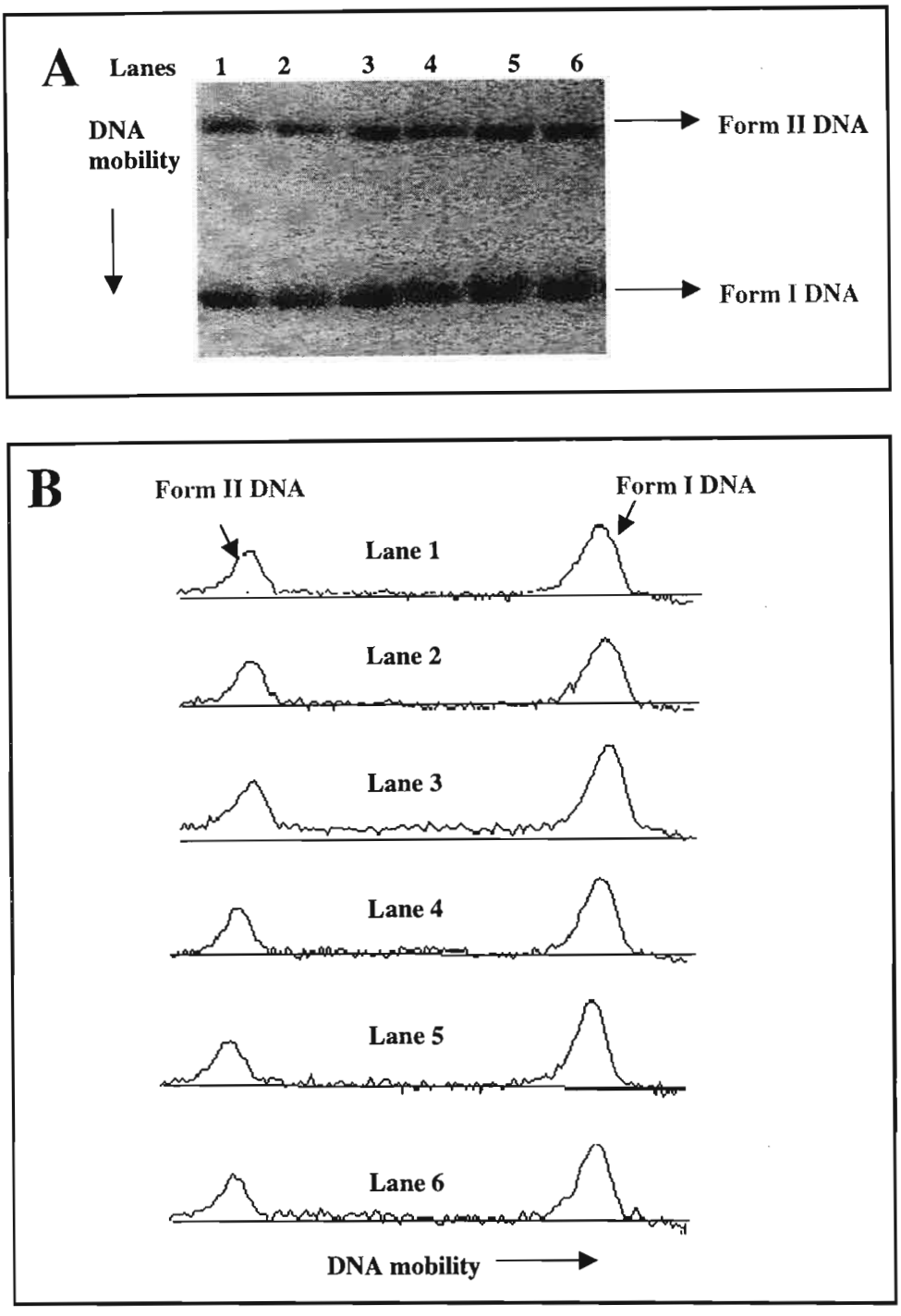

Figure 3.44 The ethidium bromide-stained agarose gel (A) and the densitometric lane graph (B) showing cleavage of ϕX174 DNA (18.85 μM) photosensitised by benzophenone-3 (50 μM). DNA samples in lanes 1-6 were irradiated for 0, 5, 10, 20, 30 and 45 minutes, respectively (RUN 1).

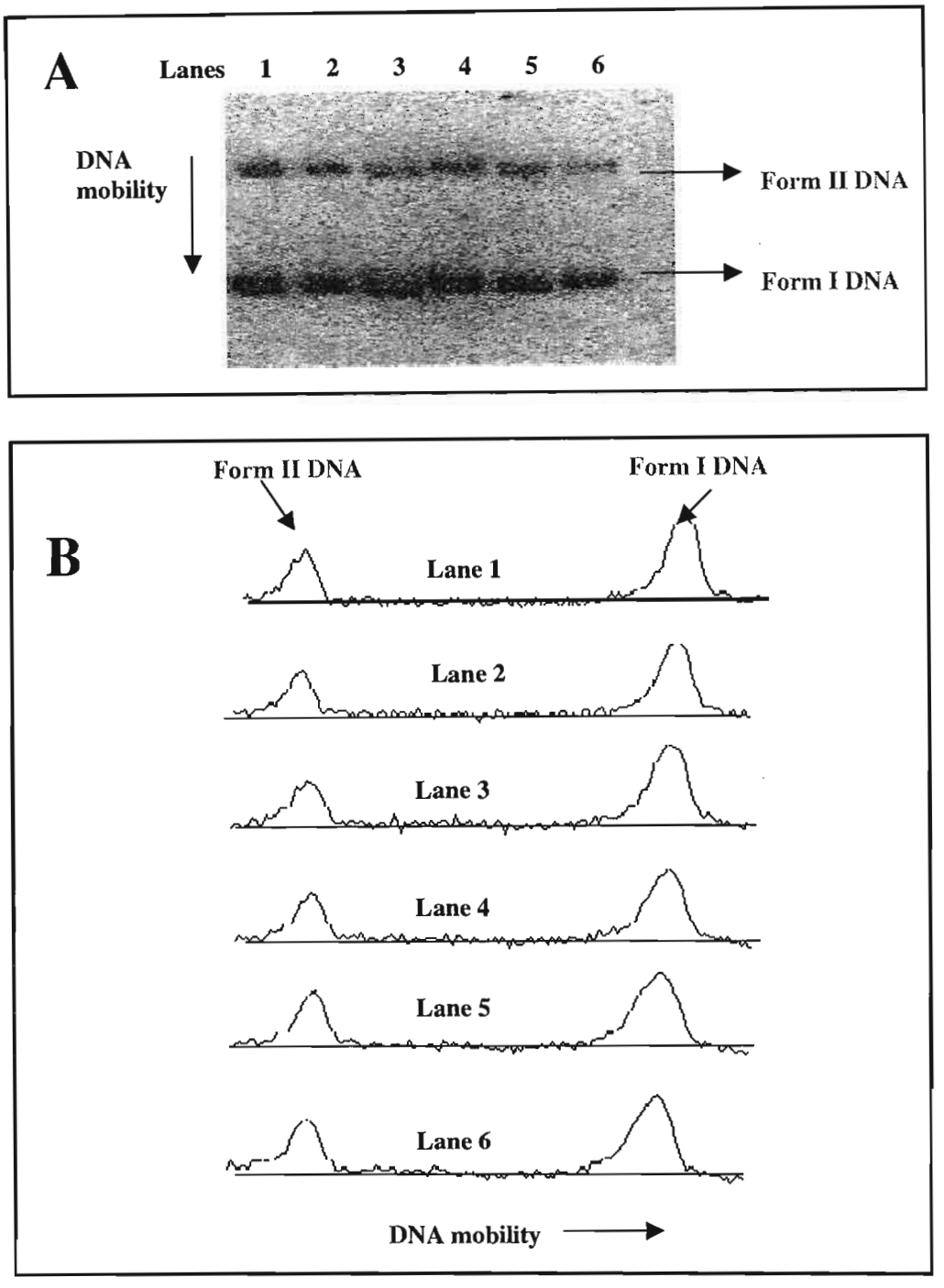

Figure 3.45: The ethidium bromide-stained agarose gel (A) and the densitometric lane graph (B) showing cleavage of ϕX174 DNA (18.85 μM) photosensitised by benzophenone-3 (50 μM). DNA samples in lanes 1-6 were irradiated for 0, 5, 10, 20, 30 and 45 minutes, respectively (RUN 2).

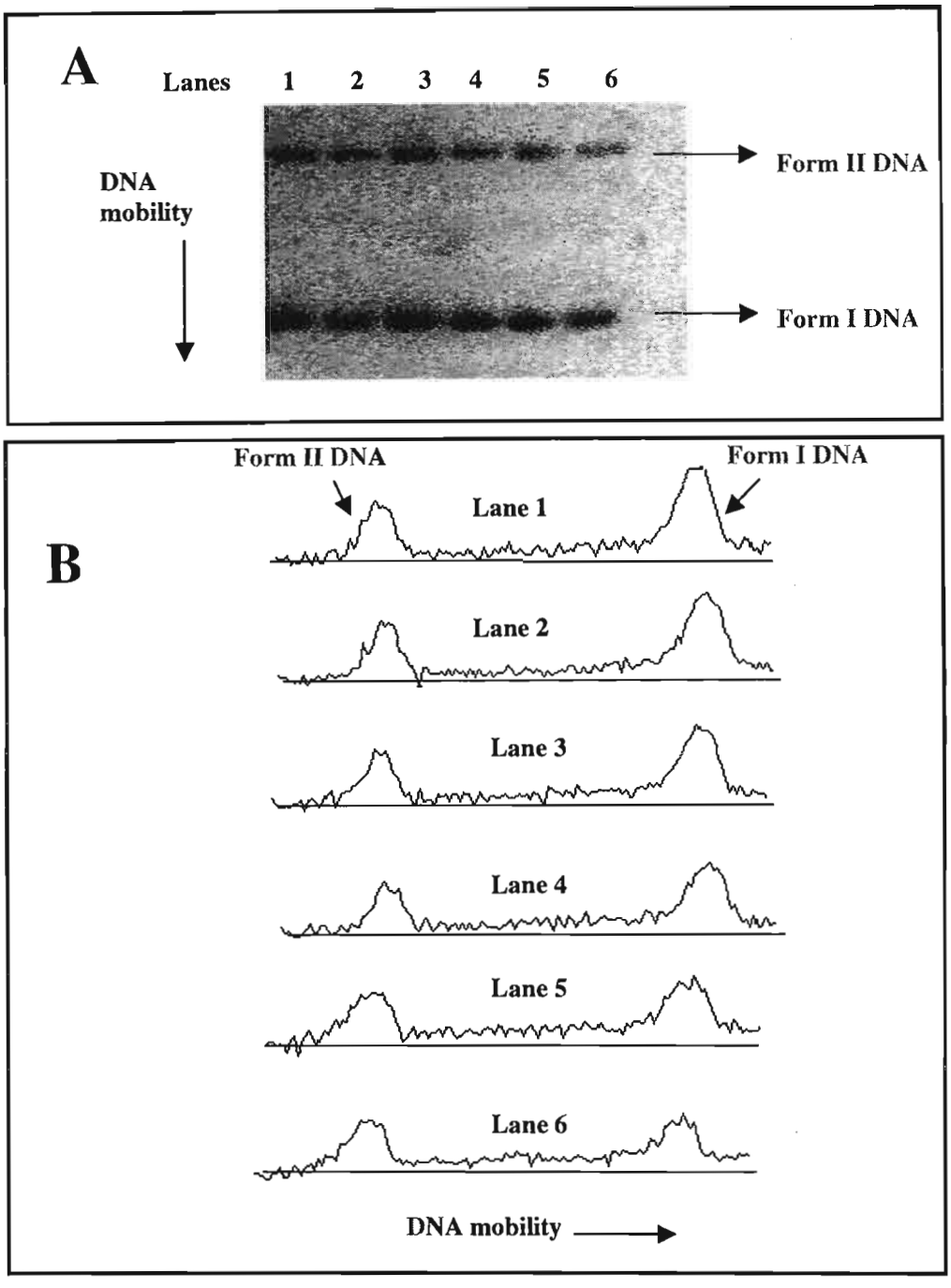

Figure 3.46: The ethidium bromide-stained agarose gel (A) and the densitometric lane graph (B) showing cleavage of ϕX174 DNA (18.85 μM) photosensitised by benzophenone-3 (50 μM). DNA samples in lanes 1-6 were irradiated for 0, 5, 10, 20, 30 and 45 minutes, respectively (RUN 3).

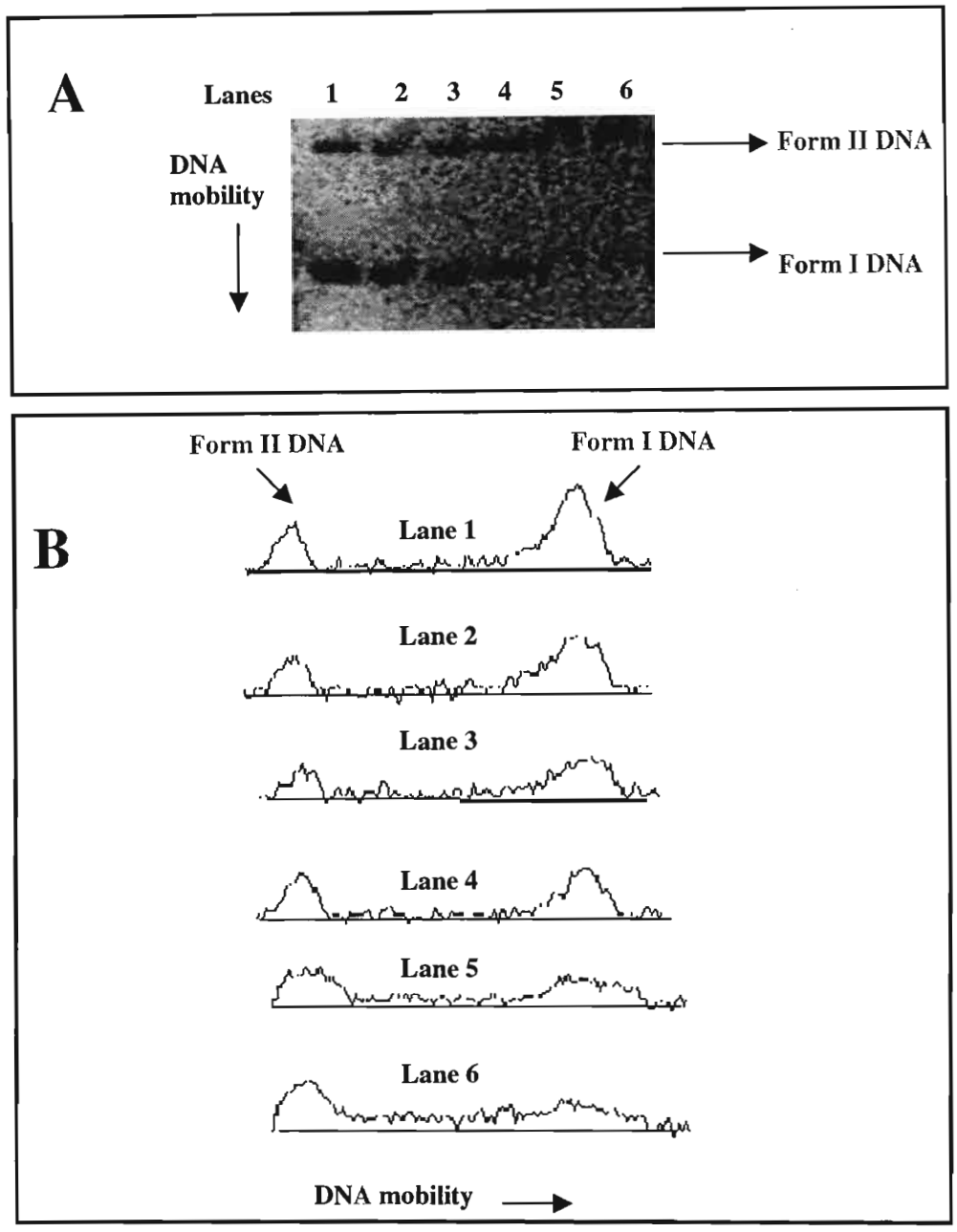

Figure 3.47: The ethidium bromide-stained agarose gel (A) and the densitometric lane graph (B) showing cleavage of ϕX174 DNA (18.85 μM) photosensitised by benzophenone-4 (50 μM). DNA samples in lanes 1-6 were irradiated for 0, 5, 10, 20, 30 and 45 minutes, respectively (RUN 1).

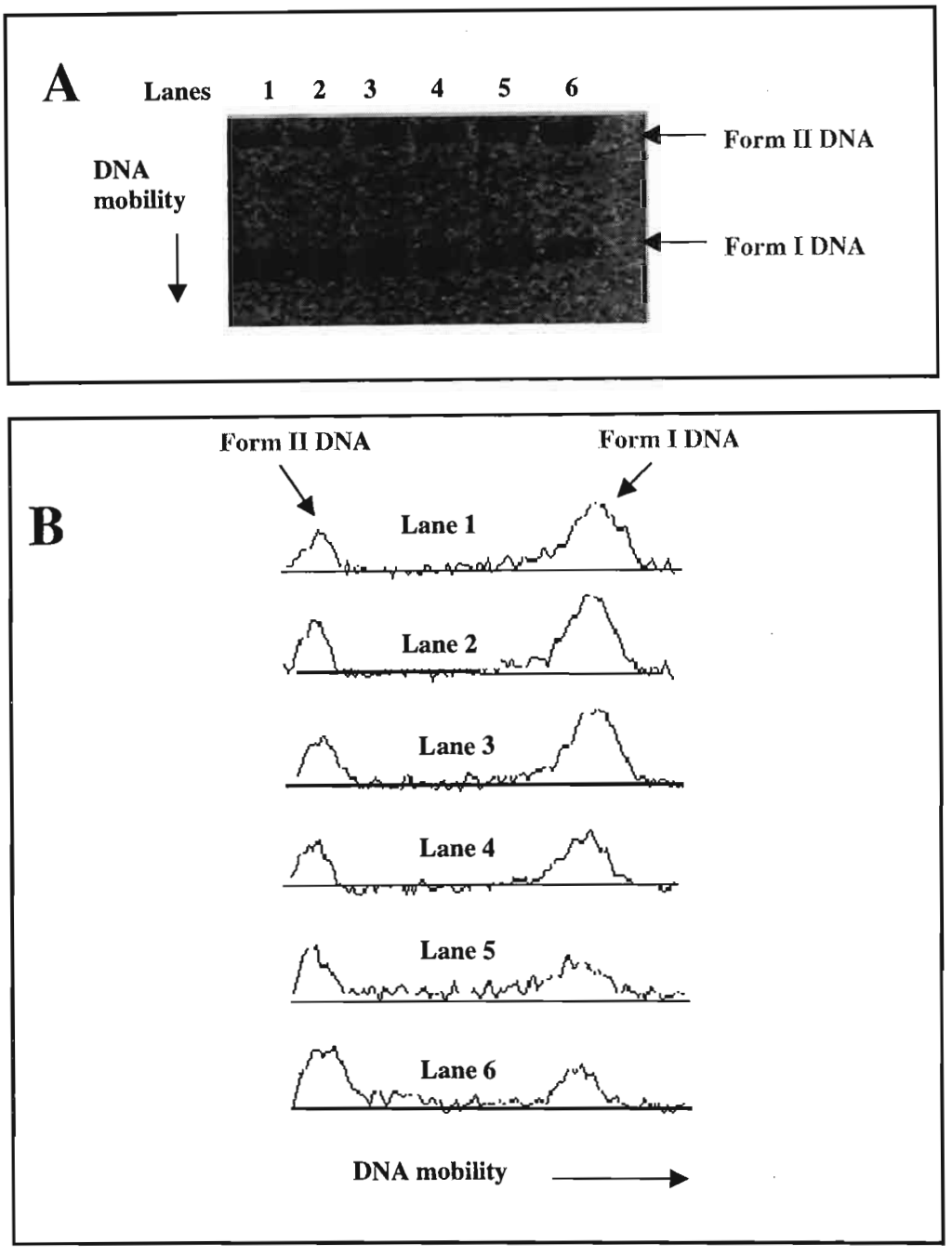

Figure 3.48: The ethidium bromide-stained agarose gel (A) and the densitometric lane graph (B) showing cleavage of ϕX174 DNA (18.85 μM) photosensitised by benzophenone-4 (50 μM). DNA samples in lanes 1-6 were irradiated for 0, 5, 10, 20, 30 and 45 minutes, respectively (RUN 2).

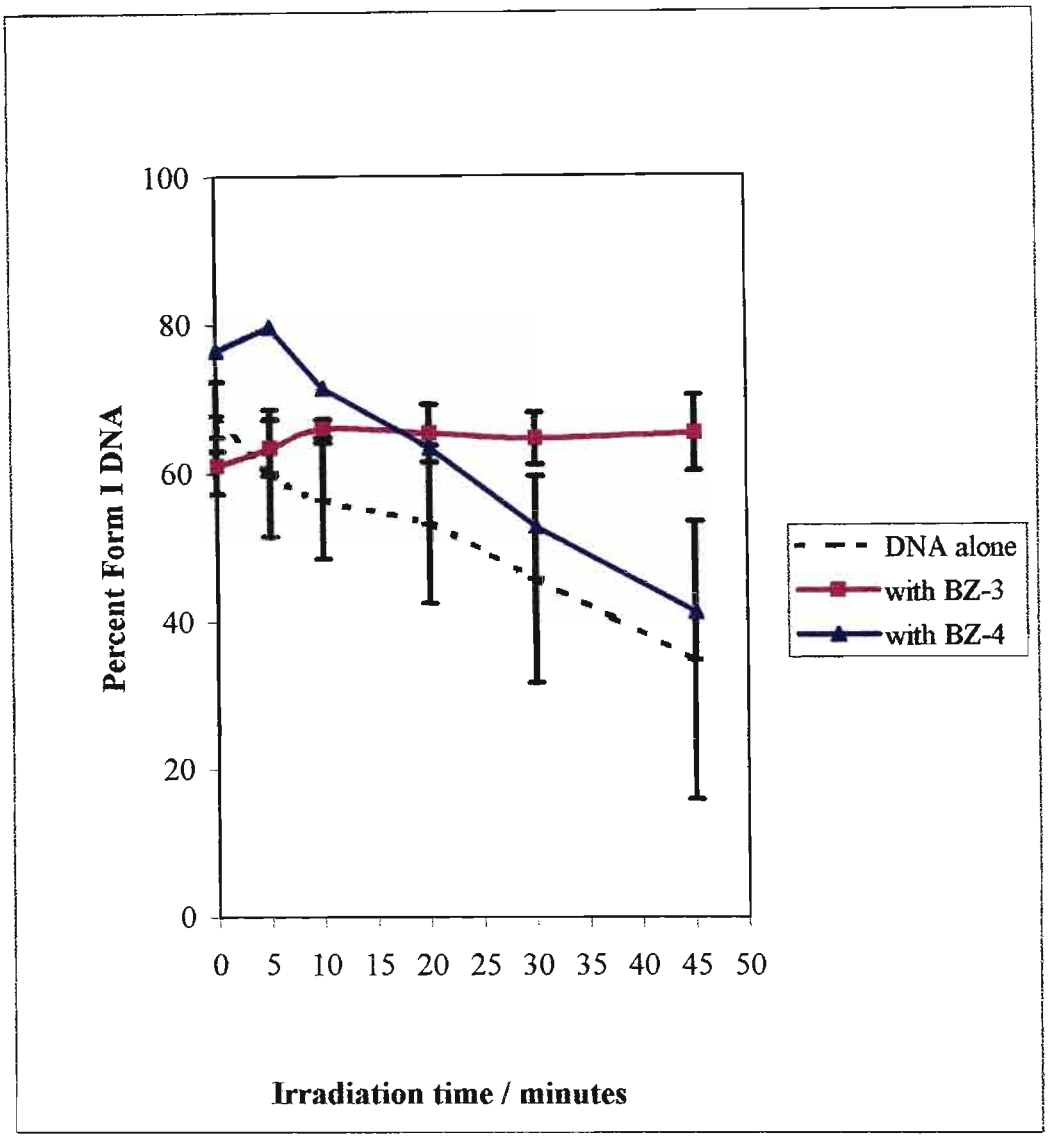

Figure 3.49: Change in the percentage of supercoiled DNA Form I induced by the irradiation of ϕX174 DNA in the presence of benzophenone-3 (BZ-3) [N=3] and benzophenone-4 (BZ-4) [N=2]. The dashed line shows the control, which represents DNA irradiated alone [N=6] and N refers to the number of replicates.

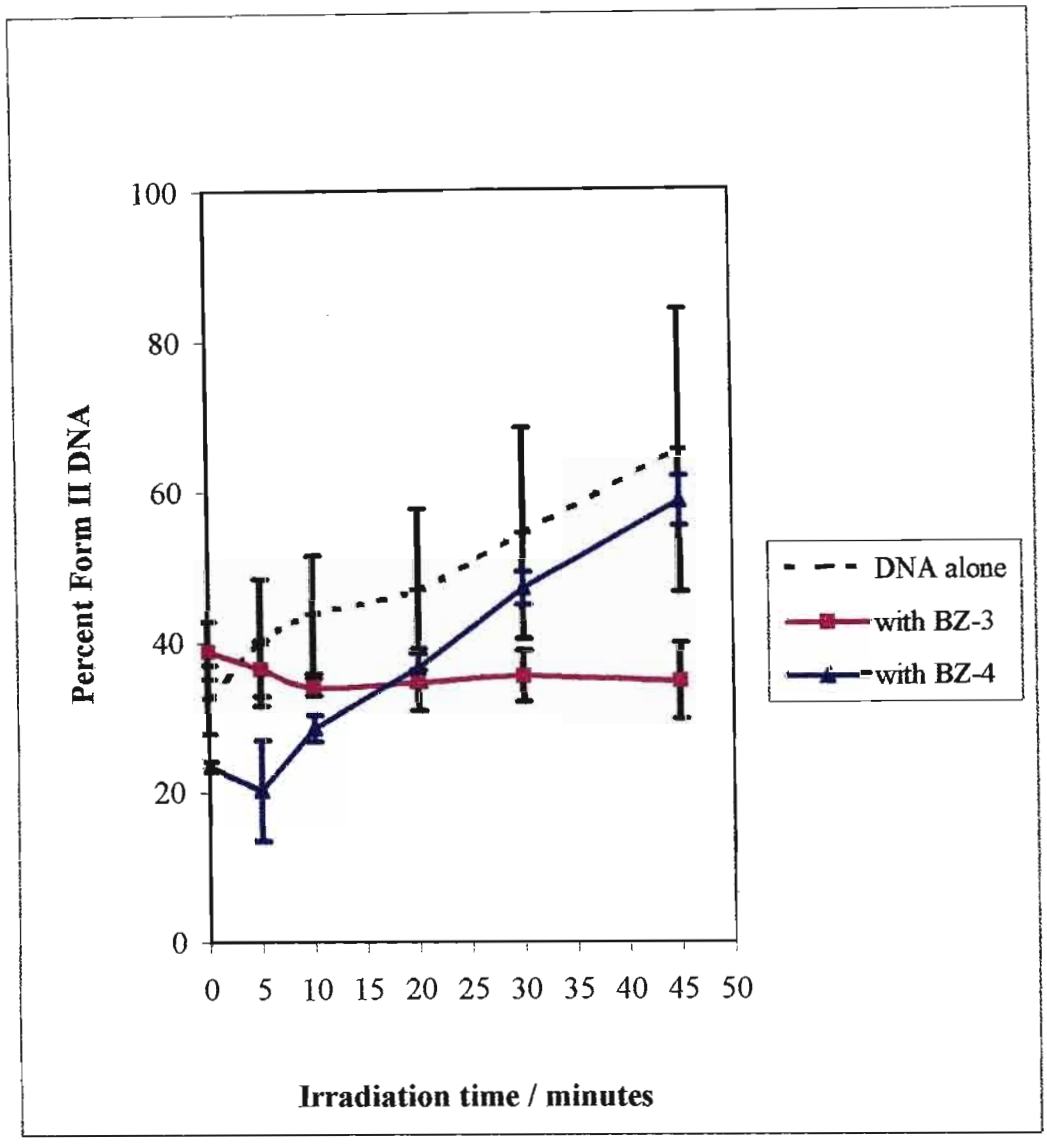

Figure 3.50: Change in the percentage of nicked circular DNA Form II induced by the irradiation of ϕX174 DNA in the presence of benzophenone-3 (BZ-3) [N=3] and benzophenone-4 (BZ-4) [N=3]. The dashed line shows the control, which represents DNA irradiated alone [N=6] and N refers to the number of replicates.

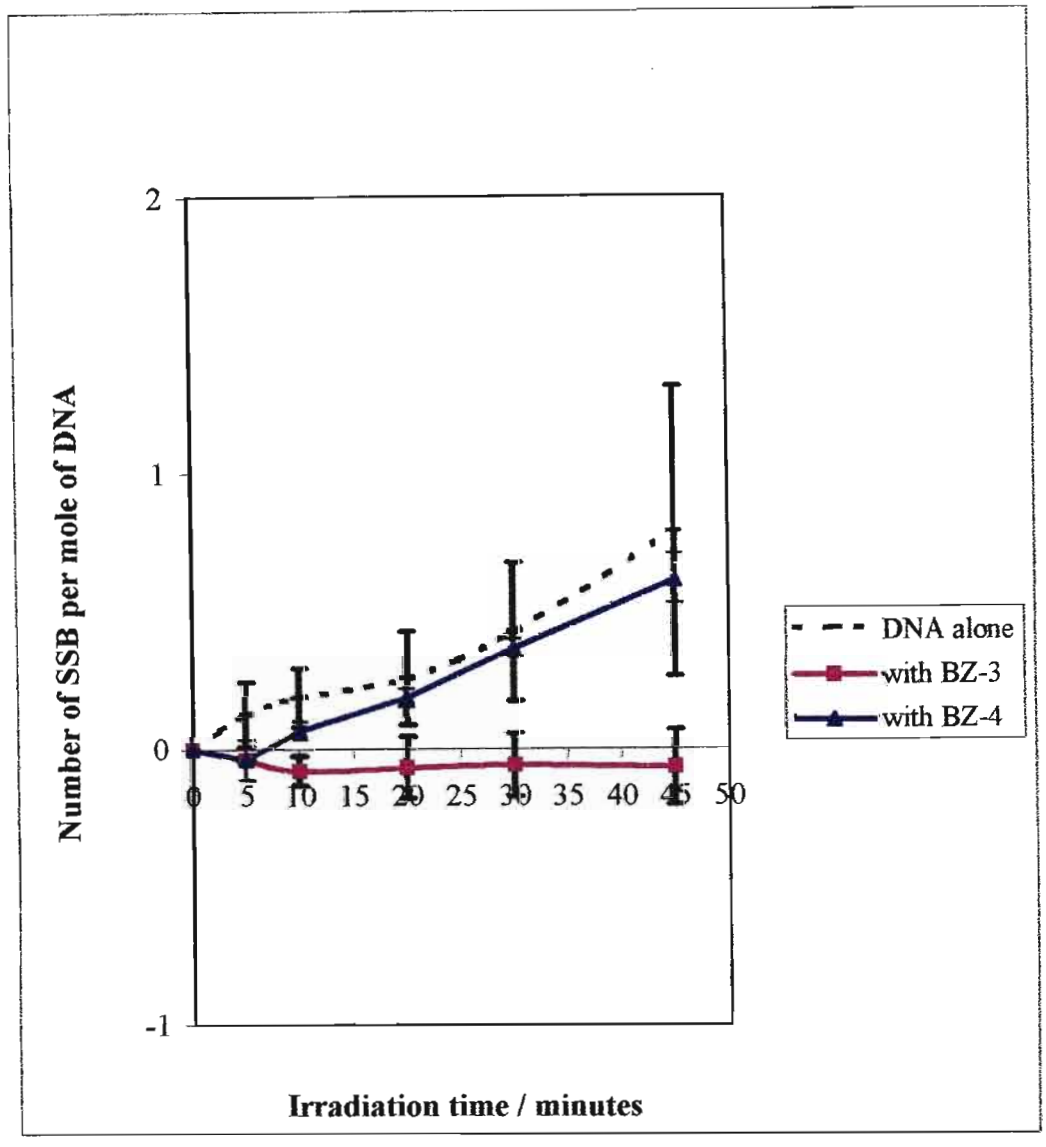

Figure 3.51: Change in the number of SSB per mole of DNA induced by the irradiation of ϕX174 DNA in the presence of benzophenone-3 (BZ-3) [N=3] and benzophenone-4 (BZ-4) [N=2]. The dashed line shows the control, which represents DNA irradiated alone [N=6], and N refers to the number of replicates.

From Figure 3.49, it is apparent that when ϕX174 DNA was irradiated in the presence of benzophenone-3, the supercoiled DNA Form I content changed only negligibly from 61% without irradiation, to 65% after 45 minutes of irradiation (Appendix B6). This implies that for the duration of the irradiation period the supercoiled DNA content remained almost constant. In the case of benzophenone-4, after 45 minutes of irradiation of the DNA in its presence, the supercoiled DNA content was decreased from 77% initially to 41% indicating that 46% of the DNA was nicked in the presence of benzophenone-4. When this is compared to the control, which demonstrated a 49% decrease in the supercoiled Form I content, the results clearly show that in the presence of benzophenone-4, the number of nicks on the supercoiled DNA was reduced, but more so in the presence of benzophenone-3. When benzophenone-3 was present the supercoiled DNA was almost completely protected from nicks irrespective of irradiation time.

From Figure 3.50, it can be seen that the nicked circular DNA Form II content was also smaller in the presence of both benzophenone-3 and benzophenone-4 compared to when they were absent. After 45 minutes of irradiation of DNA in the presence of benzophenone-3 and benzophenone-4 35% and 59% of the DNA existed as the nicked circular DNA Form II respectively compared to 65% when the DNA was irradiated alone (control). No linear DNA Form III was formed when the DNA was irradiated in the presence of either benzophenone-3 or benzophenone-4.

Also the number of SSB per DNA mole is higher when the DNA was irradiated alone, compared to when either benzophenone-3 or benzophenone-4 were present (Figure 3.51). After 45 minutes of irradiation the number of SSB produced when benzophenone-3 was present was undetectable, however, in the presence of benzophenone-4, 0.61 SSB per DNA mole was produced. The control suggests that 0.79 SSB per DNA mole was produced when the DNA was irradiated alone (Appendix B1), hence it can be seen that both benzophenone-4 and benzophenone-3 protect ϕX174 DNA from SSB. In the presence of benzophenone-3 SSB are completely prevented.

It can be concluded that DNA photocleavage was decreased both in the presence of benzophenone-3 and benzophenone-4 compared to in their absence. Both these UV absorbers protected DNA from photocleavage, with this effect being more pronounced when benzophenone-3 was present. From these results it appears that benzophenone-3 and benzophenone-4 do not cleave DNA under UV irradiation therefore their use in sunscreen formulations is acceptable.

3.3 Fluorescence spectroscopy to detect DNA binding

The Fluorescent Intercalator Displacement technique (FID) is a fast and efficient method to detect DNA binding *in vitro*. In this assay, the fluorescence from ethidium bromide was used as a reporter of DNA damage. It utilises competition of an added compound with ethidium bromide for DNA intercalation sites. The parameters selected for the assay are discussed in Section 3.3.1, the mode of interaction of ethidium bromide and DNA is described in Section 3.3.2, while in Section 3.3.3 the photocleavage efficiencies of the UV absorbers under investigation as detected by the FID assay are discussed.

3.3.1 Parameters selected for FID assay

The success of the FID assay is dependent on a number of parameters, all of which have been addressed in Section 2.4.4. A 1: 2 ethidium bromide: DNA bp ratio was used to ensure that all intercalation sites on the DNA helix are occupied. A 6:1 DNA bp: UV absorber ratio was required to provide an assay sensitive enough to depict large and sharp decreases in the fluorescence intensity. A Tris-HCl buffer with high salt concentration (0.1 M Tris-HCl) was used to ensure that binding of the ethidium bromide occurred exclusively by intercalation and not to the anionic phosphate groups on the outside of the helix. Two other parameters that had to be determined were the excitation and fluorescence monitoring wavelengths. These will now be discussed.

Fluorescence excitation wavelength

Excitation of ethidium bromide has been frequently performed directly at 510 nm, 525 nm or 546 nm (Armitage *et al.* [1994], Mohtat *et al.* [1998], Strothkamp [1994], Cain *et al.* [1978], Reinhardt & Krugh [1978] and Boger *et al.* [2001]), as well as indirectly at 260 nm (Geall & Blagbrough [2000]). The excitation wavelength for ethidium bromide had to be very carefully selected to ensure that the absorbance of ethidium bromide at the excitation wavelength was below 0.05 absorbance units, such that errors due to self-absorbance were avoided, yet the absorbance was large enough to ensure a sensitive assay. In addition, the excitation wavelength chosen should give the best resolution of peaks. The absorbance of the ethidium bromide solution (0.68×10^{-5} M) used in this assay was measured with a Cary 1E UV-Visible spectrophotometer so that the optimum excitation wavelength could be determined. The spectrum obtained appears in Figure 3.52.

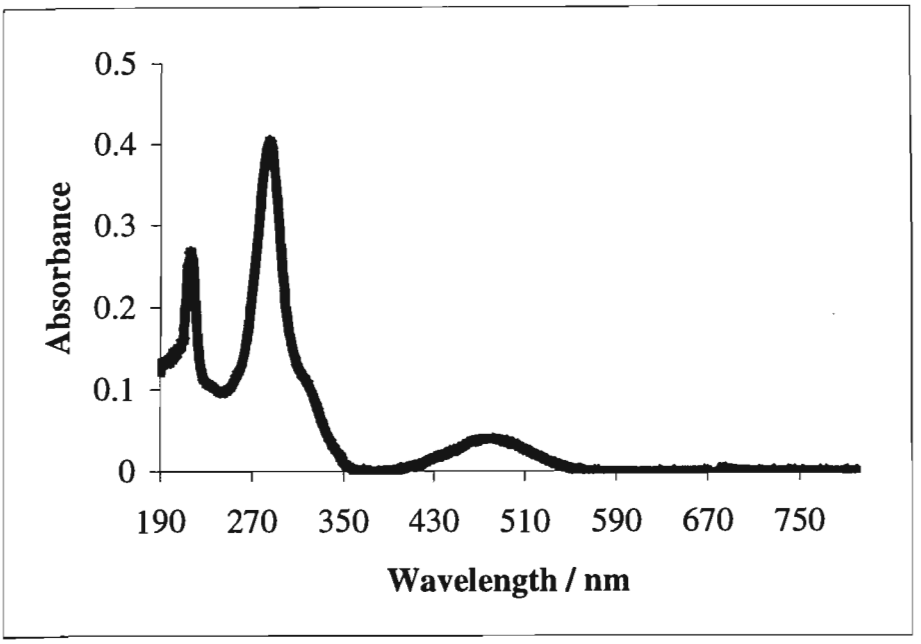

Figure 3.52: The absorption spectrum of the 0.68 x 10^{-5} M solution of ethidium bromide.

Excitation at 546 nm and 525 nm were both discarded since the absorbance of ethidium bromide at the former wavelength was 0.0049 and hence not sufficient enough to induce fluorescence, while at the latter it was 0.016 and not large enough to provide a sensitive assay. Excitation at 260 nm was also discarded since the absorbance of ethidium bromide at this wavelength was too large (0.128 absorbance units) and also gave poor resolution of fluorescence. The excitation wavelength that gave the best resolution of peaks was 510 nm. In addition the absorbance of ethidium bromide at this wavelength was 0.027 absorbance units and below the required limit of 0.05 units. Excitation of ethidium bromide at 510 nm was therefore selected to be used in this assay.

Fluorescence monitoring wavelength

The fluorescence of ethidium bromide (0.68 x 10^{-5} M) was measured with a Perkin Elmer LS 50B luminescence spectrophotometer. The spectrum was measured from 525 nm to 700 nm with excitation at 510 nm and appears in Figure 3.53. From this figure it can be seen that the maximum fluorescence of ethidium bromide occurs around 586 nm. This was chosen as the wavelength to be used to monitor the fluorescence of ethidium bromide from the FID assay.

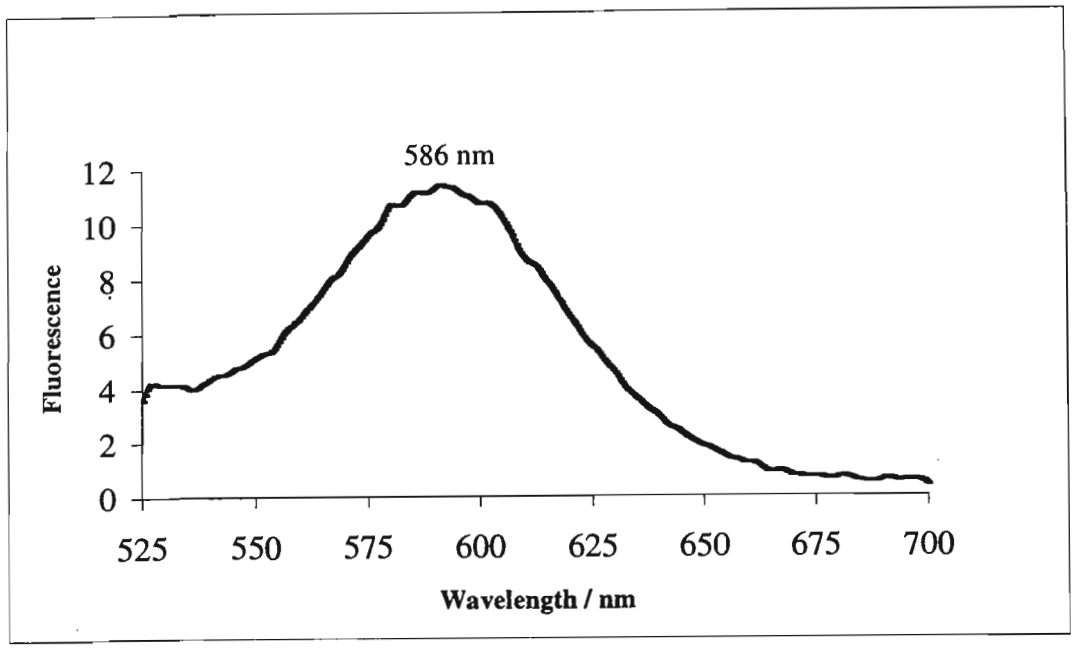

Figure 3.53: Fluorescence spectrum of ethidium bromide (0.68 x 10^{-5} M) showing maximum fluorescence at 586 nm.

None of the UV absorbers being investigated or the buffers fluoresced or absorbed light at this chosen wavelength, hence indicating that fluorescence at 586 nm would be due entirely to that of ethidium bromide.

3.3.2 The mode of interaction of ethidium bromide with DNA

The fluorescence spectra of ethidium bromide (0.68 x 10^{-5} M) both in the absence and the presence of calf thymus DNA (1.2 x 10^{-5} M bp) were measured as described in Section 2.4.6 with a Perkin Elmer LS 50B luminescence spectrophotometer. The spectra, which were measured from 525 nm to 700 nm with excitation at 510 nm, are presented in Figure 3.54.

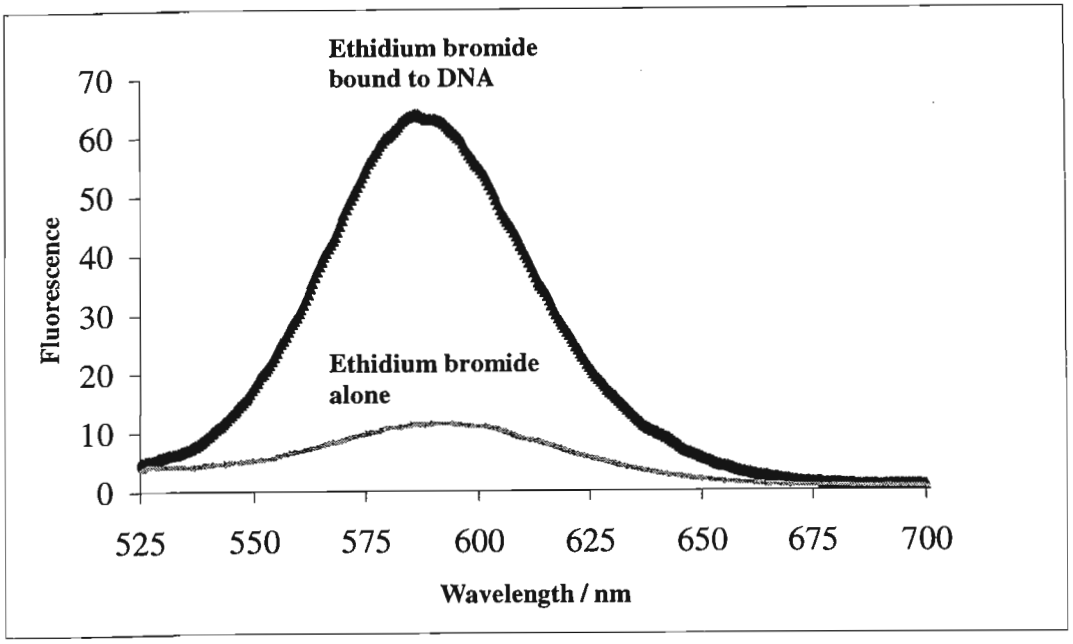

Figure 3.54: Fluorescence spectra of ethidium bromide (0.68 x 10^{-5} M) alone and ethidium bromide bound to calf thymus DNA (1.2 x 10^{-5} M bp).

It is apparent that ethidium bromide in the absence of DNA was very poorly fluorescent and depicted only a small emission peak with an intensity of 10 units at about 586 nm. In the presence of the DNA, the intensity of the fluorescence was dramatically increased to about 65 units at this emission wavelength. The increase in fluorescence upon binding to DNA as observed in Figure 3.54 has been well established in literature to be due to intercalation of the ethidium bromide between the base pairs of the DNA double helix, producing a strongly fluorescent complex.

The nature of this interaction between ethidium bromide and DNA has been well characterised in literature (Lepecq & Paoletti. [1967], Lober *et al.* [1974], Reinhardt & Krugh [1978] and Geall & Blagbrough [2000]). Ethidium bromide intercalates with the DNA by vertical stacking of the phenanthridium ring between two nucleotide bps of the DNA double helix such that the phenanthridium ring is roughly parallel to the bps (Reinhardt & Krugh [1978]) (Figure 3.55).

Ethidium bromide does not have a requirement for any particular base in binding to DNA, but it does show a preference in forming complexes with cytosine-guanine and other pyrimidine-purine sequence dinucleotides (Reinhardt & Krugh [1978]). Binding of the dye is saturated when one dye

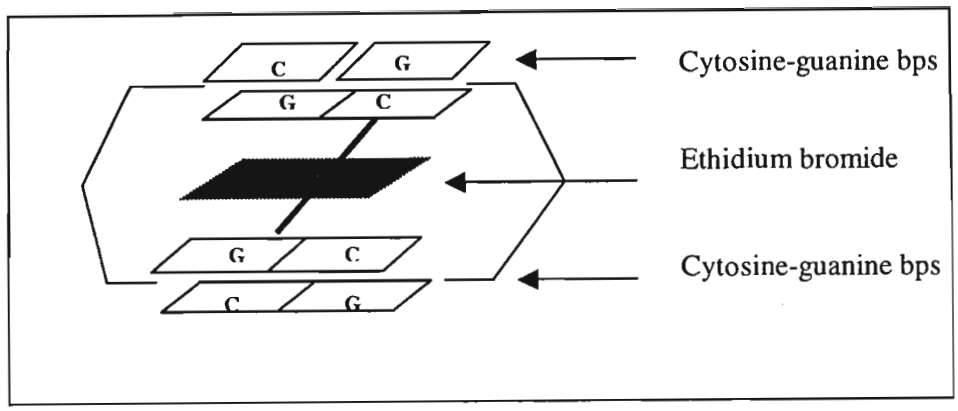

Figure 3.55: Schematic diagram showing intercalation of ethidium bromide with the DNA bps.

molecule is bound for every 4 or 5 bps (Reinhardt & Krugh [1987] and Geall & Blagbrough [2000]). This implies that there is one intercalation site for every other bp.

According to Olmstead & Kearns [1977], this fluorescence increase is due to a reduction in the rate of deactivation of the excited state of ethidium bromide. Deactivation of free ethidium bromide in aqueous solution is by proton transfer from the excited singlet state to water (Geall & Blagbrough [2000]). When ethidium bromide intercalates DNA, slow proton transfer occurs as the ethidium bromide is sterically protected from the aqueous solvent. This results in longer lifetimes for ethidium bromide and hence fluorescence enhancement.

3.3.3 DNA binding by the UV absorbers detected by the FID assay

The FID technique uses the fluorescence of ethidium bromide when bound to DNA as a useful tool to detect DNA binding by another competing compound. Any process that destroys potential DNA binding sites for ethidium bromide would result in a decrease in the ethidium bromide fluorescence intensity. However, this technique does not allow for the specific binding site on the DNA to be identified. A molecule may bind to DNA at a site different to that at which ethidium bromide binds, but due to neighbour exclusion and steric interferences, the number of binding sites available for ethidium bromide could be decreased and hence fluorescence would be reduced (Cain *et al.* [1978]). Non-intercalating compounds therefore will also compete with ethidium bromide and a

fluorescence decrease does not necessarily imply that the compound under investigation binds to DNA in a similar manner to that of ethidium bromide.

In this series of experiments the ability of the benzophenone-derived UV absorbers to bind to DNA when irradiated with UV light was investigated using the FID assay. Each UV absorber was treated as described in Section 2.4.6. Samples containing 0.36 ml of 1 x 10^{-4} M DNA bp and 1.67 x 10^{-5} M of the UV absorber were irradiated at one minute intervals for a total irradiation period of 5 minutes with an Osram HBO 500W/2 high pressure mercury lamp at wavelengths greater than 300 nm. Longer irradiation periods were not analysed since they showed larger fluctuations in results due to the extreme sensitivity of this technique. A 2.64 ml volume of ethidium bromide was then added to the irradiated sample and it was allowed to equilibrate at 25°C for 30 minutes, after which the fluorescence of ethidium bromide was measured with a Perkin Elmer LS 50B luminescence spectrometer. The excitation wavelength was 510 nm, while the fluorescence was monitored at 586 nm.

This assay was performed with a ratio of one UV absorber for every 6 DNA bps, therefore it is assumed that if each UV absorber were to react only once, then a maximum of 6% of the available binding sites could be destroyed per DNA molecule. However, large fluctuations in fluorescence readings with this assay have been reported previously in literature (Geall & Blagbrough [2000]). Therefore for each UV absorber analysed the assay was performed at least in duplicate, and the average and standard deviation was determined.

The percentage of ethidium bromide binding sites remaining after interaction of the UV absorber with the DNA was calculated from Equation 2.10. For this calculation the fluorescence intensity of the buffer was required. The fluorescence of both the Tris-HCl buffer as well as the 50% (v/v) ethanol: Tris-HCl buffer was measured and their spectra appear in Figures 3.56 and 3.57. From the spectra it can be seen that both buffers fluoresced negligibly at the wavelength of maximum fluorescence of ethidium bromide (586 nm). Therefore, when calculating the percentage of binding sites remaining, the fluorescence intensity of the buffer was taken to be zero.

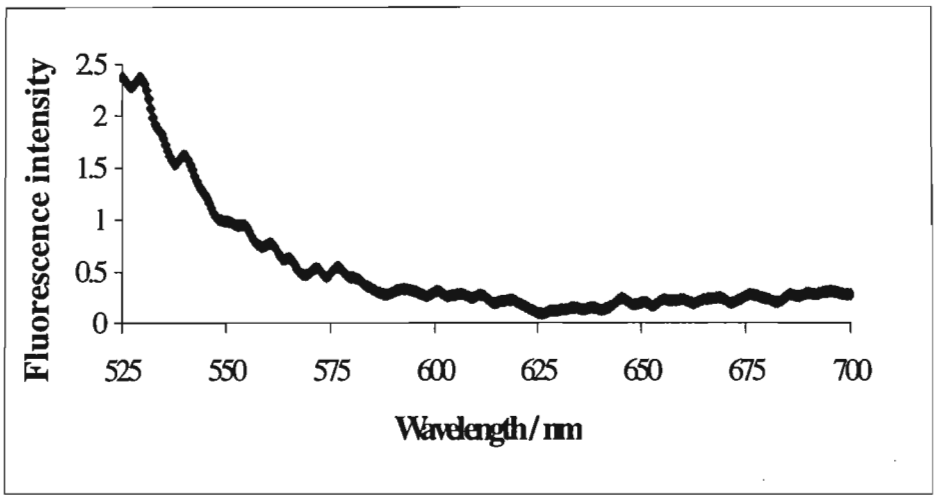

Figure 3.56: Fluorescence spectrum of Tris-HCl buffer showing negligible fluorescence at 586 nm.

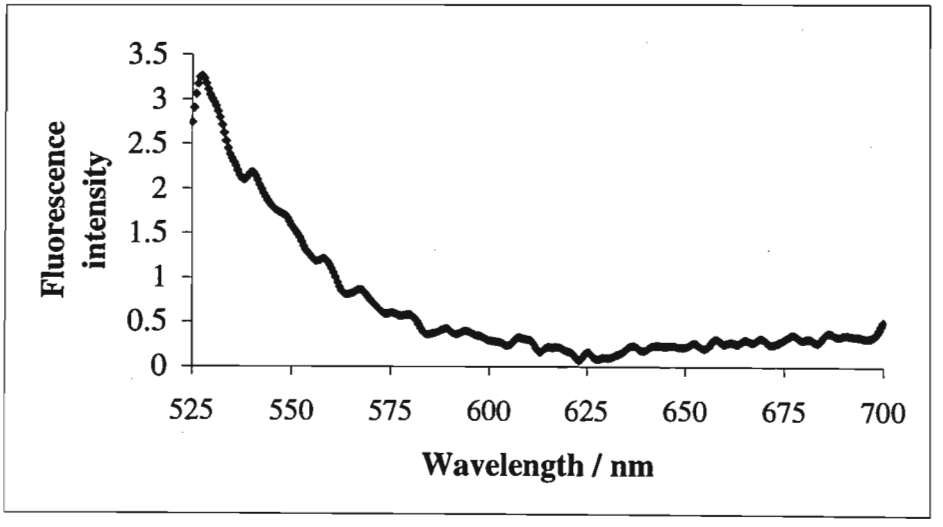

Figure 3.57 Fluorescence spectrum of 50% (v/v) ethanol: Tris-HCl buffer showing negligible fluorescence at 586 nm.

The binding interaction of ethidium bromide with DNA was investigated firstly in the absence of the UV absorbers. This served as the control, and by comparing it to the experiment, the DNA binding ability of the UV absorbers could be determined. The controls were subjected to the same conditions as the experiments. Since two different buffers were used to dissolve the UV absorbers, two control experiments had to be set up. In the first, the DNA was dissolved in Tris-HCl buffer and this served as the control for all the UV absorbers, except benzophenone-3. For benzophenone-3, however, the control consisted of DNA dissolved in 50% (v/v) ethanol: Tris-HCl buffer.

The average percentage of binding sites remaining after irradiating the DNA alone for a total irradiation period of 5 minutes in Tris-HCl buffer and 50% (v/v) ethanol: Tris-HCl buffer were calculated and the values have been plotted against irradiation time and appear in Figures 3.58 and 3.59 respectively. After 5 minutes of irradiation of DNA in both buffers, the percentage of binding sites remaining showed no significant decrease. For both controls, the overall trend suggested that all the ethidium bromide-binding sites remained intact and no binding sites were destroyed after 5 minutes of irradiation at wavelengths greater than 300 nm. According to Boger *et al.* [2001], the variations in readings for this assay may be as large as 10%, therefore the fluctuation in the results as can be seen in both figures is typical of this assay. The equations of the curves in Figures 3.58 and 3.59 are $y = 0.367x + 104$ and $y = -0.0981x + 101$ respectively.

Benzophenone, the parent compound of the UV absorbers, was the first compound to be analysed by this assay. The percentage of ethidium bromide binding sites remaining after irradiation of calf thymus DNA (1.2×10^{-5} M bp) in the presence of benzophenone (2×10^{-6} M) was calculated for the 5 minute irradiation period by means of Equation 2.10, and the results have been plotted against irradiation time in Figure 3.60.

In the presence of benzophenone, the number of DNA binding sites available to ethidium bromide decreased with irradiation time. After 5 minutes of irradiation, 7.27% of the ethidium bromide binding sites were destroyed. The slope of the graph was determined to be -1.09, when this was compared to the slope of the control (0.367), it is apparent that ethidium bromide binding to DNA was decreased by 2.96 times in the presence of benzophenone compared to when it was absent. This implies that the destroyed ethidium bromide binding sites were occupied by benzophenone.

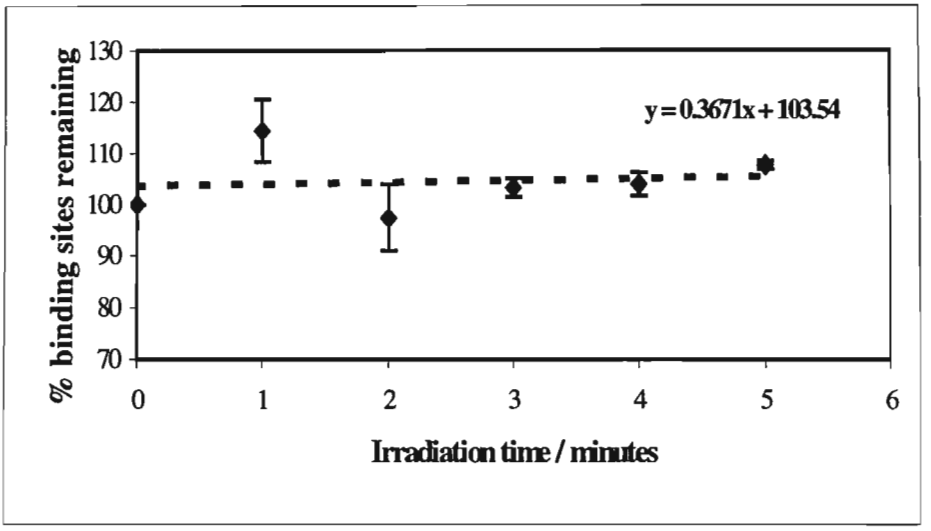

Figure 3.58: Ethidium bromide (0.6×10^{-5} M) binding to calf thymus DNA (1.2×10^{-5} M bp), irradiated in a Tris-HCl buffer (0.1 M, pH 8.0) at $\lambda > 300$ nm, in the absence of any UV absorber [N=2]. DNA binding was detected by the fluorescence of ethidium bromide at 586 nm. N refers to the number of replicates. (This served as the control for all the UV absorbers apart from benzophenone-3.)

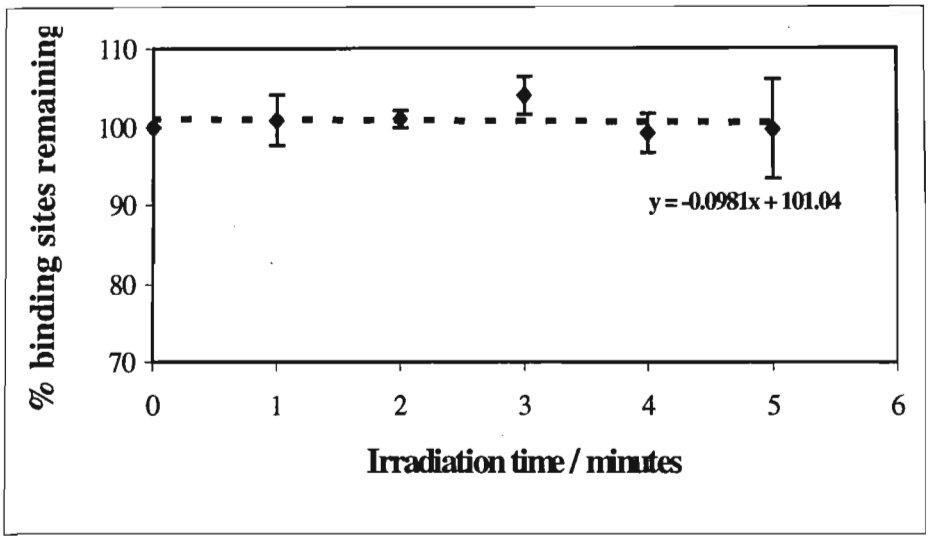

Figure 3.59: Ethidium bromide (0.6 x 10^{-5} M) binding to calf thymus DNA (1.2 x 10^{-5} M bp), irradiated in a 50% (v/v) ethanol: Tris-HCl buffer (0.1 M, pH 8.0) at $\lambda > 300$ nm, in the absence of any UV absorber [N=2]. DNA binding was detected by the fluorescence of ethidium bromide at 586 nm. N refers to the number of replicates. (This served as the control for benzophenone-3.)

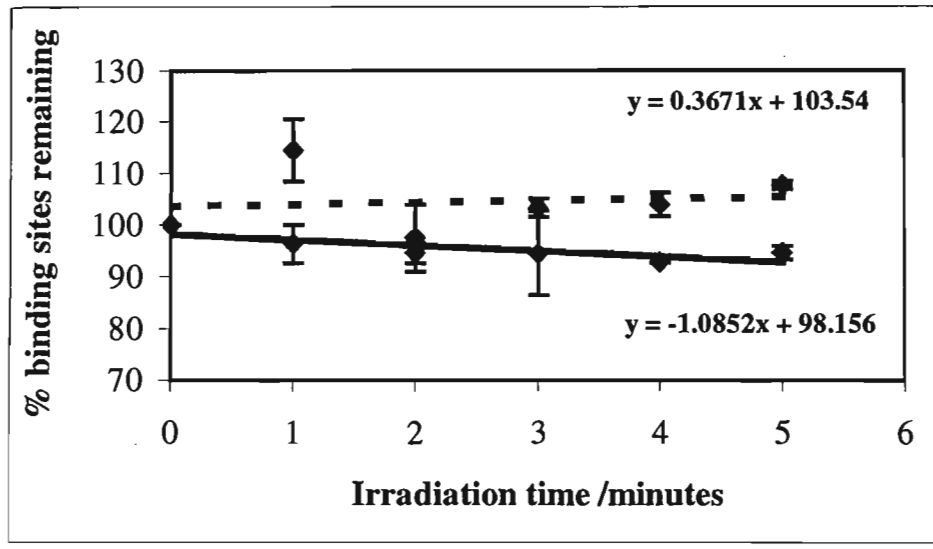

Figure 3.60: Ethidium bromide (0.6×10^{-5} M) binding to calf thymus DNA (1.2×10^{-5} M bp), irradiated in the presence of benzophenone (2×10^{-6} M) at $\lambda > 300$ nm, and detected by fluorescence at 586 nm [N=2]. The control, indicated by the dashed line, represents ethidium bromide binding to DNA in the absence of any sunscreen. N refers to the number of replicates.

The DNA binding ability of the UV absorbers under investigation in this study, were obtained similarly to that of benzophenone, and the percentage of ethidium bromide binding sites remaining after treatment of calf thymus DNA with each specific UV absorber were calculated and are plotted in Figures 3.61-3.66. From these graphs it can be seen that benzophenone-1, Uvinul DS49 and ketoprofen demonstarted comparable DNA binding patterns to that of benzophenone, while that of Eusolex 232, benzophenone-3 and benzophenone-4, differed, with this deviation being more pronounced with the latter two sunscreen agents.

For ketoprofen, benzophenone-1 and Uvinul DS49 the percentage of sites available for ethidium bromide to bind to DNA decreased with irradiation time as depicted in Figures 3.61 - 3.63. After 5 minutes of irradiation in the presence of Uvinul DS49, ketoprofen and benzophenone-1, ethidium bromide binding to DNA was decreased by 7.44%, 10.7% and 13.1% respectively (Figures 3.63, 3.61 and 3.62). The slopes of the graphs in Figures 3.61, 3.62 and 3.63 are -1.63, -2.10 and -1.52 respectively. When these values are compared to the slope of the control graph (0.367), it is clear that in the presence of ketoprofen, benzophenone-1 and Uvinul DS49, ethidium bride intercalation sites were reduced 4.45 fold, 5.57 fold and 4.14 fold respectively compared to when they were absent. This implies that the lost ethidium bromide binding sites may now be occupied by the respective UV absorbers.

Eusolex 232, however, did not display a similar reduction in ethidium bromide binding sites as observed with the UV absorbers mentioned above. DNA binding sites available to ethidium bromide, when calf thymus DNA was irradiated in the presence of Eusolex 232, appear in Figure 3.64. The slope of the graph is 0.0729 and the percentage of ethidium bromide binding sites remained almost constant for the duration of the irradiation period. This implies that Eusolex 232 did not compete with ethidium bromide binding sites on the DNA duplex. This result agrees with the work done by Stevenson & Davies [1998] and Inbaraj *et al.* [2002] who also showed the inability of Eusolex 232 to bind to calf thymus DNA.

For benzophenone-3 and benzophenone-4, two of the most commonly used sunscreens on the market, the DNA photobinding trend differed substantially from that of benzophenone. Instead of a reduction in ethidium bromide binding sites, in the presence of benzophenone-3 and benzophenone-4 the DNA sites available to ethidium bromide for binding were increased compared to in their absence (Figures 3.65 and 3.66).

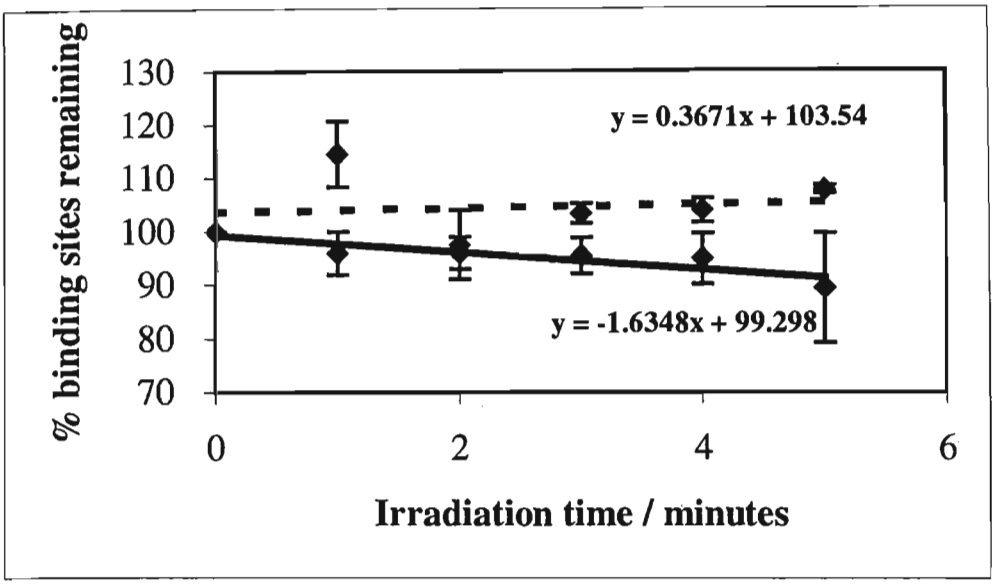

Figure 3.61: Ethidium bromide (0.6×10^{-5} M) binding to calf thymus DNA (1.2×10^{-5} M bp), irradiated in the presence of ketoprofen (2×10^{-6} M) at $\lambda > 300$ nm and detected by fluorescence at 586 nm [N=2]. The control, indicated by the dashed line, represents ethidium bromide binding to DNA in the absence of any sunscreen. N refers to the number of replicates.

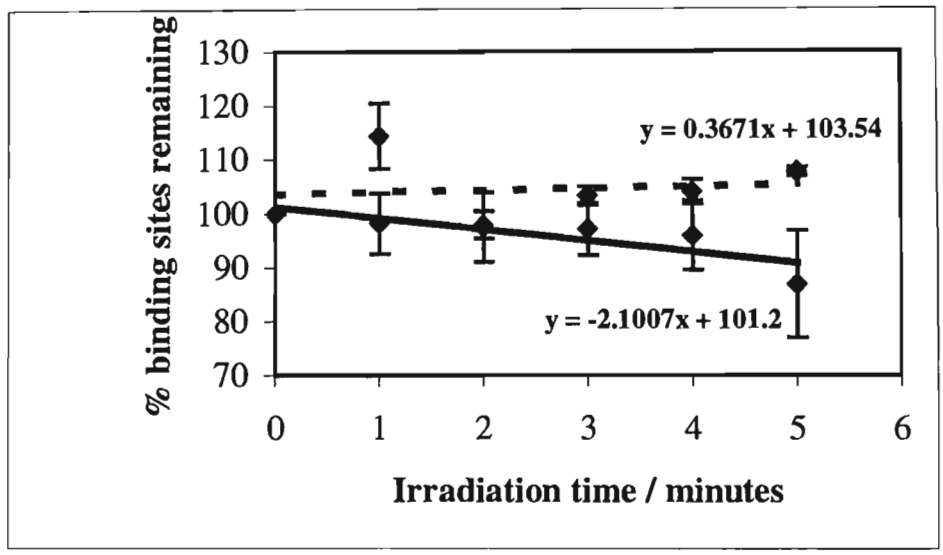

Figure 3.62: Ethidium bromide (0.6 x 10^{-5} M) binding to calf thymus DNA (1.2 x 10^{-5} M bp), irradiated in the presence of benzophenone-1 (2 x 10^{-6} M) at $\lambda > 300$ nm and detected by fluorescence at 586 nm [N=2]. The control, indicated by the dashed line, represents ethidium bromide binding to DNA in the absence of any sunscreen. N refers to the number of replicates.

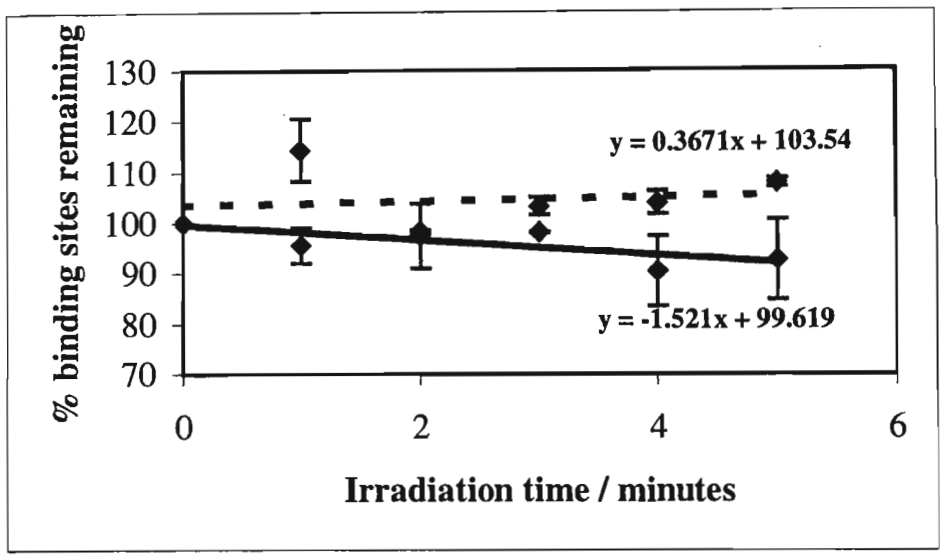

Figure 3.63: Ethidium bromide (0.6×10^{-5} M) binding to calf thymus DNA (1.2×10^{-5} M bp), irradiated in the presence of Uvinul DS49 (2×10^{-6} M) at $\lambda > 300$ nm and detected by fluorescence at 586 nm [N=2]. The control, indicated by the dashed line, represents ethidium bromide binding to DNA in the absence of any sunscreen. N refers to the number of replicates.

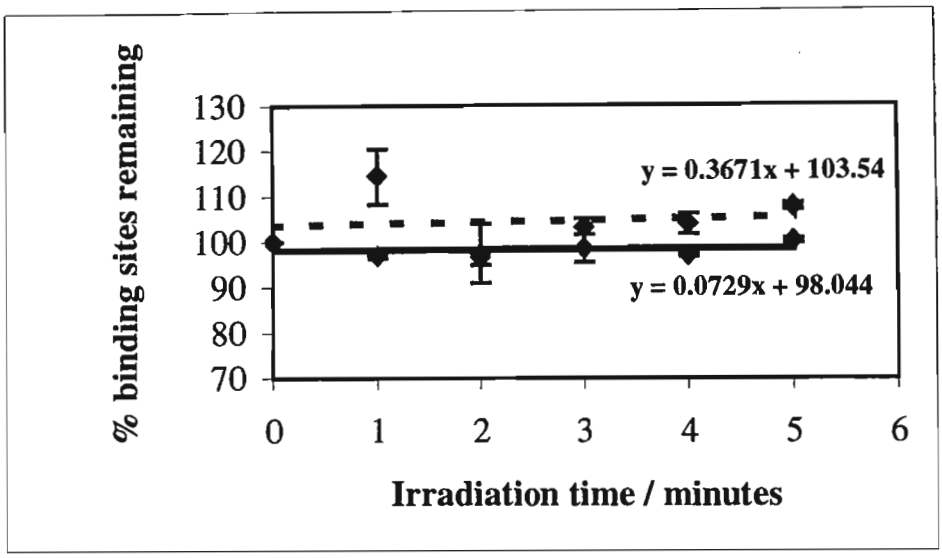

Figure 3.64: Ethidium bromide (0.6 x 10^{-5} M) binding to calf thymus DNA (1.2 x 10^{-5} M bp), irradiated in the presence of Eusolex 232 (2 x 10^{-6} M) at $\lambda > 300$ nm and detected by fluorescence at 586 nm [N=2]. The control, indicated by the dashed line, represents ethidium bromide binding to DNA in the absence of any sunscreen. N refers to the number of replicates.

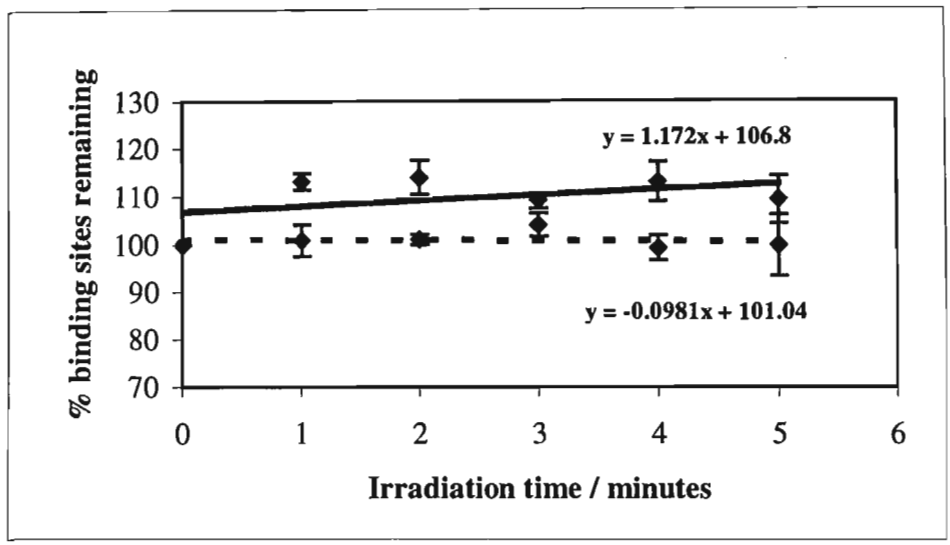

Figure 3.65: Ethidium bromide (0.6×10^{-5} M) binding to calf thymus DNA (1.2×10^{-5} M bp), irradiated in the presence of benzophenone-3 (2×10^{-6} M) at $\lambda > 300$ nm and detected by fluorescence at 586 nm [N=2]. The control, indicated by the dashed line, represents ethidium bromide binding to DNA in the absence of any sunscreen. N refers to the number of replicates.

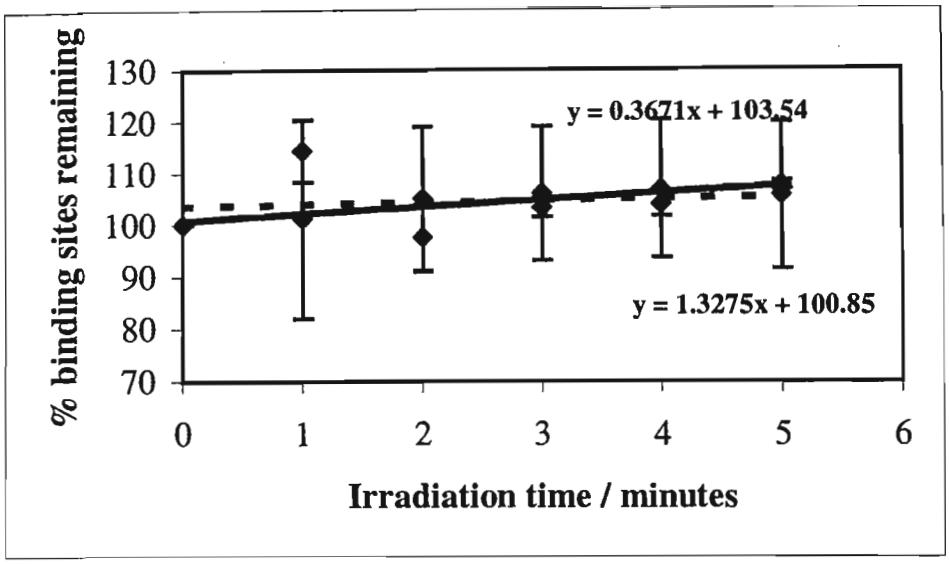

Figure 3.66: Ethidium bromide (0.6 x 10^{-5} M) binding to calf thymus DNA (1.2 x 10^{-5} M bp), irradiated in the presence of benzophenone-4 (2 x 10^{-6} M) at $\lambda > 300$ nm and detected by fluorescence at 586 nm [N=2]. The control, indicated by the dashed line, represents ethidium bromide binding to DNA in the absence of any sunscreen. N refers to the number of replicates.

The slopes of the graphs in Figures 3.65 and 3.66 are 1.17 and 1.33, while the slopes of their respective controls are -0.0981 and 0.367, thus indicating that in the presence of benzophenone-3 and benzophenone-4 the ability of ethidium bromide to bind to the DNA bases was increased by 12.0 and 3.62 times respectively compared to when they were absent.

It can be concluded that the ability of the UV absorbers studied in this investigation to bind to calf thymus DNA when irradiated with UV light decreased in the following order: benzophenone-1 > ketoprofen > Uvinul DS49 > benzophenone. Benzophenone-1 was the most efficient DNA binder. However, Eusolex 232, benzophenone-3 and benzophenone-4 did not compete with ethidium bromide for binding sites on calf thymus DNA and hence did not bind to the DNA. The latter two sunscreen agents seemed to free more intercalation sites on the DNA, and make them available to ethidium bromide for binding. This is not ideal since it implies that the extent of DNA binding by an intercalating compound would be increased in the presence of benzophenone-3 or benzophenone-4 on irradiation with calf thymus DNA and hence the damage induced to the DNA would be more severe.

3.4 Computational Results

Since it is of importance to know whether the UV absorbers investigated in this study can bind to DNA by intercalation, computational chemistry using the PM3 calculation was used to determine the low energy, most stable conformations of these structures (Section 2.5). Between 5 – 10 local minima were found for each UV absorber, and the lowest energy structure found in each case is reported below. The results obtained for benzophenone-1, benzophenone-3, benzophenone-4 and Uvinul DS49 showed similarities, and have been grouped together and are discussed in Section 3.4.1, however, Eusolex 232 showed a remarkable difference to the above-mentioned compounds and appears in Section 3.4.2.

3.4.1 Lowest energy structures for benzophenone-1, benzophenone-3, benzophenone-4 and Uvinul DS49

For benzophenone-1, benzophenone-3, benzophenone-4 and Uvinul DS49, the dihedral angles chosen for the conformational searches were C13-C8-C7-C1 and C8-C7-C1-C6 (Figure 3.67).

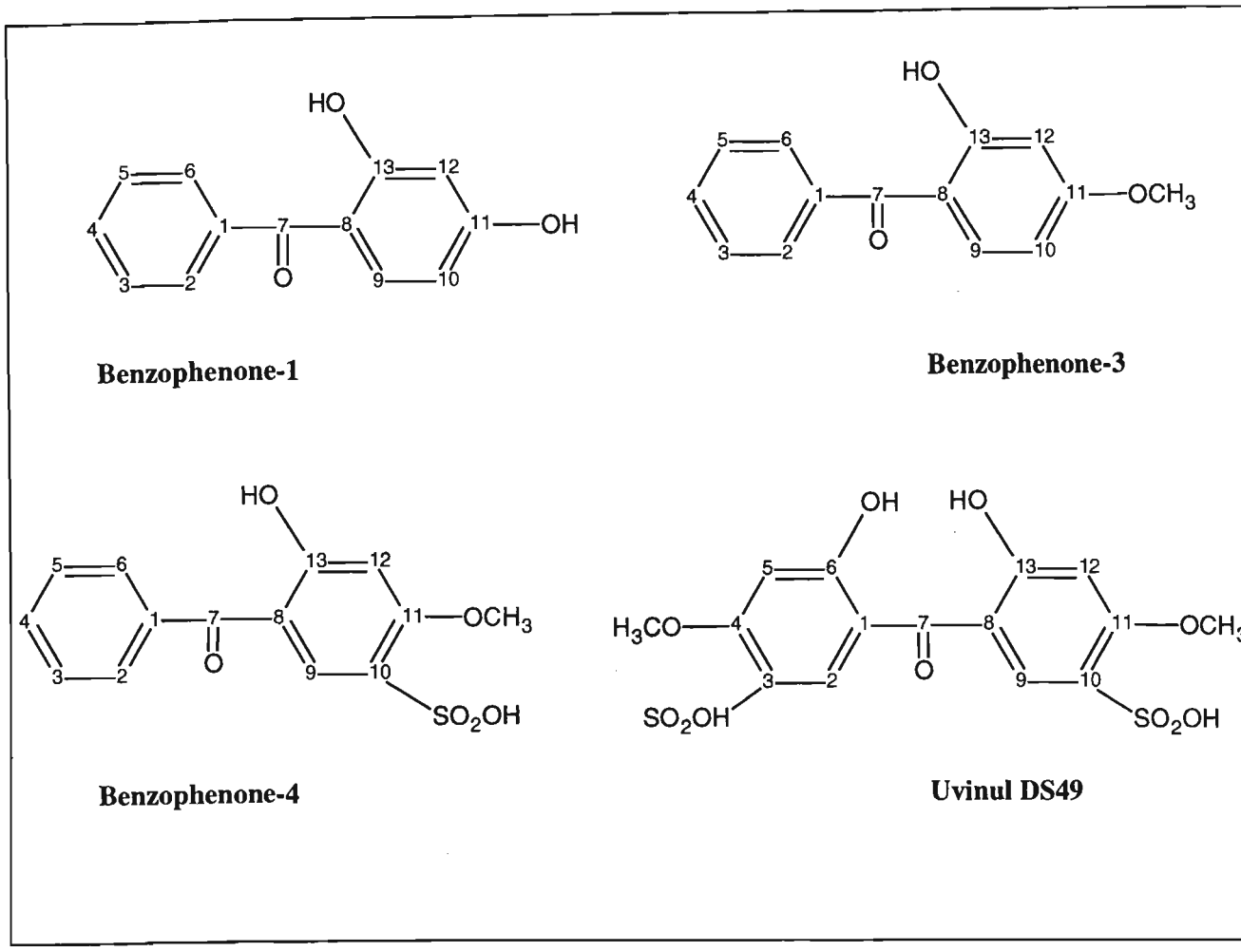

Figure 3.67: Chemical structures of benzophenone-1, benzophenone-3, benzophenone-4 and Uvinul DS49 showing the dihedral angles C13-C8-C7-C1 and C8-C7-C1-C6.

For all cases the dihedral angles were first fixed, both to 180°, thus inducing a planar structure. However, these structures proved not to be a minimum on the energy surface for these molecules, but corresponded to a maximum or transition state. The frequency calculations of the flat structures had one negative eigenvalue in each case and the movement of atoms associated with the eigenvalue resembled movement (twisting) out of the plane.

The results obtained for the computational studies appear in Table 3.1.

Table 3.1: Computational results for the optimised structures for benzophenone-1, benzophenone-3, benzophenone-4 and Uvinul DS49.

	Benzophenone-1	Benzophenone-3	Benzophenone-4	Uvinul DS49
Optimized Structure	Twisted	Twisted	Twisted	Twisted
Energy preference / kcal mol^{-1}	10	10	9	14
Dihedral angle C13-C8-C7-C1 / °	180	180	179.6	152.9
Dihedral angle C8-C7-C1-C6 / °	90.6	91.2	108.7	152.9

The lowest energy state in each case corresponded to the twisted structure. From Table 3.1, it can be seen that the optimized twisted structures for benzophenone-1, benzophenone-3, benzophenone-4 and Uvinul DS49 were preferred to the planar structures by 10 kcal mol^{-1}, 10 kcal mol^{-1}, 9 kcal mol^{-1} and 14 kcal mol^{-1}, respectively. This is not surprising since for all these molecules considerable steric hindrance is exerted in the flat structure between C6(H) and C9(H) thus preventing the planar structure from being the most stable. In addition to steric hindrance, intramolecular hydrogen bonding between C7(O) and C10(H) reaffirms the twisted structure. Also for Uvinul DS49 the difference in energy between the twisted and planar structures was higher than for the other benzophenone molecules. This can be attributed to increased steric hindrance in the flat structure in the case of Uvinul DS49 due to a larger number of functional groups on the backbone. The 14 kcal mol^{-1} preference is thus a direct result from the higher steric hindrance in the flat structure.

The optimized twisted structures for benzophenone-1, benzophenone-3, benzophenone-4 and Uvinul DS49 have dihedral angles between atoms 13, 8, 7 and 1 and between atoms 8, 7, 1 and 6 of (180°, 90.6°), (180°, 91.2°), (179.6°, 108.7°) and (152.9°, 152.9°) respectively (Table 3.1). These structures appear in Figure 3.68.

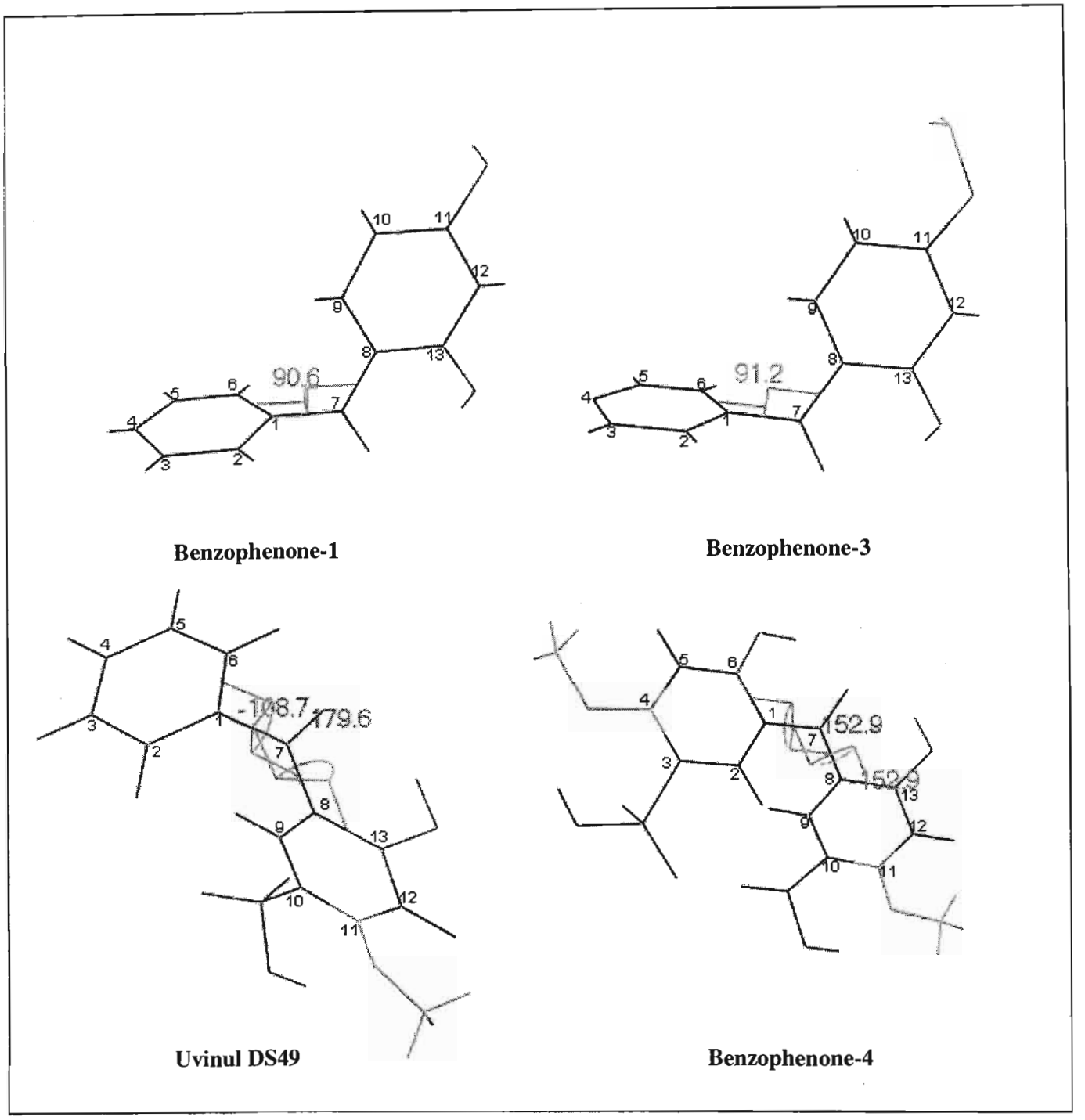

Figure 3.68: The optimized structures for benzophenone-1, benzophenone-3, benzophenone-4 and Uvinul DS49 obtained from semi-empirical PM3 calculations.

From these results it can be noted that in the case of benzophenone-4 and Uvinul DS49, the dihedral angles were larger than those of benzophenone-1 and benzophenone-3, and the optimised structures are twisted to a smaller extent as can be seen in Figure 3.67. This can be attributed to the presence of the sulphonic acid group at C10 in benzophenone-4, and at C3 and C10 in Uvinul DS49. In the sulphonic acid group the hydrogen atom is shielded and as a result the conformational search did not find the same hydrogen atom here as for the benzophenone-1 and benzophenone-3. This was noted and the structure was changed manually to have the hydrogen bond at C10, and C3 and C10 in benzophenone-4 and Uvinul DS49 respectively. Optimization of the hydrogen bonded structure of benzophenone-4 gave an energy of about 9 kcal mol^{-1} lower than the flat structure compared to about 7 kcal mol^{-1} when the hydrogen bond was not detected. This is an overestimation since it is known that a single intramolecular hydrogen bond stabilizes the structure by about 3-6 kcal mol^{-1} (March [1992]). Similar intramolecular bonding was found in Eusolex 232, which contributed to the larger dihedral angles in the optimised structure.

3.4.2 Lowest energy structure for Eusolex 232

The situation for Eusolex 232 was very different to that of the UV absorbers mentioned above (Section 3.4.1). Firstly the chemical structure of Eusolex 232 (Figure 3.69) does not display large groups exercising huge steric hinderance as with the cases above. More importantly, in Euslolex 232 π-electron delocalisation is of importance. It is well known from literature that rotational barriers involving delocalization are underestimated by PM3 (Foresman & Frisch [1996]), therefore an *ab initio* calculation in addition to the PM3 was required. With *ab initio* methodology better π-electron delocalization can be considered in the mathematical code. The results obtained from both these methods are shown in Table 3.2.

PM3 calculations

The PM3 calculation preferred a twisted structure where the dihedral angle C7-C8-C10-C11 (Figure 3.69) was approximately 30°. From the PM3 calculations it was also shown that the twisted structure was only marginally (0.1 kcal mol^{-1}) more stable than the flat structure (dihedral angle C7-C8-C10-C11 constrained at 0° and the rest of the molecule optimized using PM3). However, these calculations do not consider electron delocalisation, which has been shown to contribute

Table 3.2: Computational results for the optimized structure of Eusolex 232 as obtained from PM3 and *ab initio* calculations.

	PM3	***Ab initio***
Optimised structure	Twisted	Planar
Energy/ kcal mol^{-1}	0.1	6
Dihedral angle C7-C8-C10-C11 /°	30	0
π-electron delocalization	No	Yes

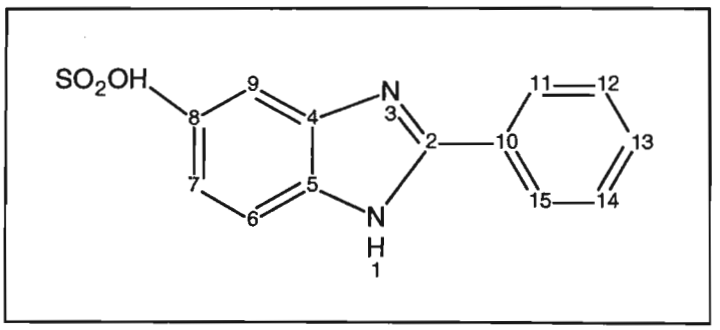

Figure 3.69: Chemical structure of Eusolex 232 showing the dihedral angle C7-C8-C10-C11.

considerably to stabilization of flat structures. These results, therefore, did not accurately predict the lowest energy state and hence *ab initio* calculations were required.

Ab initio calculations

The geometry and energy of Eusolex 232 was subsequently obtained using *ab initio* calculations at the Restricted Hartree-Fock level of theory with the 3-21+G basis set (Foresman & Frisch [1996]). Diffuse functions (+) are typically used for a more accurate description when π-electron delocalization is involved. The partially unconstrained twisted structure (where C7-C8-C10-C11 is approximately 30°, obtained from PM3 calculations) was optimised using *ab initio* methods and became perfectly flat, confirming that the lowest energy structure for Eusolex 232 should in fact be planar (Figure 3.70). Furthermore, the flat structure did not have any negative eigenvalues, confirming that the flat structure should at least be a local minimum and not a transition state. The dihedral angle C7-C8-C10-C11 was then constrained at 90.0° and the rest of the molecule optimised using the same *ab initio* method. Any unconstrained structure became planar with the *ab initio* calculation. The flat structure was more stable by about 6 kcal mol^{-1} confirming that this structure should be the global minimum, due to the large contribution towards stabilization from π-electron delocalization.

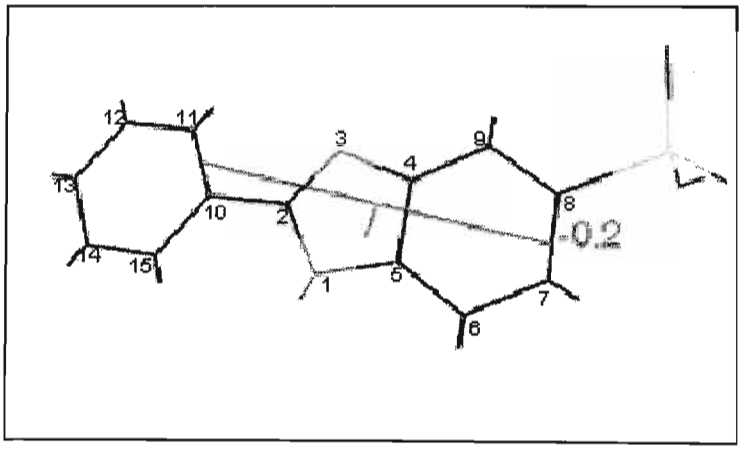

Figure 3.70 Optimized planar structure for Eusolex 232.

The flat structure of Eusolex 232 can therefore possibly intercalate with DNA and hydrogen bond formation between the nitrogen atom on Eusolex 232 and the base pairs of DNA can occur.

3.4.3 Conclusion

The computational results clearly suggest that intercalation of the following benzophenone-based UV absorbers, *i.e.*, benzophenone-1, benzophenone-3, benzophenone-4 and Uvinul DS49, with DNA will at best be very limited, since only one half could possibly interact with the base pairs of DNA. This is due to the structure of the DNA grooves, where only flat molecules are able to fit in the grooves and fully intercalate with DNA. The only analogue that could intercalate fully with DNA is Eusolex 232, since the structure is flat at room temperature. However, it should be noted that intercalation may not always lead to direct DNA cleavage and in some cases further treatment may be required (Tullius [1998]). In addition, DNA cleavage may be possible without intercalation with the base pairs.

3.5 Proposed mechanism of DNA photocleavage induced by the benzophenone-based sunscreen agents

This study, which investigated the DNA photocleavage potentials of benzophenone, benzophenone-1, benzophenone-3, benzophenone-4, Uvinul DS49 and Eusolex 232, has demonstrated some alarming results. All these UV absorbers, with the exception of benzophenone-3 and benzophenone-4, induced the cleavage of DNA when irradiated with simulated sunlight ($\lambda > 300$ nm). The possible mechanism of these interactions will now be addressed.

3.5.1 Possible pathways for DNA photocleavage

A vast amount of literature is available on agents that cleave DNA (Armitage [1998], McMillin & McNett [1998], Burrows & Muller [1998] and Pogozelski & Tullius [1998]). These agents may have mutagenic and carcinogenic effects on DNA if the damage remains unrepaired. On the other hand, some of them may be useful for the removal of harmful sequences in the DNA bases and hence find use as structural probes and therapeutic agents. With advances in medicine, new DNA cleaving agents are being sought for the treatment of various diseases such as cancers. Photocleaving agents, in particular, have gained popularity especially because the DNA cleavage event can be controlled since it is only initiated in the presence of UV light. The review article by

Armitage [1998] describes the various mechanistic pathways available to DNA photocleavage agents.

From these possible mechanisms, two distinct pathways for DNA cleavage are apparent. These are reaction of the reactive species either with the nucleobases or at the ribose sugars of the DNA leading to strand breaks. Spontaneous DNA photocleavage, however, does not occur that easily and is usually not due to reaction at the nucleobase but restricted to hydrogen atom abstraction from the sugar residue (Armitage [1998] and Pogozelski & Tullius [1998]).

Detection of the DNA photocleavage mechanism is commonly achieved with electrophoresis. However, agarose gel electrophoresis, although simple in technique, is limited in mechanistic details as compared to using gel-sequencing protocols on polyacrylamide gels. With the latter, the cleavage sites can be mapped by comparing the electrophoretic mobility of the cleavage fragments with those of a reference sequence ladder using end-labelled DNA molecules (Stevenson & Davies [1999]). It should also be noted that several photocleavage agents give spontaneous cleavage on agarose gels, however, nucleobase cleavage is only observed on guanine sites after piperidine treatment on end-labelled DNA. Also of importance is that the high sensitivity of the agarose gel technique may be misleading and may not always reveal the true type of cleavage, since a low quantum yield can produce spontaneous cleavage while a higher quantum yield DNA cleavage process may require piperidine treatment only observed on polyacrylamide gels (Armitage [1998]). Both these pathways to DNA cleavage will now be discussed in more detail.

A Reaction with a sugar residue

Reaction at the sugar residue is the most common route reported in literature to DNA photocleavage. Reaction with the sugar moiety may involve abstraction of a hydrogen atom by the photocleaving agent or by a free radical or a reactive intermediate. A reactive intermediate may form from photodegradation of the cleaving agent or from reaction with the cleaver and another molecule, while free radicals arise as a result of triplet energy transfer reactions to another molecule (such as oxygen to form singlet oxygen), which may then abstract a proton from the sugar. Photocleavers that attack at the sugar are generally expected to cleave at any sequence since a sugar residue is present in every nucleotide. However, in some cases preferential cleavage may occur as the cleaver may have higher preference for one site than another, alternatively its orientation if bound to DNA may leave some sites with higher affinity for reaction than other sites (Armitage

[1998]). Hydrogen atoms on a sugar residue that may be accessible for abstraction are shown in Figure 3.71.

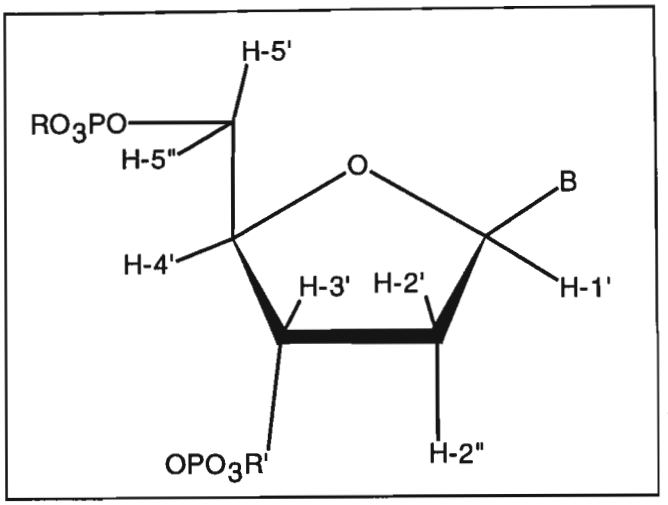

Figure 3.71: Hydrogen atoms on the sugar moiety in DNA available for abstraction (Pogozelski & Tullius [1998]).

Although all seven hydrogens are believed to be reactive towards free radicals not all have equal probability of being abstracted from DNA (Pogozelski & Tullius [1998]). Depending on the helical structure of the DNA and on the orientation of the reacting species to the sugar, some of these hydrogens may be more accessible than others. DNA can exist in two forms, that is, the B form (superhelical turns, coil to the left) or A form (superhelical turns, coil to the right). Under normal conditions, in aqueous solution, the bases stack in the B-form (McMillin & McNett [1998]) (Figure 3.72). Studies have shown that molecules that bind to the minor groove of DNA do so at the 5' and 4' positions of the sugar in B-form DNA (Pogozelski & Tullius [1998]). These positions have been shown to be most accessible to solvent and oxidizing species from the minor groove. On the other hand, the 3' position is accessible from the major groove of B-DNA.

Hydrogen abstraction at a sugar residue, generally leads to direct strand breaks with spontaneous cleavage.

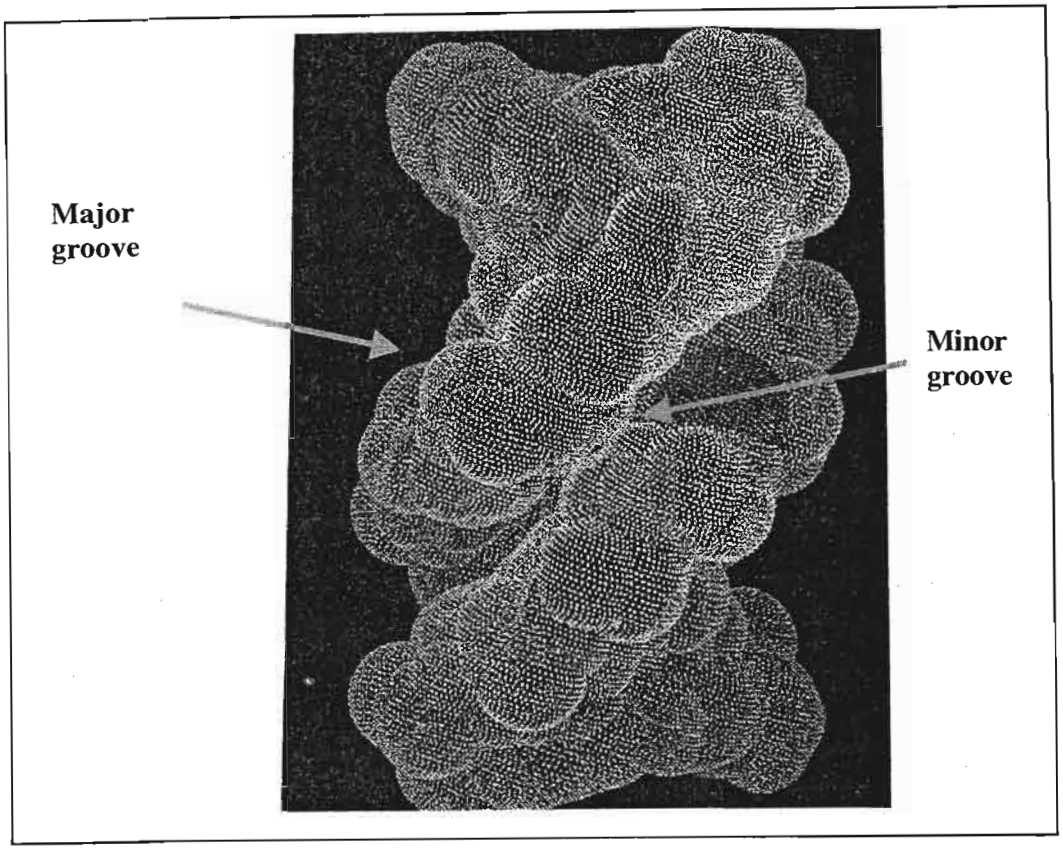

Figure 3.72: B-form DNA model showing the major and minor grooves (Pogozelski & Tullius [1998]).

B. Reaction at the DNA base

Reaction at the nucleobase generally includes (Armitage [1998]):

1) Direct electron transfer from the nucleobase to the excited photocleaver,
2) Triplet energy transfer from the excited photocleaver to oxygen, forming singlet oxygen, which then reacts with the base, or
3) Triplet energy transfer from the excited photocleaver to the base forming an adduct with the base or inducing an adduct formation between the bases.

The bases (adenine, guanine, thymine and cytosine) differ greatly in terms of their reactivities and oxidation potentials. It has been well established that photocleavers that attack nucleobases in most cases do so almost selectively at guanine. Guanine is by far the most easily oxidised and the most

reactive towards singlet oxygen (Armitage [1998]). In the first two mechanisms listed above, cleavage occurs almost exclusively at guanine, however, for adduct formation the reactive base may differ depending on the mechanism. Adduct formation between adjacent DNA bases has been found to occur commonly between two thymine dimers. Thymine has the lowest triplet state energy therefore energy transfers are highly possible.

Direct electron transfer from the nucleobase to the excited photocleaver occurs very commonly by intercalation (Figure 3.73). Examples of some common photocleavers that cleave DNA by intercalation include anthraquinones, anthracene, psoralens and riboflavin (Breslin & Schuster [1996], Armitage *et al.* [1994] and Rai *et al.* [1993]).

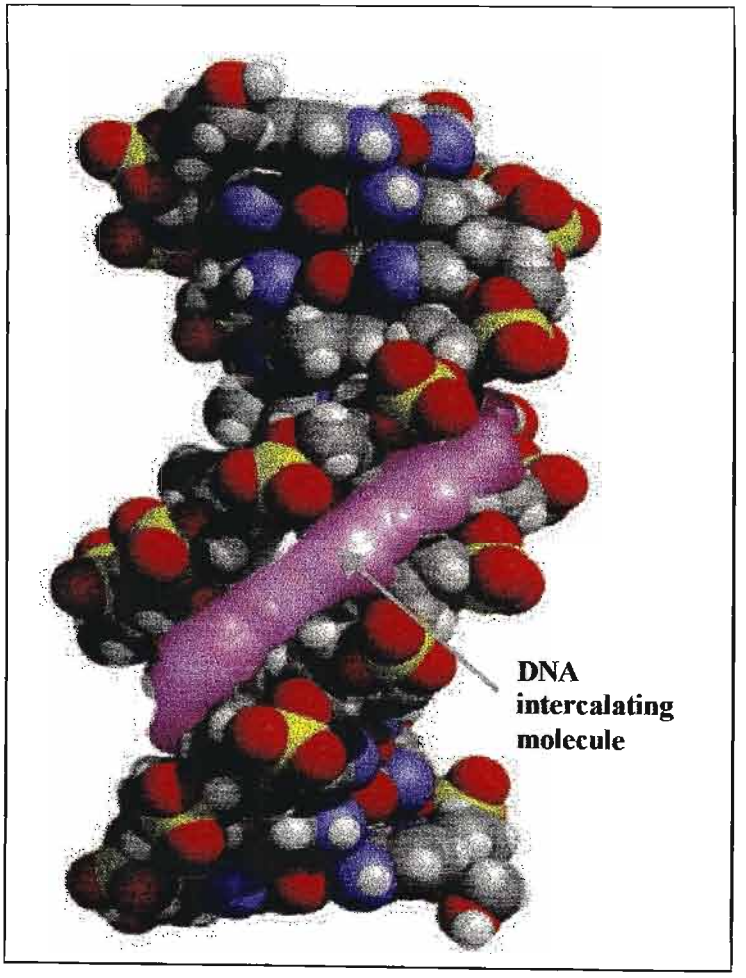

Figure 3.73: Antibiotic Distamycin A intercalates with the minor groove of DNA (Bruice P. [2001]).

However, it should be noted that binding to DNA by intercalation is not a universal requirement for direct electron transfer.

Cleavage at the base rarely leads to direct strand breaks but generally allows cleavage to occur site-specifically following an additional treatment. This may involve heat, alkali (hot piperidine or aniline) or enzymatic treatment to reveal the damage (Armitage [1998] and Burrows & Muller [1998]). The general pathway to DNA cleavage induced at the nucleobase is shown in Figure 3.74. The cleavage event is as a result of deglycosylation (removal of a sugar unit), β-elimination of the 3'-phosphate, and the formation of a modified base as shown in the figure (Burrows & Muller [1998]).

3.5.2 Postulated mechanism for DNA photocleavage by the UV absorbers

In this study, DNA photocleavage was induced spontaneously by a group of benzophenone-based sunscreens for the supercoiled DNA target investigated (ϕX174 DNA) as detected by agarose gel electrophoresis. It would therefore point to hydrogen abstraction at the sugar residue. However, from the argument above it is quite clear that nucleobase attack cannot be eliminated as the mechanism of cleavage at this stage without gel sequencing protocols being conducted. Postulated mechanisms for the sunscreen agents will now be discussed, and this will be followed by a specific mechanism for Eusolex 232, which has been identified in literature.

Benzophenone

If one considers the parent compound of the sunscreen agents under investigation, benzophenone, some insight into the DNA photocleavage behaviour of the benzophenone-based group of sunscreens can be obtained. Benzophenone has been shown to photocleave DNA, by agarose gel electrophoresis, and to bind to calf thymus DNA, as detected by the fluorescence spectroscopy technique. In addition, benzophenone has been shown to rapidly photodegrade when irradiated with UV light ($\lambda > 300$ nm), to almost 80% after only 20 minutes of irradiation. The mechanism of this photodegradation, has been discussed in Section 3.1.1, and is well known to involve the n,π^* triplet state and hydrogen atom abstraction.

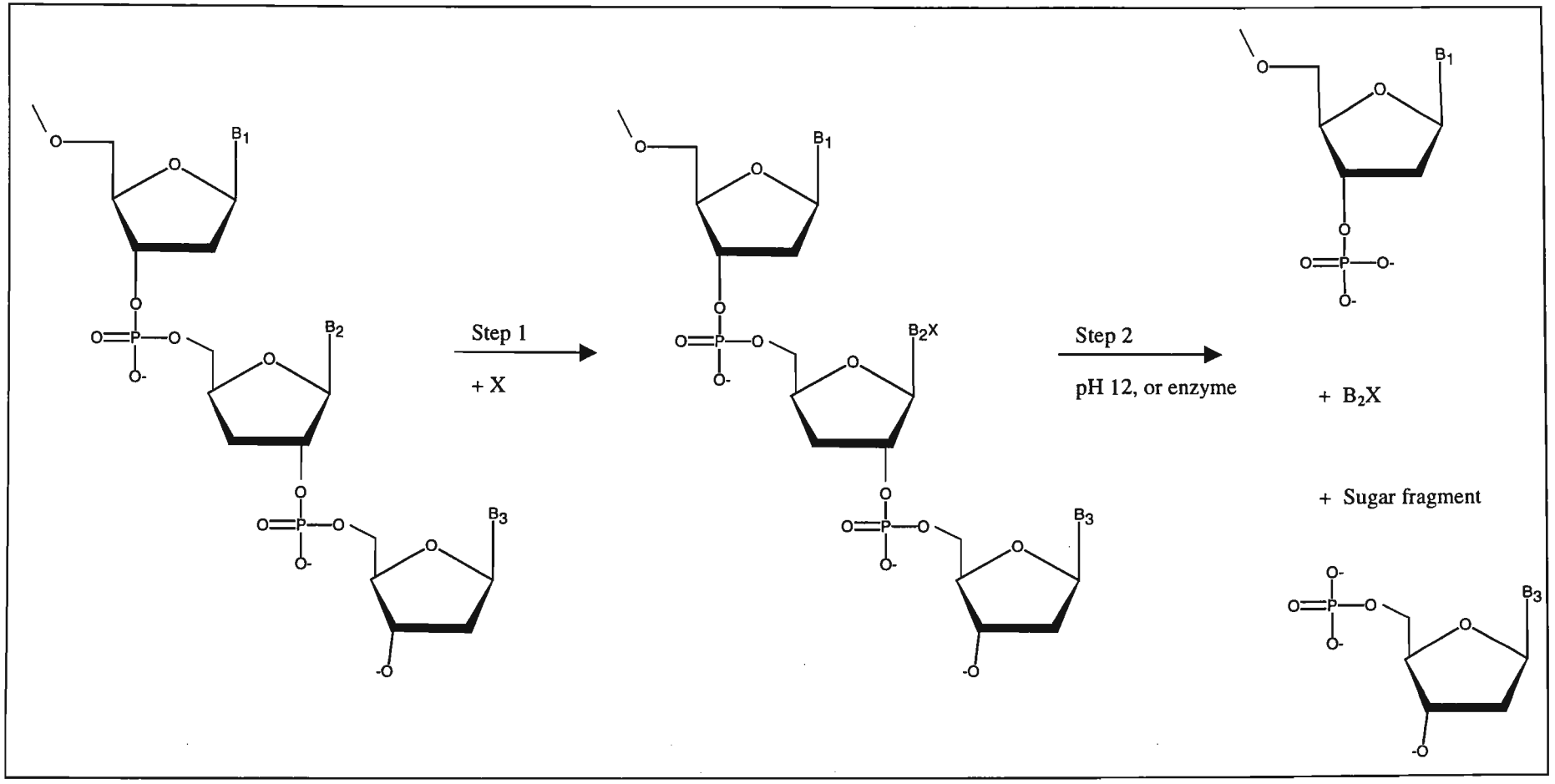

Figure 3.74: General scheme for nucleobase cleavage, where B refers to the nucleobase, and step 1 involves modification by the base damaging reagent X, followed by cleavage in step 2 using alkaline conditions or a nuclease (Burrows & Muller [1998]).

If the hydrogen abstracted were a hydrogen atom on the sugar residue of the DNA molecule, then this would lead to direct strand breaks and explain the DNA photocleavage observed by gel electrophoresis. However, an interesting observation is that photodegradation of benzophenone occurs before the time required for a significant number of single strand breaks. Single strand breaks are detected only after about 15 minutes of irradiation with UV light, as observed by gel electrophoresis, however, from the photostability experiments photodegradation of benzophenone can be seen after only 5 minutes of irradiation with the same light source. The fluorescencespectroscopy results show interaction with the DNA, or binding, within five minutes. Hence the possibility exists that cleavage arises as a result of photosensitisation reactions via triplet energy transfer from benzophenone directly to DNA, or to another molecule, which may then cleave the DNA.

The basis of these triplet energy transfer reactions has been attributed in literature to photosensitised oxidations. According to Hèléne [1987], photosensitization of DNA under aerobic conditions leads predominantly to oxidative modifications of the guanine bases, which are detected when the DNA is subsequently treated with hot piperidine. Two such photosensitised oxidation processes are possible, *i.e.*, the type I and type II processes (Foote [1991]). In the type I process, electron or hydrogen atom transfer occurs between the excited benzophenone molecule (or sensitiser) and either directly with the DNA substrate or with a solvent molecule. Transfer can actually occur in either direction, but most commonly the excited sensitiser acts as the oxidant. Abstraction of a proton from the solvent, would yield radicals or radical ions which may then be available to abstract a proton from the sugar residue and induce DNA cleavage (Foote [1991]). The type I reaction is shown in Figure 3.75.

In contrast, a type II reaction involves triplet energy transfer between the excited sensitiser to molecular oxygen (Foote [1991], Stevenson & Davies [1999]). In these reactions the triplet state quencher is oxygen because unlike most other molecules, oxygen has a triplet ground state and a low energy singlet state making triplet energy transfer highly possible. This type II reaction leads mainly to singlet molecular oxygen ($^1O_2$), which is then capable of DNA cleavage by hydrogen atom abstraction as shown in Figure 3.76.

Type I reactions

$$BP + h\nu \rightarrow {}^1BP$$
$${}^1BP \rightarrow {}^3BP$$
$${}^3BP + R-H \rightarrow BPH^{\bullet} + R^{\bullet}$$
$$R^{\bullet} \rightarrow \textit{strand breaks}$$

$$BP + h\nu \rightarrow {}^1BP$$
$${}^1BP \rightarrow {}^3BP$$
$${}^3BP + S-H \rightarrow BPH^{\bullet} + S^{\bullet}$$
$$S^{\bullet} + R-H \rightarrow S-H + R^{\bullet}$$
$$R^{\bullet} \rightarrow \textit{strand breaks}$$

Figure 3.75: Photosensitisation of DNA by Type I reactions, where BP represents benzophenone, R-H represents a proton of the DNA and S-H represents a solvent molecule.

Type II reaction

$$BP + h\nu \rightarrow {}^1BP$$
$${}^1BP \rightarrow {}^3BP$$
$${}^3BP + {}^3O_2 \rightarrow {}^1BP + {}^1O_2$$
$${}^1O_2 + DNA \rightarrow \textit{strand break}$$

Figure 3.76: Photosensitisation of DNA by type II reactions, where BP represents benzophenone, and $^3O_2$ and $^1O_2$ represent triplet and singlet oxygen respectively.

Benzophenone-1 and Uvinul DS49

Benzophenone-1 and Uvinul DS49 also cleaved DNA as detected by agarose gel electrophoresis. However, from the computational studies, the lowest energy structures for these sunscreens were non-planar. This implies that one half of the molecule could still intercalate with DNA and bind. Binding of both benzophenone-1 and Uvinul DS49 to calf thymus DNA was confirmed by the fluorescence spectroscopy experiments. However, unlike benzophenone the photodegradation of these sunscreen agents was very limited. Here again a triplet energy transfer process may be

involved as shown for benzophenone in Figures 3.75 and 3.76, which allows hydrogen abstraction (or electron transfer) from the DNA to occur by either a type I or type II process.

Benzophenone-3 and benzophenone-4

Benzophenone-3 and benzophenone-4, demonstrated a very different photocleavage pattern to that of the other sunscreen agents investigated. These UV absorbers did not cleave DNA as detected by gel electrophoresis and in fact seemed to demonstrate a protective effect. This supports studies conducted by O'Kereke *et al* [1995] and Robinson *et al* [1994] who also showed the inability of benzophenone-3 to induce damage to DNA. In addition, both benzophenone-3 and benzophenone-4 demonstrated stability towards photodecomposition under UV light. Also, from the fluorescence studies no interaction or binding with calf thymus DNA was detected. From the computational studies it was shown that both these UV absorbers possess non-planar lowest energy structures, which imply that although one half of these molecules could possibly intercalate and bind with DNA, this does not occur, as shown by the fluorescence studies. Hence benzophenone-3 and benzophenone-4 are unable to perform type I and type II photosensitised processes as discussed above for benzophenone (Figures 3.75-3.76), the latter of which has been confirmed for benzophenone-3 by Allen *et al.* [1995]. Allen and his team demonstrated that benzophenone-3 does not photosensitise the formation of singlet oxygen on irradiation with UV light, nor any other reactive oxidant species. The lack of triplet energy transfer reactions by benzophenone-3 has been also demonstrated by Wolf *et al* [1994] and Sewlall [1991], who showed that when DNA is irradiated in the presence of benzophenone-3 thymine base dimerization does not occur.

DNA photocleavage by benzophenone-3 and benzophenone-4 may be prohibited due to the substituents present on the benzophenone. Benzophenone-3, as discussed previously, contains the electron donating groups, -OH and $-OCH_3$, which are known to alter the nature of the lowest triplet from n,π^* to π,π^* (Boscá & Miranda [1998]). This is known to decrease the reactivity of the lowest triplet state. Benzophenone-4 similarly has the electron donating groups, -OH and $-OCH_3$, but in addition it also contains the electron withdrawing group $-SO_3OH$. Electron withdrawing groups are known to demonstrate high efficiency for reactivity and hydrogen abstraction (Boscá & Miranda [1998]). However, the effect of the electron-donating groups seems to dominate in the case of benzophenone-4 and reduce its reactivity. This then raises the question of how Uvinul DS49, which contains the same reactive groups as benzophenone-4, is reactive to DNA cleavage. A possible explanation for this may be that the presence of the -OH, $-OCH_3$, and the $-SO_3OH$

substituents on both of the phenyl groups of the benzophenone backbone somehow alters the photochemistry. The presence of two -SO_3OH groups may switch its reactivity in favour of the electron withdrawing effect and the n,π* triplet is unaffected and therefore DNA photocleavage is observed for Uvinul DS49.

Eusolex 232

Eusolex 232 is completely stable towards photodecomposition under UV light. This agrees with the work done by Stevenson & Davies [1998] and Inbaraj *et al.* [2002]). However, from the gel electrophoresis studies, it was shown to be a potent photocleaver of DNA, and its reactivity was the highest as compared to the other UV absorbers studied here. In addition, the computational work revealed a planar lowest energy structure for this sunscreen, thus implying that intercalation with the DNA bases was highly probable. This was in contrast to the fluorescence spectroscopy results, which showed that Eusolex 232 does not compete with the ethidium bromide for DNA binding sites since the fluorescence of the ethidium bromide remained constant during the duration of the experiment.

This was supported by studies conducted by Stevenson & Davies [1999] and Inbaraj *et al.* [2002] who showed that although Eusolex 232 does not bind to calf thymus DNA it still cleaves DNA. These researchers described the DNA cleavage mechanisms induced by Eusolex 232 as photooxidation by singlet oxygen in single stranded DNA via the type II reaction and the type I mechanism in double stranded DNA. Both these processes as mentioned before involve electron transfer between DNA and the photoexcited sensitiser. Stevenson & Davies [1999] also showed the formation of piperidine-labile cleavage sites that mapped exclusively to the guanine residue in single stranded DNA and to 5' guanines of GG (guanines situated 5' to another guanine) in double stranded DNA. This now implies that the spontaneous cleavage which was indicated from the agarose gel electrophoresis results was misleading in this case, since hydrogen abstraction from the sugar may have been in poor competition with nucleobase cleavage of which the latter was undectable with agarose gel electrophoresis.

Singlet molecular oxygen is formed via energy transfer from the excited triplet of Eusolex 232 to dissolved ground state oxygen which then modifies the guanine base and induces DNA cleavage (Stevenson & Davies [1999] and Inbaraj *et al.* [2002]). According to Inbaraj *et al.* [2002] the phosphorescence lifetime of Eusolex 232 was 2 ms, which indicates a sufficiently long-lived triplet

state that would be able to react with oxygen even at room temperature. Support for singlet oxygen as being the main source of DNA damage in single stranded DNA, was provided by the formation of 4,8-dihydro-4-hydroxy-8-oxo-2'-deoxy-guanosine in aerated solution from 2'-deoxyguanosine (Stevenson & Davies [1999]). This is a diagnostic reaction of $^1O_2$ production, which from this literature source did not occur in the absence of Eusolex 232. Further support was provided by the suppression of DNA photosensitization by Eusolex 232 in the presence of singlet oxygen quenchers (sodium azide, 1,4-diazabicyclo[2.2.2]octane and cysteine) (Stevenson & Davies [1999]). Photocleavage is not induced by singlet oxygen in double-stranded DNA, since the nucleobases are not readily accessible for reaction compared to single stranded DNA. Instead electron transfer to Eusolex 232 occurs, which leads to the formation of nucleobase radical cations situated at the 5'-guanines in GG doublets, which then act as precursors to DNA cleavage.

Bolton [1991] also showed that Eusolex 232 photosensitised thymine dimer formation via its triplet state. These Eusolex 232 photosensitised pathways are shown in Figure 3.77.

Scheme for DNA cleavage and thymine dimerisation by Eusolex 232

$$232 + h\nu \rightarrow {}^1232$$

$${}^1232 \rightarrow {}^3232$$

$${}^3232 + T(or\ {}^3O_2) \rightarrow 232 + {}^3T(or\ {}^1O_2)$$

$${}^3T + T \rightarrow T\langle\rangle T(\text{dimer})$$

$${}^1O_2 + DNA \rightarrow strand\ break$$

Figure 3.77: Mechanism of DNA photocleavageand thymine dimerisation induced by Eusolex 232, where 232 refers to Eusolex 232, and T refers to the thymine base in DNA.

It can be concluded that although Eusolex 232 is planar, it does not intercalate with DNA as would be expected. However, it still cleaves DNA via singlet oxygen triplet energy transfer. Other photosensitisers cleaving DNA in a similar manner to Eusolex 232 are riboflavin, and certain pterins which bind weakly, if at all, to duplex DNA (Stevenson & Davies [1999]).

Chapter 4

CONCLUSION

The photocleavage ability of a group of benzophenone-based UV absorbers, most of which are commonly used in sunscreen preparations, was investigated. This group of sunscreen agents included benzophenone-1 (or 2,4-dihydroxybenzophenone), benzophenone-3 (or 2-hydroxy-4-methoxy benzophenone), benzophenone-4 (or 2-hydroxy-4-methoxy benzophenone-5-sulphonic acid), 2, 2'-dihydroxy-4, 4'-dimethoxy benzophenone sulphonic acid (trade name Uvinul DS49) and 2-phenylbenzimidazole-5-sulphonic acid (trade name Eusolex 232). Agarose gel electrophoresis was used to detect DNA cleavage, while fluorescence spectroscopy techniques indicated DNA binding. This study involved irradiating buffered aqueous solutions (pH 7-8) of the benzophenone-based sunscreens in the presence of buffered aqueous solutions of DNA at wavelengths greater than 300 nm. Two types of DNA were used in this investigation, that is, single stranded ϕX174 phage DNA for the gel electrophoresis experiments and double stranded calf thymus DNA for the fluorescence spectroscopy studies. The stability of the sunscreen agents to photodecomposition in UV light was also investigated. Finally, computational studies were conducted to determine the lowest energy geometry of these sunscreen agents in an attempt to determine if intercalation of the sunscreen agents with the DNA bases was possible.

The results obtained in this investigation indicate quite clearly that benzophenone, benzophenone-1, Uvinul DS49 and Eusolex 232 are able to photocleave DNA and induce single strand breaks in the DNA helix. The mechanism of this interaction has been postulated to be type I or type II photosensitised reactions initiated by a triplet-energy transfer reaction between the excited UV absorber and DNA.

Benzophenone-3 and benzophenone-4 did not behave in a similar manner to the parent compound, benzophenone, and prevented DNA photocleavage from occurring. This is attributed to the substituents present on the benzophenone backbone. The electron donating groups, -OH and $-OCH_3$ are known to be responsible for altering the nature of the lowest triplet from n,π^* to π,π^*, which is believed to decrease the reactivity of the lowest triplet state. Nevertheless, other workers in this field (Schallreuter *et al.* [1996]) have identified reasons for concern over the use of benzophenone-3 in sunscreen formulations.

Although the parent compound, benzophenone, and the DNA photocleaver, ketoprofen, photodegraded, the other benzophenone-based UV absorbers were relatively stable over the time period investigated, which indicates that they do satisfy one of the requirements of a sunscreen absorber. However, other researchers (Serpone *et al.* [2002]) would disagree since they have shown both benzophenone-3 and Eusolex 232 to undergo photodegradation on irradiation with UV light to such an extent that their use as UV absorbers in sunscreen formulations warrants further investigation. Also, although the use of benzophenone is not permitted in sunscreen formulations by most authorities throughout the world, its use in sunscreens is still under review in Australia. This is of concern, since it is quite clear that benzophenone does not provide the intended protection against UV radiation and its use in sunscreens should not be permitted.

However, more alarming than this, is the finding that some of these UV absorbers, which are FDA approved, are able to cleave DNA. Although these studies were conducted *in vitro*, they do show that if these substances are able to penetrate skin and enter the cells then they would have the potential to damage DNA. Jiang *et al.* [1999] have provided evidence that benzophenone-3 is absorbed through the skin following topical application. According to this author's knowledge skin permeability tests for the other UV absorbers have not yet been conducted and this aspect requires urgent investigation. If these strand breaks were to occur in human DNA and if they were unrepaired, they could contribute to mutagenesis, carcinogenesis, inherited disease and eventually cell death. The photosensitising properties of Eusolex 232 are also a potential cause of concern. Its ability to induce singlet oxygen upon UV irradiation poses a threat of oxidative damage to skin tissue and the cell membranes.

With regards to the use of ketoprofen as a drug for the treatment of arthritic diseases, skin permeability is not a factor. DNA cleavage has been shown before by other workers, and has been confirmed here. Since this drug is consumed orally, it is most likely to react with DNA, but UV

light would have to reach the DNA. Therefore patients taking ketoprofen medication should avoid UV irradiation treatment.

In conclusion it should be emphasised that, before the benzophenone-based sunscreens can be considered "safe", more work needs to be done to evaluate the photochemistry *in vivo*. Until then the use of sunscreen formulations containing benzophenones should be used with caution.

REFERENCES

Agin P., Anthony F.A. and Hermansky F. (1998) *Lancet* **351**, 525.

Ainsleigh H.G. (1993) *Preventive Medicine* **22**, 132-140.

Alberts B., Bray D., Lewis J., Raff M., Roberts K. and Watson J.D. (1989) *Molecular Biology of the Cell*, Garland Publishing Inc., New York.

Aliwell S.R. (1991) *MSc thesis*, *Para*-aminobenzoic acid photosensitised dimerization of thymine, University of Natal, Durban, South Africa.

Allen J. M., Engenolf S. and Allen S. K. (1995) *Biochemical and Biophysical Research Communications* **212(3)**, 1145-1151.

Allen J.M., Gossett C.J. and Allen S.K. (1996) *Chemical Research in Toxicology* **9(3)**, 605-609.

Armitage B. (1998) *Chemical Reviews* **98(3)**, 1171-1200.

Armitage B., Yu C., Devadoss C. and Schuster G.B. (1994) *Journal of American Chemical Society* **116**, 9847-9859.

Artuso T., Bernadou J., Meunier B., Piette J. and Paillous N. (1991) *Photochemistry and Photobiology* **54(2)**, 205-213.

Atkins P.W. (1994) *Physical Chemistry* 5th Ed., Oxford University Press.

Autier, P., Dore, J., Cattaruzza, M.S., Renard, F., Luther, H., Gentiloni-Silverj, F., Zantedeschi, E., Mezzetti, M., Monjaud, I., Andry, M., Osborn, J.F., and Grivegnee, A.R. (1998). *Journal of National Cancer Institute, 90* **(24),** 1873-1880.

Avers C. J. (1984) *Genetics*, 2nd edition, Ed. van Leeuwen R.S., PWS Publishers, Wadsworth.

Berne B. and Ros A.M. (1998) *Contact Dermatitis* **38(2)**, 61-64.

Bilsland D. and Ferguson J. (1993) *Contact Dermatitis* **29(2)**, 70-73.

Birnboim H.C. and Jevcak J.J. (1981) *Cancer Research* **41**, 1889-1892.

Boger D.L., Fink B.E., Brunette S.R., Tse W.C. and Hedrick M.P. (2001) *Journal of the American Chemical Society* **123**, 5878-5891.

Bolton K. (1991) *MSc Thesis*, Studies of the photochemical reactions of thymine with selected sensitizers, University of Natal, Durban, South Africa.

Bolton K., Martincigh B.S. and Salter L.F. (1992) *Journal of Photochemistry and Photobiology A: Chemistry* **63**, 241-248.

Boscá F., Luisa M. and Miranda M.A. (2001) *Photochemistry and Photobiology* **74(5)**, 637-655.

Boscá F. and Miranda M. A. (1998) *Journal of Photochemistry and Photobiology B: Biology* **43**, 1-26.

Boscá F., Miranda M.A., Carganico G., and Mauleōn D. (1994) *Photochemistry and Photobiology* **60(2)**, 96-101.

Boyer R.F. (1993) *Modern Experimental Biochemistry* 2nd Ed., Redwood City California, Benjamin/Cummings, pp. 115-128.

Broadbent J.K. (1994) *MSc Thesis*, Photochemical studies of sunscreen constituents, University of Natal, Durban, South Africa.

Broadbent J.K., Martincigh B.S., Raynor M.W, Salter L.F., Moulder R., Sjöberg P. and Markides K.E. (1996) *Journal of chromatography A* **732**, 101-110.

Brown I.H. and Johns H.E. (1968) *Photochemistry and Photobiology* **8**, 275.

Brucat P. J. (1998) *Website:* http://itl.chem. ufl.edu /3417_s98/hyper/hyper.html, Quantum Mechanics and Spectroscopy, Date accessed:15 April 2003.

Bruice P. (2001) Organic Chemistry 3rd ed., Prentice Hall, New York, pg 1243.

Burrows C.J. and Muller J.G. (1998) *Chemical Reviews* **98(3),** 1109-1151.

Cain B.F., Baguley B.C. and Denny W.A. (1978) *Journal of Medicinal Chemistry* **21(7)**, 658-668.

Calvert J.G. and Pitts J.N. Jr. (1966) *Photochemistry*, John Wiley & Sons, 780-786.

Calvert J.G. and Pitts J.N. Jr. (1967) *Photochemistry*, New York: Wiley, 534.

Castrell J.V., Gomez-Lechon M. J., Hernandez D., Martinez L.A. and Mirand M.A. (1994) *Photochemistry and Photobiology* **60(6)**, 586-590.

Charlier M. and Hélène C. (1972) *Photochemistry and Photobiology* **15**, 71-87.

Chignell C.F., Kalyanaraman B., Mason R.P. and Sik R.H. (1980) *Photochemistry and Photobiology* **32**, 563-571.

Ciulla T.A., Van Camp J.R., Rosenfeld E. and Kochevar I. (1989) *Photochemistry and Photobiology* **51** 293-298.

Cleaver J.E. (1968) *Nature* **218**, 652-656.

Clemmett S.J. (1992) *MSc Thesis*, An investigation of acetone-photosensitised DNA kinetics, University of Natal, Durban, South Africa.

Condorelli G., Costanzo L.L., de Guidi G., Guiffrida S. and Sortino S. (1995) *Photochemistry and Photobiology* **62(1)**, 155-161.

Croke D.T., Blau W., OhUigin C. Kelly J.M. and McConnell D.J. (1988) *Photochemistry and Photobiology* **47**, 527-536.

Damiani E., Greci L., Parsons R. and Knowland J. (1999) *Free Radical Biology and Medicine* **26 (7-8)**, 809-816.

Darvay A., White I.R., Rycroft R.J. Jones A.B., Hawk J.K. and Mcfadden J.P. (2001) *British Journal of Dermatology* **145(4)**, 597-601.

De Gruijl F.R. and Van der Leun J.C. (1994) *Health Physics* **67**, 1-8.

Diffey B. (2001) *Journal of Photochemistry and Photobiology B: Biology* **64**, 105-108.

Dover J. S. and Arndt K. A. (1994) *Dermatology: Journal of the American Medical Association,* **271(21)**, 1662-1663.

Felix T, Hall B.J. and Brodbelt J.S. (1998) *Analytica Chimica Acta* **371(2-3)**, 195-203.

Foote C.S. (1991) *Photochemistry and Photobiology* **54(5)**, 659.

Foresman, J.B. (1996) *Exploring Chemistry with Electronic Structure Methods,* 2nd Ed., Frisch, Æ., Gaussian, Inc.

Franklin W.A., Lo K.M. and Haseltine W.A. (1982) *Journal of Biology and Chemistry* **257**, 13535.

Garland C.F., Garland F.C. and Gorham E.D. (1992) *American Journal of Public Health* **82(4)**, 614-615.

Gasparro F.P. (1985) *Photodermatology* **2**, 151-157.

Gasparro F.P. and Battista J. (1987) *Photochemistry and Photobiology* **45**, 495.

Geall A.J. and Blagbrough I.S. (2000) *Journal of Pharmaceutical and Biomedical Analysis* **22**, 849-859.

Glass A.G. and Hoover R.N. (1989) *The Journal of the American Medical Association* **262(15)**, 2097.

Gonzenbach H., Hill T. J. and Truscott T. G. (1992) *Journal of Photochemistry and Photobiology B: Biology* **16**, 377-379.

Green A., Williams G. and Mar C.D. (1997) *website:* www.disr.gov.au/science/pmsec/15meet/cancer/green.html, Date accessed: 1 November 2000.

Greenstock C.L. and Johns H.E. (1968) *Biochemical and Biophysical Research Communications* **30(1)**, 21-27.

Greenstock C.L., Brown I.H., Hunt J.W. and Johns H.E. (1967) *Biochemical and Biophysical Research Communications* **27**, 413.

Guilbault G.G. (1973) *Practical Fluorescence, Theory, Methods and Techniques*, Marcel Dekker Inc., New York.

Hansen J.B., Koch T., Buchardt, O., Nielsen P.E., Wirth M. and Nordēn B. (1983) *Biochemistry* **22(21)**, 4878-4886.

Harrison J.F. *website*:http://www.cem.msu.edu/~cem461/computationalchemistry.pdf, Part 1, Basics of Computational Quantum Chemistry, date accessed: 29 March 2003.

Haseltine W.A., Gordan L.K., Lindan C.P. Gafstrom R.H., Sharper N.L. and Grossman L. (1980) *Nature* **285**, 82.

Hayden C.G.J., Roberts M.S. and Benson H.A.E. (1997) *Lancet* **350**, 863.

Hehre, W.J., Yu, J., Klunzinger, P.E., Lou, L (1998) *A Brief Guide to Molecular Mechanics and Quantum Chemical Calculations*, Wavefunction, Inc.

Hélène C. (1987) *Photophysics to Photobiology*, Eds. Favre A., Ttrell R., and Cadet J., Elsevier, Amsterdam, pp. 3-22.

Hertzberg R.P. and Dervan P.B. (1984) *Biochemistry* **23**, 3934-3945.

Higginson J., Muir C.S. and Munoz N. (1992), *Human Cancer: Epidemiology and Environmental Causes, Monographs on Cancer Research*, Cambridge University Press, pp. 14-16.

Inbaraj J.J., Bilski P. and Chignell C.F. (2002) *Photochemistry and Photobiology* **75(2)**, 107-116.

Jiang R., Roberts M.S., Collins D.M. and Benson H.A. (1999) *British Journal of Clinical Pharmacology* **48(4)**, 635-637.

Kenny G.E., Sakr A., Lichtin J.L., Chou H. and Bronangh R.L. (1995) *Journal of the Society of Cosmetics and Chemistry* **46**,117-127.

Kenny G.S. (1994) *Journal of Chemical Education* **71(1)**, 77-79.

Kilfoil V. and Salter L.F. (1988) *International Journal of Chemical Kinetics* **20**, 645-649.

Knowland J., Mckensie E.A., Mchugh P.J. and Cridland N.A. (1993) *FEBS Letters* **324(3)**, 309-313.

Kochevar I.E. and Dunn D.A. (1990) *Bioorganic Photochemistry and the Nucleic Acids 1*, Ed. Morrison H., Wiley & Sons, New York, pp. 272-312.

Kowlaser K. (1998) *MSc thesis*, Photoproduct formation in the irradiated sunscreen absorber 2-ethylhexyl-*p*-methoxycinnamate, University of Natal, Durban, South Africa.

Lamola A.A. and Hammond G.S. (1965) *Journal of Chemistry and Physics* **43**, 550.

Lamola A.A. and Yamene T. (1967) *Proceedings of the National Academy of Science* **58**, 443.

Lamola A.A., Gueron M., Yamane T., Eisinger J. and Shulman R.G. (1967) *Journal of Chemistry and Physics* **47**, 2210.

Larsen H. R. (1994) *International Journal of Alternative and Complementary Medicine* **12(12)**, 17-18.

Leach A.R. (1996) *Molecular Modelling. Principles and Applications*, Addison Wesley Longman Ltd., Harlo Essex, England.

Ledger M.B. and Porter G. (1971) *Transaction of the Faraday Society*, **67**, 539.

Lee J.A.H. (1989) *Photochemistry and Photobiology* **50(4)**, 493-496.

Lepecq J.B. and Paoletti C. (1967) *Journal of Molecular Biology* **21**, 87-106.

Lerman L.S. (1961) *Journal of Molecular Biology* **3**, 18-30.

Levy S. B. (2002) http://www.emedicine.com/derm/topic510.htm, Eds: Garmyn M., Vinson R., Callen J. P., Quirk C. and Elston D.M, Date accessed: 10 December 2002.

Lewis Ricki, (2001) website: www.mhhe.com/biosci/genbio/life/articles/article22.m.html, The Mc Graw-Hill Companies, date accessed: 3 August 2002.

Lhiaubet V., Paillous N. and Chouini-Lalanne N. (2001), *Photochemistry and Photobiology* **74(5)**, 670-678.

Lloyd R.S., Hailde C.W. and Robberson D.L. (1978) *Biochemistry* **17**, 1890-1896.

Löber G., Koudelka J. and Smékal E. (1974) *Biophysical Chemistry* **2**, 158-163.

Lumb M.D. (1978) *Luminescence Spectroscopy*, Academic Press Inc. (London) Ltd.

March J. (1992) *Advanced Organic Chemistry*, 4th Ed., John Wiley and Sons, New York.

Marguery M.C., Chouini-Lalanne N., Ader J.C., and Paillous N. (1998) *Photochemistry and Photobiology* **68(5)**, 679-684.

Martincigh B. S., Allen J.M. and Allen S. K. (1997) *Sunscreen Photobiology: Molecular, Cellular and Physiological Aspects*, Ed. Gasparro F. P., Springer-Verlag and Landes Bioscience, pp. 11-45.

Masnyk T.W. and Minton K.W. (1991) *Photochemistry and Photobiology* **54(1)**, 99-107.

Mattews C.K. and van Holde K.E. (1996) *Biochemistry,* 2nd edition, Benjamin Publishing Company Inc., pp. 95-105.

McMillin D.R. and McNett K.M. (1998), *Chemical Reviews* **98(3)**, 1201-1219.

Moan J. and Dahlback A. (1992) *British Journal of Cancer* **65(6)**, 619-621.

Mohtat N., Cozens F.L., Hancock-Chen T.,Scaiano J.C., McLean J. and Kim J. (1998), *Photochemistry and Photobiology* **67(1)**, 111-118.

Morgan A.R. and Pulleyblank D.E. (1974) *Biochemical and Biophysics Research Communications* **61**, 396-403.

Morliere P., Avice O. and Melso T.S.E. (1982) *Photochemistry and Photobiology* **36**, 395-399.

Nordmeier E. (1992) *Journal of Physical Chemistry* **96**, 6045-6055.

O'Kereke C.S., Barat S.A. and Abdel-Rahman M.S. (1995) *Toxicology Letters* **80(1-3)**, 61-67.

Olmsted J. III and Kearns D.R. (1977) *Biochemistry* **16**, 3647-3654.

Osgood P.J., Moss S.H. and Davies D.J.G. (1982), *Journal of Investigative Dermatology* **79**, 354.

Panday R. (2002), *MSc. Thesis*, A photochemical investigation of two sunscreen absorbers in a polar and a non-polar medium, University of Natal, Durban, South Africa.

Patrick M.H., (1977) *Photochemistry and Photobiology* **25**, 357.

Pogozelski W.K. and Tullius T.D. (1998) *Chemical Reviews* **98(3)**, 1089-1107.

Raghunathan G., Keiber-Emmons T., Rein R. and Alderfer J. (1990) *Journal of Molecular Structure and Dynamics* **7**, 899.

Rahn R.O. and Patrick M.H. (1976) *Photochemistry and Photobiology of Nucleic Acids* 2, Ed. Wang S., Academic Press, New York, pp. 99-145.

Rai S., Kasturi C., Grayzar J., Platz M.S., Goodrich R.P., Yerram N.R., Wong V. and Tay-Goodrich B.N. (1993) *Photochemistry and Photobiology* **58(1)**, 59-65.

Reinhardt C.G. and Krugh T.R. (1978) *Biochemistry* **17(23)**, 4845-4854.

Robinson S.H., Odio M.R., Thompson E.D., Aardema M.J. and Kraus A.L. (1994) *Environmental and Molecular Mutagenesis* **23(4)**, 312-317.

Roots R., Kraft G. and Gosschalk E. (1985) *International Journal of Radiation Oncology Biology Physics* **11**, 259-265.

Roscher N.M., Lindermann M.K.O. and Kong S.K., Cho C.G. and Jiang P. (1994) *Photochemistry and Photobiology A: Chemistry* **80**, 417-421.

Sambrook J., Fritsch E.F., Maniatias T. (1989) *Molecular Cloning, A Laboratory Manual*, 2nd, Cold Spring Harbor Laboratory Press, p 65.

Sayre R. M. (1992) *Cosmetics and Toiletries* **107**, 105-109.

Sayre R.M. and Dowdy J.C. (1999) *Cosmetics and Toiletries* **114(5)**, 85-91.

Scaiano J.C., Abuin E.B. and Stewart L.C. (1982) *Journal of the American Chemical Society* **104**, 5673-5679.

Schallreuter K.U., Wood J.M., Farwell D.W., Moore J., and Edwards H.G. (1996) *Journal of Investigative Dermatology* **106**, 583-586.

Schmidt T, Ring J. and Abeck D. (1998) *Dermatology* **196(3)**, 354-357.

Schwack W. and Rudolph T. (1995) *Journal of Photochemistry and Photobiology B: Biology* **28**, 229-234.

Scott J.B.: website: www.neanderthal.-modern.com/images/dna.gif, Last updated: August 2003.

Sedly P.G. and Southern E.M. (1982) *Gel Electrophoresis of Nucleic Acids: A Practical Approach*, Ed. Rickwood D. and Harnes B.D., IRL press Ltd., pp. 39-76.

Serpone N., Salinaro A., Emeline A.V., Horikoshi S., Hidaka H. and Zhao J. (2002) *Photochemistry and Photobiological Sciences* **1**, 970-981.

Setlow R. B. (1996) *Science* **153**, 379-386.

Setlow R. Grist E., Thompson K. and Woodhead A.D. (1993) *Proceedings of the National Academy of Science USA* **90**, 6666-6670.

Setlow R.B. and Ahmed F.E (1980) *Carcinogenesis: Fundamental Mechanisms and Environmental Effects*, Ed. Pullman B. and Gelboir H., New York, p 453.

Sewlall A.S. (1999), *Honours Project* (Unpublished), An investigation of the photochemical dimerization of thymine in aqueous solution by the sunscreen absorber benzophenone-3, University of Natal, Durban, South Africa.

Shaw A, Wainschel L.A. and Shetlar M.D. (1992) *Photochemistry and Photobiology* **55(5)**, 647-656.

Sitas F., Madhoo J. and Wessie J. (1998) *website:* http://www.CANSA.co.za. The National Cancer Registry of South Africa, Date accessed: 31 October 2002.

Skoog D. A., West D. M. and Holler F. J. (1996) *Fundamentals of Analytical Chemistry* 7th ed., Saunders College Publishing, United States.

Smith D.I., Blattner F.R. and Davies J. (1976), *Nucleic Acids Research*, **3**, 343-353.

Sobell H.M., Tsai C.C., Jain S.C. and Gilbert S.G. (1977) *Journal of Molecular Biology* **114**, 333-365.

Steinberg D. C. (1996) *Sunscreen Encyclopaedia: Regulatory Update* 111.

Stevenson C. and Davies R.J.H. (1999) *Chemical Research in Toxicolgy* **12**, 38-45.

Strange C.J. (1995) Sunscreen Drug Products for Over-the-Counter Human Use; Final Monograph, Federal Registry 6427666, U.S. Food and Drug Administration **29**, 10-14, website: http://www.cfsan.fda.gov/~lrd/fr990521.html, Date accessed 31 October 2002.

Strothkamp K.G. and Strothkamp R.E. (1994) Jo*urnal of Chemical Education* **71(1)**, 77-79.

Sutherland B.M. (1982) *Photochemistry and Photobiology* **36**, 95-97.

Sztumpf-Kulikauski E., Shugar D. and Buag J.W. (1976) *Photochemistry and Photobiology* **6**, 41.

Tarras-Wahlberg N., Stenhagen G., Larkö O., Rosèn A., Wennberg A. and Wennerström O., (1999) *The Journal of Investigative Dermatology* **113(4)**, 547-553.

Thomas R.C. (1989) *MSc Thesis*, The photochemistry of DNA, University of Natal, Durban, South Africa.

Thorne H.V. (1996) *Virology* **29**, 234.

Trevisi P., Vincenzi C., Chieregato C., Guerra L. and Tosti A. (1994) *Dermatology* **189(1)**, 55-57.

Turro N.J. (1978) *Modern Molecular Photochemistry*, Benjamin/Cummings, Menlo Park, USA, pp. 90, 105, 352.

U.S. Food and Drug Administration. Sunscreen drug products for over-the-counter human use: Final monograph (2000) In: Federal Register/Rules and Regulations **64 (98)**, 27666-27693, website: http://www.cfsan.fda.gov/1lrd/fr990521.html, Date accessed: 31 October 2002.

Voss W. *Sun Protection: Dermatological and Cosmetical Aspects*, Website: http://www.dermatest.de/PB/Publikationen/PBEN/Sun_Protection/body_sun_protection.html., Date accessed: August 2001

Warburg O. and Christian W. (1942) *Biochemistry* **310,** 384-421.

Westerdahl J., Ingvar C. Masback A. and Ollsson H. (2000) *International Journal of Cancer* **87(1)**, 145-150.

Westerdahl J., Ollsson H., Masback A., Ingrar C. and Jonsson N. (1995) *Melanoma Research* **5**, 59-65.

Wolf P., Donawho C.K. and Kripke M.L. (1994) Journal *of the National Cancer Institute* **86(2)**, 99-105.

Woodruff John, *Safe sun*, website: http://www.chemsoc.org/chembytes/ezine/2001/woodruff_jul01.html, Date accessed: 3 August 2001.

Wu C. (1998) *Science News Online, Melanoma Madness*, website: www.sciencenews.org/sn-arc98/6_6_98/bob2.htm, Date accessed: 15 November 2000.

Young A.R. (1997) *Physics and Medical Biology* **42**, 789-802.

Website addresses:

1. http://216.239.39.120/translate_c?hl=en&ie=UTF-8&oe=UTF-8&u=http://www.abacovital.com/fichastecnicas/filtros/benzofenone9.htm Club of Perfumería and Cosme'tica, File of Engineering data of Raw materials, Date accessed: 4 December 2002.
2. http://216.239.39.120/translate_c?hl=en&ie=UTF-8&oe=UTF-8&u=http://www.abacovital.com/fichastecnicas/filtros/filtros.htm&prev Club of Perfumería and Cosme'tica, File of Engineering data of Raw materials, Date accessed: 4 December 2002.
3. http://216.239.39.120/translate_c?hl=en&ie=UTF-8&oe=UTF-8&u=http://www.abacovital.com/fichastecnicas/filtros/benzofenone1.htm Club of Perfumería and Cosme'tica, File of Engineering data of Raw materials, Date accessed: 4 December 2002.
4. http://herkules.oulu.fi/isbn9514266463/html/x563.html. (2002) Nf1 tumor suppressor in skin, Chapter 2.6,Oulu University Library, Date accessed: 20 September 2002.
5. http://kukulkan.mcb.arizona.edu/~mhewlett/marty/alt411/modules/dimerre.html. Formation and Repair of Pyrimidine Dimers in DNA, Date accessed: 25 September 2002.
6. http://www.emunix.emich.edu/~rwinning/genetics/mutat4.html, DNA repair, Date accessed December 2002.
7. http://www.webmo.net/curriculum/geometry_optimization/geometry_optimization_key.html (2000) Geometry Optimization Methods, WebMO, LLC, Date accesed: 20 September 2002.
8. www.health.gov.au/tga/docs/pdf/sunscrai.pdf (2001) Commonwealth Department of Health and Aged Care, Date accessed: 5 October 2002.

9. www.turnerdesigns.com/t2/doc/appnotes/s-0046.pdf), Date accessed December 2002.

APPENDIX A

A list of the materials and equipment used for the various experiments

A1: Equipment used for UV irradiation

A2: Chemicals and equipment used for UV absorption spectroscopy

A3: Chemicals and equipment used for agarose gel electrophoresis

A4: Chemicals and equipment used for fluorescence spectroscopy

A5: Equipment for computational modelling

A1 Equipment used for UV irradiation

Osram HBO 500 W/2 high pressure mercury lamp

Schreiber Power pack

10 mm Pyrex filter

NMR tubes

Quartz cuvette (10 mm pathlength)

Blak-Ray J-221 Longwave UV intensity Meter (UVP)

A2 Chemicals and equipment used for UV absorption spectroscopy

CHEMICALS	SUPPLIER INFORMATION
Tris-(hydroxymethyl)-aminomethane	Saarchem Ltd.
Sodium chloride	Skychem – Analytical grade
Hydrochloric acid	BDH Chemicals
Millipore water	Water that was purified by the Millipore Milli - Q^{50} ultra - pure water system
Ethanol	99% pure
Benzophenone	BDH Chemicals
Benzophenone-1	Uvinul 400 - BASF
Benzophenone-3	Uvinul M-40-BASF
Benzophenone-4	Uvinul MS-40-BASF
2,2'-dihydroxy-4,4'-dimethoxy benzophenone sulphonic acid	Uvinul DS-49-BASF
2-phenylbenzimidazole-5-sulphonic acid	Eusolex 232-Merck
(s). (+). Ketoprofen	Aldrich Chemicals, 99% pure

EQUIPMENT

Cary 1E UV-Visible spectrometer

Pecsa Analytical matched quartz cuvettes (10 mm pathlength)

Wisconsin aluminium steam sterilizer– Model No. 25X

Mettler AT 250 analytical balance

Millipore Milli - Q^{50} ultra - pure water system

A3 Chemicals and equipment used for agarose gel electrophoresis

CHEMICALS	SUPPLIER INFORMATION
ϕ X174 PHAGE DNA	Sigma - (store at 2 to 8°C)
di-Sodium hydrogen orthophosphate	BDH Chemicals – Analytical grade
Potassium dihydrogen orthophosphate	BDH Chemicals – Analytical grade
Sodium chloride	Skychem – Analytical grade
Millipore water	Water that was purified by the Millipore Milli - Q^{50} ultra - pure water system
Sodium hydroxide	
Ethanol	99% pure
Benzophenone	BDH Chemicals
Benzophenone-1	Uvinul 400 - BASF
Benzophenone-3	Uvinul M-40-BASF
Benzophenone-4	Uvinul MS-40-BASF
2,2'-dihydroxy-4,4'-dimethoxy benzophenone sulphonic acid	Uvinul DS-49-BASF
2-phenylbenzimidazole-5-sulphonic acid	Eusolex 232-Merck
(s). (+). Ketoprofen	Aldrich Chemicals, 99% pure
Tris-(hydroxymethyl)-aminomethane	Saarchem Ltd.
Bromophenol blue	BDH Laboratory Chemicals
Boric acid	BDH Chemicals – Analytical grade
Ethylenediamine tetra-acetic acid	BDH Chemicals
Hydrochloric acid	BDH Chemicals
Ethidium bromide	Merck
Glycerol	BDH Chemicals Ltd.
Bromophenol blue	BDH Laboratory Chemicals
Providencia Stuartii enzyme (with digestion buffer)	Sigma

EQUIPMENT

Cigen horizontal agarose gel electrophoresis apparatus

Hoefer Scientific DC power supply - PS 500 X (500 V, 400 mA)

Scientific Engineering Flask shaker

Hoefer Scientific transilluminator- Model HE 33

Matsushita communications Panasonic color CCTV camera

Mecer Premium Computers

Scion Imaging software

Syngene transilluminator

Vacutec Camera system

Syngene Genesnap software 2.60.0.14

Hoefer Scientific GS 300 Transmittance / Reflectance

Metrohm Labograph plotter - E 478XY

Wisconsin aluminium steam sterilizer – Model No. 25X

Mettler AT 250 analytical balance

Millipore Milli - Q^{50} ultra - pure water system

Gilson micropipettes 1-100 µL (P 100)

Gilson micropipettes 100-1000 µL (P 1000)

Ratiolab pipette tips

Greiner Labortecknik plastic Eppendorf tubes (1.50 ml)

A4 Chemicals and equipment used for fluorescence spectroscopy

CHEMICALS	SUPPLIER INFORMATION
Deoxyribonucleic acid (DNA) sodium salt	Sigma – Type 1, highly polymerized from Calf Thymus (store desiccated at 0-5°C)
Benzophenone	BDH Chemicals
Tris-(hydroxymethyl)-aminomethane	Saarchem Ltd.
Sodium Chloride	Skychem – Analytical grade
Hydrochloric acid	BDH Chemicals
Millipore water	Water that was purified by the Millipore Milli - Q^{50} ultra - pure water system
Ethanol	99% pure

Benzophenone	BDH Chemicals
Benzophenone-1	Uvinul 400 - BASF
Benzophenone-3	Uvinul M-40-BASF
Benzophenone-4	Uvinul MS-40-BASF
2,2'-dihydroxy-4,4'-dimethoxy benzophenone sulphonic acid	Uvinul DS-49-BASF
2-phenylbenzimidazole-5-sulphonic acid	Eusolex 232-Merck
(s). (+). Ketoprofen	Aldrich Chemicals, 99% pure
Ethidium bromide	Merck
Nitrogen gas	Afrox

EQUIPMENT

Perkin Elmer LS 50B Luminescence Spectrometer

FL Winlab Software

1 cm pathlength quartz fluorescence cuvette

Wisconsin aluminium steam sterilizer– Model No. 25X

Mettler AT 250 analytical balance

Millipore Milli - Q^{50} ultra - pure water system

Freed Electric magnetic stirrer

A5 Equipment used for the computational studies

Hyperchem software

APPENDIX B

The raw data obtained for the quantitative analysis of the ethidium bromide-stained agarose gels

B1:	Figures 3.19 - 3.24	(DNA alone-control)
B2:	Figures 3.29- 3.30	(Benzophenone)
B3:	Figures 3.31 - 3.33	(Benzophenone-1)
B4:	Figures 3.34 – 3.36	(Uvinul DS49)
B5:	Figures 3.37 – 3.39	(Eusolex 232)
B6:	Figures 3.44 – 3.46	(Benzophenone-3)
B7:	Figures 3.47 – 3.48	(Benzophenone-4)

B1: The quantitative analysis of the ethidium bromide-stained agarose gels in Figures 3.19 - 3.24 showing DNA photocleavage induced by the irradiation of DNA alone (in the absence of any UV absorber).

Figure 3.19

Lane	1	2	3	4	5	6
Irradiation time/ min	0	10	15	20	30	45
% DNA Form I	0.54	0.63	0.62	0.60	0.48	0.43
% DNA Form II	0.30	0.50	0.54	0.52	0.65	0.65
% DNA Form III	0.00	0.00	0.00	0.00	0.00	0.00
Total	0.84	1.13	1.16	1.12	1.13	1.08
% $[I]_F$	64.29	55.75	53.45	53.57	42.48	39.81
% $[II]_F$	35.71	44.25	46.55	46.43	57.52	60.19
% $[III]_F$	0.00	0.00	0.00	0.00	0.00	0.00
SSB	0.00	0.14	0.18	0.18	0.41	0.48

Figure 3.20

Lane	1	2	3	4	5	6
Irradiation time/ min	0	10	15	20	30	45
% DNA Form I	0.65	0.61	0.57	0.57	0.62	0.31
% DNA Form II	0.27	0.34	0.44	0.33	0.56	0.44
% DNA Form III	0.00	0.00	0.00	0.00	0.00	0.00
Total	0.92	0.95	1.01	0.90	1.18	0.75
% $[I]_F$	70.65	64.21	56.44	63.33	52.54	41.33
% $[II]_F$	29.35	35.79	43.56	36.67	47.46	58.67
% $[III]_F$	0.00	0.00	0.00	0.00	0.00	0.00
SSB	0.00	0.10	0.22	0.11	0.30	0.54

Figure 3.21

Lane	1	2	3	4	5	6
Irradiation time/ min	0	5	10	20	30	45
% DNA Form I	60.85	46.73	44.69	33.39	40.99	15.77
% DNA Form II	41.09	41.18	43.71	45.08	75.84	61.73
% DNA Form III	0.00	0.00	0.00	0.00	0.00	0.00
Total	101.94	87.91	88.40	78.47	116.83	77.50
% $[I]_F$	59.69	53.16	50.55	42.55	35.09	20.35
% $[II]_F$	40.31	46.84	49.45	57.45	64.91	79.65
% $[III]_F$	0.00	0.00	0.00	0.00	0.00	0.00
SSB	0.00	0.12	0.17	0.34	0.53	1.08

Figure 3.22

Lane	1	2	3	4	5	6
Irradiation time/ min	0	5	10	20	30	45
% DNA Form I	74.20	80.00	73.50	65.50	51.60	17.10
% DNA Form II	31.20	34.90	61.20	78.90	81.50	94.70
% DNA Form III	0.00	0.00	0.00	0.00	0.00	0.00
Total	105.40	114.90	134.70	144.40	133.10	111.80
% $[I]_F$	70.40	69.63	54.57	45.36	38.77	15.30
% $[II]_F$	29.60	30.37	45.43	54.64	61.23	84.70
% $[III]_F$	0.00	0.00	0.00	0.00	0.00	0.00
SSB	0.00	0.01	0.25	0.44	0.60	1.53

Figure 3.23

Lane	1	2	3	4	5	6
Irradiation time/ min	0	5	10	20	30	45
% DNA Form I	47.77	50.27	48.09	47.50	40.11	25.92
% DNA Form II	20.87	52.01	45.59	57.33	77.39	79.61
% DNA Form III	0.00	0.00	0.00	0.00	0.00	0.00
Total	68.64	102.28	93.68	104.83	117.50	105.53
% $[I]_F$	69.59	49.15	51.33	45.31	34.14	24.56
% $[II]_F$	30.41	50.85	48.67	54.69	65.86	75.44
% $[III]_F$	0.00	0.00	0.00	0.00	0.00	0.00
SSB	0.00	0.35	0.30	0.43	0.71	1.04

Figure 3.24

Lane	1	2	3	4	5	6
Irradiation time/ min	0	5	10	20	30	45
% DNA Form I	51.80	61.90	68.19	67.69	70.52	76.81
% DNA Form II	21.00	28.82	26.87	31.22	29.15	38.62
% DNA Form III	0.00	0.00	0.00	0.00	0.00	0.00
Total	72.80	90.72	95.06	98.91	99.67	115.43
% $[I]_F$	71.15	68.23	71.73	68.44	70.75	66.54
% $[II]_F$	28.85	31.77	28.27	31.56	29.25	33.46
% $[III]_F$	0.00	0.00	0.00	0.00	0.00	0.00
SSB	0.00	0.04	-0.01	0.04	0.01	0.07

The mean and standard deviation for % DNA $[I]_F$, $[II]_F$, $[III]_F$, and SSB obtained from Figures 3.19-3.24 for the irradiation of DNA alone (in the absence of any UV absorber).

	% $[I]_F$		% $[II]_F$		SSB	
Time/ min	**Mean**	**Std. Dev.**	**Mean**	**Std. Dev.**	**Mean**	**Std. Dev.**
0	67.63	4.63	32.37	4.63	0.00	0.00
5	60.02	8.49	39.98	8.49	0.13	0.12
10	56.35	7.84	43.65	7.84	0.19	0.11
20	53.09	10.70	46.91	10.70	0.26	0.17
30	45.63	13.99	54.37	13.99	0.43	0.25
45	34.65	18.81	65.35	18.81	0.79	0.52

B2 The quantitative analysis of the ethidium bromide-stained agarose gels in Figures 3.29 - 3.30 showing DNA photocleavage induced by the irradiation of DNA (18.85 μM) in the presence of benzophenone (50 μM).

Figure 3.29

Lane	1	2	3	4
Irradiation time / min	0	5	15	30
% DNA Form I	0.29	0.33	0.25	0.01
% DNA Form II	0.22	0.34	0.51	0.34
% DNA Form III	0.00	0.03	0.11	0.15
Total	0.51	0.70	0.87	0.50
% $[I]_F$	56.86	47.14	28.74	2.00
% $[II]_F$	43.14	48.57	58.62	68.00
% $[III]_F$	0.00	4.29	12.64	30.00
SSB	0.00	0.19	0.68	3.35

Figure 3.30

Lane	1	2	3	4	5	6
Irradiation time / min	0	0	10	15	30	45
% DNA Form I	0.19	0.16	0.15	0.26	0.16	0.07
% DNA Form II	0.09	0.08	0.17	0.27	0.27	0.23
% DNA Form III	0.00	0.00	0.03	0.07	0.15	0.16
Total	0.28	0.24	0.35	0.60	0.58	0.46
% $[I]_F$	67.86	66.67	42.86	43.33	27.59	15.22
% $[II]_F$	32.14	33.33	48.57	45.00	46.55	50.00
% $[III]_F$	0.00	0.00	8.57	11.67	25.86	34.78
SSB	0.00	0.02	0.46	0.45	0.90	1.49

The mean for % DNA $[I]_F$, $[II]_F$, $[III]_F$, and SSB obtained from Figures 3.29 - 3.30 for the irradiation of DNA (18.85 μM) in the presence of benzophenone (50 μM).

Time/ min	0	5	10	20	30	45
Mean % $[I]_F$	59.23	47.14	42.86	36.03	14.79	15.22
Mean % $[II]_F$	40.77	48.57	48.57	51.81	57.28	50.00
Mean % $[III]_F$	0.00	4.29	8.57	12.16	27.93	34.78
Mean SSB	0.06	0.19	0.46	0.57	2.12	1.49

B3: The quantitative analysis of the ethidium bromide-stained agarose gels in Figures 3.31 - 3.33 showing DNA photocleavage induced by the irradiation of DNA (18.85 μM) in the presence of benzophenone-1 (50 μM).

Figure 3.31

Lane	1	2	3	4	5	6
Irradiation time / min	0	5	10	20	30	45
% DNA Form I	56.63	60.97	44.83	28.58	14.51	22.99
% DNA Form II	33.80	51.84	56.25	65.16	87.28	75.48
% DNA Form III	0.00	0.00	0.00	0.00	15.76	8.26
Total	90.43	112.81	101.08	93.74	117.55	106.73
% $[I]_F$	62.62	54.05	44.35	30.49	12.34	21.54
% $[II]_F$	37.38	45.95	55.65	69.51	74.25	70.72
% $[III]_F$	0.00	0.00	0.00	0.00	13.41	7.74
SSB	0.11	0.25	0.45	0.83	1.73	1.17

Figure 3.32

Lane	1	2	3	4
Irradiation time / min	5	20	30	45
% DNA Form I	29.80	13.93	1.15	1.15
% DNA Form II	21.14	22.97	19.12	9.48
% DNA Form III	4.53	3.88	4.45	11.83
Total	55.47	40.78	24.72	22.46
% $[I]_F$	53.72	34.16	4.65	5.12
% $[II]_F$	38.11	56.33	77.35	42.21
% $[III]_F$	8.17	9.51	18.00	52.67
SSB	0.30	0.75	2.75	2.65

Figure 3.33

Lane	1	2	3	4	5	6
Irradiation time / min	0	5	10	20	30	45
% DNA Form I	58.50	60.50	16.40	8.01	8.00	13.00
% DNA Form II	27.60	73.80	129.60	111.80	82.40	104.20
% DNA Form III	0.00	0.00	13.30	12.90	24.20	56.40
Total	86.10	134.30	159.30	132.71	114.60	173.60
% $[I]_F$	67.94	45.05	10.30	6.04	6.98	7.49
% $[II]_F$	32.06	54.95	81.36	84.24	71.90	60.02
% $[III]_F$	0.00	0.00	8.35	9.72	21.12	32.49
SSB	0.04	0.45	1.92	2.46	2.31	2.24

The mean and standard deviation for % DNA $[I]_F$, $[II]_F$, $[III]_F$, and SSB obtained from Figures 3.31 – 3.33 for the irradiation of DNA (18.85 μM) in the presence of benzophenone-1 (50 μM).

	% $[I]_F$		% $[II]_F$		% $[III]_F$		SSB	
Time/ min	**Mean**	**Std. Dev.**	**Mean**	**Std. Dev.**	**Mean**	**Std. Dev.**	**Mean**	**Std. Dev.**
0	65.28	3.76	34.72	3.76	0.00	0.00	0.07	0.05
5	50.94	5.10	46.34	8.43	2.72	4.71	0.33	0.10
10	27.32	24.08	68.50	18.18	4.17	5.90	1.19	1.04
20	23.56	15.29	70.03	13.97	6.41	5.55	1.35	0.96
30	7.99	3.94	74.50	2.73	17.51	3.88	2.26	0.51
45	11.38	8.88	57.65	14.40	30.97	22.50	2.02	0.76

B4: The quantitative analysis of the ethidium bromide-stained agarose gels in Figures 3.34 – 3.36 showing DNA photocleavage induced by the irradiation of DNA (18.85 μM) in the presence of Uvinul DS49 (50 μM).

Figure 3.34

Lane	1	2	3	4	5	6
Irradiation time / min	0	5	10	20	30	45
% DNA Form I	63.82	29.55	12.10	8.13	2.08	9.03
% DNA Form II	31.01	19.24	22.88	35.08	29.88	42.45
% DNA Form III	0.00	0.00	0.00	10.87	16.88	12.01
Total	94.83	48.79	34.98	54.08	48.84	63.49
% $[I]_F$	67.30	60.57	34.59	15.03	4.26	14.22
% $[II]_F$	32.70	39.43	65.41	64.87	61.18	66.86
% $[III]_F$	0.00	0.00	0.00	20.10	34.56	18.92
SSB	0.01	0.11	0.67	1.51	2.77	1.56

Figure 3.35

Lane	1	2	3	4	5	6
Irradiation time / min	0	5	10	20	30	45
% DNA Form I	54.65	33.80	30.26	1.61	6.24	10.30
% DNA Form II	46.28	39.62	51.86	49.12	62.31	38.81
% DNA Form III	0.00	0.00	0.00	7.61	17.97	22.98
Total	100.93	73.42	82.12	58.34	86.52	72.09
% $[I]_F$	54.15	46.04	36.85	2.76	7.21	14.29
% $[II]_F$	45.85	53.96	63.15	84.20	72.02	53.84
% $[III]_F$	0.00	0.00	0.00	13.04	20.77	31.88
SSB	0.22	0.39	0.61	3.20	2.24	1.56

Figure 3.36

Lane	1	2	3	4	5	6
Irradiation time / min	0	5	10	20	30	45
% DNA Form I	58.10	28.70	17.20	2.30	17.50	0.40
% DNA Form II	15.00	52.30	106.00	92.60	97.00	44.00
% DNA Form III	0.00	0.00	0.00	11.40	25.60	23.90
Total	73.10	81.00	123.20	106.30	140.10	68.30
% $[I]_F$	79.48	35.43	13.96	2.16	12.49	0.59
% $[II]_F$	20.52	64.57	86.04	87.11	69.24	64.42
% $[III]_F$	0.00	0.00	0.00	10.72	18.27	34.99
SSB	-0.16	0.65	1.58	3.44	1.69	4.75

The mean and standard deviation for % DNA $[I]_F$, $[II]_F$, $[III]_F$, and SSB obtained from Figures 3.34 – 3.36 for the irradiation of DNA (18.85 μM) in the presence of Uvinul DS49 (50 μM).

	% $[I]_F$		% $[II]_F$		% $[III]_F$		SSB	
Time/ min	**Mean**	**Std. Dev.**	**Mean**	**Std. Dev.**	**Mean**	**Std. Dev.**	**Mean**	**Std. Dev.**
0	66.98	12.67	33.02	12.67	0.00	0.00	0.02	0.19
5	47.34	12.62	52.66	12.62	0.00	0.00	0.38	0.27
10	28.47	12.61	71.53	12.61	0.00	0.00	0.95	0.54
20	6.65	7.26	78.72	12.09	14.62	4.88	2.72	1.06
30	7.99	4.17	67.48	5.63	24.53	8.77	2.23	0.54
45	9.70	7.89	61.71	6.92	28.60	8.53	2.62	1.84

B5: The quantitative analysis of the ethidium bromide-stained agarose gels in Figures 3.37 – 3.39 showing DNA photocleavage induced by the irradiation of DNA (18.85 μM) in the presence of Eusolex 232 (50 μM).

Figure 3.37

Lane	1	2	3	4	5	6
Irradiation time / min	0	5	10	20	30	45
% DNA Form I	56.42	42.99	33.05	3.39	0.20	0.89
% DNA Form II	25.68	41.37	47.51	54.70	43.92	60.45
% DNA Form III	0.00	0.00	0.00	15.89	14.31	24.10
Total	82.10	84.36	80.56	73.98	58.43	85.44
% $[I]_F$	68.72	50.96	41.03	4.58	0.34	1.04
% $[II]_F$	31.28	49.04	58.97	73.94	75.17	70.75
% $[III]_F$	0.00	0.00	0.00	21.48	24.49	28.21
SSB	0.00	0.30	0.52	2.71	5.30	4.19

Figure 3.38

Lane	1	2	3	4	5	6
Irradiation time / min	0	5	10	20	30	45
% DNA Form I	40.73	40.28	27.59	6.49	1.82	2.56
% DNA Form II	26.66	35.12	42.30	53.37	62.17	66.85
% DNA Form III	0.00	0.00	0.00	14.26	17.26	20.95
Total	67.39	75.40	69.89	74.12	81.25	90.36
% $[I]_F$	60.44	53.42	39.48	8.76	2.24	2.83
% $[II]_F$	39.56	46.58	60.52	72.00	76.52	73.98
% $[III]_F$	0.00	0.00	0.00	19.24	21.24	23.19
SSB	0.00	0.12	0.43	1.93	3.30	3.06

Figure 3.39

Lane	1	2	3	4	5	6
Irradiation time / min	0	5	10	20	30	45
% DNA Form I	54.33	49.56	32.42	18.50	10.58	13.92
% DNA Form II	32.42	45.27	63.19	84.60	70.39	52.38
% DNA Form III	0.00	0.00	0.00	0.00	0.00	0.00
Total	86.75	94.83	95.61	103.10	80.97	66.30
% $[I]_F$	62.63	52.26	33.91	17.94	13.07	21.00
% $[II]_F$	37.37	47.74	66.09	82.06	86.93	79.00
% $[III]_F$	0.00	0.00	0.00	0.00	0.00	0.00
SSB	0.00	0.18	0.61	1.25	1.57	1.09

The mean and standard deviation for % DNA $[I]_F$, $[II]_F$, $[III]_F$, and SSB obtained from Figures 3.37 – 3.39 for the irradiation of DNA (18.85 μM) in the presence of Eusolex 232 (50 μM).

	% $[I]_F$		% $[II]_F$		% $[III]_F$		SSB	
Time/ min	**Mean**	**Std. Dev.**	**Mean**	**Std. Dev.**	**Mean**	**Std. Dev.**	**Mean**	**Std. Dev.**
0	63.93	4.29	36.07	4.29	0.00	0.00	0.00	0.00
5	52.21	1.23	47.79	1.23	0.00	0.00	0.20	0.09
10	38.14	3.74	61.86	3.74	0.00	0.00	0.52	0.09
20	10.43	6.84	76.00	5.33	13.57	11.81	1.96	0.73
30	5.22	6.86	79.54	6.44	15.24	13.30	3.39	1.87
45	8.29	11.04	74.58	4.16	17.13	15.05	2.78	1.57

B6: The quantitative analysis of the ethidium bromide-stained agarose gels in Figures 3.44 – 3.46 showing DNA photocleavage induced by the irradiation of DNA (18.85 μM) in the presence of benzophenone-3 (50 μM).

Figure 3.44

Lane	1	2	3	4	5	6
Irradiation time / min	0	5	10	20	30	45
% DNA Form I	87.00	104.20	86.50	134.20	72.80	96.50
% DNA Form II	49.00	52.30	41.90	86.00	46.10	65.60
% DNA Form III	0.00	0.00	0.00	0.00	0.00	0.00
Total	136.00	156.50	128.40	220.20	118.90	162.10
% $[I]_F$	63.97	66.58	67.37	60.94	61.23	59.53
% $[II]_F$	36.03	33.42	32.63	39.06	38.77	40.47
% $[III]_F$	0.00	0.00	0.00	0.00	0.00	0.00
SSB	0.00	-0.04	-0.05	0.05	0.04	0.07

Figure 3.45

Lane	1	2	3	4	5	6
Irradiation time / min	0	5	10	20	30	45
% DNA Form I	121.40	125.60	114.90	125.50	96.20	107.10
% DNA Form II	73.00	69.00	60.80	60.30	52.70	52.30
% DNA Form III	0.00	0.00	0.00	0.00	0.00	0.00
Total	194.40	194.60	175.70	185.80	148.90	159.40
% $[I]_F$	62.45	64.54	65.40	67.55	64.61	67.19
% $[II]_F$	37.55	35.46	34.60	32.45	35.39	32.81
% $[III]_F$	0.00	0.00	0.00	0.00	0.00	0.00
SSB	0.00	-0.03	-0.05	-0.08	-0.03	-0.07

Figure 3.46

Lane	1	2	3	4	5	6
Irradiation time / min	0	5	10	20	30	45
% DNA Form I	43.77	57.67	53.28	57.97	63.50	70.18
% DNA Form II	33.38	39.55	28.31	27.68	29.66	31.22
% DNA Form III	0.00	0.00	0.00	0.00	0.00	0.00
Total	77.15	97.22	81.59	85.65	93.16	101.40
% $[I]_F$	56.73	59.32	65.30	67.68	68.16	69.21
% $[II]_F$	43.27	40.68	34.70	32.32	31.84	30.79
% $[III]_F$	0.00	0.00	0.00	0.00	0.00	0.00
SSB	0.00	-0.04	-0.14	-0.18	-0.18	-0.20

The mean and standard deviation for % DNA $[I]_F$, $[II]_F$, $[III]_F$, and SSB obtained from Figures 3.44 – 3.46 for the irradiation of DNA (18.85 μM) in the presence of benzophenone-3 (50 μM).

	% $[I]_F$		% $[II]_F$		% $[III]_F$		SSB	
Time/ min	**Mean**	**Std. Dev.**	**Mean**	**Std. Dev.**	**Mean**	**Std. Dev.**	**Mean**	**Std. Dev.**
0	61.05	3.82	38.95	3.82	0.00	0.00	0.00	0.00
5	63.48	3.75	36.52	3.75	0.00	0.00	-0.04	0.01
10	66.02	1.17	33.98	1.17	0.00	0.00	-0.08	0.05
20	65.39	3.85	34.61	3.85	0.00	0.00	-0.07	0.11
30	64.67	3.47	35.33	3.47	0.00	0.00	-0.06	0.12
45	65.31	5.11	34.69	5.11	0.00	0.00	-0.07	0.14

B7: The quantitative analysis of the ethidium bromide-stained agarose gels in Figures 3.47 – 3.48 showing DNA photocleavage induced by the irradiation of DNA (18.85 μM) in the presence of benzophenone-4 (50 μM).

Figure 3.47

Lane	1	2	3	4	5	6
Irradiation time / min	0	5	10	20	30	45
% DNA Form I	49.07	36.44	25.41	29.30	21.98	17.55
% DNA Form II	15.45	12.17	9.54	18.28	20.87	22.63
% DNA Form III	0.00	0.00	0.00	0.00	0.00	0.00
Total	64.52	48.61	34.95	47.58	42.85	40.18
% $[I]_F$	76.05	74.96	72.70	61.58	51.30	43.68
% $[II]_F$	23.95	25.04	27.30	38.42	48.70	56.32
% $[III]_F$	0.00	0.00	0.00	0.00	0.00	0.00
SSB	0.00	0.01	0.05	0.21	0.39	0.55

Figure 3.48

Lane	1	2	3	4	5	6
Irradiation time / min	0	5	10	20	30	45
% DNA Form I	42.39	48.99	40.71	28.46	24.34	18.24
% DNA Form II	12.67	9.08	17.25	15.15	20.41	28.62
% DNA Form III	0.00	0.00	0.00	0.00	0.00	0.00
Total	55.06	58.07	57.96	43.61	44.75	46.86
% $[I]_F$	76.99	84.36	70.24	65.26	54.39	38.92
% $[II]_F$	23.01	15.64	29.76	34.74	45.61	61.08
% $[III]_F$	0.00	0.00	0.00	0.00	0.00	0.00
SSB	0.00	0.00	0.08	0.15	0.34	0.67

The mean and standard deviation for % DNA $[I]_F$, $[II]_F$, $[III]_F$, and SSB obtained from Figures 3.47 – 3.48 for the irradiation of DNA (18.85 μM) in the presence of benzophenone-4 (50 μM).

	% $[I]_F$		% $[II]_F$		% $[III]_F$		SSB	
Time/ min	Mean	Std. Dev.	Mean	Std. Dev.	Mean	Std. Dev.	Mean	Std. Dev.
0	76.52	0.66	23.48	0.66	0.00	0.00	-0.01	0.01
5	79.66	6.65	20.34	6.65	0.00	0.00	-0.04	0.08
10	71.47	1.74	28.53	1.74	0.00	0.00	0.06	0.02
20	63.42	2.60	36.58	2.60	0.00	0.00	0.18	0.04
30	52.84	2.19	47.16	2.19	0.00	0.00	0.36	0.04
45	41.30	3.36	58.70	3.36	0.00	0.00	0.61	0.08

PRESENTATIONS OF THIS WORK

1. A. Sewlall, J. Lamb and B. S. Martincigh, DNA damage photoinduced by benzophenone-based sunscreens, European Society for Photobiology Symposium on Photoprotection, Kraków, Poland, 19-22 May 2001.